Investigation of Hydrocarbon Biomarkers Preserved in the Fortescue Group in the Pilbara Craton, Western Australia

Yosuke Hoshino

A thesis submitted in fulfilment

of the requirements for the degree of

Doctor of Philosophy

2015

Department of Earth and Planetary Sciences

Faculty of Science

Macquarie University

Sydney, Australia

Statement of Authenticity

I hereby declare that this submission is my own work and to the best of my knowledge it contains no materials previously published or written by another person, or substantial proportions of material which have been accepted for the award of any other degree or diploma at Macquarie University or any other educational institution, except where due acknowledgement is made in the thesis. Any contribution made to the research by others, with whom I have worked at Macquarie University or elsewhere, is explicitly acknowledged in the thesis. I also declare that the intellectual content of this thesis is the product of my own work, except to the extent that assistance from others in the project's design and conception or in style, presentation and linguistic expression is acknowledged.

Yosuke Hoshino

Abstract

Biomarker studies on the 2.78-2.63 Ga Fortescue Group, Pilbara Craton, Western Australia, have gained tremendous attention for understanding Neoarchean ecosystems. However, there has been a serious debate about the indigeneity and syngeneity of biomarkers contained in the Group. This work focuses on the development of clean processing methods of Archean rock samples free from contamination, and the interpretation of potential Archean biomarkers to reveal information about the ancient biosphere preserved in stromatolite fossils and shales. The examined rock samples were from outcrops and drill cores, and were collected from the Kylena, Tumbiana, Maddina and Jeerinah formations in the Fortescue Group. There are plenty of stromatolite outcrops with various morphologies in the northeast part of the Pilbara region. The three drill cores recovered across the Pilbara region were also examined. Rock samples were sliced into several pieces from the outside towards the inside, so as to separately analyse the hydrocarbon content. This procedure enables recent contamination to be distinguished from indigenous hydrocarbon signatures preserved deep inside the rocks. Most samples including all drill core samples only contain trace amounts of aliphatic and aromatic hydrocarbons, at levels almost comparable but in some cases somewhat above laboratory contamination levels. The hydrocarbon distributions are characteristic of a high thermal maturity, consistent with the prehnite-pumpellyite metamorphic facies that the Fortescue Group experienced. However, one outcrop sample from the Tumbiana Formation preserves various hopanes and steranes, as well as mid-chain branched monomethylalkanes deep inside the rock, which is interpreted as indicating the presence of cyanobacteria and eukaryotes at 2.7 Ga. The finding further supports the presence of oxygen and the emergence of oxygenic photosynthesis before the Great Oxidation Event at 2.4 Ga. However, the samples which contain potential Archean biomarkers are limited, and further extensive studies will be necessary to decisively constrain the timing of evolution of cyanobacteria. In addition to the ancient cyanobacteria, recent cyanobacterial habitation on rock surfaces is indicated by the high concentration of mid-chain branched monomethylalkanes within the surface layers of the investigated rocks.

Acknowledgements

I have benefited from discussions with Martin Van Kranendonk, Roger Summons, Jochen Brocks, Kath Grey, and William Schopf who have shared their experience and knowledge with a young student.

I am indebted to the Geological Survey of Western Australia for the logistical support for the fieldwork that was essential for this study. I am grateful to David Flannery and Malcolm Walter for their companionship on my fieldwork, beneficial discussions, and the support for my stay in Australia as an international student.

The continuous support by my family was essential to complete this work.

One part of my study was carried out together with a PhD student colleague, Carl Peters. His contribution was significant. I would also like to thank my wonderful past and present colleagues in the organic geochemistry laboratory: Tim Leefmann, Sophia Bratenkov, Konstantinos Kotzakoulakis, Soumaya Abbassi, Qingyong Luo, Sarah Houlahan, Emma Flannery, Shirin Baydjanova, Tamsyn Garby, Christine Harper, and David Sala. My study has been particularly enriched by discussions with Jessica Coffey and Sargent Bray.

I was financially supported by a Macquarie University Research Excellence Scholarship, a Macquarie University Postgraduate Research Fund, an International Geological Conference travel grant, and an International Society for the Study of the Origin of Life student travel grant. The study was also funded by ARC grant No. DP1093106. I am grateful for this funding.

Part of the analytical work was performed by Se Gong and David Fuentes at the Commonwealth Scientific and Industrial Research Organisation at North Ryde, and by Jochen Brocks at the Australian National University. I also thank them for beneficial discussions.

My writing and discussion were critically reviewed by Tim Leefmann, Martin Van Kranendonk, Malcolm Walter, and my co-supervisor Norman Pearson. I owe my greatest debt to my supervisor, Simon George. I really appreciate his warm supervision and patience on my gradual progress.

Contents

List of Figures

Chapter 1

Chapter 2

Chapter 3

Chapter 4

Chapter 5

Chapter 6

Figure S6.4. Histograms of MMA (MHD, MHeD and MOD) abundances in slices 1 and 2 of the Loc. 2 sample for Ext. I and II.

Figure S6.5. Histograms of MHeD abundances in all five slices of the Loc. 3 sample for Ext. I and II.

Figure S6.6. Histograms of MMA (MHD, MHeD and MOD) abundances in slices 1 and 2 of the Loc. 4 sample for Ext. I and II.

List of Tables

Chapter 2

Chapter 3

Chapter 4

Chapter 5

Chapter 6

Chapter 7

Abbreviations

ACH	Alkylcyclohexane
ACP	Acyl carrier protein
ADO	Aldehyde deformylating oxygenase
Ar	Argon
ASE	Accelerated Solvent Extractor
ATP	Adenosine triphosphate
BChl	Bacteriochlorophyll
BHP	Bacteriohopanepolyol
BIF	Banded iron formation
BSTFA	bis-Trimethylsilyltrifluoroacetamide
$CaCO_3$	Calcium carbonate
Chl	Chlorophyll
ClO_2^-	Chlorite
ClO_3^-	Chlorate
ClO_4^-	Perchlorate
Cld	Chlorite dismutase
cm	Centimetre(s)
CuO	Copper (II) oxide
CuS	Copper monosulphide
DCM	Dichloromethane
DMDR	Dimethyldibenzothiophene ratio
DNA	Deoxyribonucleic acid
DNR-1	Dimethylnaphthalene ratio 1
eV	Electron volt(s)
EOM	Extractable organic matter
EOP	Even-over-odd preference

FAAR	Fatty acyl acyl carrier protein reductase
F-ATPase	Adenosine triphosphate synthase
FI	Fluid inclusion
Ga	Billion years before present
GOE	Great oxidation event
GC-MS	Gas chromatograph-mass spectroscopy
HC	Hydrocarbon
HCl	Hydrochloric acid
HCO	Heme-copper dioxygen reductase
HF	Hydrofluoric acid
HGT	Horizontal gene transfer
H_2O_2	Hydrogen peroxide
LECA	Last eukaryotic common ancestor
LUCA	Last universal common ancestor
Ma	Million years before present
MACH	Methylalkylcyclohexane
MAI	Methyladamantane index
MDI	Methyldiamantane index
MED	Methyleicosane
MeOH	Methanol
MHD	Methylhexadecane
MHeD	Methyheptadecane
MIF	Mass-independent fractionation
min	Minute(s)
mL	Millilitre(s)
mm	Millimetre(s)
MMA	Monomethylalkane
MND	Methylnonadecane

MNR	Methylnaphthalene ratio
MOD	Methyloctadecane
MPDF	Methylphenanthrene distribution fraction
MPI-1	Methylphenanthrene index 1
MPR	Methylphenanthrene ratio
MRM	Metastable reaction monitoring
MT	Methyltransferase
m/z	Mass to charge ratio
µL	Microlitre(s)
µm	Micrometer(s)
NADP	Nicotinamide adenine dinucleotide phosphate
ng	Nanogram(s)
NSO	Norwegian Petroleum Directorate
OEP	Odd-over-even preference
OLS	Olefin synthase
OSC	Oxidosqualene cyclase
O_2Red	Dioxygen reductase
O_2^-	Superoxide anion
PAH	Polycyclic aromatic hydrocarbon
PAL	Present atmospheric level
pg	Picogram(s)
PGE	Platinum group elements
PS	Photosystem
PTFE	Polytetrafluoroethylene
PTV	Programmable temperature vaporization
RC	Reaction centre
R_c	Calculated vitrinite reflectance

rRNA	Ribosomal ribonucleic acid
ROS	Reactive oxygen species
RuBisCO	Ribulose-1,5-bisphosphate carboxylase/oxygenase
rpm	Rotation per minute
SAM	S-adenosyl-methionine
SHC	Squalene-hopene cyclase
SIM	Single ion monitoring
SOD	Superoxide dismutase
TNR-2	Trimethylnaphthalene ratio 2
VR	Vitrinite reflectance
v / v	Volume-volume percent
UCM	Unresolved complex mixture
UV	Ultraviolet

Publications and conference presentations related to work conducted in this Ph.D

Publications

1. **Y. Hoshino**, S. C. George, 2015. Cyanobacterial inhabitation on Archean rock surfaces in the Pilbara Craton, Western Australia, *Astrobiology*, *in review.*

2. K. L. French, C. Hallmann, J. M. Hope, P. L. Schoon, J. A. Zumberge, **Y. Hoshino**, C. Peters, S. C. George, R. Buick, J. J. Brocks, R. E. Summons, 2015. Archean hydrocarbon biomarkers: Syngenetic or not?, *Proceedings of the National Academy of Sciences, in review.*

3. **Y. Hoshino**, D. T. Flannery, M. R. Walter, S. C. George, (*in prep.*) Significance of hydrocarbon biomarkers discovered in an Archean stromatolite at 2.7 Ga from the Fortescue Group, Pilbara Craton, Western Australia, *Geochimica et Cosmochimica Acta*.

4. **Y. Hoshino**, D. T. Flannery, M. R. Walter, S. C. George, 2015. Hydrocarbon biomarkers preserved in a ~2.7 Ga outcrop sample from the Fortescue Group, Pilbara Craton, Western Australia, *Geobiology* 13, 99-111.

5. D. T. Flannery, **Y. Hoshino**, M. R. Walter, M. J., S. C. George, 2012. Field observations relating to the ~2.74 Ga Mopoke Member, Kylena Formation, Fortescue Group. *Geological Survey of Western Australia Record 2012/8,* 22p.

Conference abstracts

1. **Y. Hoshino**, D. T. Flannery, M. R. Walter, S. C. George, 2014. The preservation potential of hydrocarbon biomarkers in Archean stromatolite outcrop in the Fortescue Group, Pilbara region, Western Australia. *18th Australian Organic Geochemistry Conference*, Adelaide, Australia, 30 November-2 December. Oral
2. **Y. Hoshino**, D. T. Flannery, M. R. Walter, S. C. George, 2014. Investigating the syngeneity and the paleobiology of hydrocarbon biomarkers in the Fortescue Group at 2.7-2.8 Ga, Abstracts of *Origins 2014*, Second joint international conference of the International Astrobiology Society and Bioastronomy, Nara, Japan, 6-11 July. Oral

3. D. E. Jacob, L. F. Morales, M. Amini, G. Benedix, **Y. Hoshino**, M. Mondeshki, 2014. Nanostructure and composition of marine carbonate skeletal structures, *The Australian Marine Society Association Annual Conference*, Canberra, Australia, 6-10 July.

4. **Y. Hoshino**, D. T. Flannery, M. R. Walter, S. C. George, 2013. Investigating the syngeneity and the

paleobiology of hydrocarbons in stromatolites from the Fortescue Group in the Pilbara region, Western Australia (2.7-2.8 Ga), *International Biogeoscience Conference*, Nagoya, Japan, 1-4 November. Oral

5. **Y. Hoshino**, D. T. Flannery, M. R. Walter, S. C. George, 2013. Investigating the syngeneity and the paleobiology of hydrocarbon biomarkers in the Fortescue Group at 2.7-2.8 Ga, *26th International Meeting on Organic Geochemistry*, Tenerife, Spain, 16-20 September. Poster

6. D. T. Flannery, **Y. Hoshino**, M. R. Walter, M. J. Van Kranendonk, S. C. George, 2012. The oxygenation time of Earth: insights from the Neoarchean microbialite record. *Australian Astrobiology Meeting*. University of New South Wales, Sydney, Australia, 30 June-2 July. Oral

7. **Y. Hoshino**, D. T. Flannery, M. R. Walter, S. C. George, 2012. Investigating the syngeneity and paleobiology of hydrocarbon biomarkers in the Fortescue Group at 2.7-2.8 Ga, *Australian Astrobiology Meeting*, University of New South Wales, Sydney, Australia, 30 June-2 July. Oral

8. **Y. Hoshino**, D. T. Flannery, M. R. Walter, S. C. George, 2012. Investigating the syngeneity and paleobiology of hydrocarbon in stromatolites from the Fortescue Group at 2.7-2.8 Ga, *17th Australian Organic Geochemistry Conference*, Sydney, Australia, 2-5 December. Oral

9. **Y. Hoshino**, D. T. Flannery, M. R. Walter, S. C. George, 2012. Investigating the syngeneity and paleobiology of hydrocarbon biomarkers in the Fortescue Group at 2.7-2.8 Ga, *34th International Geological Congress*, Brisbane, Australia, 5-10 August. Oral

Chapter 1.

Introduction

1.1. Oxygen and life

The rise of oxygen was one of the most important events on Earth, and significantly changed the evolutionary pathway of organisms on Earth (Dismukes et al., 2001; Knoll, 2003; Falkowski et al., 2004; Rezende, 2013; Lyons et al., 2014). The accumulation of oxygen harnessed more powerful metabolic pathways for life: aerobic respiration is 18 times more efficient than anaerobic respiration in generating adenosine triphosphate (ATP), enabling the emergence of diverse and complex multicellular organisms (Lehninger, 2008). Accumulated oxygen generated an ozone layer, which prevented the intrusion of harmful UV light and eventually enabled life to extensively diverge from the marine environment to the terrestrial world, although it is possible that biological oxygen production by cyanobacteria may have originated in terrestrial lakes (e.g. Battistuzzi and Hedges, 2009). Oxygen is also the substrate in a variety of monooxygenase and dioxygenase reactions used by all aerobic organisms for degradation of organic matter and biosynthesis of various secondary metabolites (Raymond and Segrè, 2006).

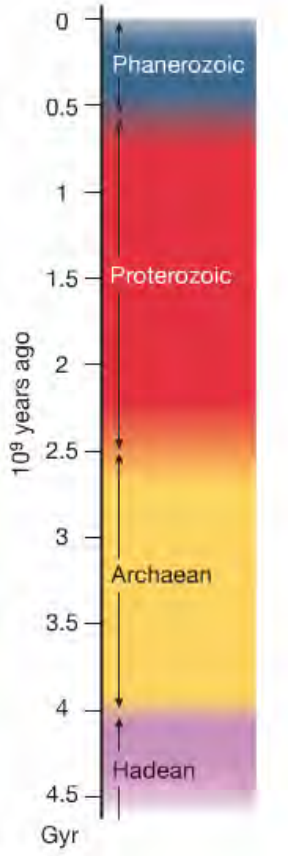

Figure 1.1. Geological time scale of Earth.

Organisms that existed before the advent of oxygen were anaerobes, which most likely utilised sulphur or iron in a similar way to some modern extremophiles. The increase of oxygen in the atmosphere and the surface of the oceans would have caused a catastrophic impact on their ecosystem, and would have forced them to retreat to some “extreme” environments

with no or only trace amounts of oxygen (Raymond and Segrè, 2006). However, oxygen also provided our ancestors the opportunity to utilise more energy. Oxygen is considered to be responsible for several major steps in biological evolution, such as multicellularity (Koch and Britton, 2008; Thannickal, 2009), the birth of eukaryotes and the Cambrian Explosion (Canfield and Teske, 1996; Knoll and Carroll, 1999). However, some anaerobic organisms can be multicellular (Danovaro et al., 2010), suggesting that the presence of oxygen was not the only factor that promoted multicellularity. The body size of organisms has also said to be correlated to the concentration of oxygen (Payne et al., 2011).

The shift of the Earth's environment from essentially anoxic to moderately oxygenated is called the Great Oxidation Event (GOE), and this occurred around 2.4-2.3 Ga (Farquhar et al., 2000; Holland, 2002; Kasting and Catling, 2003; Canfield, 2005; Holland, 2006). The GOE caused an increase of oxygen up to ~1-2 % of modern oxygen levels (Farquhar and Wing, 2003). The oxygen concentration is generally regarded to have been stable until 850 Ma, when it rose to ~20 % present atmospheric level (PAL). It peaked at 30-35 % PAL in the Carboniferous era (Holland, 2006). The rise in oxygen at 850 Ma may have been caused by the divergence of photosynthetic eukaryotes and increased productivity. In contrast, the deep oceans may have remained anoxic until the Late Proterozoic (580-550 Ma) (Johnston et al., 2009).

The key organism for the production of oxygen was cyanobacteria, the organism which first evolved oxygenic photosynthesis (see Section 1.1.2; Hohmann-Marriott and Blankenship, 2011). Furthermore, cyanobacteria are the origin of plastids, the organelles found in plants and green algae that perform oxygenic photosynthesis and also synthesise a diversity of chemical compounds important for other biochemical pathways such as aromatic amino acids, heme, isoprenoids, and fatty acids (Keeling, 2004). Although algae and plants dominate oxygen production in modern environments, their photosynthetic machinery was acquired via endosymbiosis of ancient cyanobacteria. Thus, cyanobacteria are ultimately the origin of almost all the production of oxygen on Earth (Hohmann-Marriott and Blankenship, 2011).

The origin of oxygenic photosynthesis in cyanobacteria is still enigmatic and has attracted enormous attention. Phototrophy (see Section 1.1.1) has its origin in anoxygenic photosynthesis performed by several genera of bacteria, which does not use water as electron donor and thus does not produce molecular oxygen. Oxygenic photosynthesis is considered to have evolved by the combination of two different anoxygenic photosynthetic machineries in cyanobacteria. The timing of the emergence of oxygenic photosynthesis is of importance for reconstructing the geochemical evolution of Earth, and the evolutionary pathway of oxygenic photosynthesis is also essential for a broader understanding of the biochemical evolution of organisms on Earth. It is generally assumed that the oxygen which caused the GOE was provided by oxygenic photosynthesis by cyanobacteria. However, it is not clear whether the first appearance of cyanobacteria coincides with the GOE, or dates back to the pre-GOE era. It has been widely accepted until recently that the evolution of cyanobacteria and the occurrence of the GOE were simultaneous (Kopp et al., 2005; Kirschvink and Kopp, 2008). However, new lines of evidence have indicated a certain amount of oxygen and possibly oxygenic photosynthesis before the GOE (see Sections 1.1.3 and 1.1.4; e.g. Anbar et al., 2007; Flannery and Walter, 2012).

The presence of cyanobacteria and oxygenic photosynthesis at pre-GOE time was first suggested by the discovery of cyanobacterial and eukaryotic biomarkers (see Section 1.2), molecular fossils diagnostic for specific types of organisms (Brocks et al., 1999). However, this finding has now been challenged by the suggestion that the discovered biomarkers are the result of younger contamination (Rasmussen et al., 2008). Although geochemical analysis of redox-sensitive transition elements also indicates the presence of oxygen well before the GOE, to 3.0 Ga (Anbar et al., 2007; Crowe et al., 2013; Planavsky et al., 2014), these data do not necessarily mean the existence of cyanobacteria and oxygenic photosynthesis. Thus, further biomarker evidence is still of great importance to constrain the evolutionary history of the rise of oxygen in the atmosphere and its links to cyanobacterial evolution: this is the main purpose of this study.

There are only two areas which contain relatively low grade metamorphosed Neoarchean to Paleoproterozoic crust in the world. One is the Mount Bruce Supergroup in the Pilbara Craton, Western Australia, and the other is the Transvaal Supergroup in South Africa. This study focuses on the examination of Archean biomarker evidence for cyanobacteria and eukaryotes from Neoarchean rocks of the Fortescue Group (Mount Bruce Supergroup), collected from the Pilbara region, Western Australia (see Section 1.3). There have been few thorough investigations of hydrocarbon preservation and the thermal history of these rocks, thus this study also contributes significant basic knowledge regarding Archean hydrocarbon analyses, including biomarkers.

1.1.1. Evolution of phototrophy

1.1.1.1. The phototrophic way of life

Phototrophy is a biological mechanism to utilise light energy provided by the Sun. The electrons released in this process enable phototrophic organisms (phototrophs) to reduce inorganic carbon, forming organic molecules that maintain their metabolic activity. Phototrophic organic synthesis is called photosynthesis. The solar energy exceeds any other energy sources on Earth, such as electric discharge, radioactivity, volcanism, meteorite impacts, and geothermal energy (Overmann and Garcia-Pichel, 2006). Although only 0.13 % of the available solar energy is converted into chemical energy, it is still much greater than other energy sources. Virtually all life activity is supported directly or indirectly by photosynthesis. The phototrophs which can synthesise organic molecules solely from inorganic carbon such as CO_2, CO and CH_4 are called photoautotrophs (Overmann and Garcia-Pichel, 2006), and these include:

- **Green sulphur bacteria** (belonging to Chlorobi)
- **Purple sulphur bacteria** (belonging to γ-proteobacteria)
- **Cyanobacteria**
- **Photosynthetic eukaryotes** (algae and plants)

There are also organisms which can utilise light energy to produce complex organic molecules but their carbon source is other simpler organic molecules. They are called photoheterotrophs (Overmann and Garcia-Pichel, 2006), and these include:

- **Purple non-sulphur bacteria** (belonging to α- and β-proteobacteria)
- **Green non-sulphur bacteria** (belonging to Chloroflexi)
- Some types of **Acidobacteria**
- Some types of **heliobacteria** (belonging to Firmicutes)
- A type of **Gemmatimonadetes**
- Some types of **Archaea**

Photosynthetic organisms use special molecules called chromophores to absorb light. Three types of chromophores are known: chlorophyll (Chl), bacteriochlorophyll (BChl), and retinal. Chl and BChl-based phototrophy are the most widespread mechanisms in biology on Earth. Chl and BChl are structurally very similar and are treated together from now on. Chl/BChl-based phototropy makes use of (bacterio)chlorophyll photooxidation followed by transmembrane electron transfer. In contrast, retinal-based phototrophy is the photoisomelization of retinal followed by transmembrane proton or chloride transport. Presently, no other mechanism to convert light energy into chemical energy is known.

- **Chl**-based phototrophy: cyanobacteria and all eukaryotes
- **BChl**-based phototrophy: all bacteria except for cyanobacteria
- **Retinal**-based phototrophy: some archaea and bacteria

Phototrophic organisms almost exclusively use Chl/BChl-based machinery. All bacteria use BChl as the chromophore, except for cyanobacteria. Cyanobacteria and all eukaryotes use Chl as the chromophore. In contrast, there are not many organisms that use retinal as a way to translocate protons and synthesise ATP. Such organisms include some halobacteria, proteobacteria, and some other bacteria (for a review, see Spudich and Jung, 2008; Leonid, 2014). Although these halobacteria can grow with the retinal-based phototrophy, this is only under anoxic conditions as a temporal

emergent way. This study focuses on chlorophyll-based phototrophy because cyanobacteria only use the chlorophyll-based system for energy production, although some of them possess retinal systems for sensory purpose (e.g. Anabaena).

1.1.1.2. Development of chlorophyll-based phototrophy

1.1.1.2.1. Occurrence of chlorophyll-based phototrophy

Chl/BChl-based phototrophy are found in various bacteria and some eukaryotes (algae and plants). However, the phototrophic machinery of eukaryotes was derived from cyanobacteria through endosymbiosis (Hohmann-Marriott and Blankenship, 2011). Thus, the origin of Chl/BChl-based phototrophy was almost certainly within the bacterial domain. The integral part of this phototrophy are the **reaction centres (RCs)**, protein complexes which trap light energy, and which contain Chl/BChl and some auxiliary pigments (light-harvesting complexes). Prokaryotic RCs are found in 7 out of more than 30 bacterial phyla:

- **Cyanobacteria**
- **Proteobacteria**
- **Chlorobi**
- **Chloroflexi**
- **Acidobacteria**
- **Firmicutes**
- **Gemmatimonadetes**

Not all species in each phylum are photosynthetic, except for cyanobacteria. Although some endosymbiotic cyanobacterial species cannot perform photosynthesis by gene loss (Zehr et al., 2008), all free-living cyanobacteria have the ability to photosynthesise. The patchy distribution of photosynthesis among bacteria is likely due to the combination of vertical inheritance and horizontal gene transfer of photosynthetic components, where each substructure has its own evolutionary history (Raymond et al., 2002; Olson and Blankenship, 2004).

Photoheterotroph in the phylum Gemmatimonadetes was found quite recently (Zeng et al., 2014), which possesses full functional type II RCs (see below), but does not assimilate inorganic carbon (heterotrophs). The photosynthetic machinery was probably acquired via horizontal gene transfers (HGTs) from proteobacteria (purple bacteria). This is the first confirmed example of gene transfer of chlorophyll-based phototrophy between distant bacterial phyla.

1.1.1.2.2. Reaction Centres (RCs)

RCs are protein complexes, the integral part of photosynthesis specially designed to absorb light energy. There are two types of RCs. Type I RC (RC1, FeS-type RC) has cores with [4Fe-4S] clusters as their terminal electron acceptors. In contrast, type II RC (RC2, Q-type RC, pheophytin-quinone type) has cores with quinines as terminal electron acceptors (Bryant and Frigaard, 2006). The distribution of each RC is follows:

- **Type I RC (RC1, FeS-type)**: cyanobacteria, green sulphur bacteria, heliobacteria, and acidobacteria
- **Type II RC (RC2, Q-type)**: cyanobacteria, purple bacteria, and green non-sulphur bacteria

There is no distinctive relationship between autotrophy / heterotrophy and RC type. Only cyanobacteria have both types of RCs, enabling them to use water as an electron donor and produce molecular oxygen (**oxygenic photosynthesis**). Other photosynthetic bacteria use either FeS-type or Q-type, and do not produce oxygen, because the electron donor is not water (**anoxygenic photosynthesis**). RC1 and RC2 in O_2-producing photosynthetic organisms are particularly called **photosystem I (PS I)** and **photosystem II (PS II)**.

There are two hypotheses to describe the origin of RCs (for a review, see Olson and Blankenship, 2004). The first hypothesis considers that the origin of RCs dates back into the prebiotic era, where the evolution of photosynthesis and the origin of life were closely associated with each other (e.g. Mauzerall, 1992; Hartman, 1998). The second hypothesis, in contrast, regards the advent of photosynthesis to have occurred much later than the divergence of bacteria and archaea, and for it

to have evolved from anaerobic respiration in bacteria which already had DNA, electron transport proteins, and ATP synthase (e.g. Meyer et al., 1996; Nitschke et al., 1998).

1.1.1.2.3. Evolution of RCs

It has been indicated that PS II is similar to other prokaryotic RC2 (Nitschke and Rutherford, 1991; Blankenship, 1992), and PS I is similar to RC1 (Olson et al., 1976). Thus, cyanobacterial photosynthetic machinery seems to have originated from other prokaryotes. RC1 and RC2 also seem to share a common ancestor (Mulkidjanian and Junge, 1997; Schubert et al., 1998; Vermaas, 2002).

One hypothesis of the origin of RCs argues that RC1 and RC2 evolved independently in different organisms, which diversified from a common ancestor possessing a primitive reaction centre. Then, at some point, two reaction centres fused in one organism by gene fusion and generated cyanobacteria (Blankenship, 1992; Xiong and Bauer, 2002). It has been proposed that genes for RC1 were transferred from ancestral heliobacteria to ancestral purple bacteria which already had genes for RC2 (Mathis, 1990), which is consistent with the 16S rRNA phylogeny (Fig. 1.2, Blankenship, 1992). In this hypothesis, purple bacteria and green non-sulphur bacteria are the descendants of organisms which had ancestral RC2, while heliobacteria and green-sulphur bacteria evolved from organisms which had ancestral RC1. Although the hypothesis has been accepted at least as a concept, there is no decisive evidence for the origin and evolution of RCs. Proposed phylogenetic trees for the BChl/Chl biosynthesis pathway and the RC synthesis pathway have significant discrepancies, thus it seems that each part of the phototrophic machinery experienced a different evolutionary history involving vertical gene heritance and horizontal gene transfers (Raymond et al., 2002).

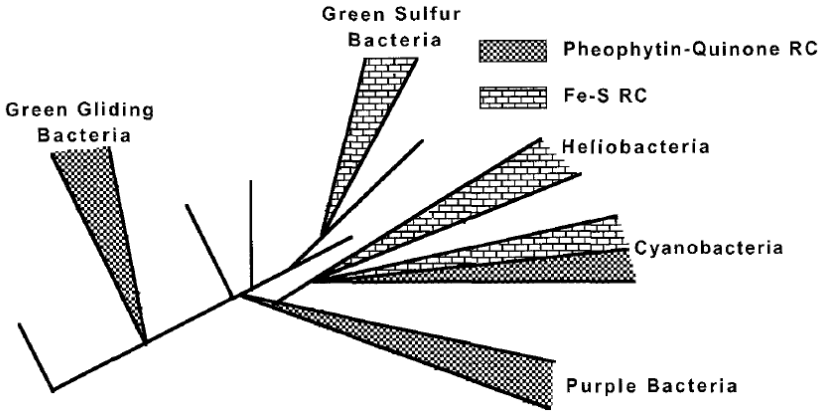

Figure 1.2. Evolutionary tree of bacteria based on 16S rRNA (Adapted from Blankenship, 1992). Green gliding bacteria correspond to green non-sulphur bacteria in the phylum Chloroflexi.

1.1.1.3. Shift from anoxygenic to oxygenic photosynthesis

There are several hypotheses to describe the transition from anoxygenic to oxygenic photosynthesis. Bicarbonate has been suggested to be an alternative and therefore a former substrate before water for O_2 production in photosynthesis. It has also been indicated that bicarbonate and manganese ion (Mn^{2+}), which were supposedly abundant in the Archean ocean, form clusters and were precursors for the modern water-oxidising protein complexes (Dismukes et al., 2001). In contrast, hydrogen peroxide (H_2O_2) has also been proposed to have been oxidised in the reaction centre using Chlorophyll d at intermediate stages before the advent of modern photosynthesis, possibly performed by purple bacteria-like organisms (Blankenship and Hartman, 1998), although the validity of this suggestion has been questioned (Dismukes et al., 2001).

Oxygenic photosynthesis is a mechanism to oxidise water to extract proton motive force for ATP synthesis, during which molecular oxygen is produced as a by-product. The main reaction of oxygenic photosynthesis is driven by four membrane protein complexes, photosystem I (PS I), photosystem II (PS II), cytochrome-b_6f and F-ATPase. The reaction is composed of water oxidation, NADP reduction, and ATP formation (for a review, see Nelson and Ben-Shem, 2004). The first two steps are catalysed by PS I and PS II, whereas the last one is by ATP synthase (F-ATPase). Water oxidation and oxygen

generation occur in the oxygen-evolving complex in PS II (for a review, see Yano and Yachandra, 2014). The cytochrome-b_6f mediates electron transport between PS II and PS I and creates the proton motive force. Obtained electrons and protons are used for ATP synthesis and to fix CO_2 to carbohydrates via the Calvin-Benson cycle.

1.1.2. Evolution of cyanobacteria

1.1.2.1. What are cyanobacteria?

Cyanobacteria are gram-negative photosynthetic bacteria, and are one of the most divergent organisms on Earth. They are major primary producers and play an important role in biogeochemical cycles of N, C and O. 30 % of modern oxygen annual production on Earth is estimated to be produced by cyanobacteria. Cyanobacteria thrive in a wide range of environment, including freshwater, oceans, soils, and some harsh conditions such as hot springs, saline lakes and ice lakes (Falkowski 1997). Cyanobacteria were previously known as blue-green algae because they were thought to be part of the eukaryotic algae. 16S rRNA sequence analyses, however, revealed that cyanobacteria belong to the domain Bacteria (Flores et al., 2008).

Cyanobacteria are the only performer of oxygenic photosynthesis in prokaryotes. The evolution of oxygenic photosynthesis by cyanobacteria had a significant impact on evolutionary pathways of life on early Earth. Oxygenic photosynthesis is essential to almost all of the modern organisms because any aerobic metabolisms are based on oxygen, and also many anaerobic activities are supported by organic matter ultimately produced by photoautotrophic carbon assimilations. Although oxygenic photosynthesis is nowadays dominantly performed by plants and green algae (photosynthetic eukaryotes), the chloroplasts where photosynthesis is carried out in plants and algae are evolutionarily the endosymbiotic descendants of cyanobacteria (Hohmann-Marriott and Blankenship, 2011). Thus, all oxygenic photosynthesis on Earth originated from cyanobacteria.

Synechococcus and *Prochlorococcus* are two major groups of marine unicellular cyanobacteria that dominate the vast majority of the world's oceans (for a review, see Scanlan, 2012). *Prochlorococcus*

contributes about 45 % of CO_2 fixation, and *Synechococcus* contributes 21 % in the sub-tropical North Atlantic Ocean (Jardillier et al., 2010). Thus, these marine cyanobacterial groups are primary contributors to oceanic CO_2 fixation.

1.1.2.2. Taxonomy of cyanobacteria

Despite the universal presence of cyanobacteria and their great importance for the habitability of Earth, their taxonomy and classification are still being debated (Kauff and Büdel, 2011). Cyanobacteria are traditionally classified into five groups according to their morphologies (Rippka et al., 1979; Schirrmeister et al., 2011) (Fig. 1.3):

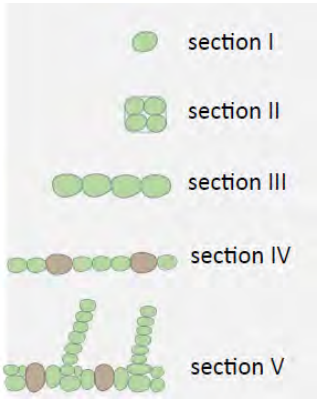

Figure 1.3. Morphologies of cyanobacteria (adapted from Schirrmeister et al., 2011)

Section I. Unicellular (Chroococcales)

Section II. Baeocystous (Pleurocapsales)

Section III. Filamentous (Oscillatoriales)

Section IV. Heterocystous (Nostocales)

Section V. Ramified or True Branching (Stigonematales)

Section I and II refer to unicellular species and section III-V correspond to multicellular species. Section I includes spheroidal, solitary and colonial unicellular cyanobacteria. These reproduce by fission and budding (e.g. *Gloeocapsa*). Section II contains unicellular or pseudofilamentous cyanobacteria. These reproduce by multiple fissions giving rise to daughter cells called baeocytes (e.g. *Pleurocapsa*). Section III is composed of multicellular filamentous cyanobacteria, but they are undifferentiated (e.g. *Oscillatoria, Spirulina*). Section IV encompasses filamentous cyanobacteria that display irreversible cellular differentiation into akinetes (climate-resistant spores) and heterocysts (N_2 fixing cells) (e.g. *Nostoc*). Section V comprises morphologically more complex filamentous cyanobacteria forming heterocysts and exhibiting true branching (e.g. *Fischerella*).

Nevertheless, cyanobacterial subdivisions are polyphyletic (Schirrmeister et al., 2011), and the classification based on cell organization, and metabolism does not reflect evolutionary relationships. Section II, IV and V are generally monophyletic, respectively, and section IV and V can be further grouped together, but Sections I and III do not form monophyletic lineages (Schopf, 2012).

Recently, the diversification of multicellularity in cyanobacteria has been associated with the GOE (Tomitani et al., 2006; Schirrmeister et al., 2011; Schirrmeister et al., 2013). It was suggested that multicellularity could have played a key role in triggering cyanobacterial evolution and the drastic increase of atmospheric oxygen at the GOE. However, it is not clear whether multicellularity caused the GOE, or whether the increase of oxygen triggered the development of multicellularity. The very origin of cyanobacteria (unicellular species) could be as early as 3.0 Ga (Schirrmeister et al., 2013).

1.1.2.3. Evolution of cyanobacteria

Little is known about the evolution of cyanobacteria. Cyanobacteria have two photo-sensing protein complexes, PS I and PS II, whereas any other phototrophic bacteria have only either PS I or PS II-like reaction centres. The combination of PS I and PS II enables cyanobacteria to perform oxygenic photosynthesis producing molecular oxygen (Hohmann-Marriott and Blankenship, 2011). Cyanobacteria may have acquired the PS I-like photosystem from heliobacteria, and the PS II-like one from proteobacteria (see Section 1.1.1.2.3).

Recently, melainabacteria have been discovered to have a close relationship to cyanobacteria (Di Rienzi et al., 2013; Hofer, 2013). Melainabacteria have neither PS I nor PS II, which complicates the interpretation of cyanobacterial evolution because they indicate that proto-cyanobacteria did not have any photosynthetic machinery, and thus needed to acquire two photosystems one by one, or simultaneously. Thus, there is a large missing link between melainabacteria and cyanobacteria.

Gloeobacter violaceus is a rod-shaped unicellular cyanobacterium which branched off the earliest from other cyanobacteria (Honda et al., 1999). This is the only cyanobacteria which lacks the thylakoids where photosynthesis is performed in other cyanobacteria. Instead, photosynthesis of

Gloeobacter is carried out on the plasma membrane. They also lack many genes for photosystem I and II (Nakamura et al., 2003). Thus, *Gloeobacter* is considered to be the closest species to the ancestors of cyanobacteria.

It is generally regarded that all cyanobacteria are photosynthetic. However, there are a few species of cyanobacteria which do not perform oxygenic photosynthesis. The N_2-fixing marine cyanobacterium UCYN-A lacks PS II (Zehr et al., 2008; Tripp et al., 2010). UCYN-A has a unique photofermentative metabolism which uses the remaining PS I, and is in a symbiotic relationship with a photosynthetic unicellular alga, prymnesiophyte (Thompson et al., 2012; Thompson et al., 2014). An intracellular N_2-fixing bacterium, which is closely related to diazotrophic cyanobacteria of the *Cyanothece sp.*, is another example of a cyanobacterium lacking photosynthetic pathways (Kneip et al., 2008). The cyanobacterium has an endosymbiotic relationship with the host diatom *Rhopalodia gibba*. Genes encoding photosynthesis seem to have been lost during the long symbiotic relationship because they were no longer required (Moran and Wernegreen, 2000). Thus, it is not correct to say that all cyanobacteria perform oxygenic photosynthesis, but it is still arguable that all free living cyanobacteria carry out oxygenic photosynthesis.

1.1.2.4. Other biological oxygen-production mechanisms

Besides oxygenic photosynthesis, three biological pathways to produce molecular oxygen have been discovered: (1) the detoxification (dismutation) of reactive oxygen species, (2) chlorite respiration, and (3) nitrite-driven anaerobic methane oxidation (Ettwig et al., 2010). Dismutation is a chemical reaction during which two identical molecules react with each other, and generate two different products. These three pathways do not need light. Instead, they take advantage of oxidants with a more positive redox potential than the O_2/H_2O couple. However, the total amount of produced oxygen by these pathways is estimated to be small and cannot compare with oxygenic photosynthesis. Nevertheless, they may have existed in the distant past and could have been associated with early aerobic metabolisms (Kool et al., 2014).

Reactive oxygen species (ROS), such as superoxide anion (O_2^-) is dismutated by superoxide dismutase (SOD) producing molecular oxygen

$2\ O_2^- + 2\ H^+ \rightarrow H_2O_2 + O_2$

Also, H_2O_2 is dismutated by catalases forming water and oxygen.

$2\ H_2O_2 \rightarrow 2\ H_2O + O_2$

These reactions are a part of the water-water cycle which detoxicate deleterious ROS unavoidably generated during aerobic metabolism and oxygenic photosynthesis (Latifi et al., 2009). Dismutation of ROS ends up regenerating oxygen which was transformed to ROS, thus is not a mechanism to actively produce oxygen.

Some types of β-proteobacteria can carry out the dismutation of the toxic intermediate chlorite (ClO_2^-) and concomitant production of molecular oxygen, catalysed by chlorite dismutase for chemoorganotrophic respiration (Rikken et al., 1996; van Ginkel et al., 1996; Hagedoorn et al., 2002), or for monooxygenase-dependent antibiotics biosynthesis (Bab-Dinitz et al., 2006).

$ClO_2^- \rightarrow Cl^- + O_2$

These chlorite-reducing bacteria can use chlorate (ClO_3^-) or perchlorate (ClO_4^-) as a terminal electron acceptor. They are facultative aerobes, and can grow in anoxic environments using the chlorite-derived oxygen for aerobic respiration. Their respiration is involved with chlorate reductase and chlorite dismutase (Cld), reducing chlorate or perchlorate to chlorite, then to chloride and molecular oxygen. Oxygen is not derived from water, but from chlorite itself (Lee 2008). Cld belongs to the CDE superfamily of heme enzymes, named after three closely related enzyme groups; CFP, DyP, and EfeB (Goblirsch et al., 2011). Cld homologs have been also found in both bacteria and archaea, although they cannot grow with chlorate as an electron acceptor (Mlynek et al., 2011).

Methane-oxidising bacterium "*Candidatus methylomirabilis oxyfera*" metabolise methane "aerobically" under an anoxic environment. The bacterium lacks any homologues to known

anaerobic methanotrophic pathways, but instead has a complete set of aerobic methane oxidation pathways involving particulate methane monooxygenase (Ettwig et al., 2012). *M. oxyfera* enables the aerobic reactions using internally-produced oxygen through NO dismutation. It has been suggested that eight NO molecules are dismutated to four molecules of N_2 and O_2. Then, three O_2 molecules are consumed for methane oxidation, and residual O_2 seems to be used for respiration of one of the terminal oxidases (Wu et al., 2011). *M. oxyfera* produces some novel bacteriohopanepolyols (BHPs), which may be exclusive biomarkers for this species, including 3-methyl-BHP-hexol and BHP-hexol (Kool et al., 2014). Interestingly, ^{13}C-labelling experiments indicates that the carbon atom in discovered BHPs do not come from CH_4, but rather from bicarbonate/CO_2. This finding implies that BHPs derived from methanotrophs do not necessarily show a characteristically depleted carbon isotopic ratio (Kool et al., 2014).

1.1.3. Evidence of oxygen before the GOE

There have been numerous lines of evidence for the presence of oxygen before the GOE, as described below. However, the mere presence of oxygen does not necessarily support the emergence of oxygenic photosynthesis before the GOE, as oxygen can be produced either abiologically to concentrations of up to 10^{-5} present atmospheric level (PAL) (Haqq-Misra et al., 2011), or by other biological pathways (Ettwig et al., 2010). For example, some aerobic metabolisms indeed work at very low oxygen concentrations down to nanomolar range (Waldbauer et al., 2011), and the evolution of some aerobic enzymes seem to date back to the common ancestors of bacteria and archaea back in the Paleoarchean or Hadean (Brochier-Armanet et al., 2009). This has led some researchers to hypothesise that the development of aerobic metabolism occurred before the advent of oxygenic photosynthesis (The early respiration hypothesis, Castresana and Saraste, 1995). However, it is not constrained how much oxygen existed before the GOE. Most evidence indicate nonzero amounts of oxygen, but very low (e.g. Anbar et al., 2007; Garvin et al., 2009; Li et al., 2013; Wille et al., 2013). It is not clear when oxygenic photosynthesis arose during the course of the

evolution of the aerobic biosphere. However, recent data suggest that the prevailing view of an early Earth that was completely anoxic with organisms that only developed aerobic metabolisms at, or after the GOE, needs to be modified. Instead, it has been suggested that organisms were adapted to micro-aerobic conditions, and continuously evolved in association with the rise of oxygen throughout the entire Precambrian (Wang et al., 2011; Kim et al., 2012). Note that this does not reduce the significance of the GOE and oxygenic photosynthesis for triggering the greater diversification of organisms on our planet.

1.1.3.1. Abiogenic O_2 production and early respiration hypothesis

Trace amounts of atmospheric oxygen can be produced abiogenically by photochemical reactions of H_2O and CO_2 (Kasting et al., 1979; Kasting and Walker, 1981; Kasting et al., 1984), and these might have enabled the evolution of oxygen-related metabolisms such as aerobic respiration before the development of oxygenic photosynthesis (the early respiration hypothesis, Castresana et al., 1994; Castresana and Saraste, 1995; Pereira et al., 2001; Brochier-Armanet et al., 2009). However, it has generally been stated that the possible amount of abiologically produced oxygen is too low for aerobic metabolism; for example, at 10^{-14} present atmospheric level (PAL) (Siebert et al., 2005). However, the study by Haqq-Misra et al. (2011) indicated that the oxygen concentration obtained by abiogenic photochemical reactions may have been locally much higher than previously thought (1.5 x 10^{-5} PAL), and thus allowed the performance of aerobic respiration on pre-photosynthetic Earth.

1.1.3.2. Geochemical evidence for the rise of oxygen

1.1.3.2.1. Redox-sensitive metals

Some transition metal elements are sensitive to the redox state of the atmosphere or oceans. Their abundance and/or isotopic ratios can be used to indicate the presence of oxygen before the GOE based on the redox-dependent solubility. Some elements are insoluble in oxidised forms, but soluble in reduced forms; for example, iron (Fe). In contrast, other elements are insoluble in reduced forms and soluble in oxidised forms; for example, molybdenum (Mo), rhenium (Re) and chromium (Cr).

The enrichment of Mo and Re in the 2.5 Ga Mount McRae Formation in Western Australia suggests that these metals were derived from oxidative weathering of crustal sulphide minerals (pyrite), and that therefore a small amount of oxygen existed more than 50 million years before the GOE (Anbar et al., 2007). An O_2 concentration of only 10^{-5} PAL was estimated to be enough to account for the observed Mo/Re enrichment in these rocks. The Mo and Re behaviour coincides with the shift of sulphur isotopic ratios at 2.5 Ga from slightly positive to negative in the same formation (Kaufman et al., 2007). The shift to negative $\delta^{34}S$ is interpreted as the onset of widespread microbial sulphate reduction, stimulated by the increase of sulphate concentration in oceans caused by oxidative weathering of crustal sulphides. The data suggest that oxygen levels exceeded at least 10^{-6} PAL in the world's oceans at 2.5 Ga. A high abundance of Re and a low abundance of Mo observed in the 2.6-2.5 Ga black shales from the Cambellrand-Malmani carbonate platform in South Africa was interpreted to be the result of dissolved oxygen in the bottom waters on the platform slope adjacent to a large Archean ocean basin, based on different mechanisms of Re and Mo removal (Kendall et al., 2010).

Isotope ratios are also useful indicators for the presence of atmospheric oxygen. A large offset of ^{98}Mo isotope ratios relative to ^{95}Mo ($\delta^{98/95}Mo$) from rocks in a nearshore setting in the c. 2.95 Ga Sinqeni Formation, Pongola Supergroup, South Africa was indicated to be caused by oxygenic photosynthesis (Planavsky et al., 2014). Mo isotopic ratios are strongly associated with Mn(II) oxidation under oxic conditions (Siebert et al., 2003; Barling and Anbar, 2004; Tossell, 2005). The necessary oxygen concentration for Mn(II) oxidation is much higher than abiogenic oxygen production (~ 10^{-5} PAL). Thus, the presence of Mn oxidation suggests oxygenic photosynthesis.

The investigated 3.0 Ga Sinqeni Formation retained ^{98}Mo signatures for Mn oxidation despite subsequent reduction of the host Mn oxides during younger diagenesis (Planavsky et al., 2014). Many other $\delta^{98/95}Mo$-based studies have also suggested the presence of oxygen before the GOE, including in shales of the 2.5 Ga Mount McRae Formation in Australia (Duan et al., 2010), and the 2.6-2.5 Ga Ghaap Group in the Transvaal Supergroup in South Africa (Wille et al., 2007; Voegelin et al., 2010). In

contrast, a study suggested no measurable redox cycle of the redox-sensitive elements Mo and Cr, and an anoxic condition around 3.5-2.8 Ga (Wille et al., 2013).

Cr isotopes are also redox indicators for oxidative weathering. The depletion of ^{53}Cr in a 3.0 Ga palaeosol and its concomitant enrichment in shallow water iron formation from the Pongola Supergroup, South Africa has been attributed to the oxidative weathering of Cr-containing soils and transport of water-soluble Cr(VI) to oceans (Crowe et al., 2013). This coincides with the suggested presence of oxygen at 2.95 Ga, in the same group, by the Mo isotope study mentioned above (Planavsky et al., 2014). Oxidation of Cr(III) in soil to water soluble Cr(VI) enriches heavy ^{53}Cr in Cr(VI) caused by the isotopic fractionation during oxidation (Zerkle et al., 2012). Further, Cr(III) oxidation is facilitated by the presence of manganese oxides, which in turn are produced by microorganisms under oxic conditions (Tebo et al., 2005; Stüeken et al., 2012). The estimated oxygen level by Crowe et al. (2013) is at least 6×10^{-5} PAL at 3.0 Ga.

Furthermore, redox-dependent solubilities of PGE, and particularly the Re-Os pair, are used as proxies for atmospheric/oceanic oxygen levels. PGE consist of ruthenium (Ru), rhodium (Rh), palladium (Pd), osmium (Os), iridium (Ir), and platinum (Pt). These show different solubilities in water depending on their redox state. The rise of oxygen in the Archean has been suggested by PGE-Re data combined with Mo isotope analysis (Siebert et al., 2005; Wille et al., 2007). The 3.23 Ga Fig Tree Group sedimentary rocks in the Barberton Greenstone Belt, South Africa, do not show any difference in PGE-Re abundance pattern nor Mo fractionation from komatiites in the same locality, suggesting the absence of elevated oxygen concentrations (Siebert et al., 2005; Wille et al., 2007). In contrast, 2.64-2.5 Ga Ghaap Group black shales in the Transvaal Supergroup and 2.7 Ga black shale in the Manjeri Formation in the Belingwe Greenstone Belt in Zimbabwe show increased Mo concentrations and fractionations, as well as Re and Os enrichment, indicating elevated oxygen around 2.7-2.6 Ga (Siebert et al., 2005; Wille et al., 2007).

1.1.3.2.2. Banded Iron Formations (BIFs)

BIFs are a major characteristic of Precambrian geology, and are possible evidence for the presence of oxygen, although other mechanisms of their formation have been widely discussed. BIFs are laminated marine sedimentary rocks characterised by alternating laminations of iron-bearing layers and iron-poor layers of silica (James, 1954; James, 1983; Klein, 2005; Trendall, 2009; Bekker et al., 2010). BIFs are exclusive to the Precambrian, ranging in age mostly from 3.8 Ga to 1.8 Ga, primarily in the late Archean (2.7-2.5 Ga) and the Paleoproterozoic (2.5-1.8 Ga), but also in the Paleo- to Mesoarchean (3.8 Ga) and Neoproterozoic (0.7 Ga) (Nutman et al., 1997; Bekker et al., 2004; Klein, 2005; Holland, 2006). Thus, the peak of BIF deposition bridges the GOE when the atmospheric composition on Earth drastically changed (Anbar et al., 2007), and have been used to reveal the composition of the Archean and the Proterozoic ocean and ancient microbial activities.

There is no consensus on the origin of BIFs. That is, the mechanism of dissolved Fe(II) oxidation into the precipitation of solid phase Fe(III). There are two potential hypotheses (for a recent review, see Posth et al., 2014). Fe(II) oxidation by molecular oxygen produced by cyanobacterial photosynthesis is a biological mechanism proposed for BIF formation (Cloud, 1965; Cloud, 1973), which hints at the presence of molecular oxygen before the GOE. It was argued that even if there were low oxygen conditions before the GOE, there may have been locally oxygenated areas produced by cyanobacterial blooms (Cloud, 1965).

Alternatively, oxidation of Fe(II) by microaerobic chemoautotrophs (Holm, 1989), and anoxygenic Fe(II)-oxidising photoautotrophs coupled by CO_2 fixation has been proposed as the origin of BIFs before the evolution of oxygenic photosynthesis (Garrels et al., 1973; Hartman, 1984; Widdel et al., 1993; Kappler et al., 2005). In this scenario, the presence of oxygen is not necessary. Anoxygenic photoautotrophs utilising Fe(II) and sulphur may have been the key organisms for primary production on early Earth, considering the high abundance of these chemical species in the Archean

(Canfield et al., 2006). There is a possibility that the BIF formation may be a mixture of these two mechanisms, depending on time and space.

1.1.3.2.3. Sulphur mass-independent fractionation (S-MIF) signals

The S-MIF is an excellent indicator for the oxygenation of Earth's atmosphere (Farquhar et al., 2000; Pavlov and Kasting, 2002). The amount of sulphur isotopic fractionation ($\Delta^{33}S$) is controlled by mass-dependent fractionations such as kinetic and equilibrium fractionations, and MIF such as spin-forbidden photochemical reactions. MIF is rare in nature, and the examples have been found for oxygen and sulphur so far (Clayton et al., 1973; Heidenreich and Thiemens, 1986; Farquhar et al., 2000). S-MIF signals are supplied by elemental sulphur (S^0) produced by SO_2 photolysis in the atmosphere under anoxic conditions. In contrast, in oxic environments, volcanic SO_2 is readily oxidised to SO_4^{2-}, preventing S^0 formation and MIF signal generation. It has been demonstrated that $\Delta^{33}S$ largely deviate in Precambrian rocks before 2.45 Ga (Farquhar et al., 2000; Fig. 1.4). This indicates the absence of atmospheric oxygen before that time, and is one of the most powerful evidence for the GOE at 2.45 Ga.

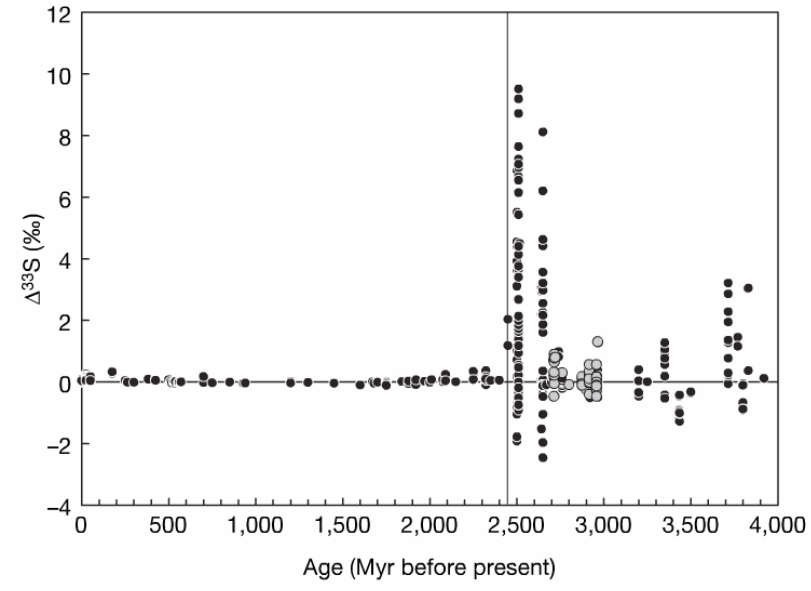

Figure 1.4. $\Delta^{33}S$ versus age for rock samples (adapted from Farquhar et al., 2007).

Although the S-MIF signals have been used to indicate anoxic environments throughout the Archean, the intervals of low $\Delta^{33}S$ at 3.0-2.8 Ga may represent transient oxygenation events (Ohmoto et al., 2006). However, it has also been demonstrated that small, but non-zero, MIF signals indeed occurred during the intervals and anoxic environments persisted (Farquhar et al., 2007). The low S-MIF signals have been attributed to variations in the relative abundance of trace gas species such as SO_2, or to fluctuation in UV radiation. Dogamal-Goldman et al. (2008) suggested that an organic haze could have affected the MIF signal intensity by shielding UV radiation responsible for the MIF photochemistry. However, Crowe et al. (2013) revealed that the possible presence of oxygen (~3 x 10^{-4} PAL) at 3.0 Ga indicated by Cr isotope fractionation coincides with the MIF anomaly period, and the anomaly may be associated with the temporal rise of oxygen as originally suspected. The S-MIF anomaly also coincides with the suggested first glaciation events on Earth at c. 2.9 Ga, which might have occurred due to the decrease of CH_4 in accordance with the rise of oxygen (Holland, 2006).

1.1.3.2.4. Carbon isotope ratios ($\delta^{13}C$)

It is well known that sedimentary organic matter in the Precambrian is depleted in ^{13}C (Fig. 1.5), and has been used to indicate the presence of microbial life since at least 3.8 Ga (Hayes et al., 1983).

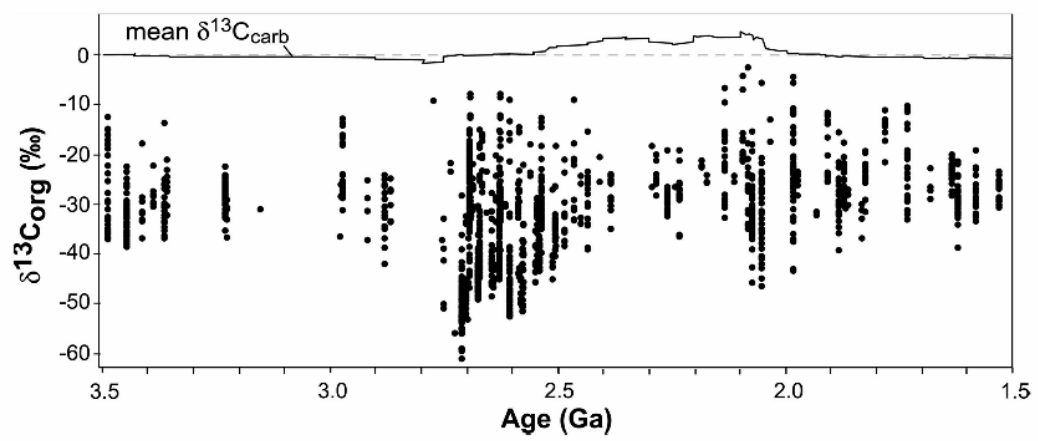

Figure 1.5. Kerogen and total organic carbon $\delta^{13}C$ values relative to inorganic carbon $\delta^{13}C$ compositions (top curve) for marine carbonate rocks (adapted from Eigenbrode and Freeman, 2006).

^{13}C depletion is also used to indicate the presence of a certain aerobic metabolism, which necessarily requires oxygen. Eigenbrode and Freeman (2006) argued that the wide range of ^{13}C depletion between -60.9 and -28.1 ‰ around 2.7-2.6 Ga is associated with a diversification of microbial ecology in the shallow water from purely anaerobic methanotrophy to aerobic metabolisms driven by cyanobacterial oxygen production at 2.7 Ga. The drastic decrease in $\delta^{13}C$ at 2.7 Ga may represent the onset of methane assimilation stimulated by the high availability of electron acceptors as a consequence of oxygen production (Coleman et al., 1981; Barling and Anbar, 2004), although the evidence for cyanobacteria from conventionally collected drill core samples is now doubted (French et al., 2013). The consistency in the observed depleted $\delta^{13}C$ values among three different formations at 2.9 Ga has been used to argue for the presence of oxygenic photosynthesis by 2.9 Ga (Nisbet et al., 2007).

1.1.3.2.5. Nitrogen isotope ratio ($\delta^{15}N$)

Transient elevated values of ^{15}N isotope ratios have been reported from the 2.5 Ga organic-rich Mount McRae shale in the Hamersley Basin in Australia (Garvin et al., 2009) and the 2.7 Ga shale in the Campbellrand-Malmani platform in South Africa (Godfrey and Falkowski, 2009), indicating the presence of aerobic nitrification/denitrification pathways, and consequently the temporal rise of oxygen in surface oceans before the GOE. Isotopic fractionation occurs during denitrification. The oxygen level was estimated to be from $< 10^{-6}$ to $\leq 10^{-5}$ PAL (Garvin et al., 2009). It was suggested that nitrification and denitrification drove the loss of fixed N, causing the low availability of N and thus constraining the growth of oxygen-producing plankton, which then delayed the accumulation of atmospheric oxygen (Godfrey and Falkowski, 2009).

1.1.3.2.6. Oxygen before 3.0 Ga

A minority of researchers argue that the Earth was fully oxygenated already at 3.5 Ga (e.g. Ohmoto, 1997; Ohmoto et al., 2006; Hoashi et al., 2009), but this is not widely accepted because it contradicts much geochemical data that are consistent with anoxic environments before 3.0 Ga. The higher abundance of uranium (U) than that of thorium (Th) in the 3.8 Ga Isua metasedimentary rocks may

suggest the presence of oxygen because U is soluble in oxidised forms and mobile, whereas Th is immobile in both oxidised and reduced forms (Rosing and Frei, 2004). However, such an isotopic behaviour seems limited to the Isua metasedimentary rocks, and lower grade Archean sedimentary rocks do not show a similar trend (Wille et al., 2013). Thus, the validity of this hypothesis is uncertain (Van Kranendonk, 2014).

1.1.3.3. Biochemical evidence for the rise of oxygen

Biochemical evidence for the presence of oxygen is generally based on the reconstruction of oxygen-related genes or enzyme phylogeny. However, their time estimation is not solely based on biochemical data, but also on geological evidence (see Methodology in David and Alm, 2011; Wang et al., 2011). Thus, biochemical data can be complementary to geological data, but cannot be the sole evidence. The antiquity of some aerobic enzymes dating back to the divergence of bacteria and archaea implies the presence of oxygen well before the GOE. The gradual development of aerobic metabolisms may coincide with the emergence of oxygenic photosynthesis, but the relationship between them is still unclear.

1.1.3.3.1. Oxygen-related gene diversification

A recent phylogenomic study indicated that oxygen-related genes drastically increased around 3.0 Ga, and continued to increase towards present (David and Alm, 2011). The highest growth rate of oxygen-related genes was at 3.0 Ga, not at 2.5 Ga, the timing of the GOE, and thus the advent of cyanobacteria was estimated by these authors to be around 3.0 Ga, as well. The predicted early rise of oxygen coincides well with geochemical data arguing for the rise of oxygenic photosynthesis by 3.0 Ga (e.g. Crowe et al., 2013; Planavsky et al., 2014).

The presence of some oxygen-related genes dates back to the oldest age of the calculation (≤ 3.8 Ga), which may represent biological responses against abiogenic oxygen production. Also, the increase of oxygen-related genes already starts before the spike at 3.0 Ga or a younger age (David and Alm, 2011, see Supplementary Fig. 10), which may reflect a gradual adaptation towards primitive aerobic

metabolisms under microaerobic conditions, or the early emergence of oxygenic photosynthesis. Indeed, enzymes using oxidised forms of nitrogen such as N_2O and NO_3^- grow concomitantly over time, indicating the presence of an aerobic nitrogen cycle by the late Archean as also suggested by geochemical data (Garvin et al., 2009; Godfrey and Falkowski, 2009). Also, enzymes using copper and molybdenum increase over time in the late Archean, corresponding to the increased availability of these elements in oxidising atmosphere and oceans (Crowe et al., 2013).

1.1.3.3.2. Oxygen-related protein domain development

The molecular clock study based on protein domain structures of oxygen-related enzymes suggests the appearance of aerobic metabolisms at 2.9 Ga, and aerobic respirations at 2.8 Ga (Wang et al., 2011; Kim et al., 2012; Saito, 2012). Similar to the gene diversification pattern, the number of protein domain structures associated with aerobic metabolisms has grown gradually since 2.9 Ga, with no particular shift at the GOE, indicating that the development of aerobic metabolisms was more gradual, and earlier, than commonly regarded (Fig. 1.6).

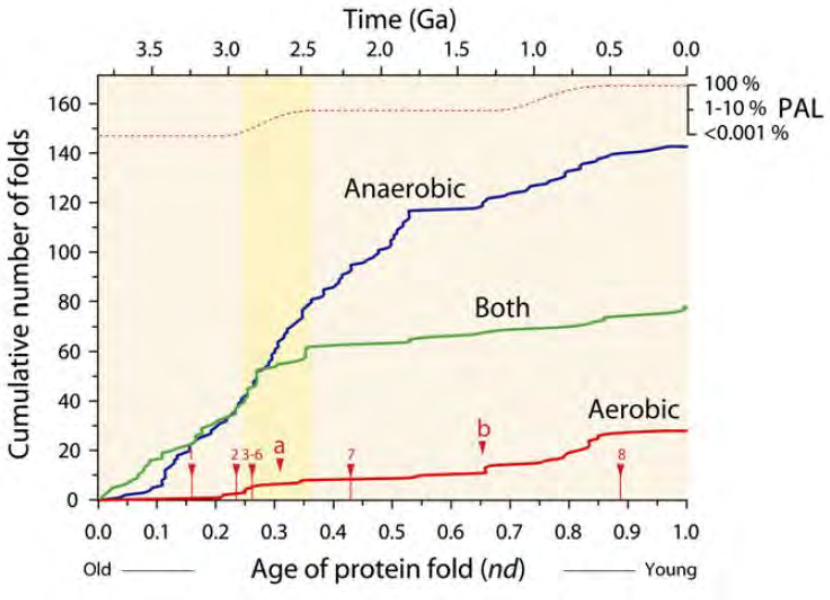

Figure 1.6. Accumulation of aerobic protein domains. (adapted from Wang et al., 2011).

1.1.3.3.3. Evolution of oxygen-related enzymes

Oxidosqualene cyclases (OSCs) are triterpene cyclases that catalyse the cyclisation of oxidosqualene, producing various sterols found in all eukaryotes (Desmond and Gribaldo, 2009). There are closely related enzymes, Squalene-hopene cyclases (SHCs), catalysing the same cyclisation of squalene forming diverse hopanoids, possible surrogates of sterols in bacteria (Kannenberg and Poralla, 1999). OSCs require oxygen to process the reactions, whereas SHCs do not. Phylogenetic study suggests that the bacterial SHC enzymes and eukaryotic OSCs have a common origin, and diverged much earlier than the cyanobacterial SHC group (Frickey and Kannenberg, 2009). This study is not consistent with the proposed evolution of eukaryotic sterol synthesis after oxygenic photosynthesis (e.g. Desmond and Gribaldo, 2009). The last eukaryotic common ancestor (LECA) would have had the ability to synthesise sterols. Thus, if the advent of the LECA coincides with the SHC/OSC divergence, the development of eukaryotes and oxygen-involved sterol synthesis precede that of cyanobacteria, indicating the presence of oxygen before oxygenic photosynthesis. In contrast, if the emergence of the LECA was triggered by the rise of oxygen along with the development of oxygenic photosynthesis, its timing was later than the divergence of SHCs and OSCs. In this case, sterols may have been produced before the development of oxygenic photosynthesis and LECA, or the substrate of ancient OSCs may not have been oxidosqualene, which implies that the products of ancient OSC catalysis may not have been sterols.

Another examples of oxygen-related enzymes are superoxide dismutases (SODs). Oxygen contributed to the diversification of life on Earth, but at the same time, oxygen can also be deleterious to life. Oxygen can be reduced to reactive oxygen species (ROS), such as singlet oxygen ($^1O_2$), and superoxide (O_2^-) in the course of aerobic metabolism and oxygenic photosynthesis. ROS can react with lipids, pigments and proteins to cause irreversible damage to a cell (for a review, see Imlay, 2003). Thus, organisms have had to evolve various defence mechanisms against the toxic effects of ROS.

ROS are removed by a series of enzymatic activity, in which SODs is most extensively studied. SODs catalyse the disproportionation of O_2^- into H_2O_2 and O_2. Four types of SOD have been identified based on the metal element used (Fe, Mn, Cu/Zn, and Ni). Fe-SOD is considered to be the most primitive form of SOD, which is consistent with the availability of Fe ions in the Archean ocean (Ilbert and Bonnefoy, 2013). The origin of SOD is probably earlier than the advent of cyanobacteria, and even earlier than the divergence of bacteria and archaea because most of the primitive bacteria have SODs.

In addition, dioxygen reductase (O_2Red) is a key enzyme for aerobic respiration. It is the last enzyme of the aerobic respiratory chains, and catalyses the reduction of O_2 to water (Wikstrom, 1977). O_2Red belongs to two protein superfamilies: the cytochrome *bd* (Cyt-*bd*) and the heme-copper O_2Red (HCO) superfamily. The HCO superfamily consists of three groups (A, B and C) based on the sequence similarity (Pereira et al., 2001). According to a recent study by Brochier-Armanet (2009), cyt-*bd* have a bacterial origin and were widely spread within bacteria and a few archaea. A-O_2Red are the most ancient of four O_2Red and likely emerged prior to the divergence of archaea and bacteria (Castresana et al., 1994; Castresana and Saraste, 1995; Brochier-Armanet et al., 2009), indicating their appearance before the advent of oxygenic photosynthesis in cyanobacteria.

1.1.4. Evidence for oxygenic photosynthesis before the GOE

The evidence for oxygenic photosynthesis is necessarily the evidence for the presence of cyanobacteria, or the evidence for the presence of eukaryotes, because eukaryotic metabolisms are largely based on oxygen which requires oxygenated environments and ultimately oxygenic photosynthesis as a source of oxygen. The evidence for cyanobacteria in the ancient geological record has been indicated by (1) stromatolites, (2) microfossils, (3) carbon isotope ratios consistent with Rubisco enzyme, a key enzyme in Calvin-Benson cycle, (4) biomarkers for cyanobacteria, and (5) genome studies of cyanobacteria (for a review, see Schopf et al., 2007; Schopf, 2012; Hallmann and Summons, 2014; Summons and Hallmann, 2014). Eukaryotes can also be suggested by microfossils,

carbon isotopic data, and genomic analyses. The proposed evidence is highly controversial and a general consensus is still not formed.

1.1.4.1. Stromatolites

Stromatolites are microbially mediated finely laminated rock structures composed of typically carbonate minerals (e.g. $CaCO_3$). The term was initially coined by (Kalkowsky, 1908). There are several examples of modern living stromatolites, for example the Shark Bay in Western Australia (Allen et al., 2009; Garby et al., 2013), and the Highborne Cay in Bahamas (Baumgartner et al., 2009; Foster et al., 2009). However, the presence of stromatolites is limited to restricted areas such as hot springs and hypersaline lagoons, because the slow-growing microbial mats can easily be disturbed by grazing or burrowing metazoans. In contrast, stromatolite-like laminar structures are abundant in the Precambrian, probably due to the lack of disturbing metazoans. In modern stromatolites, cyanobacteria are major contributors to the development of these lithified structures. By analogy, many ancient stromatolites are typically assumed to be produced by cyanobacteria as well, although the action of other microbes is well known and some stromatolites or other microbially-induced sedimentary structures are formed by non-cyanobacterial communities.

Well described examples of Archean stromatolites include: the 2.7 Ga Fortescue Group in Western Australia, with domical, pseudocolumnar and branching stromatolites; the 3.0 Ga Insuzi Group of South Africa, with stratiform and conical stromatolites; and the 3.4 Ga Strelly Pool Chert Formation and the 3.5 Ga Dresser Formation of Western Australia, which contain domical, stratiform and close-packed conical stromatolites (Walter, 1983; Allwood et al., 2006; Schopf et al., 2007; Van Kranendonk et al., 2008; Schopf, 2012). There is no guarantee that these ancient stromatolites were built by cyanobacteria. The primary producer could have been anaerobic anoxygenic photosynthetic bacteria. Furthermore, abiological production of stromatolite-like morphologies has been proposed (e.g. Grotzinger and Rothman, 1996), which renders the interpretation of ancient stromatolites difficult. However, macroscale microbial morphology studies have been used to argue that the

presence of conical stromatolites (*Conophyton*) at 2.7 Ga in the Fortescue Group in the Pilbara region, Western Australia can be a sign of oxygenic photosynthesis, by comparing these rocks with modern analogues at Shark Bay in Western Australia (Bosak et al., 2009; Flannery and Walter, 2012; Flannery, 2013).

Currently, the evolution of cyanobacteria at some point before the GOE around 3.0-2.5 Ga has gradually gained support (e.g. Van Kranendonk, 2014), but an oxygenated Earth before 3.0 Ga is contentious (e.g. Hoashi et al., 2009).

1.1.4.2. Microfossils

Cyanobacterial fossil records are abundant in the Precambrian, and include both unicellular and multicelluar (filamentous) morphologies (Schopf, 2002, 2012). Cyanobacteria generally have larger cell sizes and more complex morphologies compared to other bacteria and archaea because they need as large as possible a surface area to maximise light absorption. Extracellular sheaths and envelopes, composed of carbohydrates, are relatively recalcitrant to degradation and are preserved among various components in cyanobacteria. Cell walls are less common. The peptidoglycan-containing (cell wall forming polymer composed of sugars and amino acids) thick lateral walls are better preserved than the thinner peptidoglycan-deficient transverse walls (Schopf, 2012).

The microfossils of filamentous cyanobacteria are mainly limited to after the GOE, corresponding to the suggested diversification of multicellularity at the GOE (Schirrmeister et al., 2013). This observation is also consistent with the property of heterocysts that are characteristic of multicellular cyanobacteria to protect nitrogenase enzymes for N_2 fixation from oxygenated environments. However, some microfossils of multicellular cyanobacteria predate the GOE, and their authenticity has long been debated (Schopf, 1993; Schopf, 2002; Brasier et al., 2006).

The oldest unambiguous cyanobacterial microfossils have been found in the Kasegalik and McLeary formations of the Belcher Subgroup in Canada at 2.1 Ga (Hofmann, 1976). Both unicellular and

multicellular cyanobacteria are also found in 2.0 Ga stromatolites of the Franceville Group in Gabon (Amard and Bertrand-Sarfati, 1997). There are several reports of pre-GOE microfossils (e.g. Walsh, 1992; Kazmierczak and Altermann, 2002; Tice and Lowe, 2004; Schopf, 2006), and some of them argue for the presence of cyanobacteria back to 3.5 Ga by their filamentous morphologies (Schopf and Packer, 1987; Schopf, 1993; Altermann and Kazmierczak, 2003; Schopf et al., 2007).

However, microfossils of non-photosynthetic filamentous microorganisms at 3.2 Ga have been found in a massive sulphide deposit from the Pilbara Craton in Australia, and this suggests that the filamentous morphology alone cannot be interpreted as photosynthetic filamentous cyanobacteria (Rasmussen, 2000). Furthermore, it has been suggested that a microfossil-like structure can be abiotically formed by amorphous graphite within metalliferous hydrothermal vein chert and volcanic glass (Brasier et al., 2002; García-Ruiz et al., 2003; Brasier et al., 2006). However, the Raman spectroscopy measurements of Archean microfossil-like specimens revealed that they are composed of carbonaceous kerogen, indicating the biogenicity (Schopf et al., 2002). Both microfossil and stromatolite evidence have the same problems regarding being able to distinguish them from similar but abiotic morphologies. Another problem with microfossils is proving that they are derived from cyanobacteria, and not from other microorganisms.

1.1.4.3. Carbon isotope ratios

The carbon isotope ratios ($\delta^{13}C$) of sedimentary rocks in the Precambrian have values around -30 ‰ for organic carbon, a similar value to the modern RuBisCO metabolism, characteristic of biological CO_2 fixation via photosynthesis (O'Leary, 1988; Des Marais, 2001; Schidlowski, 2001), whereas it is approximately 0 ‰ for carbonate carbon. The isotopic depletion of organic carbon in the 3.4 Ga Strelley Pool Formation and the 3.5 Ga Dresser Formation in Western Australia has been used to indicate the presence of photoautotrophy and possibly cyanobacteria in the Paleoarchean (Hayes et al., 1983; House et al., 2003).

However, it cannot be resolved whether the carbon fixation was photosynthetic or not, because other fixation pathways can also explain the difference. Chemoautotrophic organisms such as methanogens and anoxygenic phototrophs can also produce similar fractionations (Schidlowski, 1983). Also, abiological carbon isotope fractionation of a similar magnitude is possible (McCollom and Seewald, 2006). As discussed in section 1.1.3.2.4, a wide range of ^{13}C depletion in the 2.7 Ga Tumbiana Formation, Western Australia may reflect the presence of a shallow-water phototrophic ecosystem, possibly dominated by cyanobacteria, and a deep-water methanotrophic ecosystem (Eigenbrode and Freeman, 2006), but the evidence for cyanobacteria used in the study is now contested (French et al., 2013).

1.1.4.4. Biomarkers

The presence of cyanobacteria and oxygenic photosynthesis can be tracked by their chemical fossils, especially diagnostic biomarkers for cyanobacteria and eukaryotes. Since the first report of the pre-GOE biomarkers (Brocks et al., 1999), there has been several studies suggesting the presence of oxygenic photosynthesis at 2.7-2.8 Ga, well before the GOE (Brocks et al., 2003a; Ventura et al., 2007; Eigenbrode et al., 2008; Waldbauer et al., 2009; Coffey, 2011). However, these findings are now debated (Rasmussen et al., 2008; Brocks, 2011) (see Section 1.2.2 and Chapter 2). Also, one of the originally proposed cyanobacterial biomarker (2α-methyhopane; Summons et al., 1999) is now known to be produced by several other bacterial taxa which do not produce oxygen (Rashby et al., 2007; Ricci et al., 2013). A more sophisticated method to analyse ancient biomarkers has been developed by slicing rock samples and checking the biomarker concentration gradients (Sherman et al., 2007; Coffey, 2011) (see Chapter 2). Also, another group of cyanobacterial biomarkers (mid-chain branched monomethylalkanes) are now sought for additional biomarker evidence (Shiea et al., 1990; Thiel et al., 1999).

1.1.4.5. Multicellularity of cyanobacteria

Genomic studies of cyanobacteria suggest that the diversification of cyanobacterial multicellularity corresponded to the timing of the GOE, which in turn implies the earlier evolution of cyanobacteria

with unicellularity before the GOE (Tomitani et al., 2006; Schirrmeister et al., 2011; Schirrmeister et al., 2013). A molecular clock calculation suggests the initial appearance of cyanobacteria back to 3.0 Ga (Schirrmeister et al., 2013), which coincides with some geochemical results which suggest the presence of oxygen around the same time (e.g. Crowe et al., 2013). Also, the most ancient cyanobacterium (*G. violaceus*) is known to produce C-2 methylated hopanoids and mid-chain branched monomethylalkanes. Thus, if the discovered biomarkers before the GOE are syngenetic, they may be the remains of simple cyanobacteria with unicellularity.

As already discussed in Section 1.1.3.3, other phylogenomic studies also indicate the appearance of cyanobacteria around 3.0-2.9 Ga (David and Alm, 2011; Wang et al., 2011; Kim et al., 2012). Further, the diversification of aerobic genes before the GOE may also be associated with the earlier emergence of cyanobacteria and oxygenic photosynthesis (David and Alm, 2011).

1.1.4.6. Gap between the GOE and earlier evolution of oxygenic photosynthesis

The earlier evolution of cyanobacteria and oxygenic photosynthesis lead to the need for an explanation of why the concentration of oxygen was suppressed until the onset of the GOE. It is assumed that the source-sink balance of oxygen gradually shifted towards oxygen accumulation and eventually triggered the GOE (Kasting, 2013; Lyons et al., 2014). There are both non-biological and biological mechanisms that can be used to explain the delay of oxygen accumulation. Non-biological mechanisms include changes in the ratio of C and S relative to H in volcanic gases with Earth's maturation (Holland, 2002, 2009), hydrogen escape to space and the concomitant oxidation of continents (Catling et al., 2001; Claire et al., 2006), a switch from submarine to subaerial outgassing with the shift to more oxidised gases (Kump and Barley, 2007; Gaillard et al., 2011), oxidation of ferrous iron depositing BIFs (Cloud, 1973; Isley and Abbott, 1999), and changes in volcanic gassing rates (Van Kranendonk, 2014). Biological mechanisms consist of depletion of Ni leading to a decrease of methanogenesis and subsequently an increase of oxygen (Konhauser, 2009), increased availability of Mo and V enhancing primary productivity (Zerkle et al., 2006; Scott et al., 2011), and changes in

the rate of serpentisation of seafloor by the evolution of nitrogenase protection in cyanobacteria (Kasting and Canfield, 2012). There is no consensus which factor was dominant.

1.2. Biomarkers

1.2.1. Usefulness of biomarker research

Biomarkers are organic molecules preserved within sedimentary rocks that indicate the presence of particular types of organisms or metabolisms at the time of deposition (for a review, see Brocks and Summons, 2003; Brocks and Pearson, 2005; Peters et al., 2005). Biomarkers can mean either functionalised original biomolecules produced by host organisms preserved in modern or recent sediments, or molecular fossils reduced to hydrocarbon skeletons via thermal alteration in ancient sedimentary rocks. Original biomolecules include carbohydrates, lipids, proteins, amino acids, and DNA. Most compounds are readily biologically degraded and thermally unstable so that they rarely remain unchanged over geological time (Briggs and Summons, 2014). However, hydrocarbon skeletons of some compounds such as lipids are highly recalcitrant, and can remain intact for hundreds of millions of years. Historically, biomarkers have been utilised in the petroleum industry to estimate the thermal history and age of reservoired oil, and to correlate crude oil with potential source rocks (Brocks and Grice, 2011). More recently, biomarkers have gained attention in geobiology for understanding past ecosystems (e.g. Hinrichs et al., 1999; Summons et al., 1999) and as paleoenvironmental proxies (e.g. Schouten et al., 2002).

Biomarkers with resistant hydrocarbon skeletons are generated from deposited organic matter through biological and chemical reactions during diagenesis. Firstly, most organic carbon is digested and/or metabolised, and further subject to biodegradation, and recycled back to carbon dioxide and water, and only 0.1 % of organic matter is incorporated into sediments (Holser et al., 1988). Then, an array of subsequent chemical processes including recondensation, polymerisation and sulphurisation form an amorphous macromolecular aggregate called kerogen, which is highly resistant to further degradation and chemical weathering (Tissot and Welte, 1984). Later, thermal alteration (60-150 °C)

of kerogen leads to the cracking of chemical bonds which releases small fragments, the solvent-soluble organic matter sometimes called bitumen or extractable organic matter (EOM) (Koopmans et al., 1996). EOM is composed of aliphatic and aromatic hydrocarbons including biomarkers, and polar compounds (Mycke et al., 1987). At higher temperatures, biomarkers and other hydrocarbons undergo thermal isomerisation and epimerisation, and their composition provides information on the thermal history of the sample (thermal maturity parameters) (Peters et al., 2005).

1.2.2. Biomarkers in the Archean

Presently, the oldest certainly indigenous biomarkers come from the 1.64 Ga Barney Creek Formation of the McArthur Basin in northern Australia (Summons et al., 1988; Brocks et al., 2005). Proposed biomarker evidence before 1.8 Ga is highly controversial because of the general lack of preservation of older rocks, and the common high burial metamorphism that older rocks have been exposed to. All known sedimentary rocks older than 1.8 Ga have experienced metamorphism of at least zeolite to prehnite-pumpellyite facies, at temperatures of 175-280 °C. At such temperatures, bitumen is largely cracked to gas and is expelled from rocks. However, the existence of biomarkers at >200 °C has been reported (Price, 1993; Price, 2000; Price and DeWitt, 2001). Also, a kinetic model study of petroleum degradation suggests the persistence of hydrocarbons to 250 °C (Pepper and Dodd, 1995; Dominé et al., 2002). Thus, it is possible that ancient sedimentary rocks still preserve intact molecular fossils.

Biomarkers including hopanes and steranes have been found in fluid inclusions in the Paleoproterozoic 2.45 Ga fluvial metaconglomerate of the Matinenda Formation, Canada (Dutkiewicz et al., 2006; George et al., 2008). The oldest biomarker reports are from the 2.7 Ga Fortescue Group in Western Australia (Brocks et al., 1999; Brocks et al., 2003a). Several additional lines of evidence for Archean biomarkers have been found in the Pilbara region (Eigenbrode et al., 2008; Coffey, 2011), the 2.7 Ga metasedimentary rocks from Timmins, Canada (Ventura et al., 2007), and also in the Transvaal Supergroup in South Africa, which is another site containing only slightly metamorphosed

Archean crust (Waldbauer et al., 2009). If proven by further work, these discovered biomarkers suggest the presence of cyanobacteria and eukaryotes, and ultimately oxygenic photosynthesis well before the GOE at 2.4-2.3 Ga. However, some researchers have rebutted the evidence for pre-GOE biomarkers, by demonstrating that in some cases these biomarkers are contaminants (Rasmussen et al., 2008; Brocks, 2011). Therefore, a more comprehensive and detailed examination is crucial.

1.2.3. Biomarkers for cyanobacteria and eukaryotes

Biomarkers for cyanobacteria are mid-chain branched monomethylalkanes (MMAs) and 2α-methylhopanes. Biomarkers for eukaryotes are steranes (Brocks and Summons, 2003). Hopanes are diagenetically altered compounds from hopanoids, a group of squalene-derived lipid components mainly found in bacteria. 2α-methylhopanes are derived from hopanoids with a methyl group attached to the C-2 position. Steranes are diagenetically altered compounds from sterols, a diverse group of oxidosqualene-derived lipid components, almost only found in eukaryotes. Currently, high abundance of mid-chain branched MMAs is attributed to cyanobacteria, although small amount of mid-chain branched MMAs can also be produced by thermal rearrangement reactions (see Section 1.2.5.4). In contrast, biological sources of 2α-methylhopanes include not only cyanobacteria, but also several genera of proteobacteria and actinobacteria (see Section 1.2.4.4). Thus, 2α-methylhopanes cannot be used as sole evidence for cyanobacteria, but combined with the presence of mid-chain branched MMAs, 2α-methylhopanes may be used to constrain the more specific taxa within the cyanobacterial clade. Hopanoids and sterols are closely related to each other in terms of their function and evolutionary history, thus are discussed together in the following sections.

1.2.4. Hopanoids and sterols

1.2.4.1. Hopanoids and sterols in cell membranes

It is critical for cells to maintain the integrity of cell membranes. Membranes are permeability barrier to solutes, and are responsible for the maintenance of cell integrity and signal transduction. The responses of a cell to outside stress are changes in protein, sterol, hopanoid, and carotenoid content, as well as changes in membrane lipid composition (de Carvalho and Fernandes, 2010).

Sterols are the major non-polar lipids of cell membranes and play an important role in the physiology and biochemistry of all eukaryotes. They control the fluidity and permeability of the cells, forming a liquid-order phase (Simons and Ikonen, 1997; van Meer et al., 2008). Sterols are also involved in membrane-related metabolic processes, and are the precursors for a wide array of metabolites, such as antibiotics and hormones (e.g. Siedenburg and Jendrossek, 2011). Sterols further participate in the formation of lipid rafts, which form platforms that function in signal transduction in higher organisms (Hancock, 2006).

Hopanoids are primarily found in bacteria as cytoplasm membrane components, and relatively common in cyanobacteria, α-, β-, and γ-proteobacteria including methanotrophic bacteria and nitrogen-fixing bacteria, and ammonium-oxidising (anammox) planctomycetales (Kannenberg and Poralla, 1999; Talbot et al., 2008). Their structural similarity to sterols led to the hypothesis that hopanoids are bacterial surrogates of sterols in eukaryotes (Ourisson et al., 1987). Although there are numerous studies about sterol functions (e.g. van Meer et al., 2008; Lingwood and Simons, 2010), those of hopanoids in bacterial membranes are poorly investigated. A few studies suggest that hopanoids have similar functions to steroids but are probably less effective (Sáenz et al., 2012; Poger and Mark, 2013).

1.2.4.2. Biosynthesis of hopanoids and sterols

Both hopanoids and sterols are triterpenoids, a large class of natural compounds built of C_5 isoprenyl units that occur in almost all organisms on Earth (Mahato et al., 1992). Hopanoids are pentacyclic, and sterols are tetracyclic with a hydroxyl group derived from the epoxy group of oxidosqualene. Hopanoids are synthesised from C_{30} squalene by squalene-hopene cyclase (SHC), whereas sterols are produced from oxidosqualene by oxidosqualene cyclase (OSC) (Fig. 1.7). Oxidosqualene is derived from squalene by squalene monooxygenase, which requires oxygen for its synthesis. Thus, the presence of sterols indicates oxic conditions. Hopanoid synthesis involves the formation of 5 ring structures, 13 covalent bonds, and 9 stereocenters in one reaction, which is the most complex one-

step enzymatic reaction in biochemistry (Xu et al., 2004; Siedenburg and Jendrossek, 2011). Sterol synthesis is similarly complex, and generates lanosterol, a precursor to ergosterol in fungi, and cholesterol in animals, or cycloartenol in plants.

SHCs and OSCs are distantly related in amino acid sequences, forming two distinctive groups: a bacterial clade (SHCs) and a eukaryotic clade (OSCs) (Figs 1.7 and 1.8, Frickey and Kannenberg, 2009; Racolta et al., 2012). Although hopanoid distribution is limited to only about 10 % of the entire bacterial domain (Pearson et al., 2007; Pearson et al., 2009), SHCs are widespread in a variety of bacterial clades. As already discussed in Section 1.1.3.3.3, SHCs and OSCs probably share a common ancestor (Frickey and Kannenberg, 2009).

Previously, hopanoids were only found in aerobic bacteria and thought to be biomarkers for oxic environments (Rohmer et al., 1984). However, the biosynthesis of hopanoids in anaerobes has been reported, including in some facultative anaerobes (Neunlist et al., 1985; Neunlist et al., 1988; Llopiz et al., 1992), fermentative anaerobic bacteria (Renoux and Rohmer, 1985), obligate anaerobic ammonium-oxidising (anammox) planctomycetes (Sinninghe-Damsté et al., 2004), and some sulphate-reducing bacteria (Fischer et al., 2005; Härtner et al., 2005; Blumenberg et al., 2006; Eickhoff et al., 2013). These observations show the occurrence of hopanoids not only in aerobic conditions, but also in anaerobic conditions (Thiel et al., 2003).

Some eukaryotes such as plants, mosses, fungi and ciliates can produce hopanoids. Some of them are produced by OSCs using oxidosqualenes, unlike bacteria. Others are produced by SHCs, although these SHCs are apparently obtained by horizontal gene transfers (HGTs) from bacteria, and the amount is usually low (Ourisson et al., 1987). There are also a few bacteria known to contain sterols, including γ-proteobacteria, δ-proteobacteria (myxobacteria), and the planctomycete (Bird et al., 1971; Bouvier et al., 1976; Kohl et al., 1983; Bode et al., 2003; Pearson et al., 2003). These sterols are produced by OSC homologs which are grouped within eukaryotic OSC clade, indicating HGTs from eukaryotes (Pearson et al., 2003; Desmond and Gribaldo, 2009; Frickey and Kannenberg, 2009). In

addition, the sterols produced by these bacteria do not have any extended side chain (Pearson et al., 2003).

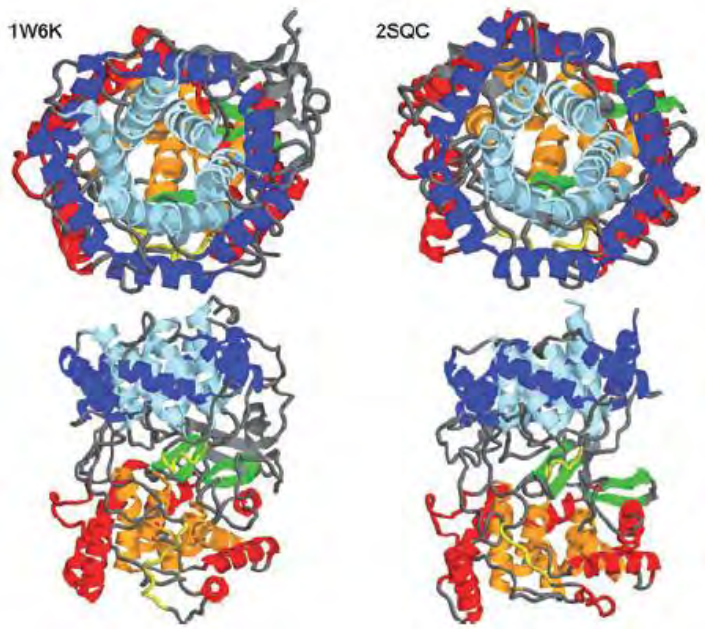

Figure 1.7. Structures of oxidosqualene cyclase (OSC; left) and squalene-hopene cyclase (SHC; right). Top view towards the catalytic cavity (upper part) and side view (lower part). In side view, domain 1 (upper part) and domain 2 (lower part) (adapted from Frickey and Kannenberg, 2009).

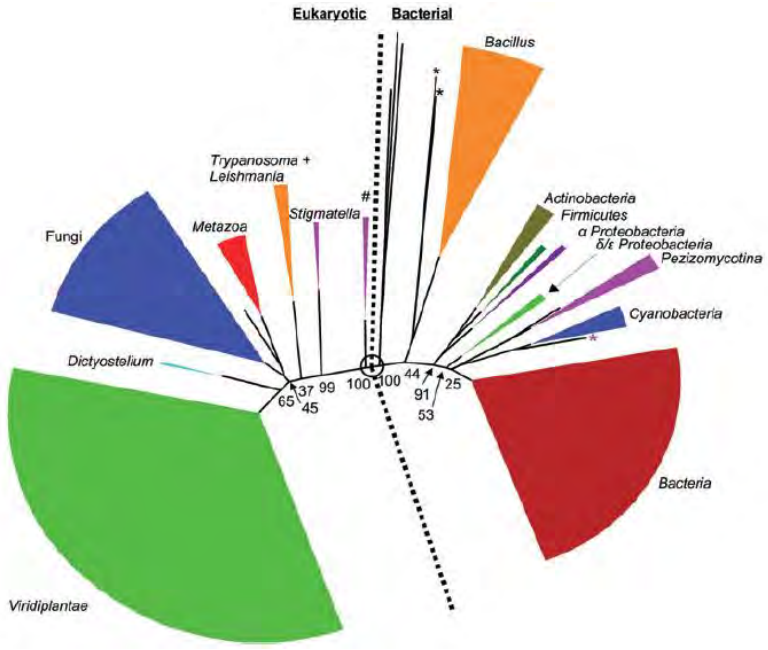

Figure 1.8. Phylogenetic tree of the protein family of triterpene cyclases (adapted from Frickey and Kannenberg, 2009).

1.2.4.3. Diversity of hopanoids

There are numerous types of hopanoids produced by bacteria and some eukaryotes depending on the species and inhabiting environments (e.g. Talbot et al., 2008). The varying characteristics of hopanoids are the basic C_{30} pentacyclic structure (Fig. 1.9), the C_5 extended side chain with several functional groups, diastereomers at C-22, the methylation of the hopanoid A-ring (C-2α/β, C-3β), double bond(s) on the A-D rings, and the formation of composite hopanoids with an additional moiety that is linked to the C-35 terminal functional group. The side chain functions as a head group, and the pentacyclic structure works as hydrophobic moiety in a lipid membrane.

Diploptene (I) and diplopterol (II) are two principal C_{30} basic hopanoids that are quite common in bacteria (Fig. 1.9, Talbot et al., 2008). C_{35} bacteriohopanepolyols (BHPs) are hopanoids having a C_5 side chain with several hydroxyl group derived from D-ribose moiety of S-adenosyl-methionine (SAM) (Flesch and Rohmer, 1988; Bradley et al., 2010), such as 30,32,33,34,35-bacteriohopanepentol (IIIa). Due to this synthesis mechanism, the carbon number of an extended side chain is always only five. An additional moiety connected to the side chain varies. Cyanobacteria have some unique hopanoids, including BHT cyclitol ether (IIIb), 35-O-β-amino-deoxyglucopyranosyl-bacteriohopanetetrol (IIIc), 35-O-β-3,5-anhydro-galacturonopyranosyl-bacteriohopanetetrols (IIId), 35-O-β–galacturonosyl-bacteriohopanetetrol (IIIe), and 35-O-α-altruronopyranosylacterio-hopanetetrol (IIIf) (Fig. 1.9, Talbot et al., 2008). These hopanoids are sometimes further methylated at the C-2 position (see next section).

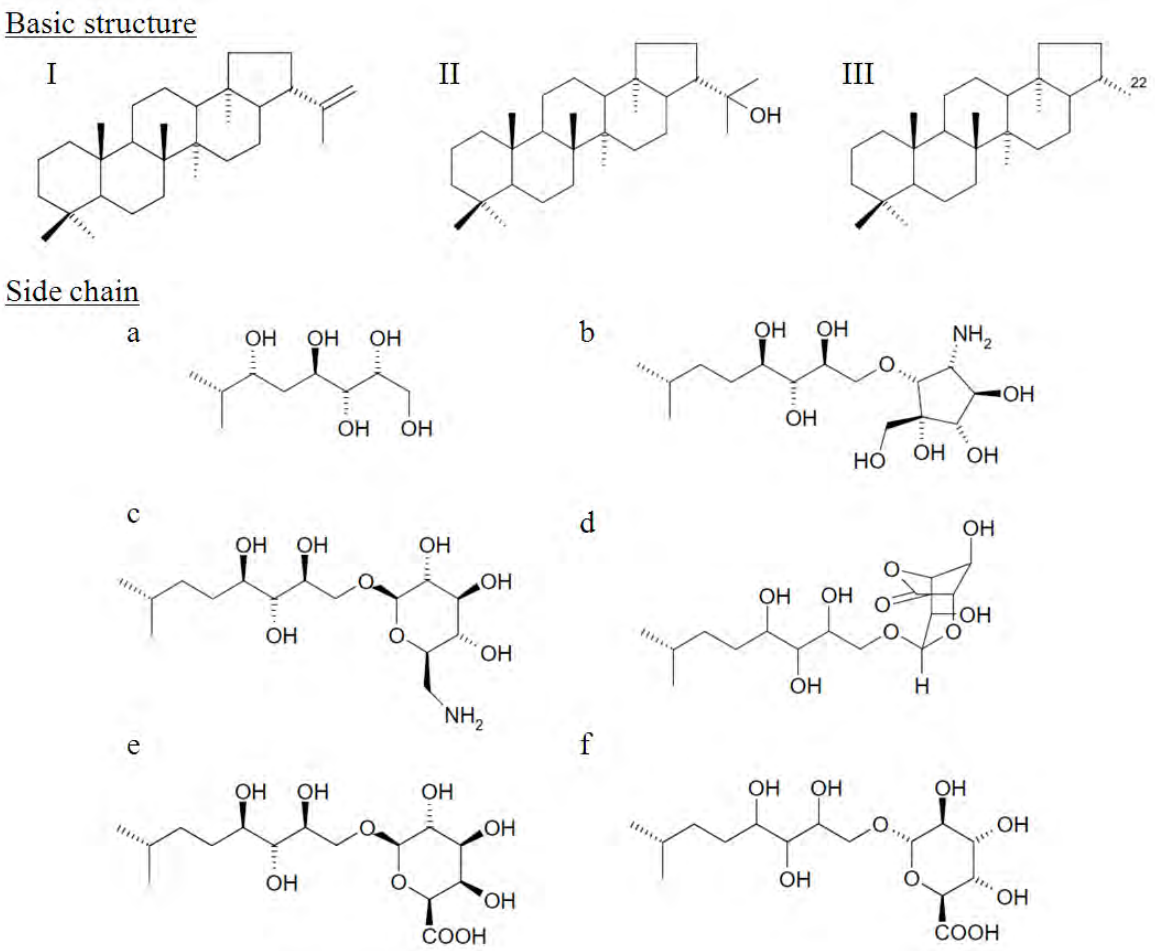

Figure 1.9. Structures of hopanoids.

1.2.4.4. C-2 and C-3 methylated hopanoids

Methylation at the C-2 and C-3 positions of the A-ring has been paid particularly attention as specific biomarkers to certain types of organisms. C-2 methylated BHPs (Fig. 1.10) are commonly found in cyanobacteria (Rohmer et al., 1984; Summons et al., 1999; Talbot et al., 2008). The diagenetic rearrangement compounds of C-2 methylated BHPs, 2α-methylhopanes, were once thought to be specific biomarkers for cyanobacteria (Brocks et al., 1999; Summons et al., 1999). However, it has now been shown that various proteobacteria (Bisseret et al., 1985; Zundel and Rohmer, 1985b; Vilcheze et al., 1994; Bravo et al., 2001; Rashby et al., 2007), purple non-sulphur bacteria (Welander et al., 2010), and acidobacteria (Welander et al., 2010) can produce C-2 methylated hopanoids. It is now also clear that not all cyanobacteria (only 19 % of all sequenced cyanobacterial genera) possess

the gene *hpnP* which encodes the enzyme responsible for methylating hopanoids at the C-2 position (Welander et al., 2010; Ricci et al., 2013). Thus, 2α-methylhopanes cannot be solely used to indicate the presence of cyanobacteria. However, accompanied with other evidence, it might be able to use 2α-methylhopanes to constrain the types of cyanobacteria. So far, no cultured modern marine cyanobacteria are known to synthesise 2-methylhopanoids; 2-methylhopanoid-producing cyanobacteria are all from freshwater or soil environments (Talbot et al., 2008; Sáenz et al., 2011).

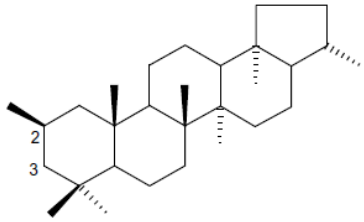

Figure 1.10. C-2 methylated hopanoid.

C-3 methylation was first reported in acetic acid bacteria (Rohmer and Ourisson, 1976), and in aerobic methanotrophs (Zundel and Rohmer, 1985a, b). 3β-Methylhopanes, diagenetic products of C-3 methylated BHPs, are generally regarded as biomarkers for methanotrophs, with characteristically depleted carbon isotope ratios (Summons et al., 1994; Jahnke et al., 1999). However, a recently published taxonomic distribution of the gene *hpnR* encoding C-3 methylation shows that they are widely distributed among various taxa, although they are limited to bacteria with an aerobic metabolism (Welander and Summons, 2012). Thus, 3β-methylhopanes cannot be indicators for methanotrophy without supporting evidence of carbon isotopic data, but they can still indicate aerobic respiration. The enzymes HpnP and HpnR are both radical S-adenosylmethionine (SAM) domain proteins (Eickhoff et al., 2013).

1.2.4.5. Diversity of sterols

Most eukaryotes (animals, fungi, land plants, and many protists) can produce various types of sterols (Peters et al., 2005; Volkman, 2005) (Fig. 1.11). Cyclisation of C_{30} oxidosqualene produces lanosterol or cycloarterol. These compounds are further modified by various enzymatic activities. Lanosterol is

converted to zymosterol, which eventually forms either C_{28} ergosterol or C_{27} cholesterol. On the other hand, cycloarterol is transformed to 24-methylenelophenol, and further to C_{28} campesterol or C_{29} stigmasterol (Desmond and Gribaldo, 2009). Animals form cholesterol as the final product, fungi synthesise ergosterol, and land plants generate a mixture of phytosterols, including C_{29} β-sitosterol, stigmasterol and campesterol, as the major representatives. Microalgae (microphytes) generate a wide range of sterols depending on the class, family, genus and species. They typically carry an ethyl group at C-24 and unusual desaturations at various positions (Volkman, 2003).

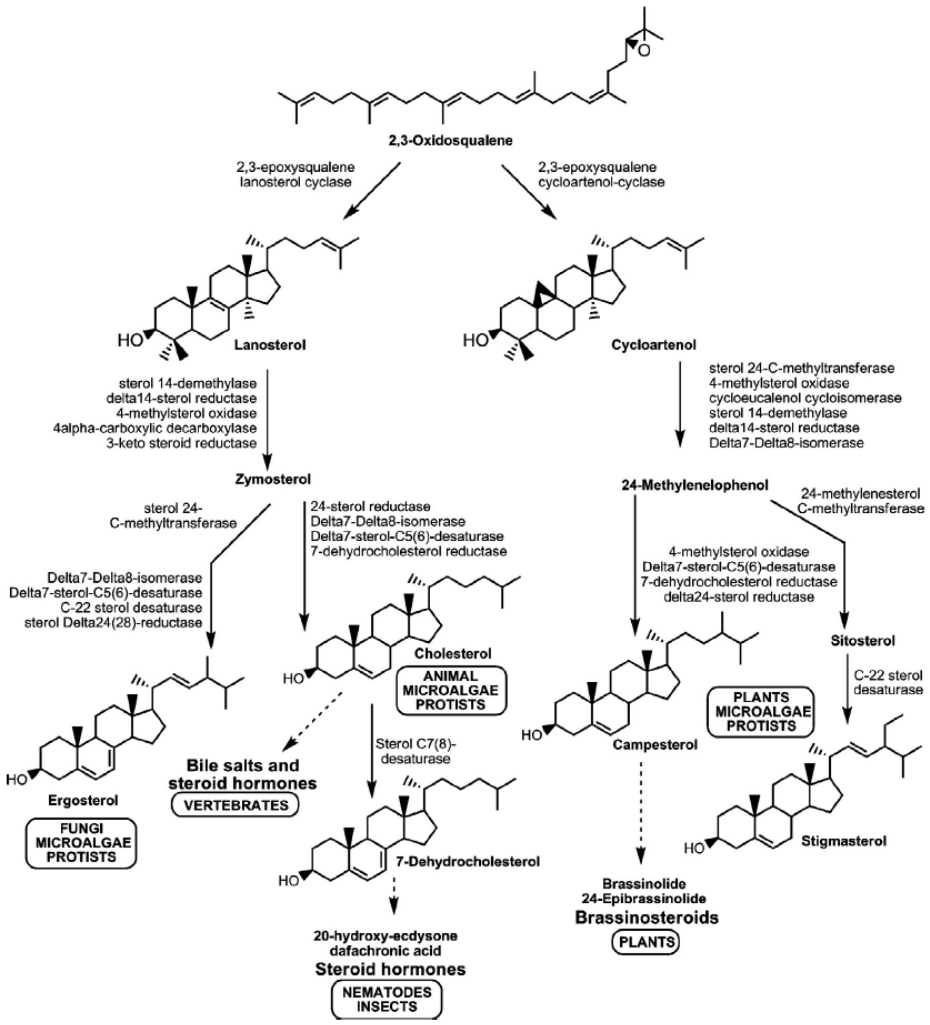

Figure 1.11. Structures of sterols (adapted from Tomazic et al., 2014).

1.2.4.6. Diagenesis of hopanoids and sterols

The polycyclic ring structure of hopanoids and sterols is highly recalcitrant to degradation. Diagenetic hopanoid products (geohopanoids) have been described as the "most abundant natural products on Earth" (Ourisson and Albrecht, 1992). Although there is a wide array of hopanoids and sterols with various functional groups, these functional groups are removed through diagenesis by dehydration and reduction, leaving only hydrocarbon skeletons (hopanes and steranes).

Rearrangement and/or removal of methyl groups on the hopane ring structure generates various kinds of hopanes such as C_{29} norneohopane, C_{28} bisnorhopane, C_{27} trisnorhopane and C_{29}/C_{30} diahopane, in addition to the original C_{30} hopane. These compounds have several stereoisomers by C-H bond directions (α/β), and by stereocentres (R/S) such as 17α(H),21β(H)-hopane and 17β(H),21α(H)-hopane. The side chain of C_{35} BHPs may lose carbons from the side chain, producing a C_{30}-C_{35} homologous series of hopanes (homohopanes). The methyl group at the C-2 or C-3 is generally retained and can be diagnostic for methylhopanoid-producing organisms. Steranes also undergo similar transformation, leading to the production of C_{27}-C_{30} diasteranes as well as C_{27}-C_{30} steranes. Although most eukaryotic taxonomical information is lost during diagenesis, steranes and diasteranes can still indicate the presence of eukaryotes and oxic environments.

1.2.5. Mid-chain branched monomethylalkanes (MMAs)

1.2.5.1. Geological occurrence of mid-chain branched MMAs

MMAs have been identified in various sediments and crude oils from modern environments to the Precambrian. Especially, mid-chain branched MMAs are considered to be characteristic constituents of cyanobacterial lipids and biomarkers for cyanobacteria (Han et al., 1968; Gelpi et al., 1970; Han and Calvin, 1970; Shiea et al., 1990; Summons and Walter, 1990; Shiea et al., 1991; Köster et al., 1999; Thiel et al., 1999; Dembitsky et al., 2001). Mid-chain branched MMAs occur in about two thirds of the cyanobacterial species examined so far, and cyanobacteria are the only microorganisms known to produce them (Shiea et al., 1990). In pure-cultured cyanobacteria, the biosynthesis of mid-chain branched MMAs is mainly limited to 7-methylheptadecanes (7-MHeD), but some cyanobacteria

produce other isomers / homologues in the C_{16}-C_{21} range, with one report suggests homologues up to C_{28} (Paoletti et al., 1976), depending on the species and the culture conditions (Shiea et al., 1990). Some dimethylalkanes (e.g. 7,11-dimethylalkane) and trimethylalkanes have also been used as evidence for cyanobacteria (Köster et al., 1999; Lu et al., 2003), although their occurrence in a wide range of cyanobacteria has not yet been examined as for MMAs. Similarly, the origin of > C_{21} long-chain MMAs in geological samples is still poorly understood, although these are generally considered to not originate from cyanobacteria. Proposed sources of long-chain MMAs include insects, leaf waxes, freshwater algae, heterotrophic bacteria, and sulphide-oxidising bacteria (Lu et al., 2003).

The assignment of MMAs observed in geological samples as having a cyanobacterial origin is not straightforward. There are several reports that geological samples of Holocene to Tertiary age contain a limited distribution pattern of MMAs that is similar to that observed in modern cyanobacteria (Robinson and Eglinton, 1990; Kenig et al., 1995; Thiel et al., 1999). The high abundance of mid-chain branched MMAs relative to other isomers in fluid inclusion oils from the Jurassic was suggested to be of cyanobacterial origin (George et al., 2002). There are many examples of further ancient MMAs into the Precambrian era (Makushina et al., 1978; Klomp, 1986b; Fowler and Douglas, 1987; Summons, 1987; Summons et al., 1988; Warton et al., 1997; Höld et al., 1999; Brocks et al., 2003b). Elevated concentrations of MMAs relative to *n*-alkanes are frequently present in Proterozoic and lower Paleozoic sediments, for example in the early Cambrian Chandler Formation in the Amadeus basin in Australia (Summons, 1987), in the terminal Proterozoic to Cambrian Huqf Formation of Oman (Klomp, 1986b), in Neoproterozoic oils from eastern Siberia (Fowler and Douglas, 1987), in bitumens from the Mesoproterozoic McArthur basin in Australia (Summons et al., 1988), in Paleoproterozoic fluid inclusions from the Matinenda Formation in Australia (George et al., 2008) and even in Archaean sediments from the Tumbiana Formation in Australia (Brocks et al., 2003b).

However, these geological samples have a homogeneous distribution of MMA isomers, unlike the heterogeneous distribution of modern cyanobacterial origin. Some geological examples show

confined distributions, but they do not match any modern examples (Makushina et al., 1978; Fowler and Douglas, 1987; Höld et al., 1999). Furthermore, the C_{17} *n*-alkane is commonly of similar relative abundance as other *n*-alkanes in these geological samples, whereas the C_{17} *n*-alkane is usually the dominant *n*-alkane in cyanobacterial mats. The C_{17} *n*-alkane may have been subject to selective biodegradation or rearrangement. A selective decrease of *n*-alkanes relative to MMAs was reported from Holocene cyanobacterial mats (Kenig et al., 1995), and preferential biodegradation of all *n*-alkanes is well known (Wenger et al., 2002).

1.2.5.2. Biosynthesis of hydrocarbons by cyanobacteria

All cyanobacteria possess the pathway to synthesise long-chain hydrocarbons from fatty acids (Coates et al., 2014). However, the role of hydrocarbons in cyanobacteria is as yet poorly understood. Although various possibilities exist including prevention of grazing from herbivores, chemical signalling, prevention of desiccation, enhanced buoyancy, or membrane fluidity or stability, none of them has been directly confirmed (Coates et al., 2014).

There are two metabolic pathways to synthesise hydrocarbons in cyanobacteria, which were identified quite recently. The first pathway is a two-step conversion of fatty acids to fatty aldehydes (even-numbered) and next to alkanes (odd-numbered), which is catalysed by a fatty acyl ACP reductase (FAAR) and an aldehyde deformylating oxygenase (ADO) (**FAAR/ADO pathway**) (Schirmer et al., 2010; Li et al., 2012). The second is conversion of fatty acyl-ACP to terminal alkene (odd-numbered) by an elongation-decarboxylation mechanism which is catalysed by olefin synthase (OLS), a type of polyketide synthase (**OLS pathway**) (Mendez-Perez et al., 2011) (Fig. 1.12).

All cyanobacteria possess either pathway, but no single species has both (Coates et al., 2014). The FAAR/ADO pathway is taxonomically widely distributed among cyanobacteria and is most likely an ancestral form of hydrocarbon synthesis pathway. The OLS pathway is only found in a small number of cyanobacteria and likely evolved later than the FAAR/ADO pathway. The OLS pathway forms a cohesive phylogenetic clade with only a few exceptions where these species may have obtained the

OLS pathway via HGTs. The distribution of these two pathways is not known in other bacterial clades, but it has not been thoroughly studied yet.

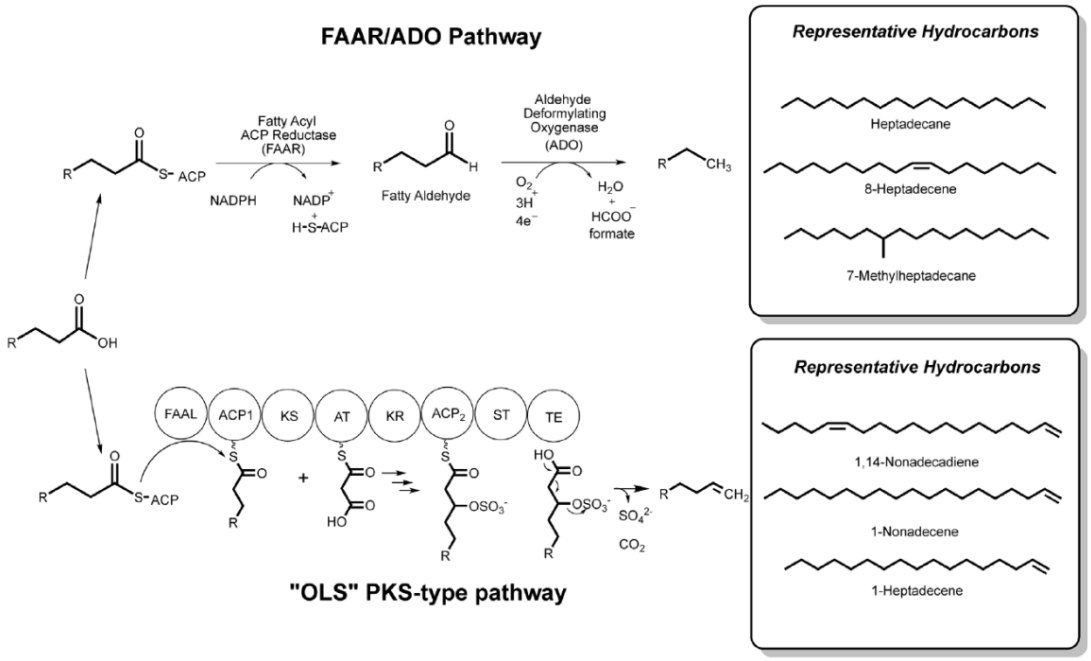

Figure 1.12. Hydrocarbon synthesis pathways in cyanobacteria (adapted from Coates et al., 2014).

In the FAAR/ADO pathway, ADO-catalysed reaction is an oxygen-dependent reaction. Whereas FAAR is found in various organisms, ADO is unique to cyanobacteria (Li et al., 2012). There was a hypothesis that the ADO catalysed reaction is oxygen-independent (Das et al., 2011; Eser et al., 2011), but the reaction was proved to require oxygen (Li et al., 2011; Li et al., 2012). The phylogenetic relationships of FAAR and 16S rRNA of cyanobacteria are generally similar to each other, whereas that of ADO is not congruent, which may indicate an ADO gene duplication at a very early stage (Liu et al., 2013), or a difference of selective pressure between FAAR and ADO. Some parts of the OLS pathway are homologous to fatty acid biosynthesis (Jenke-Kodama et al., 2005; Jenke-Kodama and Dittmann, 2009). The terminal double bond is a unique signature of the OLS pathway.

1.2.5.3. Biosynthesis of mid-chain branched MMAs in cyanobacteria

Saturated hydrocarbons including mid-chain branched MMAs are only produced by cyanobacteria which employ the FAAR/ADO pathway (Coates et al., 2014). Cyanobacteria which use the OLS

pathway exclusively produce alkenes. The position of the methyl group in MMA is diverse (2- to 8-MMA) among cyanobacterial species and also depends on the surrounding environments, but 7-MMA is generally predominant as well as *n*-C_{17}. Mid-chain branched MMAs are generally observed only in limited clades including heterocystous, ramified, and particularly filamentous cyanobacteria, but there are a few reports of mid-chain branched MMAs in unicellular cyanobacteria as well (Han et al., 1968; Gelpi et al., 1970; Liu et al., 2013; Coates et al., 2014), including the most ancient cyanobacterium *G. violaceus* (Coates et al., 2014). Some experimental studies indicate that 7- and 8-MMAs are derived from cis-vaccenic acid (11-octadecenoic acids, C_{18}) by addition of a methyl group from SAM to its double bond through a methyltransferase, followed by the subsequent reduction and decarboxylation of the fatty acids (Han et al., 1968; Fehler and Light, 1970; Fehler and Light, 1972; Bird and Lynch, 1974; Ladygina et al., 2006). However, the enzyme responsible for the methylation has yet to be identified.

There are several examples of aliphatic-methylating methyltransferases (MTs); mycolic acid cyclopropane synthase (Huang et al., 2002), methylene-fatty-acid-phospholipid synthase (Akamatsu and Law, 1970), sterol 24-C-methyltransferase (Nes et al., 1998), geranyl diphosphate 2-C-methyltransferase (Komatsu et al., 2008), and botryococcene C-methyltransferase (Niehaus et al., 2012). The MT which drives the methylation at the C-2/C-3 position in hopanoids is an additional example (Welander et al., 2010). It is assumed that the last universal common ancestor (LUCA) possessed as many as twenty SAM-binding proteins from at least five distinct fold classes (Kozbial and Mushegian, 2005). The following evolution of MTs was so diverse that no MT appears to be conserved across the three domains of life. MTs have been adapted to clade-specific or even species-specific functions (Liscombe et al., 2012). It could mean that such specifically-produced molecules within a clade or a species can be used as biomarkers to identify them in geological records.

1.2.5.4. Diagenetic pathways to produce MMAs

Mid-chain branched MMAs can also be produced through diagenesis of organic matter, which may hamper the identification of their specific biological sources. Possible geological pathways include:

(1) diagenetic transformations of functionalised lipid components such as carboxylic acids (fatty acids) (Summons, 1987; Summons et al., 1988); (2) isomerisation of original *iso*- or *anteiso*-alkane isomers through a long-term thermodynamic equilibrium (Hoering, 1981; Klomp, 1986a); and (3) acid-clay-mineral catalysed conversion from α-olefins which are formed by thermal cracking of *n*-alkanes (Kissin, 1987). However, no diagenetic pathway has been discovered that selectively produces mid-chain branched MMAs such as 7-MMA at C_{17}-C_{20}. Thus, solely diagenetic processes cannot explain the selective high abundance of mid-chain branched MMAs.

1.3. Geology of the Fortescue Group

The Fortescue Group has been well studied and described in detail (e.g. Thorne and Trendall, 2001; Coffey et al., 2013). The group forms the basal member of the Mount Bruce Supergroup, and overlies Palaeoarchaean granite-greenstone basement rocks of the Pilbara Craton. The Fortescue Group was deposited between 2775 and 2630 Ma during one or more periods of rifting and extensive volcanism (Thorne and Trendall, 2001). The group is predominantly composed of subaerial tholeiitic flood basalts, with subordinate siliciclastic, volcaniclastic and carbonate units. The Pilbara Craton was located at ~50° south during the time of Fortescue Group deposition, and may have been part of a larger supercontinent along with the Kaapvaal Craton in South Africa (de Kock et al., 2009).

The Fortescue Group in the Pilbara region is divided into four sub-basins (Fig 1.13). The metamorphic grade of the Fortescue Group is limited to the prehnite-pumpellyite facies (175-280 °C) in the northwest and northeast sub-basins, whereas the south sub-basin was subject to actinolite facies metamorphism (300-350 °C). These temperatures are low compared to many other Archean terrains (Smith et al., 1982). The depositional environment of Fortescue Group sedimentary units is still under debate, and was either a marine setting (Packer, 1990; Thorne and Trendall, 2001; Sakurai et al., 2005), or a lacustrine setting (Kriewaldt and Ryan, 1967; Walter, 1983; Buick, 1992; Blake et al., 2004; Bolhar and Van Kranendonk, 2007; Awramik and Buchheim, 2009; Coffey et al., 2013; Flannery, 2013). The marine setting is favoured by the laterally uniform lithofacies, and by the north to south

thickening of the stratigraphic successions. In contrast, abrupt vertical and lateral facies changes, symmetrical wave ripples, and desiccation cracks support a periodically exposed lacustrine setting (Coffey et al., 2013).

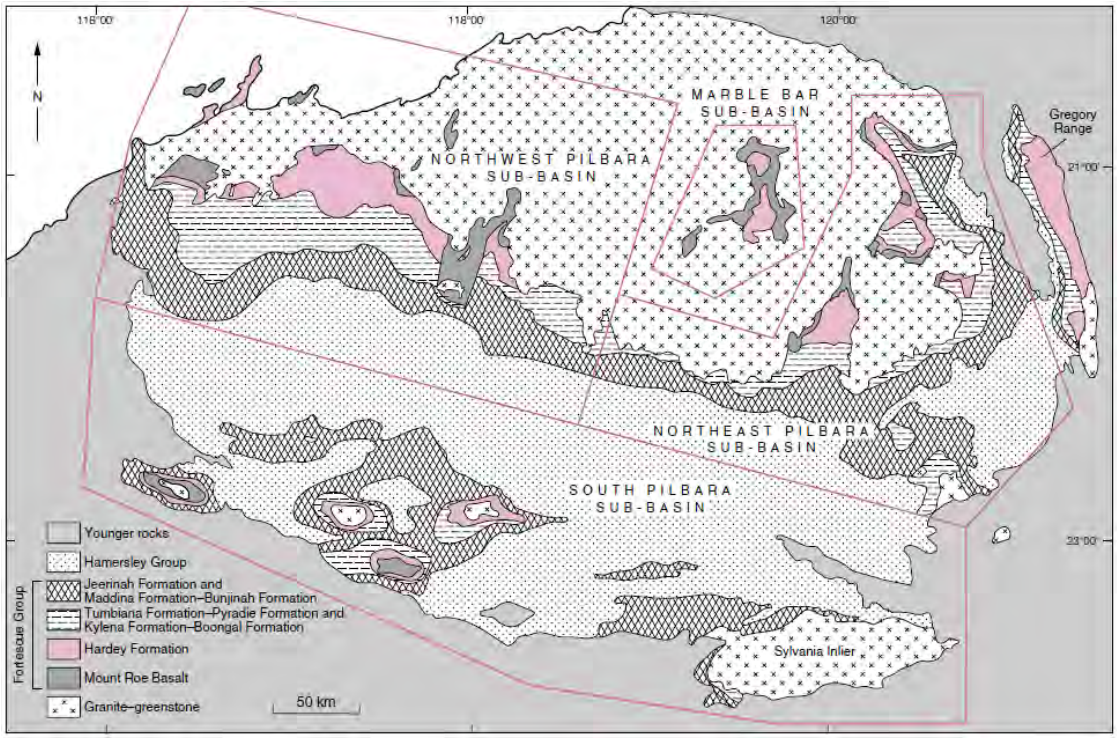

Figure 1.13. Geological map of the Fortescue Group in the Pilbara region, Western Australia (adapted from Thorne and Trendall, 2001).

The rock samples studied in this thesis were collected from the northeast sub-basin, where stromatolitic carbonate rocks are well preserved from several different formations (Fig. 1.14), including: the Mopoke Member in the c. 2.74 Ga Kylena Formation; the Meentheena Member in the c. 2.72 Ga Tumbiana Formation; the Kuruna Member in the c. 2.7 Ga Maddina Formation; and the Woodiana Member in the c. 2.67 Ga Jeerinah Formation.

The Kylena Formation is dominated by subaerial lava flows, with thin layers of carbonate, volcaniclastic and siliciclastic sedimentary rocks (Smithies, 1998). The formation unconformably overlies sandstones and volcaniclastic rocks of the Hardy Formation, and is overlain by the Tumbiana Formation. The Kylena Formation is divided into upper and lower lava flow units, with an intervening thin sedimentary layer (the Mopoke Member) that contains stromatolitic carbonate rocks. No direct

radiometric dates are available for the Mopoke Member, but it was deposited between 2741±3 Ma, the age of the lower Kylena Formation, and 2724±3 Ma, the age of the overlying Tumbiana Formation (Blake et al., 2004). Carbon isotopic ratios of organic matter ($\delta^{13}C_{org}$) in carbonate rocks from the Mopoke Member range from -40.7 to -29.8 ‰ (Flannery, 2013).

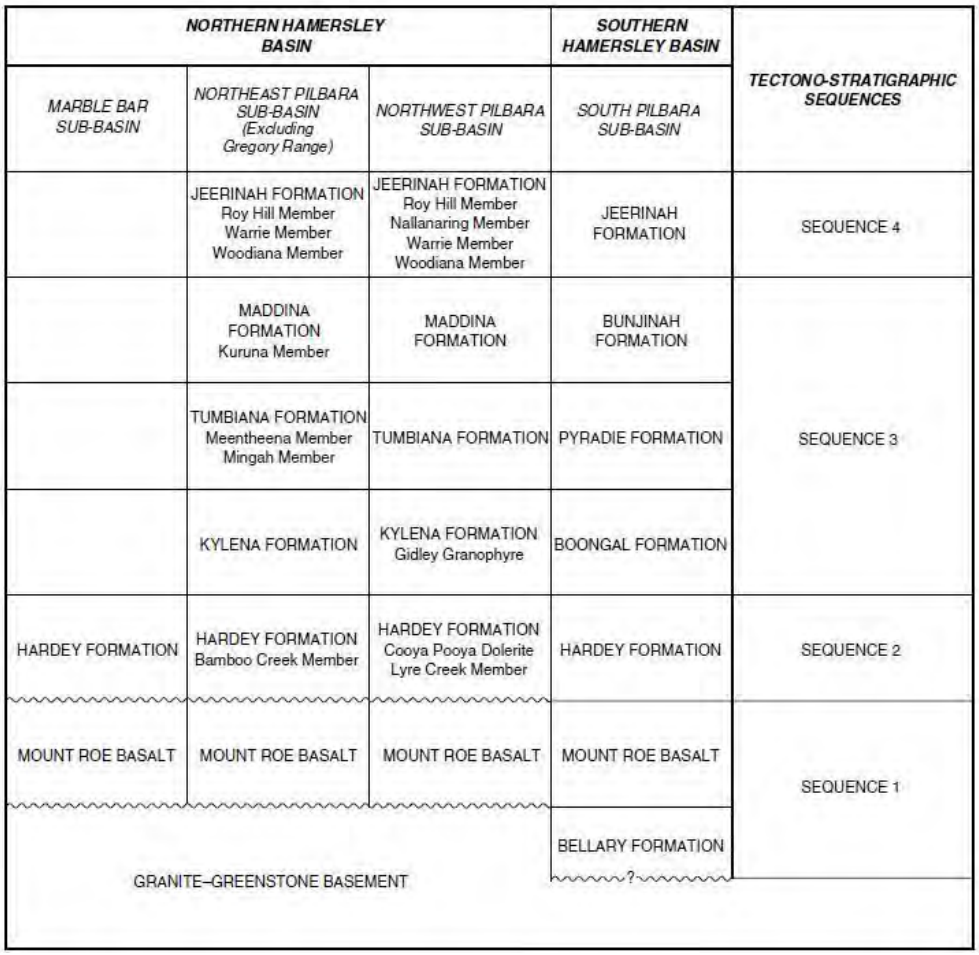

Figure 1.14. Fortescue Group stratigraphy (adapted from Thorne and Trendall, 2001).

The Tumbiana Formation was deposited between subaerial lava flows of the underlying Kylena and overlying Maddina formations. It is divided into the Mingah Member - consisting predominantly of sandstones and subaerial lava flows with volcaniclastic and minor carbonate rocks - and the overlying Meentheena Member, which consists of dark, prominently outcropping, stromatolitic limestones and recessive mudstones (Lipple, 1975; Thorne and Hickman, 1998). The age of the Tumbiana Formation is constrained by radiometric dating from lavas in the Kylena Formation at 2741±3 Ma (Blake et al.,

2004) and in the Maddina Formation at 2717±2 Ma (Kojan and Hickman, 1998; Nelson, 1998), from detrital zircons recovered from Tumbiana Formation tuffaceous sandstones at 2715±6 Ma (Arndt et al., 1991), and from zircons derived from a Mingah Member felsic tuff at 2721±4 Ma (Blake et al., 2004).

Carbon isotope ratios of organic matter ($\delta^{13}C_{org}$) from the Tumbiana Formation are amongst the lowest known from the Precambrian geological record, with values as negative as -60.9 ‰ (Strauss and Moore, 1992). Bimodal distributions of $\delta^{13}C_{org}$ in the Tumbiana Formation, a shallow-water ecosystem dominated by photoautotrophs (-57 to -28 ‰) and a deep-water ecosystem dominated by methanotrophs (-40 to -45 ‰), have been reported (Eigenbrode and Freeman, 2006; Thomazo et al., 2009; Coffey et al., 2013).

The Maddina Formation is predominantly a unit of subaerial lava flows, but contains stromatolitic carbonates as a minor component (Thorne and Trendall, 2001). This formation conformably overlies the Tumbiana Formation. A sedimentary unit within the Maddina Formation, the Kuruna Member, consists of sandstone, mudstone, tuff, chert, lapillistone, and stromatolitic carbonate rocks. The age of the Kuruna Member is constrained by a U-Pb date of 2717±2 Ma for an overlying Maddina Formation rhyolite (Nelson, 1998) and a date of 2721±4 Ma foer the underlying Tumbiana Formation (Blake et al., 2004). The Kuruna Member is divided into three units, with the stromatolites occurring together with abundant accretionary lapilli in the middle unit, between a lower mudstone unit and an upper siltstone unit. $\delta^{13}C_{org}$ for a Kuruna carbonate rock is -46.3 ‰ (Strauss and Moore, 1992).

The Jeerinah Formation is mostly composed of argillite with minor sandstone, dolomite, chert and volcanic rocks (Thorne and Trendall, 2001). Stromatolites are contained in the basal Woodiana Member. Other parts of the Jeerinah Formation are mostly mudstone. The age of the Woodiana Member is between 2717 Ma for the underlying Maddina Formation (Kojan and Hickman, 1998) and 2629±5 Ma, obtained from overlying rocks of the Jeerinah Formation (Arndt et al., 1991; Nelson et al., 1999; Trendall et al., 2004). A $\delta^{13}C_{org}$ of -45.5 ‰ was reported for the Woodiana Member in the

Tambrey area (Packer, 1990). Another study shows $\delta^{13}C_{org}$ of 39.7-27.1 ‰ for the Woodiana Member in the Mt. Florence area, interpreted to be due to a mixed input of photoautotrophs and methanotrophs (Kakegawa and Nanri, 2006).

The nonzero MIF signals, the absence of sulphate minerals, and the presence of detrital pyrite indicate anoxic depositional environments for the Fortescue Group. Nevertheless, conical stromatolitic morphologies (Conophytons) similar to extant cyanobacterial tufted mats may indicate the presence of cyanobacteria at that time (Flannery, 2013). Also, as discussed in Sections 1.1.3.2.4 and 1.1.4.3, the depletion of ^{13}C may also reflect the phototrophic activities of cyanobacteria (Eigenbrode and Freeman, 2006; Coffey et al., 2013).

1.4. References

Akamatsu, Y. and Law, J.H. (1970) Enzymatic alkylenation of phospholipid fatty acid chains by extracts of Mycobacterium phlei. Journal of Biological Chemistry 245, 701-708.

Allen, M.A., Goh, F., Burns, B.P. and Neilan, B.A. (2009) Bacterial, archaeal and eukaryotic diversity of smooth and pustular microbial mat communities in the hypersaline lagoon of Shark Bay. Geobiology 7, 82-96.

Allwood, A., Walter, M., Kamber, B., Marshall, C. and Burch, I. (2006) Stromatolite reef from the Early Archaean era of Australia. Nature 441, 714-718.

Altermann, W. and Kazmierczak, J. (2003) Archean microfossils: a reappraisal of early life on Earth. Research in Microbiology 154, 611-617.

Amard, B. and Bertrand-Sarfati, J. (1997) Microfossils in 2000 Ma old cherty stromatolites of the Franceville Group, Gabon. Precambrian Research 81, 197-221.

Anbar, A.D., Duan, Y., Lyons, T.W., Arnold, G.L., Kendall, B., Creaser, R.A., Kaufman, A.J., Gordon, G.W., Scott, C., Garvin, J. and Buick, R. (2007) A whiff of oxygen before the Great Oxidation Event? Science 317, 1903-1906.

Arndt, N.T., Nelson, D.R., Compston, W., Trendall, A.F. and Thorne, A.M. (1991) The age of the Fortescue Group, Hamersley Basin, Western Australia, from ion microprobe zircon U-Pb results. Australian Journal of Earth Sciences 38, 261-281.

Awramik, S.M. and Buchheim, H.P. (2009) A giant, Late Archean lake system: The Meentheena Member (Tumbiana Formation; Fortescue Group), Western Australia. Precambrian Research 174, 215-240.

Bab-Dinitz, E., Shmuely, H., Maupin-Furlow, J., Eichler, J. and Shaanan, B. (2006) Haloferax volcanii PitA: an example of functional interaction between the Pfam chlorite dismutase and antibiotic biosynthesis monooxygenase families? Bioinformatics (Oxford, England) 22, 671-675.

Barling, J. and Anbar, A.D. (2004) Molybdenum isotope fractionation during adsorption by manganese oxides. Earth and Planetary Science Letters 217, 315-329.

Battistuzzi, F.U. and Hedges, S.B. (2009) A Major Clade of Prokaryotes with Ancient Adaptations to Life on Land. Molecular Biology and Evolution 26, 335-343.

Baumgartner, L., Spear, J., Buckley, D., Pace, N., Reid, R., Dupraz, C. and Visscher, P. (2009) Microbial diversity in modern marine stromatolites, Highborne Cay, Bahamas. Environmental Microbiology 11, 2710-2719.

Bekker, A., Holland, H.D., Wang, P.L., Rumble, D., Stein, H.J., Hannah, J.L., Coetzee, L.L. and Beukes, N.J. (2004) Dating the rise of atmospheric oxygen. Nature 427, 117-120.

Bekker, A., Slack, J.F., Planavsky, N., Krapež, B., Hofmann, A., Konhauser, K.O. and Rouxel, O.J. (2010) Iron Formation: The Sedimentary Product of a Complex Interplay among Mantle, Tectonic, Oceanic, and Biospheric Processes. Economic Geology 105, 467-508.

Bird, C.W. and Lynch, J.M. (1974) Formation of hydrocarbons by micro-organisms. Chemical Society Reviews 3, 309-328.

Bird, C.W., Lynch, J.M., Pirt, F.J., Reid, W.W., Brooks, C.J.W. and Middleditch, B.S. (1971) Steroids and Squalene in Methylococcus capsulatus grown on Methane. Nature 230, 473-474.

Bisseret, P., Zundel, M. and Rohmer, M. (1985) 2. 2β-Methylhopanoids from Methylobacterium organophilum and Nostoc muscorum, a new series of prokaryotic triterpenoids. European Journal of Biochemistry 150, 33-34.

Blake, T.S., Buick, R., Brown, S.J.A. and Barley, M.E. (2004) Geochronology of a late Archaean flood basalt province in the Pilbara Craton, Australia; constraints on basin evolution, volcanic and sedimentary accumulation, and continental drift rates. Precambrian Research 133, 143-173.

Blankenship, R. and Hartman, H. (1998) The origin and evolution of oxygenic photosynthesis. Trends in biochemical sciences 23, 94-97.

Blankenship, R.E. (1992) Origin and early evolution of photosynthesis. Photosynthesis Research 33, 91-111.

Blumenberg, M., Krüger, M., Nauhaus, K., Talbot, H., Oppermann, B., Seifert, R., Pape, T. and Michaelis, W. (2006) Biosynthesis of hopanoids by sulfate-reducing bacteria (genus Desulfovibrio). Environmental Microbiology 8, 1220-1227.

Bode, H.B., Zeggel, B., Silakowski, B., Wenzel, S.C., Reichenbach, H. and Müller, R. (2003) Steroid biosynthesis in prokaryotes: identification of myxobacterial steroids and cloning of the first bacterial 2,3(S)-oxidosqualene cyclase from the myxobacterium Stigmatella aurantiaca. Molecular Microbiology 47, 471-481.

Bolhar, R. and Van Kranendonk, M.J. (2007) A non-marine depositional setting for the northern Fortescue Group, Pilbara Craton, inferred from trace element geochemistry of stromatolitic carbonates. Precambrian Research 155, 229-250.

Bosak, T., Liang, B., Sim, M.S. and Petroff, A.P. (2009) Morphological record of oxygenic photosynthesis in conical stromatolites. Proceedings of the National Academy of Sciences 106, 10939-10943.

Bouvier, P., Rohmer, M., Benveniste, P. and Ourisson, G. (1976) Delta8(14)-steroids in the bacterium Methylococcus capsulatus. The Biochemical journal 159, 267-271.

Bradley, A.S., Pearson, A., Sáenz, J.P. and Marx, C.J. (2010) Adenosylhopane: The first intermediate in hopanoid side chain biosynthesis. Organic Geochemistry 41, 1075-1081.

Brasier, M., McLoughlin, N., Green, O. and Wacey, D. (2006) A fresh look at the fossil evidence for early Archaean cellular life. Philosophical Transactions of the Royal Society B: Biological Sciences 361, 887-902.

Brasier, M.D., Green, O.R., Jephcoat, A.P., Kleppe, A.K., Van Kranendonk, M.J., Lindsay, J.F., Steele, A. and Grassineau, N.V. (2002) Questioning the evidence for Earth's oldest fossils. Nature 416, 76-81.

Bravo, J., Perzl, M., Härtner, T., Kannenberg, E. and Rohmer, M. (2001) Novel methylated triterpenoids of the gammacerane series from the nitrogen-fixing bacterium Bradyrhizobium japonicum USDA 110. European journal of biochemistry / FEBS 268, 1323-1331.

Briggs, D.E.G. and Summons, R.E. (2014) Ancient biomolecules: Their origins, fossilization, and role in revealing the history of life. BioEssays 36, 482-490.

Brochier-Armanet, C., Talla, E. and Gribaldo, S. (2009) The multiple evolutionary histories of dioxygen reductases: Implications for the origin and evolution of aerobic respiration. Molecular biology and evolution 26, 285-297.

Brocks, J.J. (2011) Millimeter-scale concentration gradients of hydrocarbons in Archean shales: Live-oil escape or fingerprint of contamination? Geochimica Et Cosmochimica Acta 75, 3196-3213.

Brocks, J.J., Buick, R., Logan, G.A. and Summons, R.E. (2003a) Composition and syngeneity of molecular fossils from the 2.78 to 2.45 billion-year-old Mount Bruce Supergroup, Pilbara Craton, Western Australia. Geochimica Et Cosmochimica Acta 67, 4289-4319.

Brocks, J.J., Buick, R., Summons, R.E. and Logan, G.A. (2003b) A reconstruction of Archean biological diversity based on molecular fossils from the 2.78 to 2.45 billion-year-old Mount Bruce Supergroup, Hamersley Basin, Western Australia. Geochimica Et Cosmochimica Acta 67, 4321-4335.

Brocks, J.J. and Grice, K. (2011) Biomarkers (molecular fossils). Springer, 147-167.

Brocks, J.J., Logan, G.A., Buick, R. and Summons, R.E. (1999) Archean molecular fossils and the early rise of eukaryotes. Science 285, 1033-1036.

Brocks, J.J., Love, G.D., Summons, R.E., Knoll, A.H., Logan, G.A. and Bowden, S.A. (2005) Biomarker evidence for green and purple sulphur bacteria in a stratified Palaeoproterozoic sea. Nature 437, 866-870.

Brocks, J.J. and Pearson, A. (2005) Building the biomarker tree of life. Reviews in Mineralogy and Geochemistry 59, 233-258.

Brocks, J.J. and Summons, R.E. (2003) 8.03 - Sedimentary Hydrocarbons, Biomarkers for Early Life, in: Editors-in-Chief: Heinrich, D.H., Karl, K.T. (Eds.), Treatise on Geochemistry. Pergamon, Oxford, pp. 63-115.

Bryant, D.A. and Frigaard, N.-U. (2006) Prokaryotic photosynthesis and phototrophy illuminated. Trends in microbiology 14, 488-496.

Buick, R. (1992) The antiquity of oxygenic photosynthesis; evidence from stromatolites in sulphate-deficient Archaean lakes. Science 255, 74-77.

Canfield, D., Rosing, M. and Bjerrum, C. (2006) Early anaerobic metabolisms. Philosophical transactions of the Royal Society of London. Series B, Biological sciences 361, 1819-1836.

Canfield, D.E. (2005) The early history of atmospheric oxygen: Homage to Robert M. Garrels. Annual Review of Earth and Planetary Sciences 33, 1-36.

Canfield, D.E. and Teske, A. (1996) Late Proterozoic rise in atmospheric oxygen concentration inferred from phylogenetic and sulphur-isotope studies. Nature 382, 127-132.

Castresana, J., Lübben, M., Saraste, M. and Higgins, D. (1994) Evolution of cytochrome oxidase, an enzyme older than atmospheric oxygen. The EMBO journal 13, 2516-2525.

Castresana, J. and Saraste, M. (1995) Evolution of energetic metabolism: the respiration-early hypothesis. Trends in biochemical sciences 20, 443-448.

Catling, D.C., Zahnle, K.J. and McKay, C.P. (2001) Biogenic methane, hydrogen escape, and the irreversible oxidation of early Earth. Science 293, 839-843.

Claire, M.W., Catling, D.C. and Zahnle, K.J. (2006) Biogeochemical modelling of the rise in atmospheric oxygen. Geobiology 4, 239-269.

Clayton, R.N., Grossman, L. and Mayeda, T.K. (1973) A Component of Primitive Nuclear Composition in Carbonaceous Meteorites. Science 182, 485-488.

Cloud, P. (1973) Paleoecological Significance of the Banded Iron-Formation. Economic Geology 68, 1135-1143.

Cloud, P.E. (1965) Significance of the Gunflint (Precambrian) Microflora: Photosynthetic oxygen may have had important local effects before becoming a major atmospheric gas. Science 148, 27-35.

Coates, R., Podell, S., Korobeynikov, A., Lapidus, A., Pevzner, P., Sherman, D., Allen, E., Gerwick, L. and Gerwick, W. (2014) Characterization of cyanobacterial hydrocarbon composition and distribution of biosynthetic pathways. PloS one 9, e85140.

Coffey, J.M. (2011) A paleoenvironmental study of the 2.7 Ga Tumbiana Formation, Fortescue Basin, Western Australia. Ph.D. dissertation, University of New South Wales, Sydney.

Coffey, J.M., Flannery, D.T., Walter, M.R. and George, S.C. (2013) Sedimentology, stratigraphy and geochemistry of a stromatolite biofacies in the 2.72Ga Tumbiana Formation, Fortescue Group, Western Australia. Precambrian Research 236, 282-296.

Coleman, D.D., Risatti, J.B. and Schoell, M. (1981) Fractionation of carbon and hydrogen isotopes by methane-oxidizing bacteria. Geochimica Et Cosmochimica Acta 45, 1033-1037.

Crowe, S., Døssing, L., Beukes, N., Bau, M., Kruger, S., Frei, R. and Canfield, D. (2013) Atmospheric oxygenation three billion years ago. Nature 501, 535-538.

Danovaro, R., Dell'Anno, A., Pusceddu, A., Gambi, C., Heiner, I. and Mobjerg Kristensen, R. (2010) The first metazoa living in permanently anoxic conditions. BMC Biology 8, 30.

Das, D., Eser, B., Han, J., Sciore, A. and Marsh, E. (2011) Oxygen-independent decarbonylation of aldehydes by cyanobacterial aldehyde decarbonylase: a new reaction of diiron enzymes. Angewandte Chemie (International ed. in English) 50, 7148-7152.

David, L.A. and Alm, E.J. (2011) Rapid evolutionary innovation during an Archaean genetic expansion. Nature 469, 93-96.

de Carvalho, C.C. and Fernandes, P. (2010) Production of metabolites as bacterial responses to the marine environment. Marine drugs 8, 705-727.

de Kock, M.O., Evans, D.A.D. and Beukes, N.J. (2009) Validating the existence of Vaalbara in the Neoarchean. Precambrian Research 174, 145-154.

Dembitsky, V.M., Dor, I., Shkrob, I. and Aki, M. (2001) Branched Alkanes and Other Apolar Compounds Produced by the Cyanobacterium Microcoleus vaginatusfrom the Negev Desert. Russian Journal of Bioorganic Chemistry 27, 130-140.

Des Marais, D.J. (2001) Isotopic Evolution of the Biogeochemical Carbon Cycle During the Precambrian. Reviews in Mineralogy and Geochemistry 43, 555-578.

Desmond, E. and Gribaldo, S. (2009) Phylogenomics of Sterol Synthesis: Insights into the Origin, Evolution, and Diversity of a Key Eukaryotic Feature. Genome Biology and Evolution 1, 364–381.

Di Rienzi, S., Sharon, I., Wrighton, K., Koren, O., Hug, L., Thomas, B., Goodrich, J., Bell, J., Spector, T., Banfield, J. and Ley, R. (2013) The human gut and groundwater harbor non-photosynthetic bacteria belonging to a new candidate phylum sibling to Cyanobacteria. eLife 2, e01102.

Dismukes, G., Klimov, V., Baranov, S., Kozlov, Y., DasGupta, J. and Tyryshkin, A. (2001) The origin of atmospheric oxygen on Earth: the innovation of oxygenic photosynthesis. Proceedings of the National Academy of Sciences of the United States of America 98, 2170-2175.

Dogamal-Goldman, S. D., Kasting, J. F., Johnston, D. T., Farquhar, J. (2008) Organic haze, glaciations and multiple sulfur isotopes in the Mid-Archean Era. Earth and Planetary Science Letters 269, 29-40.

Dominé, F., Bounaceur, R., Scacchi, G., Marquaire, P.-M., Dessort, D., Pradier, B. and Brevart, O. (2002) Up to what temperature is petroleum stable? New insights from a 5200 free radical reactions model. Organic Geochemistry 33, 1487-1499.

Duan, Y., Anbar, A.D., Arnold, G.L., Lyons, T.W., Gordon, G.W. and Kendall, B. (2010) Molybdenum isotope evidence for mild environmental oxygenation before the Great Oxidation Event. Geochimica Et Cosmochimica Acta 74, 6655-6668.

Dutkiewicz, A., Volk, H., George, S., Ridley, J. and Buick, R. (2006) Biomarkers from Huronian oil-bearing fluid inclusions: An uncontaminated record of life before the Great Oxidation Event. Geology 34, 437-440.

Eickhoff, M., Birgel, D., Talbot, H.M., Peckmann, J. and Kappler, A. (2013) Bacteriohopanoid inventory of Geobacter sulfurreducens and Geobacter metallireducens. Organic Geochemistry 58, 107-114.

Eigenbrode, J.L. and Freeman, K.H. (2006) Late Archean rise of aerobic microbial ecosystems. Proceedings of the National Academy of Sciences 103, 15759-15764.

Eigenbrode, J.L., Freeman, K.H. and Summons, R.E. (2008) Methylhopane biomarker hydrocarbons in Hamersley Province sediments provide evidence for Neoarchean aerobiosis. Earth and Planetary Science Letters 273, 323-331.

Eser, B., Das, D., Han, J., Jones, P. and Marsh, E. (2011) Oxygen-independent alkane formation by non-heme iron-dependent cyanobacterial aldehyde decarbonylase: investigation of kinetics and requirement for an external electron donor. Biochemistry 50, 10743-10750.

Ettwig, K., Butler, M., Le Paslier, D., Pelletier, E., Mangenot, S., Kuypers, M.M., Schreiber, F., Dutilh, B., Zedelius, J., de Beer, D., Gloerich, J., Wessels, H., van Alen, T., Luesken, F., Wu, M., van de Pas-Schoonen, K., Op den Camp, H., Janssen-Megens, E., Francoijs, K.-J., Stunnenberg, H., Weissenbach, J., Jetten, M. and Strous, M. (2010) Nitrite-driven anaerobic methane oxidation by oxygenic bacteria. Nature 464, 543-548.

Ettwig, K., Speth, D., Reimann, J., Wu, M.L., Jetten, M.S.M. and Keltjens, J.T. (2012) Bacterial oxygen production in the dark. Frontiers in Microbiology 3, 273.

Falkowski, P., Katz, M., Knoll, A., Quigg, A., Raven, J., Schofield, O. and Taylor, F. (2004) The evolution of modern eukaryotic phytoplankton. Science 305, 354-360.

Farquhar, J., Bao, H. and Thiemens, M. (2000) Atmospheric Influence of Earth's Earliest Sulfur Cycle. Science 289, 756-758.

Farquhar, J., Peters, M., Johnston, D., Strauss, H., Masterson, A., Wiechert, U. and Kaufman, A. (2007) Isotopic evidence for Mesoarchaean anoxia and changing atmospheric sulphur chemistry. Nature 449, 706-709.

Farquhar, J. and Wing, B.A. (2003) Multiple sulfur isotopes and the evolution of the atmosphere. Earth and Planetary Science Letters 213, 1-13.

Fehler, S. and Light, R. (1970) Biosynthesis of hydrocarbons in Anabaena variabilis. Incorporation of [methyl-14C]- and [methyl-2H3]methionine into 7- and 8-methylheptadecanes. Biochemistry 9, 418-422.

Fehler, S.W.G. and Light, R.J. (1972) Biosynthesis of methylheptadecanes in Anabaena variabilis. In vitro incorporation of S-[methyl-14C]-adenosylmethionine. Biochemistry 11, 2411-2416.

Fischer, W.W., Summons, R.E. and Pearson, A. (2005) Targeted genomic detection of biosynthetic pathways: anaerobic production of hopanoid biomarkers by a common sedimentary microbe. Geobiology 3, 33-40.

Flannery, D.T. (2013) Palaeobiology of the Neoarchean Fortescue Group, Pilbara Craton, Western Australia. Ph.D. dissertation, University of Sydney.

Flannery, D.T. and Walter, M.R. (2012) Archean tufted microbial mats and the Great Oxidation Event: new insights into an ancient problem. Australian Journal of Earth Sciences 59, 1-11.

Flesch, G. and Rohmer, M. (1988) Prokaryotic hopanoids: the biosynthesis of the bacteriohopane skeleton. Formation of isoprenic units from two distinct acetate pools and a novel type of carbon/carbon linkage between a triterpene and D-ribose. European journal of biochemistry / FEBS 175, 405-411.

Flores, F.G., Herrero, A. and Flores, E. (2008) The cyanobacteria: molecular biology, genomics, and evolution. The Publisher.

Foster, J., Green, S., Ahrendt, S., Golubic, S., Reid, R., Hetherington, K. and Bebout, L. (2009) Molecular and morphological characterization of cyanobacterial diversity in the stromatolites of Highborne Cay, Bahamas. The ISME journal 3, 573-587.

Fowler, M.G. and Douglas, A.G. (1987) Saturated hydrocarbon biomarkers in oils of Late Precambrian age from Eastern Siberia. Organic Geochemistry 11, 201-213.

French, K.L., Hallman, C., Hope, J.M., Buick, R., Brocks, J.J. and Summons, R.E. (2013) Archean hydrocarbon biomarkers: Archean or not?, Goldschmidt 2013 Conference Abstract.

Frickey, T. and Kannenberg, E. (2009) Phylogenetic analysis of the triterpene cyclase protein family in prokaryotes and eukaryotes suggests bidirectional lateral gene transfer. Environmental Microbiology 11, 1224-1241.

Gaillard, F., Scaillet, B. and Arndt, N. (2011) Atmospheric oxygenation caused by a change in volcanic degassing pressure. Nature 478, 229-232.

Garby, T.J., Walter, M.R., Larkum, A.W.D. and Neilan, B.A. (2013) Diversity of cyanobacterial biomarker genes from the stromatolites of Shark Bay, Western Australia. Environmental Microbiology 15, 1464-1475.

García-Ruiz, J.M., Hyde, S.T., Carnerup, A.M., Christy, A.G., Van Kranendonk, M.J. and Welham, N.J. (2003) Self-Assembled Silica-Carbonate Structures and Detection of Ancient Microfossils. Science 302, 1194-1197.

Garrels, R.M., Perry, E.A. and Mackenzie, F.T. (1973) Genesis of Precambrian Iron-Formations and the Development of Atmospheric Oxygen. Economic Geology 68, 1173-1179.

Garvin, J., Buick, R., Anbar, A.D., Arnold, G.L. and Kaufman, A.J. (2009) Isotopic Evidence for an Aerobic Nitrogen Cycle in the Latest Archean. Science 323, 1045-1048.

Gelpi, E., Schneider, H., Mann, J. and Oro, J. (1970) Hydrocarbons of geochemical significance in microscopic algae. Phytochemistry 9, 603-612.

George, S. and Ahmed, M. (2002) Use of aromatic compound distributions to evaluate organic maturity of the Proterozoic middle Velkerri Formation, McArthur Basin, Australia. The Sedimentary Basins of Western Australia III: Proceedings of the West Australasian Basins Symposium (WABS) III.

George, S., Volk, H., Ruble, T. and Brincat, M. (2002) Evidence for a new oil family in the Nancar Trough area, Timor Sea. APPEA journal 42, 387-404.

George, S.C., Volk, H., Dutkiewicz, A., Ridley, J. and Buick, R. (2008) Preservation of hydrocarbons and biomarkers in oil trapped inside fluid inclusions for > 2 billion years. Geochimica Et Cosmochimica Acta 72, 844-870.

Goblirsch, B., Kurker, R., Streit, B., Wilmot, C. and DuBois, J. (2011) Chlorite dismutases, DyPs, and EfeB: 3 microbial heme enzyme families comprise the CDE structural superfamily. Journal of Molecular Biology 408, 379-398.

Godfrey, L.V. and Falkowski, P.G. (2009) The cycling and redox state of nitrogen in the Archaean ocean. Nature Geoscience 2, 725-729.

Grotzinger, J.P. and Rothman, D.H. (1996) An abiotic model for stromatolite morphogenesis. Nature 383, 423-425.

Hagedoorn, P.L., De Geus, D.C. and Hagen, W.R. (2002) Spectroscopic characterization and ligand binding properties of chlorite dismutase from the chlorate respiring bacterial strain GR 1. European Journal of Biochemistry 269, 4905-4911.

Hallmann, C. and Summons, R.E. (2014) 6.5 - Paleobiological Clues to Early Atmospheric Evolution, in: Holland, H.D., Turekian, K.K. (Eds.), Treatise on Geochemistry (Second Edition). Elsevier, Oxford, pp. 139-155.

Han, J. and Calvin, M. (1970) Branched alkanes from blue-green algae. Journal of the Chemical Society D Chemical Communications, 1490-1491.

Han, J., McCarthy, E.D., Melvin, C. and Benn, M.H. (1968) Hydrocarbon constituents of the blue-green algae Nostoc muscorum, Anacystis nidulans, Phormidium luridium and Chlorogloea fritschii. Journal of the Chemical Society C Organic, 2785-2791.

Hancock, J. (2006) Lipid rafts: contentious only from simplistic standpoints. Nature reviews. Molecular cell biology 7, 456-462.

Haqq-Misra, J., Kasting, J. and Lee, S. (2011) Availability of O_2 and H_2O_2 on pre-photosynthetic Earth. Astrobiology 11, 293-302.

Hartman, H. (1984) The evolution of photosynthesis and microbial mats: A speculation on banded iron formations, in: Cohen, Y., Castenholz, R.W., Halvorson, H.O. (Eds.), Microbial Mats, Stromatolites. Alan R Liss, New York, pp. 451-453.

Hartman, H. (1998) Photosynthesis and the origin of life. Origins of life and evolution of the biosphere : the journal of the International Society for the Study of the Origin of Life 28, 515-521.

Härtner, T., Straub, K. and Kannenberg, E. (2005) Occurrence of hopanoid lipids in anaerobic Geobacter species. FEMS microbiology letters 243, 59-64.

Hayes, J.M., Kaplan, I.R. and Wedeking, K.M. (1983) Precambrian organic geochemistry, preservation of the record, in: Schopf, J.W. (Ed.), Earth's earliest biosphere, its origin and evolution. Princeton University Press, Princeton, pp. 93-134, 543.

Heidenreich, J.E. and Thiemens, M.H. (1986) A non-mass-dependent oxygen isotope effect in the production of ozone from molecular oxygen: The role of molecular symmetry in isotope chemistry. The Journal of Chemical Physics 84, 2129-2136.

Hinrichs, K.-U., Hayes, J.M., Sylva, S.P., Brewer, P.G. and DeLong, E.F. (1999) Methane-consuming archaebacteria in marine sediments. Nature 398, 802-805.

Hoashi, M., Bevacqua, D.C., Otake, T., Watanabe, Y., Hickman, A.H., Utsunomiya, S. and Ohmoto, H. (2009) Primary haematite formation in an oxygenated sea 3.46 billion years ago. Nature Geoscience 2, 301-306.

Hoering, T.C. (1981) Monomethyl acyclic hydrocarbons in petroleum and rock extracts. Carnegie Institute of Washington Yearbook 80, 389-393.

Hofer, U. (2013) Bacterial evolution: Getting to the bottom of Cyanobacteria. Nature Review Microbiology 11, 818-819.

Hofmann, H.J. (1976) Precambrian Microflora, Belcher Islands, Canada: Significance and Systematics. Journal of Paleontology 50, 1040-1073.

Hohmann-Marriott, M. and Blankenship, R. (2011) Evolution of photosynthesis. Annual review of plant biology 62, 515-548.

Höld, I.M., Schouten, S., Jellema, J. and Damsté, J.S.S. (1999) Origin of free and bound mid-chain methyl alkanes in oils, bitumens and kerogens of the marine, Infracambrian Huqf Formation (Oman). Organic Geochemistry 30, 1411-1428.

Holland, H.D. (2002) Volcanic gases, black smokers, and the great oxidation event. Geochimica Et Cosmochimica Acta 66, 3811-3826.

Holland, H.D. (2006) The oxygenation of the atmosphere and oceans. Philosophical Transactions of the Royal Society B: Biological Sciences 361, 903-915.

Holland, H.D. (2009) Why the atmosphere became oxygenated: a proposal. Geochimica Et Cosmochimica Acta 73, 5241-5255.

Holm, N.G. (1989) The $^{13}C/^{12}C$ ratios of siderite and organic matter of a modern metalliferous hydrothermal sediment and their implications for banded iron formations. Chemical Geology 77, 41-45.

Holser, W.T., Schilowski, M., Mackenzie, F.T. and Maynard, J.B. (1988) Biogeochemical cycles of carbon and sulfur, in: Gregor, C.B., Garreis, R.M., Mackenzie, F.T., Maynard, J.B. (Eds.), Chemical cycles in the evolution of the Earth, New York, pp. 105-173.

Honda, D., Yokota, A. and Sugiyama, J. (1999) Detection of seven major evolutionary lineages in cyanobacteria based on the 16S rRNA gene sequence analysis with new sequences of five marine Synechococcus strains. Journal of Molecular Evolution 48, 723-739.

House, C.H., Schopf, J.W. and Stetter, K.O. (2003) Carbon isotopic fractionation by Archaeans and other thermophilic prokaryotes. Organic Geochemistry 34, 345-356.

Huang, C.-c., Smith, C.V., Glickman, M., Jacobs, W.R. and Sacchettini, J.a.J.C. (2002) Crystal Structures of Mycolic Acid Cyclopropane Synthases from Mycobacterium tuberculosis. Journal of Biological Chemistry 277, 11559-11569.

Ilbert, M. and Bonnefoy, V. (2013) Insight into the evolution of the iron oxidation pathways. Biochimica et biophysica acta 1827, 161-175.

Imlay, J.A. (2003) Pathways of oxidative damage. Annual Reviews in Microbiology 57, 395-418.

Isley, A.E. and Abbott, D.H. (1999) Plume-related mafic volcanism and the deposition of banded iron formation. J. Geophys. Res. 104, 15461-15477.

Jahnke, L., Summons, R., Hope, J. and Des Marais, D. (1999) Carbon isotopic fractionation in lipids from methanotrophic bacteria II: the effects of physiology and environmental parameters on the biosynthesis and isotopic signatures of biomarkers. Geochimica Et Cosmochimica Acta 63, 79-93.

James, H.L. (1954) Sedimentary facies of iron-formation. Economic Geology 49, 235-293.

James, H.L. (1983) Distribution of Banded Iron-Formation in space and time, in: Trendall, A.F., Morris, R.C. (Eds.), Iron-Formation: Facts and Problems. Elsevier, Amsterdam, pp. 471-490.

Jardillier, L., Zubkov, M.V., Pearman, J. and Scanlan, D.J. (2010) Significant CO_2 fixation by small prymnesiophytes in the subtropical and tropical northeast Atlantic Ocean. The ISME journal 4, 1180-1192.

Jenke-Kodama, H. and Dittmann, E. (2009) Evolution of metabolic diversity: Insights from microbial polyketide synthases. Phytochemistry 70, 1858-1866.

Jenke-Kodama, H., Sandmann, A., Müller, R. and Dittmann, E. (2005) Evolutionary implications of bacterial polyketide synthases. Molecular biology and evolution 22, 2027-2039.

Johnston, D., Wolfe-Simon, F., Pearson, A. and Knoll, A. (2009) Anoxygenic photosynthesis modulated Proterozoic oxygen and sustained Earth's middle age. Proceedings of the National Academy of Sciences of the United States of America 106, 16925-16929.

Kakegawa, T. and Nanri, H. (2006) Sulfur and carbon isotope analyses of 2.7 Ga stromatolites, cherts and sandstones in the Jeerinah Formation, Western Australia. Precambrian Research 148, 115-124.

Kalkowsky, E. (1908) Oolith und Stromatolith im norddeutschen Buntsandstein. Zeitschrift der deutschen geologischen Gesellschaft, 68-125.

Kannenberg, E. and Poralla, K. (1999) Hopanoid biosynthesis and function in bacteria. Naturwissenschaften 86, 168-176.

Kappler, A., Pasquero, C., Konhauser, K.O. and Newman, D.K. (2005) Deposition of banded iron formations by anoxygenic phototrophic Fe (II)-oxidizing bacteria. Geology 33, 865-868.

Kasting, J., Pollack, J. and Crisp, D. (1984) Effects of high CO_2 levels on surface temperature and atmospheric oxidation state of the early Earth. Journal of atmospheric chemistry 1, 403-428.

Kasting, J. and Walker, J. (1981) Limits on oxygen concentration in the prebiological atmosphere and the rate of abiotic fixation of nitrogen. Journal of Geophysical Research 86, 1147-1158.

Kasting, J.F. (2005) Methane and climate during the Precambrian era. Precambrian Research 137, 119-129.

Kasting, J.F. (2013) What caused the rise of atmospheric O_2? Chemical Geology 362, 13-25.

Kasting, J.F. and Canfield, D.E. (2012) The global oxygen cycle, in: Knoll, A.H., Canfield, D.E., Konhauser, K. (Eds.), Fundamentals of geobiology. Wiley-Blackwell, Oxford, pp. 93-104.

Kasting, J.F. and Catling, D. (2003) Evolution of a habitable planet. Annual Review of Astronomy and Astrophysics 41, 429-463.

Kasting, J.F., Liu, S.C. and Donahue, T.M. (1979) Oxygen levels in the prebiological atmosphere. Journal of Geophysical Research 84, 3097-3107.

Kauff, F. and Büdel, B. (2011) Phylogeny of Cyanobacteria: An Overview. Springer, 209-224.

Kaufman, A.J., Johnston, D.T., Farquhar, J., Masterson, A.L., Lyons, T.W., Bates, S., Anbar, A.D., Arnold, G.L., Garvin, J. and Buick, R. (2007) Late Archean Biospheric Oxygenation and Atmospheric Evolution. Science 317, 1900-1903.

Kazmierczak, J. and Altermann, W. (2002) Neoarchean biomineralization by benthic cyanobacteria. Science 298, 2351.

Keeling, P. (2004) Diversity and evolutionary history of plastids and their hosts. American journal of botany 91, 1481-1493.

Kendall, B., Reinhard, C.T., Lyons, T.W., Kaufman, A.J., Poulton, S.W. and Anbar, A.D. (2010) Pervasive oxygenation along late Archaean ocean margins. Nature Geoscience 3, 647-652.

Kenig, F., Damsté, J.S.S., Dalen, A.C.K.-v., Rijpstra, W.I.C., Huc, A.Y. and Leeuw, J.W.d. (1995) Occurrence and origin of mono-, di-, and trimethylalkanes in modern and Holocene cyanobacterial mats from Abu Dhabi, United Arab Emirates. Geochimica Et Cosmochimica Acta 59, 2999-3015.

Kim, K., Qin, T., Jiang, Y.-Y., Chen, L.-L., Xiong, M., Caetano-Anollés, D., Zhang, H.-Y. and Caetano-Anollés, G. (2012) Protein domain structure uncovers the origin of aerobic metabolism and the rise of planetary oxygen. Structure 20, 67-76.

Kirschvink, J.L. and Kopp, R.E. (2008) Palaeoproterozoic ice houses and the evolution of oxygen-mediating enzymes: the case for a late origin of photosystem II. Philosophical Transactions of the Royal Society B: Biological Sciences 363, 2755-2765.

Kissin, Y.V. (1987) Catagenesis and composition of petroleum: Origin of n-alkanes and isoalkanes in petroleum crudes. Geochimica Et Cosmochimica Acta 51, 2445-2457.

Klein, C. (2005) Some Precambrian banded iron-formations (BIFs) from around the world: Their age, geologic setting, mineralogy, metamorphism, geochemistry, and origins. American Mineralogist 90, 1473-1499.

Klomp, U.C. (1986a) The chemical structure of a pronounced series of iso-alkanes in South Oman Crudes, in: Leythaeuser, D., Rullkcöte, J. (Eds.), Advances in Organic Geochemistry Part II. Pergamon Journals, Oxford, pp. 807-814.

Klomp, U.C. (1986b) The chemical structure of a pronounced series of iso-alkanes in South Oman crudes. Organic Geochemistry 10, 807-814.

Kneip, C., Voss, C., Lockhart, P. and Maier, U. (2008) The cyanobacterial endosymbiont of the unicellular algae Rhopalodia gibba shows reductive genome evolution. BMC Evolutionary Biology 8, 30.

Knoll, A. (2003) Life on a Young Planet: The First Three Billion Years of Evolution on Earth. Princeton University Press, Princeton.

Knoll, A. and Carroll, S. (1999) Early animal evolution: emerging views from comparative biology and geology. Science 284, 2129-2137.

Koch, L. and Britton, S. (2008) Aerobic metabolism underlies complexity and capacity. The Journal of physiology 586, 83-95.

Kohl, W., Gloe, A. and Reichenbach, H. (1983) Steroids from the Myxobacterium Nannocystis exedens. Journal of General Microbiology 129, 1629-1635.

Kojan, C.J. and Hickman, A.H. (1998) Late Archaean volcanism in the Kylena and Maddina Formations, Fortescue Group, west Pilbara. Western Australia Geological Survey, Annual Review 1997–98, 43-53.

Komatsu, M., Tsuda, M., mura, S., Oikawa, H. and Ikeda, H. (2008) Identification and functional analysis of genes controlling biosynthesis of 2-methylisoborneol. Proceedings of the National Academy of Sciences 105, 7422-7427.

Konhauser, K. (2009) Biogeochemistry: Deepening the early oxygen debate. Nature Geoscience 2, 241-242.

Kool, D.M., Talbot, H.M., Rush, D., Ettwig, K. and Sinninghe Damsté, J.S. (2014) Rare bacteriohopanepolyols as markers for an autotrophic, intra-aerobic methanotroph. Geochimica et Cosmochimica Acta 136, 114-125.

Koopmans, M.P., De Leeuw, J.W., Lewan, M.D. and Sinninghe Damste, J.S. (1996) Impact of dia- and catagenesis on sulphur and oxygen sequestration of biomarkers as revealed by artificial maturation of an immature sedimentary rock. Organic Geochemistry 25, 391-426.

Kopp, R.E., Kirschvink, J.L., Hilburn, I.A. and Nash, C.Z. (2005) The Paleoproterozoic snowball Earth; a climate disaster triggered by the evolution of oxygenic photosynthesis. Proceedings of the National Academy of Sciences of the United States of America 102, 11131-11136.

Köster, J., Volkman, J.K., Rullkötter, J., Scholz-Böttcher, B.M., Rethmeier, J. and Fischer, U. (1999) Mono-, di- and trimethyl-branched alkanes in cultures of the filamentous cyanobacterium Calothrix scopulorum. Organic Geochemistry 30, 1367-1379.

Kozbial, P. and Mushegian, A. (2005) Natural history of S-adenosylmethionine-binding proteins. BMC structural biology 5, 19.

Kriewaldt, M. and Ryan, G.R. (1967) Western Australia Geological Survey 1:250,000 Geological Series, Pyramid. Explanatory Notes: Sheet SF/50-7., 1-39.

Kump, L. and Barley, M. (2007) Increased subaerial volcanism and the rise of atmospheric oxygen 2.5 billion years ago. Nature 448, 1033-1036.

Ladygina, N., Dedyukhina, E. and Vainshtein, M. (2006) A review on microbial synthesis of hydrocarbons. Process Biochemistry 41, 1001-1014.

Latifi, A., Ruiz, M. and Zhang, C.-C. (2009) Oxidative stress in cyanobacteria. FEMS microbiology reviews 33, 258-278.

Lehninger, A. (2008) Principles of Biochemistry. Freeman and Company, New York.

Leonid, B. (2014) Eubacterial rhodopsins - Unique photosensors and diverse ion pumps. Biochimica et biophysica acta 1837, 553-561.

Li, N., Chang, W.-C., Warui, D., Booker, S., Krebs, C. and Bollinger, J. (2012) Evidence for only oxygenative cleavage of aldehydes to alk(a/e)nes and formate by cyanobacterial aldehyde decarbonylases. Biochemistry 51, 7908-7916.

Li, N., Nørgaard, H., Warui, D., Booker, S., Krebs, C. and Bollinger, J. (2011) Conversion of fatty aldehydes to alka(e)nes and formate by a cyanobacterial aldehyde decarbonylase: cryptic redox by an unusual dimetal oxygenase. Journal of the American Chemical Society 133, 6158-6161.

Li, W., Czaja, A.D., Van Kranendonk, M.J., Beard, B.L., Roden, E.E. and Johnson, C.M. (2013) An anoxic, Fe(II)-rich, U-poor ocean 3.46 billion years ago. Geochimica et Cosmochimica Acta 120, 65-79.

Lingwood, D. and Simons, K. (2010) Lipid rafts as a membrane-organizing principle. Science 327, 46-50.

Liscombe, D., Louie, G. and Noel, J. (2012) Architectures, mechanisms and molecular evolution of natural product methyltransferases. Natural product reports 29, 1238-1250.

Liu, A., Zhu, T., Lu, X. and Song, L. (2013) Hydrocarbon profiles and phylogenetic analyses of diversified cyanobacterial species. Applied Energy 111, 383-393.

Llopiz, P., Neunlist, S. and Rohmer, M. (1992) Prokaryotic triterpenoids: O-alpha-D-glucuronopyranosyl bacteriohopanetetrol, a novel hopanoid from the bacterium Rhodospirillum rubrum. The Biochemical journal 287 (Pt 1), 159-161.

Lu, H., Peng, P.a. and Sun, Y. (2003) Molecular and stable carbon isotopic composition of monomethylalkanes from one oil sand sample: source implications. Organic Geochemistry 34, 745-754.

Lyons, T., Reinhard, C. and Planavsky, N. (2014) The rise of oxygen in Earth's early ocean and atmosphere. Nature 506, 307-315.

Mahato, S., Nandy, A. and Roy, G. (1992) Triterpenoids. Phytochemistry 31, 2199-2149.

Makushina, V.M., Arefev, O.A., Zabrodina, M.N. and Petrov, A.A. (1978) New relic alkanes of petroleums. Neftekhimiya 18, 847-851.

Mathis, P. (1990) Compared structure of plant and bacterial photosynthetic reaction centers. Evolutionary implications. Biochimica et Biophysica Acta - Bioenergetics 1018, 163-167.

Mauzerall, D. (1992) Light, iron, Sam Granick and the origin of life. Photosynthesis Research 33, 163-170.

McCollom, T.M. and Seewald, J.S. (2006) Carbon isotope composition of organic compounds produced by abiotic synthesis under hydrothermal conditions. Earth and Planetary Science Letters 243, 74-84.

Mendez-Perez, D., Begemann, M. and Pfleger, B. (2011) Modular synthase-encoding gene involved in α-olefin biosynthesis in Synechococcus sp. strain PCC 7002. Applied and environmental microbiology 77, 4264-4267.

Meyer, T.E., Van Beeumen, J.J., Ambler, R.P. and Cusanovich, M.A. (1996) The evolution of electron transfer proteins in photosynthetic bacteria and denitrifying pseudomonads, in: Baltscheffsky, H. (Ed.), Origin and Evolution of Biological Energy Conversion. VCH Publishers, New York, pp. 71–108.

Mlynek, G., Sjöblom, B., Kostan, J., Füreder, S., Maixner, F., Gysel, K., Furtmüller, P., Obinger, C., Wagner, M., Daims, H. and Djinović-Carugo, K. (2011) Unexpected diversity of chlorite dismutases: a catalytically efficient dimeric enzyme from Nitrobacter winogradskyi. Journal of Bacteriology 193, 2408-2417.

Moran, N.A. and Wernegreen, J.J. (2000) Lifestyle evolution in symbiotic bacteria: insights from genomics. Trends in Ecology & Evolution 15, 321-326.

Mulkidjanian, A.Y. and Junge, W. (1997) On the origin of photosynthesis as inferred from sequence analysis. Photosynthesis Research 51, 27-42.

Mycke, B., Narjes, F. and Michaelis, W. (1987) Bacteriohopanetetrol from chemical degradation of an oil shale kerogen. Nature 326, 179-181.

Nakamura, Y., Kaneko, T., Sato, S., Mimuro, M., Miyashita, H., Tsuchiya, T., Sasamoto, S., Watanabe, A., Kawashima, K., Kishida, Y., Kiyokawa, C., Kohara, M., Matsumoto, M., Matsuno, A., Nakazaki, N., Shimpo, S., Takeuchi, C., Yamada, M. and Tabata, S. (2003) Complete Genome Structure of Gloeobacter violaceus PCC 7421, a Cyanobacterium that Lacks Thylakoids. DNA Research 10, 137-145.

Nelson, D.R. (1998) Compilation of SHRIMP U-Pb zircon geochronology data. . Western Australia Geological Survey, Record 1998/2.

Nelson, D.R., Trendall, A.F. and Altermann, W. (1999) Chronological correlations between the Pilbara and Kaapvaal cratons. Precambrian Research 97, 165-189.

Nelson, N. and Ben-Shem, A. (2004) The complex architecture of oxygenic photosynthesis. Nature Reviews Molecular Cell Biology 5, 971-982.

Nes, W., McCourt, B., Zhou, W., Ma, J., Marshall, J., Peek, L. and Brennan, M. (1998) Overexpression, purification, and stereochemical studies of the recombinant (S)-adenosyl-L-methionine: delta 24(25)-to delta 24(28)-sterol methyl transferase enzyme from Saccharomyces cerevisiae. Archives of biochemistry and biophysics 353, 297-311.

Neunlist, S., Bisseret, P. and Rohmer, M. (1988) The hopanoids of the purple non-sulfur bacteria *Rhodopseudomonas palustris* and *Rhodopseudomonas acidophila* and the absolute configuration of bacteriohopanetetrol. European journal of biochemistry / FEBS 171, 245-252.

Neunlist, S., Holst, O. and Rohmer, M. (1985) Prokaryotic triterpenoids - the hopanoids of the purple non-sulphur bacterium *Rhodomicrobium vannielii*: an aminotriol and its aminoacyl derivatives, N-tryptophanyl and N-ornithinyl aminotriol. European Journal of Biochemistry 147, 561-568.

Niehaus, T., Kinison, S., Okada, S., Yeo, Y.-s., Bell, S., Cui, P., Devarenne, T. and Chappell, J. (2012) Functional identification of triterpene methyltransferases from Botryococcus braunii race B. The Journal of biological chemistry 287, 8163-8173.

Nisbet, E.G., Grassineau, N.V., Howe, C.J., Abell, P.I., Regelous, M. and Nisbet, R.E.R. (2007) The age of Rubisco: the evolution of oxygenic photosynthesis. Geobiology 5, 311-335.

Nitschke, W., Mühlenhoff, U. and Liebl, U. (1998) Evolution, in: Raghavendra, A. (Ed.), Photosynthesis: a Comprehensive Treatise. Cambridge University Press, Cambridge, pp. 285-304.

Nitschke, W. and Rutherford, A. (1991) Photosynthetic reaction centres: variations on a common structural theme? Trends in biochemical sciences 16, 241-245.

Nutman, A., Mojzsis, S. and Friend, C. (1997) Recognition of ≥3850 Ma water-lain sediments in West Greenland and their significance for the early Archaean Earth. Geochimica Et Cosmochimica Acta 61, 2475-2484.

O'Leary, M.H. (1988) Carbon Isotopes in Photosynthesis. Bioscience 38, 328-337.

Ohmoto, H. (1997) When did the Earth's atmosphere become oxic? Geochem. News 93, 12-13, 26-27.

Ohmoto, H., Watanabe, Y., Ikemi, H., Poulson, S.R. and Taylor, B.E. (2006) Sulphur isotope evidence for an oxic Archaean atmosphere. Nature 442, 908-908.

Olson, J.M. and Blankenship, R.E. (2004) Thinking about the evolution of photosynthesis. Photosynthesis Research 80, 373-386.

Olson, J.M., Prince, R.C. and Brune, D.C. (1976) Reaction center complexes from green bacteria, Chlorophyll Proteins, Reaction Centers and Photosynthetic Membranes. Brookhaven National Laboratory, Upton, New York, pp. 238–246.

Ourisson, G. and Albrecht, P. (1992) Hopanoids. 1. Geohopanoids: the most abundant natural products on Earth? Accounts of Chemical Research 25, 398-402.

Ourisson, G., Rohmer, M. and Poralla, K. (1987) Prokaryotic Hopanoids and other Polyterpenoid Sterol Surrogates. Annual Review of Microbiology 41, 301-333

Overmann, J. and Garcia-Pichel, F. (2006) The phototrophic way of life. Springer, 32-85.

Packer, B.M. (1990) Sedimentology, Paleontology and Isotope-Geochemistry of Selected Formations in the 2.7 Billion-Year-Old Fortescue Group, Western Australia. Ph.D dissertation, University of Calfornia, Los Angeles.

Paoletti, C., Pushparaj, B., Florenzano, G., Capella, P. and Lercker, G. (1976) Unsaponifiable matter of green and blue-green algal lipids as a factor of biochemical differentiation of their biomasses: I. Total unsaponifiable and hydrocarbon fraction. Lipids 11, 258-265.

Pavlov, A. and Kasting, J. (2002) Mass-independent fractionation of sulfur isotopes in Archean sediments: strong evidence for an anoxic Archean atmosphere. Astrobiology 2, 27-41.

Payne, J.L., McClain, C.R., Boyer, A.G., Brown, J.H., Finnegan, S., Kowalewski, M., Krause Jr, R.A., Lyons, S.K., McShea, D.W. and Novack-Gottshall, P.M. (2011) The evolutionary consequences of oxygenic photosynthesis: a body size perspective. Photosynthesis Research 107, 37-57.

Pearson, A., Budin, M. and Brocks, J.J. (2003) Phylogenetic and biochemical evidence for sterol synthesis in the bacterium *Gemmata obscuriglobus*. Proceedings of the National Academy of Sciences of the United States of America 100, 15352-15357.

Pearson, A., Flood Page, S., Jorgenson, T., Fischer, W. and Higgins, M. (2007) Novel hopanoid cyclases from the environment. Environmental Microbiology 9, 2175-2188.

Pearson, A., Leavitt, W.D., Saenz, J.P., Summons, R.E., Tam, M.C.M. and Close, H.G. (2009) Diversity of hopanoids and squalene hopene cyclases across a tropical land sea gradient. Environmental Microbiology 11, 1208-1223.

Pepper, A.S. and Dodd, T.A. (1995) Simple kinetic models of petroleum formation. Part II: oil-gas cracking. Marine and Petroleum Geology 12, 321-340.

Pereira, M., Santana, M. and Teixeira, M. (2001) A novel scenario for the evolution of haem-copper oxygen reductases. Biochimica et biophysica acta 1505, 185-208.

Peters, K.E., Walters, C.C. and Moldowan, J.M. (2005) The biomarker guide: Biomarkers and isotopes in the environment and human history. Cambridge University Press Volume 1.

Planavsky, N.J., Asael, D., Hofmann, A., Reinhard, C.T., Lalonde, S.V., Knudsen, A., Wang, X., Ossa, F.O., Pecoits, E., Smith, A.J.B., Beukes, N.J., Bekker, A., Johnson, T.M., Konhauser, K.O., Lyons, T.W. and Rouxel, O.J. (2014) Evidence for oxygenic photosynthesis half a billion years before the Great Oxidation Event. Nature Geoscience 7, 283-286.

Poger, D. and Mark, A. (2013) The Relative Effect of Sterols and Hopanoids on Lipid Bilayers: When Comparable Is Not Identical. The journal of physical chemistry. B 117, 16129-16140.

Posth, N.R., Canfield, D.E. and Kappler, A. (2014) Biogenic Fe(III) minerals: From formation to diagenesis and preservation in the rock record. Earth-Science Reviews 135, 103-121.

Price, L.C. (1993) Thermal stability of hydrocarbons in nature: Limits, evidence, characteristics, and possible controls. Geochimica Et Cosmochimica Acta 57, 3261-3280.

Price, L.C. (2000) Organic metamorphism in the California petroleum basins: Chap. B—Insights from extractable bitumen and saturated hydrocarbons. U. S. Geological Survey Bulletin B, 2174-B.

Price, L.C. and DeWitt, E. (2001) Evidence and characteristics of hydrolytic disproportionation of organic matter during metasomatic processes. Geochimica et Cosmochimica Acta 65, 3791-3826.

Racolta, S., Juhl, P., Sirim, D. and Pleiss, J. (2012) The triterpene cyclase protein family: a systematic analysis. Proteins 80, 2009-2019.

Rashby, S.E., Sessions, A.L., Summons, R.E. and Newman, D.K. (2007) Biosynthesis of 2-methylbacteriohopanepolyols by an anoxygenic phototroph. Proceedings of the National Academy of Sciences of the United States of America 104, 15099-15104.

Rasmussen, B. (2000) Filamentous microfossils in a 3,235-million-year-old volcanogenic massive sulphide deposit. Nature 405, 676-679.

Rasmussen, B., Fletcher, I.R., Brocks, J.J. and Kilburn, M.R. (2008) Reassessing the first appearance of eukaryotes and cyanobacteria. Nature 455, 1101-1104.

Raymond, J. and Segrè, D. (2006) The effect of oxygen on biochemical networks and the evolution of complex life. Science 311, 1764-1767.

Raymond, J., Zhaxybayeva, O., Gogarten, J.P., Gerdes, S.Y. and Blankenship, R.E. (2002) Whole-genome analysis of photosynthetic prokaryotes. Science 298, 1616-1620.

Renoux, J. and Rohmer, M. (1985) Prokaryotic triterpenoids. New bacteriohopanetetrol cyclitol ethers from the methylotrophic bacterium Methylobacterium organophilum. European journal of biochemistry / FEBS 151, 405-410.

Rezende, E. (2013) Evolution. Better oxygen delivery. Science 340, 1293-1294.

Ricci, J., Coleman, M., Welander, P., Sessions, A., Summons, R., Spear, J. and Newman, D. (2013) Diverse capacity for 2-methylhopanoid production correlates with a specific ecological niche. The ISME journal 8, 675-684.

Rikken, G.B., Kroon, A.G.M. and Ginkel, C.G.v. (1996) Transformation of (per)chlorate into chloride by a newly isolated bacterium: reduction and dismutation. Applied Microbiology and Biotechnology 45, 420-426.

Rippka, R., Deruelles, J., Waterbury, J.B., Herdman, M. and Stanier, R.Y. (1979) Generic assignments, strain histories and properties of pure cultures of cyanobacteria. Journal of General Microbiology 111, 1-61.

Robinson, N. and Eglinton, G. (1990) Lipid chemistry of Icelandic hot spring microbial mats. Organic Geochemistry 15, 291-298.

Rohmer, M., Bouvier-Nave, P. and Ourisson, G. (1984) Distribution of Hopanoid Triterpenes in Prokaryotes. Journal of General Microbiology 130, 1137-1150.

Rohmer, M. and Ourisson, G. (1976) Structure des bactériohopanetétrols d'acetobacter xylinum. Tetrahedron Letters 17, 3633-3636.

Rosing, M.T. and Frei, R. (2004) U-rich Archaean sea-floor sediments from Greenland; indications of >3700 Ma oxygenic photosynthesis. Earth and Planetary Science Letters 217, 237-244.

Sáenz, J., Sezgin, E., Schwille, P. and Simons, K. (2012) Functional convergence of hopanoids and sterols in membrane ordering. Proceedings of the National Academy of Sciences of the United States of America 109, 14236-14240.

Sáenz, J.P., Wakeham, S.G., Eglinton, T.I. and Summons, R.E. (2011) New constraints on the provenance of hopanoids in the marine geologic record: Bacteriohopanepolyols in marine suboxic and anoxic environments. Organic Geochemistry 42, 1351-1362.

Saito, M. (2012) The rise of oxygen and aerobic biochemistry. Structure 20, 1-2.

Sakurai, R., Ito, M., Ueno, Y., Kitajima, K. and Maruyama, S. (2005) Facies architecture and sequence-stratigraphic features of the Tumbiana Formation in the Pilbara Craton, northwestern Australia; implications for depositional environments of oxygenic stromatolites during the late Archean. Precambrian Research 138, 255-273.

Scanlan, D.J. (2012) Marine Picocyanobacteria, in: Whitton, B.A. (Ed.), Ecology of Cyanobacteria II: Their Diversity in Space and Time. Science+Business Media, pp. 503-533.

Schidlowski, M. (1983) Evolution of photoautotrophy and early atmospheric oxygen levels. Precambrian Research 20, 319-335.

Schidlowski, M. (2001) Carbon isotopes as biogeochemical recorders of life over 3.8 Ga of Earth history: evolution of a concept. Precambrian Research 106, 117-134.

Schirmer, A., Rude, M.A., Li, X., Popova, E. and Del Cardayre, S.B. (2010) Microbial biosynthesis of alkanes. Science 329, 559-562.

Schirrmeister, B., Antonelli, A. and Bagheri, H. (2011) The origin of multicellularity in cyanobacteria. BMC Evolutionary Biology 11, 45.

Schirrmeister, B., de Vos, J., Antonelli, A. and Bagheri, H. (2013) Evolution of multicellularity coincided with increased diversification of cyanobacteria and the Great Oxidation Event. Proceedings of the National Academy of Sciences of the United States of America 110, 1791-1796.

Schopf, J., Kudryavtsev, A., Agresti, D., Wdowiak, T. and Czaja, A. (2002) Laser--Raman imagery of Earth's earliest fossils. Nature 416, 73-76.

Schopf, J.W. (1993) Microfossils of the Early Archean Apex chert: new evidence of the antiquity of life. Science 260, 640-646.

Schopf, J.W. (2002) The fossil record: tracing the roots of the cyanobacterial lineage. Springer, 13-35.

Schopf, J.W. (2006) Fossil evidence of Archaean life. Philosophical Transactions of the Royal Society B: Biological Sciences 361, 869-885.

Schopf, J.W. (2012) The Fossil Record of Cyanobacteria, in: Whitton, B.A. (Ed.), Ecology of Cyanobacteria II: Their Diversity in Space and Time. Springer Science+Business Media, pp. 15-36.

Schopf, J.W., Kudryavtsev, A.B., Czaja, A.D. and Tripathi, A.B. (2007) Evidence of Archean life: Stromatolites and microfossils. Precambrian Research 158, 141-155.

Schopf, J.W. and Packer, B.M. (1987) Early Archean (3.3-Billion to 3.5-Billion-Year-Old) Microfossils from Warrawoona Group, Australia. Science 237, 70-73.

Schouten, S., Hopmans, E.C., Schefuß, E. and Sinninghe Damsté, J.S. (2002) Distributional variations in marine crenarchaeotal membrane lipids: a new tool for reconstructing ancient sea water temperatures? Earth and Planetary Science Letters 204, 265-274.

Schubert, W., Klukas, O., Saenger, W., Witt, H., Fromme, P. and Krauss, N. (1998) A common ancestor for oxygenic and anoxygenic photosynthetic systems: a comparison based on the structural model of photosystem I. Journal of Molecular Biology 280, 297-314.

Scott, C.T., Bekker, A., Reinhard, C.T., Schnetger, B., Krapež, B., Rumble, D. and Lyons, T.W. (2011) Late Archean euxinic conditions before the rise of atmospheric oxygen. Geology 39, 119-122.

Sherman, L.S., Waldbauer, J.R. and Summons, R.E. (2007) Improved methods for isolating and validating indigenous biomarkers in Precambrian rocks. Organic Geochemistry 38, 1987-2000.

Shiea, J., Brassel, S.C. and Ward, D.M. (1991) Comparative analysis of extractable lipids in hot spring microbial mats and their component photosynthetic bacteria. Organic Geochemistry 17, 309-319.

Shiea, J., Brassell, S.C. and Ward, D.M. (1990) Mid-chain branched mono- and dimethyl alkanes in hot spring cyanobacterial mats: A direct biogenic source for branched alkanes in ancient sediments? Organic Geochemistry 15, 223-231.

Siebert, C., Kramers, J.D., Meisel, T., Morel, P. and Nägler, T.F. (2005) PGE, Re-Os, and Mo isotope systematics in Archean and early Proterozoic sedimentary systems as proxies for redox conditions of the early Earth. Geochimica Et Cosmochimica Acta 69, 1787-1801.

Siebert, C., Nägler, T.F., von Blanckenburg, F. and Kramers, J.D. (2003) Molybdenum isotope records as a potential new proxy for paleoceanography. Earth and Planetary Science Letters 211, 159-171.

Siedenburg, G. and Jendrossek, D. (2011) Squalene-hopene cyclases. Applied and environmental microbiology 77, 3905-3915.

Simons, K. and Ikonen, E. (1997) Functional rafts in cell membranes. Nature 387, 569-572.

Sinninghe-Damsté, J.S., Rijpstra, W.I.C., Schouten, S., Fuerst, J.A., Jetten, M.S.M. and Strous, M. (2004) The occurrence of hopanoids in planctomycetes: implications for the sedimentary biomarker record. Organic Geochemistry 35, 561-566.

Smith, R.E., Perdrix, J.L. and Parks, T.C. (1982) Burial Metamorphism in the Hamersley Basin, Western Australia. Journal of Petrology 23, 75-102.

Smithies, R.H. (1998) Geology of the Mount Wohler 1:100 000 Sheet, Geological Survey of Western Australia. Explanatory Notes 1, 19.

Spudich, J.L. and Jung, K.H. (2008) Microbial Rhodopsins. Protein Science Encyclopedia.

Strauss, S. and Moore, T. (1992) Abundances and isotopic compositions of carbon and sulfur speciedin whole rock and kerogen samples, in: Schopf, J.W., Klein, K. (Eds.), The Proterozoic biosphere: a amultidisciplinary study. Cambridge University Press, Cambridge, pp. 709-808.

Stüeken, E.E., Catling, D.C. and Buick, R. (2012) Contributions to late Archaean sulphur cycling by life on land. Nature Geoscience 5, 722-725.

Summons, R., Jahnke, L. and Roksandic, Z. (1994) Carbon isotopic fractionation in lipids from methanotrophic bacteria: relevance for interpretation of the geochemical record of biomarkers. Geochimica Et Cosmochimica Acta 58, 2853-2863.

Summons, R.E. (1987) Branched alkanes from ancient and modern sediments: Isomer discrimination by GC/MS with multiple reaction monitoring. Organic Geochemistry 11, 281-289.

Summons, R.E. and Hallmann, C. (2014) 12.2 - Organic Geochemical Signatures of Early Life on Earth, in: Holland, H.D., Turekian, K.K. (Eds.), Treatise on Geochemistry (Second Edition). Elsevier, Oxford, pp. 33-46.

Summons, R.E., Jahnke, L.L., Hope, J.M. and Logan, G.A. (1999) 2-Methylhopanoids as biomarkers for cyanobacterial oxygenic photosynthesis. Nature 400, 554-557.

Summons, R.E., Powell, T.G. and Boreham, C.J. (1988) Petroleum geology and geochemistry of the Middle Proterozoic McArthur Basin, Northern Australia: III. Composition of extractable hydrocarbons. Geochimica Et Cosmochimica Acta 52, 1747-1763.

Summons, R.E. and Walter, M.R. (1990) Molecular fossils and microfossils of prokaryotes and protists from Proterozoic sediments. American Journal of Science 290-A, 212-244.

Talbot, H.M., Summons, R.E., Jahnke, L.L., Cockell, C.S., Rohmer, M. and Farrimond, P. (2008) Cyanobacterial bacteriohopanepolyol signatures from cultures and natural environmental settings. Organic Geochemistry 39, 232-263.

Tebo, B.M., Johnson, H.A., McCarthy, J.K. and Templeton, A.S. (2005) Geomicrobiology of manganese(II) oxidation. Trends in microbiology 13, 421-428.

Thannickal, V. (2009) Oxygen in the evolution of complex life and the price we pay. American journal of respiratory cell and molecular biology 40, 507-510.

Thiel, V., Blumenberg, M., Pape, T., Seifert, R. and Michaelis, W. (2003) Unexpected occurrence of hopanoids at gas seeps in the Black Sea. Organic Geochemistry 34, 81-87.

Thiel, V., Jenisch, A., Wörheide, G., Löwenberg, A., Reitner, J. and Michaelis, W. (1999) Mid-chain branched alkanoic acids from "living fossil" demosponges: a link to ancient sedimentary lipids? Organic Geochemistry 30, 1-14.

Thomazo, C., Ader, M., Farquhar, J. and Philippot, P. (2009) Methanotrophs regulated atmospheric sulfur isotope anomalies during the Mesoarchean (Tumbiana Formation, Western Australia). Earth and Planetary Science Letters 279, 65-75.

Thompson, A., Carter, B., Turk-Kubo, K., Malfatti, F., Azam, F. and Zehr, J. (2014) Genetic diversity of the unicellular nitrogen-fixing cyanobacteria UCYN-A and its prymnesiophyte host. Environmental Microbiology Online version.

Thompson, A.W., Foster, R.A., Krupke, A., Carter, B.J., Musat, N., Vaulot, D., Kuypers, M.M.M. and Zehr, J.P. (2012) Unicellular cyanobacterium symbiotic with a single-celled eukaryotic alga. Science 337, 1546-1550.

Thorne, A.M. and Trendall, A.F. (2001) Geology of the Fortescue Group, Pilbara Craton, Western Australia. Bulletin - Geological Survey of Western Australia, 249.

Tice, M. and Lowe, D. (2004) Photosynthetic microbial mats in the 3,416-Myr-old ocean. Nature 431, 549-552.

Tissot, B.P. and Welte, D.H. (1984) Petroleum Formation and Occurrence, 2nd edition. Springer-Verlag, Berlin.

Tomazic, M., Poklepovich, T., Nudel, C. and Nusblat, A. (2014) Incomplete sterols and hopanoids pathways in ciliates: Gene loss and acquisition during evolution as a source of biosynthetic genes. Molecular phylogenetics and evolution 74, 122-134.

Tomitani, A., Knoll, A., Cavanaugh, C. and Ohno, T. (2006) The evolutionary diversification of cyanobacteria: molecular-phylogenetic and paleontological perspectives. Proceedings of the National Academy of Sciences of the United States of America 103, 5442-5447.

Tossell, J.A. (2005) Calculating the partitioning of the isotopes of Mo between oxidic and sulfidic species in aqueous solution. Geochimica Et Cosmochimica Acta 69, 2981-2993.

Trendall, A. (2009) The significance of iron-formation in the Precambrian stratigraphic record, in: Altermann, W., Corcoran, P.L. (Eds.), Precambrian sedimentary environ ments: a modern approach to ancient depositional systems. Blackwell Publishing Ltd., Oxford, pp. 33-66.

Trendall, A.F., Compston, W., Nelson, D.R., Laeter, J.R.D. and Bennett, V.C. (2004) SHRIMP zircon ages constraining the depositional chronology of the Hamersley Group, Western Australia. Australian Journal of Earth Sciences 51, 621-644.

Tripp, H., Bench, S., Turk, K., Foster, R., Desany, B., Niazi, F., Affourtit, J. and Zehr, J. (2010) Metabolic streamlining in an open-ocean nitrogen-fixing cyanobacterium. Nature 464, 90-94.

van Ginkel, C., Rikken, G., Kroon, A. and Kengen, S. (1996) Purification and characterization of chlorite dismutase: a novel oxygen-generating enzyme. Archives of microbiology 166, 321-326.

Van Kranendonk, M., Philippot, P., Lepot, K., Bodorkos, S. and Pirajno, F. (2008) Geological setting of Earth's oldest fossils in the ca. 3.5 Ga Dresser Formation, Pilbara Craton, Western Australia. Precambrian Research 167, 93-124.

Van Kranendonk, M.J. (2014) Earth's early atmosphere and surface environments: A review. Geological Society of America Special Papers 504, 105-130.

van Meer, G., Voelker, D. and Feigenson, G. (2008) Membrane lipids: where they are and how they behave. Nature reviews. Molecular cell biology 9, 112-124.

Ventura, G., Kenig, F., Reddy, C., Schieber, J., Frysinger, G., Nelson, R., Dinel, E., Gaines, R. and Schaeffer, P. (2007) Molecular evidence of Late Archean archaea and the presence of a subsurface hydrothermal biosphere. Proceedings of the National Academy of Sciences of the United States of America 104, 14260-14265.

Vermaas, W.F.J. (2002) Evolution of photosynthesis, Encyclopedia of Life Sciences. Nature Publishing Group, London, pp. 1-18.

Vilcheze, C., Llopiz, P., Neunlist, S., Poralla, K. and Rohmer, M. (1994) Prokaryotic triterpenoids: new hopanoids from the nitrogen-fixing bacteria *Azotobacter vinelandii*, *Beijerinckia indica* and *Beijerinckia mobilis*. Microbiology 140, 2749-2753.

Voegelin, A.R., Nägler, T.F., Beukes, N.J. and Lacassie, J.P. (2010) Molybdenum isotopes in late Archean carbonate rocks: Implications for early Earth oxygenation. Precambrian Research 182, 70-82.

Volkman, J.K. (2005) Sterols and other triterpenoids: source specificity and evolution of biosynthetic pathways. Organic Geochemistry 36, 139-159.

Volkman, J.V. (2003) Sterols in microorganisms. Applied Microbiology and Biotechnology 60, 495-506.

Waldbauer, J.R., Newman, D.K. and Summons, R.E. (2011) Microaerobic steroid biosynthesis and the molecular fossil record of Archean life. Proceedings of the National Academy of Sciences 108, 13409-13414.

Waldbauer, J.R., Sherman, L.S., Sumner, D.Y. and Summons, R.E. (2009) Late Archean molecular fossils from the Transvaal Supergroup record the antiquity of microbial diversity and aerobiosis. Precambrian Research 169, 28-47.

Walsh, M. (1992) Microfossils and possible microfossils from the Early Archean Onverwacht Group, Barberton Mountain Land, South Africa. Precambrian Research 54, 271-293.

Walter, M. (1983) Archean stromatolites: Evidence of the Earth's earliest benthos, in: Schopf, J. (Ed.), Earth's Earliest Biosphere: It's Origin and Evolution. Princeton University Press, Princeton, pp. 187-213.

Wang, M., Jiang, Y.-Y., Kim, K., Qu, G., Ji, H.-F., Mittenthal, J., Zhang, H.-Y. and Caetano-Anollés, G. (2011) A universal molecular clock of protein folds and its power in tracing the early history of aerobic metabolism and planet oxygenation. Molecular biology and evolution 28, 567-582.

Wang, W., Zhou, Z.-Y. and Yu, P. (2005) Relations Between Vitrinite Reflectance, Peek Temperature and its Neighboring Temperature Variation Rate: A Comparison of Methods. Chinese Journal of Geophysics 48, 1443-1453.

Warton, B., Alexander, R. and Kagi, R.I. (1997) Identification of some single branched alkanes in crude oils. Organic Geochemistry 27, 465-476.

Welander, P.V., Coleman, M.L., Sessions, A.L., Summons, R.E. and Newman, D.K. (2010) Identification of a methylase required for 2-methylhopanoid production and implications for the interpretation of sedimentary hopanes. Proceedings of the National Academy of Sciences 107, 8537-8542.

Welander, P.V. and Summons, R.E. (2012) Discovery, taxonomic distribution, and phenotypic characterization of a gene required for 3-methylhopanoid production. Proceedings of the National Academy of Sciences 109, 12905-12910.

Wenger, L.M., Davis, C.L. and Isaksen, G.H. (2002) Multiple controls on petroleum biodegradation and impact on oil quality. SPE Reservoir Evaluation & Engineering 5, 375-383.

Widdel, F., Schnell, S., Heising, S., Ehrenreich, A., Assmus, B. and Schink, B. (1993) Ferrous iron oxidation by anoxygenic phototrophic bacteria. Nature 362, 834-836.

Wikstrom, M.K. (1977) Proton pump coupled to cytochrome c oxidase in mitochondria. Nature 266, 271-273.

Wille, M., Kramers, J.D., Nägler, T.F., Beukes, N.J., Schröder, S., Th, M., Lacassie, J.P. and Voegelin, A.R. (2007) Evidence for a gradual rise of oxygen between 2.6 and 2.5 Ga from Mo isotopes and Re-PGE signatures in shales. Geochimica Et Cosmochimica Acta 71, 2417-2435.

Wille, M., Nebel, O., Van Kranendonk, M.J., Schoenberg, R., Kleinhanns, I.C. and Ellwood, M.J. (2013) Mo–Cr isotope evidence for a reducing Archean atmosphere in 3.46–2.76 Ga black shales from the Pilbara, Western Australia. Chemical Geology 340, 68-76.

Wu, M., de Vries, S., van Alen, T., Butler, M., Op den Camp, H., Keltjens, J., Jetten, M. and Strous, M. (2011) Physiological role of the respiratory quinol oxidase in the anaerobic nitrite-reducing methanotroph 'Candidatus Methylomirabilis oxyfera'. Microbiology (Reading, England) 157, 890-898.

Xiong, J. and Bauer, C. (2002) A cytochrome b origin of photosynthetic reaction centers: an evolutionary link between respiration and photosynthesis. Journal of Molecular Biology 322, 1025-1037.

Xu, R., Fazio, G. and Matsuda, S. (2004) On the origins of triterpenoid skeletal diversity. Phytochemistry 65, 261-291.

Yano, J. and Yachandra, V. (2014) Mn_4Ca Cluster in Photosynthesis: Where and How Water is Oxidized to Dioxygen. Chemical reviews 114, 4175-4205.

Zehr, J., Bench, S., Carter, B., Hewson, I., Niazi, F., Shi, T., Tripp, H. and Affourtit, J. (2008) Globally distributed uncultivated oceanic N2-fixing cyanobacteria lack oxygenic photosystem II. Science 322, 1110-1112.

Zeng, Y., Feng, F., Medová, H., Dean, J. and Kobližek, M. (2014) Functional type 2 photosynthetic reaction centers found in the rare bacterial phylum Gemmatimonadetes. Proceedings of the National Academy of Sciences of the United States of America 111, 7795-7800.

Zerkle, A.L., Claire, M.W., Domagal-Goldman, S.D., Farquhar, J. and Poulton, S.W. (2012) A bistable organic-rich atmosphere on the Neoarchaean Earth. Nature Geoscience 5, 359-363.

Zerkle, A.L., House, C.H., Cox, R.P. and Canfield, D.E. (2006) Metal limitation of cyanobacterial N_2 fixation and implications for the Precambrian nitrogen cycle. Geobiology 4, 285-297.

Zundel, M. and Rohmer, M. (1985a) Prokaryotic triterpenoids 1. 3β-Methylhopanoids from *Acetobacter* species and *Methylococcuscapsulatus*. European Journal of Biochemistry 150, 23-27.

Zundel, M. and Rohmer, M. (1985b) Prokaryotic triterpenoids 3. The biosynthesis of 2β-methylhopanoids and 3β-methylhopanoids. European Journal of Biochemistry 150, 35-39.

Chapter 2.

Methodology and contamination source identification and monitoring

2.1. Difficulties of Precambrian biomarker research

The search for Precambrian biomarkers has always been a struggle with trace contamination problems. Hydrocarbons were first extracted from Archean rocks more than 30 years ago, but their significance was discounted after amino acids of recent origin were found in the same rocks (Hayes et al., 1983). In the late 1990s the discovery of biomarkers for cyanobacteria and eukaryotes in the Archean Fortescue Group, Western Australia revitalised Archean biomarker research (Brocks et al., 1999). Subsequently, several additional studies discovered the same biomarkers, suggesting the presence of cyanobacteria and eukaryotes in the Archean (Brocks et al., 2003; Eigenbrode et al., 2008; Waldbauer et al., 2009; Coffey, 2011). However, these findings are now called into question again. It has been shown that kerogen and pyrobitumen in Archean drill cores are strongly depleted in ^{13}C, which is inconsistent with the isotopic data of extracted bitumens from the same cores which yielded supposedly Archean biomarkers (Rasmussen et al., 2008). Thus, the detected biomarkers are suspected to be from later migration or contamination. Furthermore, the spatial distribution of hydrocarbon biomarkers in some drill cores from the Fortescue Group suggests that the biomarkers are not indigenous (Brocks, 2011).

The examination of the spatial distribution of biomarkers using slice experiments as reported by Brocks (2011) is indeed an effective method to prove the indigeneity of detected hydrocarbons. A limited distribution of hydrocarbons on rock surfaces is a characteristic of contamination from surrounding environments (Sherman et al., 2007). In contrast, indigenous hydrocarbons show the opposite distribution pattern, i.e. they are more abundant inside a rock compared to on the outside

of the same rock, because the middle of the rock is protected and would be less subject to weathering. Thus, the spatial analyses of hydrocarbon concentrations can distinguish indigenous biomarker signals from later contamination. The slice method was applied by Coffey (2011) to investigate the Fortescue Group outcrop rocks, but the experimental contamination level was in some samples comparable to the amount of indigenous hydrocarbons present (less than ng amounts). In this study, essentially the same method was applied, but the experimental contamination level was reduced to the pg range, which allowed the identification of indigenous hydrocarbons with improved certainty.

2.2. Rock sampling

2.2.1. Outcrop rocks

Rock samples were selected at the outcrop based on their size and degree of fracturing. All collected rocks were at least 10 cm long in their smallest dimension, and were thus large enough to carry out slice experiments. Even if they did not have apparent fractures on the outside, once they were sliced, small fractures became visible inside many of the samples. Some of the fractured parts of samples were removed before crushing, but it was impossible to eliminate all fractures because there were many microscopic scale fractures not visible with the naked eye. Thus, any of the outcrop rock samples could have been subjected to later contamination. Even if a rock was contaminated through fractures, contaminants are expected to be distinguished by the slice method (Section 2.3.1). Collected rocks were covered with aluminium foil, sealed in plastic pails at the sites, and transported to the Macquarie University organic geochemistry laboratory by air freight.

2.2.2. Drill core sampling

Drill cores analysed in this study came from the Agouron Institute Drilling Project (French et al., 2013). The aim of the project was to critically examine the syngeneity of Archean biomarkers. Thus, the drilling protocols were designed to be strictly free from contamination. Only filtered water was used as the drilling fluid, so as to minimise hydrocarbon contamination. The drill cores were immediately

packed in Teflon bags filled with Ar gas, and were kept frozen during transport and storage until the last moment of experiment. More details of the drilling and sampling protocols are given in Chapter 5.

2.3. General solvent extraction procedure in the laboratory

The general extraction procedure for hydrocarbons is described here and is generally common to all the studies described in this thesis, although there were some minor modifications of the solvent extraction and analysis procedure for each study (described in detail in the later chapters). As the individual studies are submitted manuscripts, or are being prepared for submission, the overlapping parts are included here. The detailed contamination estimation procedure is described in Section 2.4.

2.3.1. Rock cutting

The rock samples were sliced using a diamond blade from the outside of the sample towards the inside, producing approximately 1 cm thick slices (Fig. 2.1, left). For details of the saw blades used, see Section 2.4.4. Each slice was cut into approximately 1 cm^3 pieces (Fig. 2.1, right). A basaltic lava flow from a nearby locality was tested as a procedural blank, before processing the actual samples. A solvent mixture of dichloromethane (DCM) and methanol (MeOH) (9:1, v/v) was used to extract hydrocarbons from the samples (see Section 2.4.3 for solvent details). All solvents were checked for purity by gas chromatography-mass spectroscopy (GC-MS) as described below. All glassware was combusted in an oven at 400 °C for 3 h before use. Between each slice experiment, all equipment was washed with Milli-Q water, MeOH and DCM and checked for purity by GC-MS (see Sections 2.4.4 and 2.4.5).

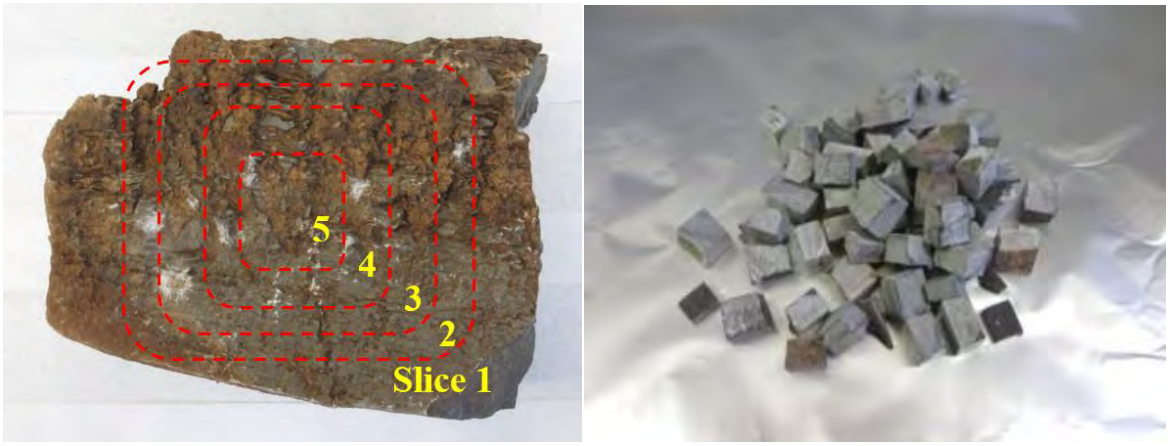

Figure 2.1. Outcrop rock slicing (left) and rock pieces after cutting (right, slice 1). The sample in the image is a stromatolite from the outcrop described in Chapter 3).

2.3.2. Rock crushing

Fine particles on the rock surfaces were removed by water washing and ultrasonication in filtered water for 10 min. Organic contamination on the surfaces was removed by ultrasonication with DCM and MeOH (9:1, v/v) for two cycles of 10 min, using a new solvent mixture each time. The last solvent mixture was analysed by GC-MS for purity and surface checking. If the cleaning was insufficient, additional ultrasonication steps were performed until the contamination level was < 1 ng. The rock was then ground to < 200 mesh grain size in a tungsten carbide ring-mill (Rocklab; Fig. 2.2). The mill was cleaned between samples (see Section 2.4.5).

Figure 2.2. Inside of the ring-mill crusher.

2.3.3. First solvent extraction (Ext. I)

Extraction of hydrocarbons from the rock powder was carried out by ultrasonication with 200 mL of the solvent mixture as described above, for two cycles of 10 min. Between the sonications, the solution was stirred using a glass rod and left to stand still for a few minutes. The solvent was collected in a round-bottom flask. The powder was further sonicated with a fresh 100 mL aliquot of DCM for 10 min to retrieve organic residues, particularly aliphatic hydrocarbons, in the mixed slurry of powder and solvent. The second solvent aliquot was added to the first solvent.

The extraction solution volume was reduced by rotary evaporation to 30-40 mL and centrifuged for 3 min at 2,000 rpm to remove suspended rock particles. The volume was then further reduced by rotary evaporation to approximately 5 mL. If the amount of suspended solids was low, the centrifuge step was omitted and the solvent was directly reduced to approximately 5 mL. Even after the centrifuge step, there were still some very fine rock particles suspended in the solvent for all samples. These were removed by filtering the solvent/sample mixture through silica gel (silica gel 60, 0.063-0.200 mm, Merck), which was pre-extracted and activated at 120 °C for > 4 hours before use. Column fractionation of the extractable organic matter (EOM) was not performed because the yield was very small (< 100 ng / g sample), the interference between aliphatic and aromatic hydrocarbons was not serious, and also to prevent the loss of hydrocarbons.

The EOM was spiked with three compounds as internal standards by adding 1 mL of a DCM solution containing about 50 ng of each: anthracene-d_{10} (98 atom %D, Isotec), p-terphenyl-d_{14} (98 atom %D, Isotec), and tetraeicosane-d_{50} (98 atom %D, Isotec). The volume of solvent containing the EOM was further reduced on a hot plate at 40 °C under a gentle nitrogen flow, until approximately 50 µL remained.

2.3.4. Second solvent extraction (Ext. II)

For some samples, the residual rock powder was treated with hydrochloric acid (HCl; 36%, RCI Labscan) to remove carbonate minerals such as calcite, dolomite and siderite. 100-150 mL of the HCl solution were added to the powder (~100 g) on a hot plate at 70 °C until effervescence stopped (Fig.

2.3). The resulting solution was washed with 500 mL of filtered water six times. The surplus acid-water mixture was discarded and the remaining powder slurry was air dried. Extraction of the decarbonated rock powder was performed as described in Section 2.3.3 for the first extraction.

Figure 2.3. HCl treatment.

Acid treatment of the rock powders was found to release a large amount of elemental sulphur, which can damage GC-MS instruments and interfere with hydrocarbon identification and quantification. Thus, elemental sulphur was removed by treatment of the EOM with activated copper. 5 g of copper particles (metal turnings, TG, Chem-Supply) were first treated with 36% HCl to remove CuO surficial layers and any remaining CuS residues from the previous experiment, and then washed with MeOH twice and DCM twice. The activated copper was added to the EOM and stirred for a minute. This simple procedure was enough to remove most sulphur, so that the reflux of the solution was not performed. Then, the copper particles were removed by decanting the EOM solution. The EOM solution was spiked with standards and prepared for GC-MS using the same procedure as for the first extraction (see Section 2.3.3).

2.3.5. Third solvent extraction (Ext. III)

For some samples, the powder residue was further treated with hydrofluoric acid (HF) (40%, Merck) to remove silicate minerals. Only 4 g of powder were used because of the danger caused by the reaction of large sample amounts with HF. 20 mL of HF solution were added to the powder in a Teflon container on a hot plate at 70 °C, and then left for 3-4 h (Fig. 2.4). This was repeated three

times to make sure the reaction was completed. The resulting solution was washed with filtered water three times. The surplus water was discarded and the remaining solution was air dried. Then, the solvent extraction procedure was repeated as described in Section 2.3.3 for the first extraction.

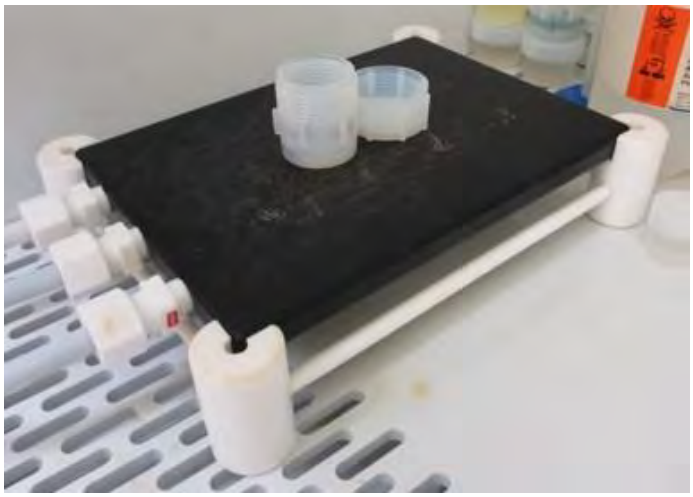

Figure 2.4. HF treatment.

2.3.6. Gas Chromatography-Mass Spectroscopy (GC-MS)

Benchtop GC-MS analysis was carried out on an Agilent GC (6890N) coupled to an Agilent Mass Selective Detector (5975B). 1 µL of the EOM solution was injected into a Programmable Temperature Vaporization (PTV) inlet operating in splitless mode with a J&W DB5MS column (length 60 m, inner diameter 0.25 mm, film thickness 0.25 µm). The inlet was ramped from 35 °C (3 min isothermal) to 310 °C (0.5 min isothermal) at a rate of 700 °C / min. Helium was used as the carrier gas (1.5 mL / min), and the temperature of the GC oven was ramped from 30 °C (2 min isothermal) to 310 °C (30 min isothermal) at a rate of 4 °C / min. The MS data were acquired in single ion monitoring mode, and in scan mode for organic-rich samples. Individual hydrocarbon identification was based on comparison of relative GC retention times and mass spectra with those previously reported. Semi-quantitative analyses were performed using the tetraeicosane-d_{50} internal standard, not taking into account any response factors. The other two standards were used to check sensitivity and repeatability of the measurement, but were not used for the quantification.

2.3.7. Further biomarker analysis

Biomarkers such as hopanes and steranes were detected in low amounts uing the benchtop GC-MS analysis procedure, and quantification was impossible except for a few compounds. Therefore, the samples were further analysed at the CSIRO North Ryde laboratories using a Thermo Trace Ultra GC interfaced with a high resolution Thermo DFS GC-MS system. GC was carried out on a J&W DB5MS column (length 60 m, inner diameter 0.25 mm, film thickness 0.25 μm). Helium was used as the carrier gas (1.5 mL / min). 1 μL of the EOM solution was injected into a splitless inlet operating at 260 °C in splitless mode. The MS was tuned to 1,000 resolution (electron energy 70 eV; source temperature 280 °C). The GC oven was ramped from 40 °C (2 min isothermal) to 200 °C at a rate of 4 °C / min, then to 310 °C (30 min isothermal) at a rate of 2 °C / min. The MS data were firstly acquired in single ion monitoring mode. For some samples, observed biomarkers were further analysed by metastable reaction monitoring (MRM). However, their abundance was too low to detect by MRM measurement. Thus, their identification was performed using their retention times and mass spectra, in comparison with the NSO-1 reference oil (Weiss et al., 2000).

2.4. Possible contamination sources during extraction

There are several contamination sources during rock preparation and solvent extraction (Table 2.1).

Table 2.1. Possible contamination sources during the rock preparation and solvent extraction steps.

	Contamination source	**Section**
1	Rotary evaporator	2.4.1
2	Glassware	2.4.2
3	Organic solvents	2.4.3
4	Rock saws	2.4.4
5	Rock crushing in ring-mill	2.4.5
6	Organic residues on rock surfaces	2.4.6
7	Spatula	2.4.7
8	Internal standard solution	2.4.8
9	Accelerated Solvent Extractor (ASE)	2.4.9

.

2.4.1. Rotary evaporator

The rotary evaporator (Rotavapor R-210, BUCHI) can be a serious contamination source, especially when the instrument is shared with other operators. Observations were made that solvent such as hexane may boil during operation, and some organic matter from the sample could adhere to the inside surfaces of the glass vapour duct, which may cause cross-contamination of the following samples. Furthermore, if the pressure is not low enough, the solvent vapour may condense on the glass surface before reaching the condenser, dissolve compounds adhering to the glass surface, and flow back into the round-bottom flask, thereby contaminating the original solution. The degree of contamination varied from time to time, but it could be as high as 100 ng.

The O-ring used to seal the rotary evaporator can be a source of contamination as well. Theoretically, it should never come into contact with the EOM solution. However, in reality, the condensed solvent liquid from the vapour could, under certain pressure conditions, contact the O-ring and elute some of its components, such as siloxanes, *n*-alkanes, and unresolved mixtures of phthalates, particularly around *n*-C_{21} to *n*-C_{30}. This typically occurred when too high a pressure was used.

The ultimate solution to prevent cross contamination on the rotary evaporator was to not share the instrument with anyone, but this was impossible. Thus, a more practical solution that was applied in this study was to rinse the inside of the rotary with organic solvents (DCM and MeOH) before use. In the study by Coffey (2011), contamination by the rotary evaporator caused serious contaminations in some of her samples.

2.4.2. Glassware

Glassware can also be a serious source of contamination in any organic geochemistry laboratory due to adhering organic residues from previous experiments of other users. For glassware cleaning, the glassware was first submerged in a detergent (Decon 90) solution overnight in a bucket, and then washed with filtered water. However, this procedure proved to be insufficient to reduce hydrocarbon contamination below 100 ng. Treatment with chromic acid is an alternative for removing organic residues on glassware, but proved to be insufficient as well. In this study, the only

effective way for reducing hydrocarbon contamination to the pg level was found to be the combustion of glassware in an oven at 400 °C for >3 hours. The study by Coffey (2011) did not consider the contamination problem of glassware.

2.4.3. Organic solvents

The contamination level of hydrocarbons in DCM and MeOH varies with manufacturer and with grade of solvent purchased. 100 mL aliquots of solvent from several companies/brands were tested. The DCM used in this study contained trace amounts of C_{19-25} *n*-alkanes up to 0.1 pg / mL. In addition to *n*-alkanes, naphthalene and phenanthrene were sometimes detected, at concentrations of less than 0.1 pg / mL. Specific biomarkers such as hopanes and steranes were never detected in any of the solvents.

DCM (Scharlau, GC residue analysis) was used for the first study (Chapter 3). However, the contamination level suddenly increased when using different lots of the same solvent brand purchased at a different time, and therefore, a different product (Macron, H485-10) was chosen for the following studies (Chapter 4 and thereafter). This shows that a solvent product which is deemed to be adequately clean at the start of an experiment is not necessarily always clean for later experiments. This may be caused by contamination during the solvent production processes, or by subtle method changes in purification processes during manufacture. Thus, purity tests of all solvents are required on a regular basis.

The MeOH used in this study (Honeywell Burdick & Jackson, GC230-4) had a higher contamination level for C_{14-28} *n*-alkanes as compared to DCM (up to 0.7 pg / mL). However, as only 10 mL of MeOH were used for the solvent extraction step (max 7 pg / 10 mL), total solvent contamination levels could be kept in the pg range.

2.4.4. Rock saws

Three different sized rock saws (Dembicon, JBS-CPC20S, saw blade diameter / thickness: 500 mm / 4.0 mm; Diatrenn, D0, saw blade diameter / thickness: 310 mm / 0.9 mm; BUEHLER, BUE11-4267, saw blade diameter / thickness: 178 mm / 0.6 mm) were used to cut the rock samples. Some big

outcrop rocks were first cut by the largest saw, and then following cuts were made by the middle-sized saw. Smaller outcrop rocks were cut by the middle-sized saw only. Drill core samples were cut exclusively by the small-sized precision saw.

The small-sized precision saw blade was covered with lubricant at the time of product delivery. The lubricant contained various aliphatic hydrocarbons such as *n*-alkanes, methylalkanes, and regular isoprenoids, aromatic hydrocarbons such as naphthalene and phenanthrene, and hopanes and steranes. The saw blade was scrubbed with a metal brush, and then sonicated in a metal container with the DCM/MeOH solvent extraction mixture several times. The saw blade was further combusted twice in an oven at 300° C for >3 hours. Consequently, the contamination level of the small-sized precision saw dropped below the detection limit of the benchtop GC-MS (used in all the studies), and was ~20 pg by analysis on the DFS/Autospec GC-MS system (used in Chapters 4 and 5), except for some *n*-alkanes up to C_{30} with a maximum at C_{18} (a few ng). There also was a small unresolved complex mixture (UCM) with a maximum around *n*-C_{17} to *n*-C_{20} (less than 1 ng). These *n*-alkanes and the UCM were never eliminated, even after combustion. However, the contamination level of the procedural blank was lower than that of the saw, and the distribution of *n*-alkanes was also different from that of the saw. Furthermore, the UCM from the saw blade were never observed in the procedural blank, nor indeed identifiably in any of the samples. Therefore, the contamination of the small-sized precision saw does not seem to have affected any of the actual samples.

It was not possible to reduce the amount of contamination from the bigger saws to that of the small-sized precision saw due to their larger sizes. Contamination included various aliphatic and aromatic compounds, such as *n*-alkanes, regular isoprenoids, naphthalene, phenanthrene, retene, hopanes, steranes, and a large amount of a high molecular weight UCM with a maximum around *n*-C_{25} to *n*-C_{28}. However, these contaminants were not observed in any of the procedural blanks, except for *n*-alkanes, naphthalene and phenanthrene. In a similar way as for the small-sized saw, the abundance of these contaminants in the procedural blank was lower than that in the saw blanks, and the distribution of *n*-alkanes in the blank was also different from that in the saw blanks. Retene and the high molecular weight UCM were never detected in the procedural blank or the actual samples. Even

if some of these contaminants migrated onto the rock surfaces from the saw blade during cutting, they were removed by the subsequent cleaning processes before crushing (see Section 2.3.2). Also, hydrocarbon migration into the inside of each rock cube must have been negligible (see also Section 2.4.6).

2.4.5. Rock crushing in ring-mill

A tungsten carbide ring-mill crusher (Rocklab) was used exclusively for this project, and was not used for any other projects. The major contamination problem for the ring-mill crusher is carry-over from the previous crushing experiment. The ring-mill crusher was scrubbed with a metal brush and washed with tap water and then filtered water. After the ring-mill crusher was air dried, 40-50 mL of DCM and MeOH (9:1, v/v) were added and the ring-mill crusher was shaken manually for 30 seconds 10 times. Between each solvent rinse, the solvent was replaced. The ring-mill crusher was further shaken mechanically using a milling head at 700 rpm for 30 seconds 5 times. Between each solvent rinse, the solvent was replaced, as above. If the cleaning was insufficient, further mechanical cleaning was performed until the contamination level was < 1 ng (Fig. 2.5a).

2.4.5.1. Manual cleaning

At the beginning of the study, the ring-mill crusher was washed manually only. The rinse was repeated 10 times. However, even if the manual cleaning resulted in a contamination level <1 ng (C_{14}-C_{36} *n*-alkanes, and occasionally naphthalene and phenanthrene), more than 1 ng of contamination reappeared following any additional mechanical cleaning. Likely, the manual cleaning could not remove particle residues adsorbed on the crusher walls completely, which may have been the source of the reappearing hydrocarbons. Indeed, an extraction of a stromatolitic carbonate rock (Chapter 3) followed by manual cleaning and the extraction of a basalt blank sample showed similar distribution patterns of hydrocarbons for both samples. This indicated that manual cleaning was not sufficient to remove all organic residues.

2.4.5.2. Rocklab mechanical cleaning

The efficiency of mechanical cleaning was tested using a Rocklab milling head. The ring-mill crusher with solvent was shaken at 700 rpm for 30 seconds, which was repeated up to 25 times (Fig. 2.5a). *n*-Alkanes were generally found to be the largest contamination components, and amounts of other aliphatic and aromatic hydrocarbons were less than *n*-alkanes. The result of mechanical cleaning was not different from that of manual cleaning until the 10^{th} rinse (mill 10), but mechanical cleaning continuously reduced contamination level, and eventually achieved a 0.1 ng residual level. However, except for occasional cross-contamination between samples by the rotary evaporator and/or glassware, the ring-mill crusher was still the primary contamination source.

One characteristic of the mechanical cleaning is that the cleaning is more effective for heavier and/or larger hydrocarbons (Fig. 2.5b). A plausible explanation for this effect is that hydrocarbons are partitioned by the equilibrium between liquid state in the solvent and adsorbed state on the crusher wall, and heavier and more bulky molecules are more favoured to stay in the solvent than to stick to the walls. This may be caused by the microscopic irregular surfaces of the crusher walls, which favour adsorption of lighter/smaller molecules. After mill 20, the amount of organic residues remained almost constant, which may indicate that the signal from newly dissolved hydrocarbons into the solvent is within experimental error.

2.4.5.3. Ring-mill crusher O-ring

The O-ring used in the ring-mill crusher lid can be a serious contamination source. It supposedly never contacts the actual samples. However in reality, fine-grained powder can get in contact with the O-ring. Rubber O-rings typically contain *n*-alkanes and unresolved phthalate mixtures around *n*-C_{21} to *n*-C_{30}, which can migrate into the crushed sample powder to varying degrees. Desirable contamination-free O-rings are made of viton (Viton 75 duro) and Polytetrafluoroethylene (PTFE). Silicon O-rings are clean in terms of hydrocarbons, but they contain large amounts of siloxanes which may co-elute with target hydrocarbon peaks in the GC-MS chromatograms and thus hamper the identification of hydrocarbons. PTFE may be the cleanest, but is also the most rigid of the three materials, i.e. only expensive PTFE O-rings precisely designed and produced to fit the crusher could

have been used. Viton has a few phthalates, but their distinctive peaks on GC-MS do not co-elute with the target hydrocarbon peaks. Therefore, for this study, a viton O-ring was chosen.

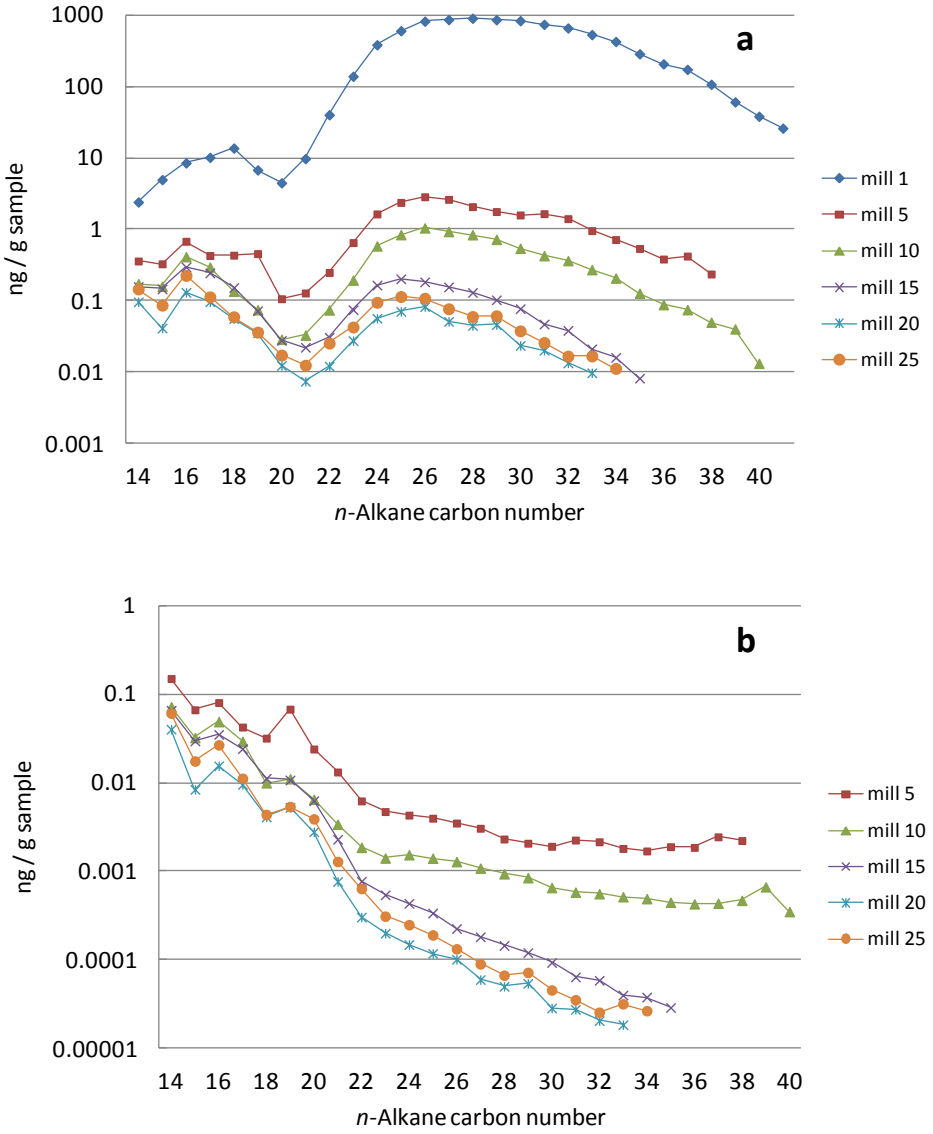

Figure 2.5. a. *n*-Alkane concentration changes through mechanical cleaning (mill *i* indicates the solvent used for the *i*th rinse), b. *n*-alkane amounts relative to the mill 1.

2.4.6. Organic residues on rock surfaces

Hydrocarbons derived from the surface rinse and those from the inside of the rock generally had a similar distribution pattern (Fig. 2.6). Furthermore, the abundance of extracted hydrocarbons was typically much higher than that from the rock surfaces (10 times in the case of the inner-most slice of Chapter 3 sample). Although it is possible that the extracted hydrocarbons from the rock surface are all derived from saw contamination, the composition of extracted hydrocarbons did not have the

characteristics of saw contamination such as a large high molecular weight UCM and retene. Furthermore, it would be an unusual coincidence that the composition of the saw-derived hydrocarbons was very similar to that from the internal part of the samples. Therefore, the organic residues on the rock surfaces after solvent rinse are interpreted to not be saw contamination. Instead, in this case (and for many other samples analysed) it is likely that the sample wash from the rock surface mainly contains hydrocarbons originally from the rock sample matrix, but in lower abundance due to the inefficient solvent extraction procedure (ultrasonication of rock cubes), compared to ultrasonication of crushed rock powder.

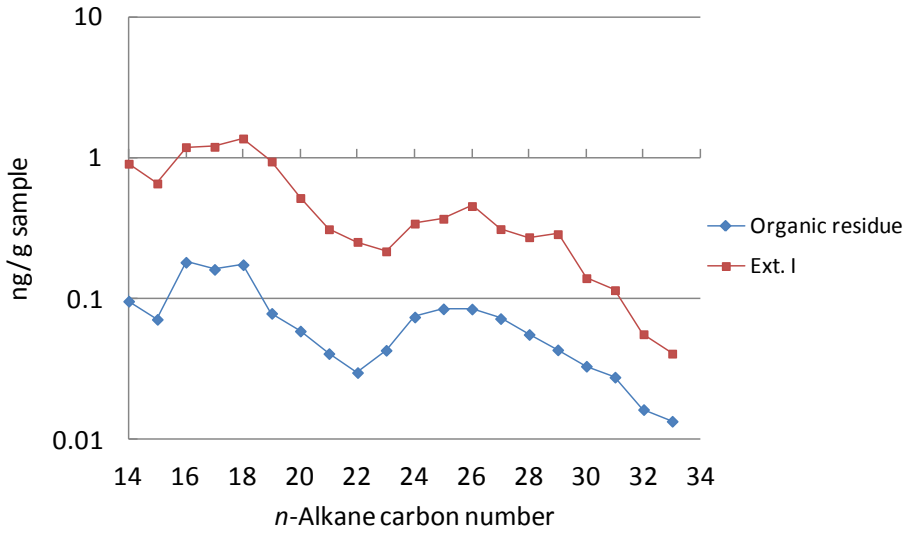

Figure 2.6. *n*-Alkane distribution from sample surface and the first extraction (Ext. I). The sample is the inner-most slice of Chapter 3 sample.

2.4.7. Spatula

The stainless steel spatula was wiped with a paper towel to remove fine particles from its surface and sonicated with DCM and MeOH (9:1, v/v) for 1 min twice. The organic residue from the spatula was tested using the second sonicated solvent. *n*-Alkanes from *n*-C_{14} to *n*-C_{29} were detected in low amounts (up to 50 pg). Thus the spatula was not a serious source of contamination compared to the crusher.

2.4.8. Internal standard solution

The internal standard solution can become contaminated during repetitious usage, so regular testing of just the standard solution is desirable. In addition, the standard compounds may degrade with time. At first, 1-bromoeicosane was used as one of the standards, but the use of this compound was discontinued in favour of the other three compounds (see Section 2.3.3) after the observation that the 1-bromoeicosane had started to degrade. In particular, compounds which require cold storage need to be handled carefully as they are very prone to degradation.

2.4.9. Accelerated Solvent Extractor (ASE)

ASE is a common instrument used for the solvent extraction of geological samples. However, it was not employed in this study because trace contamination of aliphatic and aromatic hydrocarbons >100 ng was observed in a test experiment using a baked sand blank. Furthermore, some parts of the system cannot be replaced, and each EOM from successive runs travels through the same plumbing system, which can only be rinsed between runs. As the instrument was shared with other users, who were carrying out a wide range of studies including extraction of much richer samples than this Archean project, cross-contamination would have been unavoidable.

2.5. Sampling locations

Stromatolite samples and drill core samples were collected from various localities as shown in Fig. 2.7. Six stromatolite rocks (ST1-6), and three drill cores (AIDP-1, 2 and 3) were examined in this study. Two basaltic rocks (BS1 and 2) were also analysed as procedural blanks.

A brief description of each sample is given in Table 2.2. Chapter 3 discusses the slice experiment on one stromatolite outcrop (ST1), and then Chapter 4 deals with the slice experiment on another stromatolite sample from a different outcrop (ST2). Chapter 5 focuses on the drill core samples (AIDP-1, 2 and 3). Chapter 6 analyse four stromatolite samples (ST1-4) and one basaltic rock (BS1). Chapter 7 discusses all the samples from the previous chapters, and other samples (ST5, ST6 and BS2).

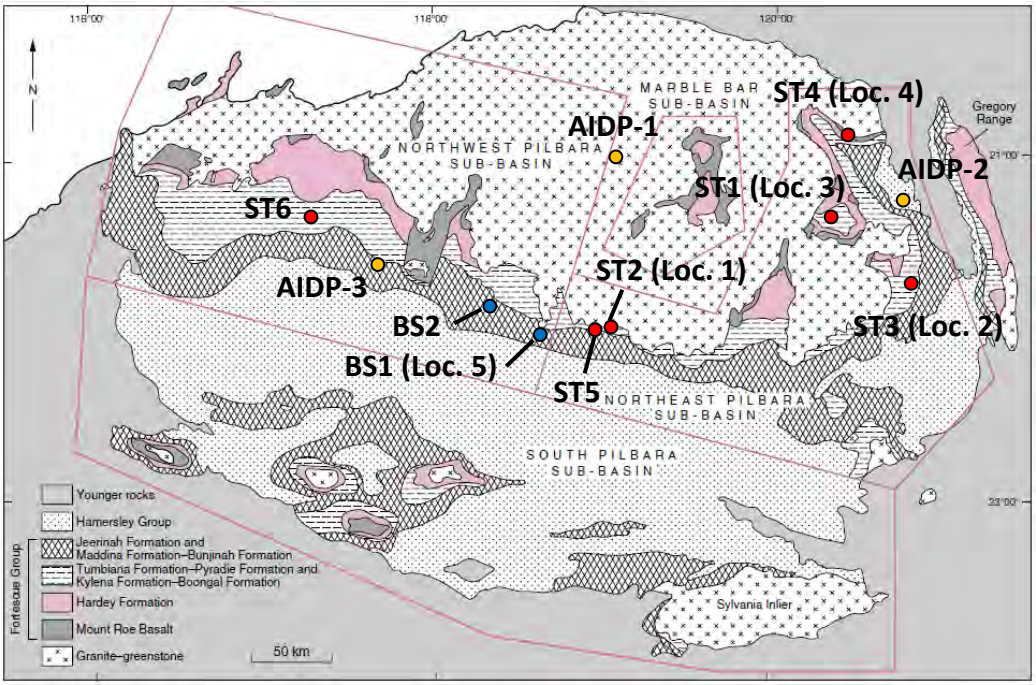

Figure 2.7. Sampling locations of stromatolite rocks and drilling sites in this study. Red circles indicate stromatolite outcrop; orange circles indicate drill cores; and blue circles indicate basalt lava flow outcrop. Loc. is the abbreviation for sample names in Chapter 6.

Table 2.2. Sample list of analysed rocks

Sample	Formation	Chapter	Sample name in Chapter
ST1	Tumbiana	3, 6 and 7	Loc. 3 (Chapter 6)
ST2	Tumbiana	4, 6 and 7	Loc. 1 (Chapter 6)
ST3	Kylena	6 and 7	Loc. 2 (Chapter 6)
ST4	Tumbiana	6 and 7	Loc. 4 (Chapter 6)
ST5	Tumbiana	7	-
ST6	Jeerinah	7	-
AIDP-1[a]	-	5 and 7	1
AIDP-2[a]	-	5 and 7	2-1, 2-2, 2-3 and 2-4
AIDP-3[a]	-	5 and 7	3
BS1	Maddina	3-6, and 7	Loc. 5 (Chapter 6)
BS2	Maddina	7	-

[a]Samples come from several different formations (see Chapter 5).

2.6. References

Brocks, J.J. (2011) Millimeter-scale concentration gradients of hydrocarbons in Archean shales: Live-oil escape or fingerprint of contamination? Geochimica Et Cosmochimica Acta 75, 3196-3213.

Brocks, J.J., Buick, R., Logan, G.A. and Summons, R.E. (2003) Composition and syngeneity of molecular fossils from the 2.78 to 2.45 billion-year-old Mount Bruce Supergroup, Pilbara Craton, Western Australia. Geochimica Et Cosmochimica Acta 67, 4289-4319.

Coffey, J.M. (2011) A paleoenvironmental study of the 2.7 Ga Tumbiana Formation, Fortescue Basin, Western Australia. Ph.D. dissertation, University of New South Wales, Sydney.

Eigenbrode, J.L., Freeman, K.H. and Summons, R.E. (2008) Methylhopane biomarker hydrocarbons in Hamersley Province sediments provide evidence for Neoarchean aerobiosis. Earth and Planetary Science Letters 273, 323-331.

French, K.L., Hallman, C., Hope, J.M., Buick, R., Brocks, J.J. and Summons, R.E. (2013) Archean hydrocarbon biomarkers: Archean or not?, Goldschmidt 2013 Conference Abstract.

Hayes, J.M., Kaplan, I.R. and Wedeking, K.M. (1983) Precambrian organic geochemistry, preservation of the record, in: Schopf, J.W. (Ed.), Earth's earliest biosphere, its origin and evolution. Princeton University Press, Princeton, pp. 93-134, 543.

Rasmussen, B., Fletcher, I.R., Brocks, J.J. and Kilburn, M.R. (2008) Reassessing the first appearance of eukaryotes and cyanobacteria. Nature 455, 1101-1104.

Sherman, L.S., Waldbauer, J.R. and Summons, R.E. (2007) Improved methods for isolating and validating indigenous biomarkers in Precambrian rocks. Organic Geochemistry 38, 1987-2000.

Waldbauer, J.R., Sherman, L.S., Sumner, D.Y. and Summons, R.E. (2009) Late Archean molecular fossils from the Transvaal Supergroup record the antiquity of microbial diversity and aerobiosis. Precambrian Research 169, 28-47.

Weiss, H.M., Wilhelms, A., Mills, N., Scotchmer, J., Hall, P.B., Lind, K. and Brekke, T. (2000) NIGOGA - The Norwegian Industry Guide to Organic Geochemical Analyses [online], http://www.npd.no/engelsk/nigoga/default.htm.

Chapter 3.

Hydrocarbons preserved in a ~2.7 Ga outcrop sample from the Fortescue Group, Pilbara Craton, Western Australia

Y. Hoshino [1,2], D. T. Flannery [2,3], M. R. Walter [2,3], S. C. George [1,2]

[1] *Department of Earth and Planetary Sciences, Macquarie University, Sydney, Australia*

[2] *Australian Centre for Astrobiology, University of New South Wales, Australia*

[3] *School of Biotechnology and Biomolecular Sciences, University of New South Wales, Australia*

Statement of authors' contribution

This Chapter is a published article in *Geobiology*. This paper has been formatted to conform to the font and referencing style adopted in this thesis. Figures and tables included within the text are prefixed with the chapter number.

I am the primary author (95% of the effort). I collected the sample with the help of David Flannery (University of New South Wales, Australia). I examined the sample, including sample cutting, grinding, and solvent extractions. I performed gas chromatography-mass spectroscopy. I processed and interpreted all the data derived from the measurements. I wrote and designed the structure of the paper. All co-authors carefully reviewed and provided feedback and valuable refinements on the final version of the manuscript, and approved it for submission and publication. Neither this manuscript nor one with similar content under our authorship has been published or is being considered for publication elsewhere, except as described above.

Abstract

The hydrocarbons preserved in an Archean rock were extracted and their composition and distribution in consecutive slices from the outside to the inside of the rock were examined. The 2.7 Ga rock was collected from the Fortescue Group in the Pilbara region, Western Australia. The bitumen I (solvent extracted rock) and bitumen II (solvent extracted hydrochloric acid-treated rock) fractions have different hydrocarbon compositions. Bitumen I contains only trace amounts of aliphatic hydrocarbons and virtually no aromatic hydrocarbons. In contrast, bitumen II contains abundant aliphatic and aromatic hydrocarbons. The difference seems to reflect the weathering history and preservational environment of the investigated rock. Aliphatic hydrocarbons in bitumen I are considered to be mainly from later hydrocarbon inputs, after initial deposition and burial, and are therefore not indigenous. The lack of aromatic hydrocarbons in bitumen I suggests a severe weathering environment since uplift and exposure of the rock at the Earth's surface in the Cenozoic. On the other hand, the high abundance of aromatic hydrocarbons in bitumen II suggests bitumen II hydrocarbons have been physically isolated from removal by their encapsulation within carbonate minerals. The richness of aromatic hydrocarbons and the relative scarcity of aliphatic hydrocarbons may reflect the original compositions of organic materials biosynthesised in ancient organisms in the Archean era, or the high thermal maturity of the rock. Cyanobacterial biomarkers were observed in the surficial slices of the rock, which may indicate that endolithic cyanobacteria inhabited the surface outcrop. The distribution of aliphatic and aromatic hydrocarbons implies a high thermal maturity, which is consistent with the lack of any specific biomarkers such as hopanes and steranes, and the prehnite-pumpellyite facies metamorphic grade.

3.1. Introduction

It is widely accepted that the oxygenation of the previously anaerobic Earth was the result of the evolution of oxygenic photosynthesis in cyanobacteria (Lyons et al., 2014). Most researchers agree that atmospheric and surface oceanic O_2 concentrations rose between 2.45 Ga and 2.33 Ga during the Great Oxidation Event (GOE) (Holland, 2002; Bekker et al., 2004). However, some lines of evidence, including biomarker analyses, have suggested the rise of O_2 well before the GOE (e.g. Brocks et al., 1999; Anbar et al., 2007; Waldbauer et al., 2009; Planavsky et al., 2014).

Biomarkers are hydrocarbons preserved as part of the extractable organic matter within sedimentary rocks. Biomarkers may be directly deposited and incorporated into sediments, or may be the product of diagenetic reactions of organic matter in the sediments and sedimentary rocks, after which they can remain for long periods of geological time (Eglinton et al., 1964; Waldbauer et al., 2009). Biomarkers can be linked to specific biological metabolic pathways and are used to identify specific types of organisms (e.g. Brocks and Summons, 2003; Grice and Eiserbeck, 2014). Hopanes are biomarkers for the domain bacteria (Ourisson et al., 1987). In particular, 2α-methylhopanes were considered diagnostic biomarkers for cyanobacteria (Summons et al., 1999), although it is now known that cyanobacteria are not the sole source of these biomarkers, as they can also be derived from some anoxygenic phototrophs (Rashby et al., 2007; Welander et al., 2010). Steranes, which are biomarkers for the domain eukarya, require O_2 for the biosynthesis of their parent molecules and are thus indicators for the presence of O_2 and oxygenic photosynthesis (Summons et al., 2006).

The presence of these biomarkers in Archean rocks was first reported from the 2.7 Ga carbonates in the Fortescue and Hamersley groups in the Pilbara region in Western Australia (Brocks et al., 1999). The Pilbara is one of two main areas preserving relatively pristine Archean crust dating back to 2.5-3.5 Ga (Arndt et al., 1991; Buick et al., 1995). Archean biomarkers have been reported from both the Pilbara region (Brocks et al., 2003a; Eigenbrode et al., 2008; Coffey, 2011) and also the Transvaal Supergroup in South Africa (Waldbauer et al., 2009). Biomarkers have also been reported from fluid

inclusions in the fluvial metaconglomerate of the 2.45 Ga Matinenda Formation, Canada (Dutkiewicz et al., 2006; George et al., 2008).

However, some researchers have contested the evidence for pre-GOE biomarkers by demonstrating that these biomarkers are contaminants in some cases. It has been shown that kerogen and pyrobitumen in Archean drill cores are strongly depleted in ^{13}C. This is inconsistent with the isotopic values of supposedly Archean biomarkers reported bitumens extracted from the same cores (Rasmussen et al., 2008). Thus, the detected biomarkers are suspected to be from later migration or contamination. Furthermore, the spatial distribution of hydrocarbon biomarkers in some drill cores from the Fortescue Group suggests that the biomarkers are not indigenous (Brocks, 2011). The oldest widely-accepted biomarkers are reported from the McArthur Basin and McArthur Group sediments deposited between 1.6 and 1.4 Ga (Jackson et al., 1986; Summons et al., 1988; Brocks et al., 2005; Volk et al., 2005; Flannery and George, 2014), and the syngeneity and indigeneity of organic matter reported in older rocks continue to be debated. In order to address this issue, contamination from experimental procedures and hydrocarbon migration from the outside needs to be investigated and minimised. In this study, concentrations of contaminants were kept very low, enabling small amounts of indigenous organic matter including biomarkers to be unambiguously detected.

Another approach for investigating the syngeneity and indigeneity of hydrocarbons is to measure concentration gradients by successively slicing samples from the outside, and then investigating each slice separately (Brocks, 2001; Sherman et al., 2007; Flannery and George, 2014). Recent contamination from the external environment is likely to have a maximum concentration at the surface of the rock in the outer slice, and is expected to decline in concentration in the inner slices. On the other hand, any indigenous organic compounds may be more protected deep inside the rock and may there retain their original concentrations, and reduce in concentrations towards the outer slices due to partial or complete removal by weathering. In this study, slice experiments were used to show a variety of indigenous organic compound candidates and their distribution throughout the rock.

There have been few studies that have comprehensively measured hydrocarbon compositions and spatial distributions including biomarkers for Archean rocks (Brocks, 2001; Brocks et al., 2003a; Brocks, 2011; Coffey, 2011). Thus, the detection of any hydrocarbons would advance understanding of ancient ecosystems and improve estimates of the preservation history of these systems over geological time, regardless of the presence of biomarkers.

3.2. Geological setting and sample

The sample was collected from Meentheena Member outcrop (Tumbiana Formation, Fortescue Group) in the northeast Pilbara sub-basin in Western Australia (Fig. 3.1) (Thorne and Trendall, 2001).

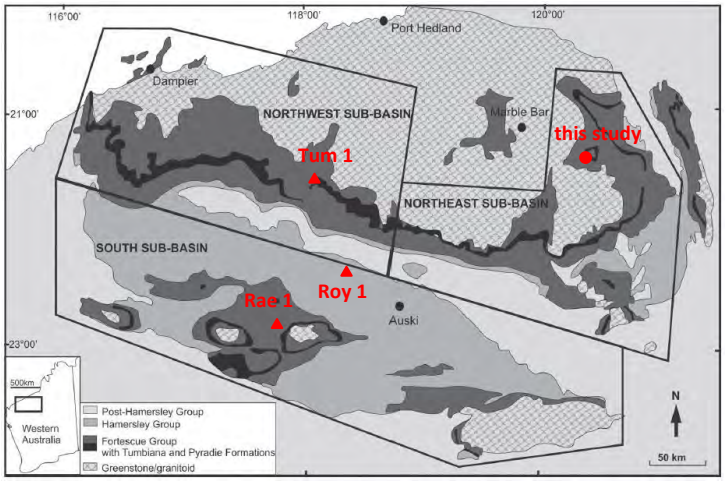

Figure 3.1. Location map showing the Fortescue Group and the Tumbiana Formation in the Pilbara Craton in Western Australia. The red dot shows the sampling location (grid reference lodged with the GSWA). The red triangles show the sampling locations of Brocks et al. (2003a). Map modified after Thorne and Trendall, 2001.

The Pilbara Craton includes Paleo- to Mesoarchean granitoid-greenstone basement and unconformably overlying volcano-sedimentary rocks of the Mt Bruce Supergroup, which was deposited between 2.78 and 2.45 Ga. The Fortescue Group is the basal member of the Mt. Bruce Supergroup and was deposited between 2.78 and 2.63 Ga during a period of rifting and extensive volcanism (Thorne and Trendall, 2001). The Tumbiana Formation is a thin unit of siliciclastic, volcaniclastic and carbonate rocks deposited between subaerial lava flows of the underlying Kylena and overlying Maddina Formations. It is divided into the Mingah Member and the overlying

Meentheena Member, the latter consisting mostly of stromatolitic limestone and recessive shale (Lipple, 1975). The Meentheena Member experienced prehnite-pumpellyite facies metamorphism (175-280 °C) in the northeast and northwest sub-basins, and actinolite facies metamorphism (300-350 °C) in the southern sub-basin. The former temperatures are thus low compared to those experienced by other Archean rocks in the Pilbara Region (Smith et al., 1982).

The Meentheena Member was deposited in either a shallow marine environment (e.g. Thorne and Trendall, 2001; Sakurai et al., 2005) or a lacustrine environment (e.g. Walter, 1983; Awramik and Buchheim, 2009; Coffey et al., 2013). The sample analysed is a micritic carbonate composed of centimetre-scale, coniformly-laminated pseudocolumnar and columnar stromatolites, linked by regularly-occurring interconnecting laminae (Figs 3.2 and 3.3). This unit is underlain by a metre-scale, roughly equidimensional domical stromatolites. A basaltic lava flow from the nearby overlying Maddina Formation was sampled for use as a procedural blank.

Figure 3.2. Field photograph of the investigated locality showing metre-scale domical stromatolites in the Meentheena Member immediately underlying the sampled material. The red circle indicates where the sample rock was collected.

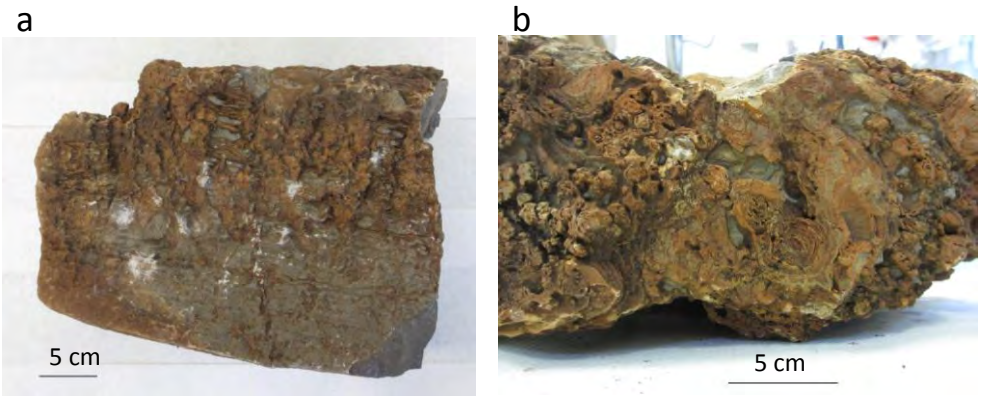

Figure 3.3. Photographs of the investigated stromatolite sample; (a) top view, and (b) partially enlarged side view.

3.3. Experimental Procedure

3.3.1. Solvents and glassware

Dichloromethane (DCM) (Scharlau, GC residue analysis) and methanol (MeOH) (Honeywell Burdick & Jackson, GC230-4) (9:1 v/v) were used to extract hydrocarbons from the sample. All solvents were checked for purity by gas chromatography-mass spectroscopy (GC-MS) as described below. All glassware was combusted in an oven at 400 °C for 3 hours before use.

3.3.2. Sample preparation

The rock sample was sliced using a diamond blade (Diatrenn, D0) from the outside towards the inside, producing approximately 1 cm thick slices. Each slice was then cut into approximately 1 cm^3 pieces. Approximately 100 g of rock was used for the analysis of each slice. The procedural blank was processed first. Between each slice experiment all equipment, including the saw blade, was washed with filtered water, MeOH and DCM and checked for purity by GC-MS.

Fine particles on sample surfaces were removed by ultrasonication in filtered water for 10 min. Organic contamination on surfaces was removed by ultrasonication in a mixture of DCM and MeOH (9:1, v/v) for two cycles of 10 min., with a new solvent mixture each time. The last solvent mixture was analysed by GC-MS for purity and surface checking. If the cleaning was not sufficient, additional ultrasonication was performed until the contamination level was < 1 ng.

The rock was then ground to < 200 mesh grain size in a ring-mill. The mill was cleaned between samples. Fine particles in the mill were removed by water washing and scrubbing by a metal brush. The mill was then repeatedly rinsed with a solvent mixture of the same composition as described above. If the cleaning was insufficient, additional rinsing of the ring-mill was performed until the contamination level was < 1 ng.

3.3.3. First solvent extraction (Ext. I)

Extraction of hydrocarbons from the rock powder was carried out by ultrasonication with 200 mL of the solvent mixture described above for two cycles of 10 min. Between the sonications, the solution was stirred using a glass rod and left to stand still for a few minutes. The solvent was collected in a round-bottom flask. The powder was further sonicated with a fresh 100 mL aliquot of DCM for 10 min to retrieve organic residues, particularly aliphatic hydrocarbons, in the mixed slurry of powder and solvent. The second solvent was added to the first solvent. An instrument such as an Accelerated Solvent Extractor was not used because of the possibility of contamination.

The obtained solution volume was reduced by rotary evaporation to 30-40 mL. The solution was then centrifuged for 3 min at 2,000 rpm to remove suspended rock particles. The volume was then further reduced by rotary evaporation to approximately 5 mL. If the amount of suspended solids was low, the centrifuge step was omitted and the solvent was directly reduced to approximately 5 mL. Even after the centrifuge step, there were still some very fine rock particles suspended in the solvent. These were removed by filtering the solvent/sample mixture through silica gel (silica gel 60, 0.063-0.200 mm, Merck), which was activated at 120 °C for > 4 hours before use. Column fractionation of the extractable organic matter (EOM) was not performed because the yield was very small (< 100 ng / g sample), and therefore the interference between hydrocarbon peaks was not serious, and also to prevent the loss of hydrocarbons.

The EOM was spiked with three compounds as internal standards by adding 1 mL of a DCM solution containing about 50 ng of each: anthracene-d_{10} (98 atom %D, Isotec), p-terphenyl-d_{14} (98 atom %D, Isotec), and tetraeicosane-d_{50} (98 atom %D, Isotec). The volume of solvent containing the EOM was

further reduced on a hot plate at 40 °C under a gentle nitrogen flow, until approximately 50 µL remained.

3.3.4. Second solvent extraction (Ext. II)

After the first solvent extraction, the residual rock powder was treated with hydrochloric acid (HCl; 36%, RCI Labscan) to remove the carbonate minerals. 100-150 mL of HCl solution was added to the powder (~100 g) on a hot plate at 70 °C until effervescence stopped. The resultant solution was washed with 500 mL of filtered water six times. The surplus acid-water mixture was discarded and the remaining powder slurry was air dried. Extraction of the decarbonated rock powder was performed as described above for the first extraction. Acid treatment was found to release a large amount of elemental sulphur, which can damage GC-MS instruments and interfere with hydrocarbon identification and quantification. Thus, elemental sulphur was removed by treatment of the EOM with activated copper. 5 g of copper particles (metal turnings, TG, Chem-Supply) were first treated with 36% HCl to remove CuO surficial layers and any remaining CuS residues from the previous experiment, and then washed with MeOH twice and DCM twice. The activated copper was added to the EOM and stirred for a minute. This simple procedure was enough to remove most sulphur so that reflux of the solution was not performed. Then, the copper particles were removed. The resultant EOM was spiked with standards and prepared for GC-MS using the same procedure as for the first extraction.

3.3.5. Gas Chromatography-Mass Spectroscopy (GC-MS)

GC-MS analysis was carried out on an Agilent GC (6890N) coupled to an Agilent Mass Selective Detector (5975B). 1 µL of the EOM solution was injected into a Programmable Temperature Vaporization (PTV) inlet operating in splitless mode with a J&W DB5MS column (length 60 m, inner diameter 0.25 mm, film thickness 0.25 um). The inlet was ramped from 35 °C (3 min. isothermal) to 310 °C (0.5 min. isothermal) at a rate of 700 °C / min. Helium was used as the carrier gas (1.5 mL / min.), and the temperature of the GC oven was ramped from 30 °C (2 min. isothermal) to 310 °C (30 min. isothermal) at a rate of 4 °C / min. The MS data were acquired in single ion monitoring mode.

Hydrocarbon identification was based on comparisons of relative GC retention times and mass spectra with those previously reported. Semi-quantitative analyses were performed using the tetraeicosane-d_{50} internal standard, not taking into account any response factor. The other two standards were used to check sensitivity and repeatability of the measurement, but were not used for the quantification.

3.4. Results

Each slice was labelled from 1 (the outer-most layer) to 5 (the inner-most layer), and analysed for its aliphatic hydrocarbons, aromatic hydrocarbons, and any biomarkers.

3.4.1. The first solvent extraction (Ext. I)

3.4.1.1. Aliphatic hydrocarbons

n-Alkanes have a heterogeneous distribution throughout the rock (Fig. 3.4a). Slice 1 has a distinctive peak at *n*-C_{17}, which is three times larger than *n*-C_{16} and *n*-C_{18}. Slices 2 to 4 also have maxima at *n*-C_{17}, but the relative abundance of *n*-C_{17} to *n*-C_{16} and *n*-C_{18} for slices 2-4 is lower than that for slice 1. Contrarily, slice 5 only has a slight even-over-odd preference (EOP) between *n*-C_{15} and *n*-C_{19}, which may indicate a different origin of organic matter in slice 5 from that in other slices. The amount of *n*-alkanes > *n*-C_{21} decreases from the outside slice towards the inside slice, with the exception of slice 2. This may reflect variation in the degree of influence of the hydrocarbon input from the outside of the sample towards the inside. The outermost layer (slice 1) has a clear odd-over-even preference (OEP) between *n*-C_{26} and *n*-C_{34}, indicating higher plant input (Eglinton and Hamilton, 1967), but the inner slices 2 to 5 do not have a similar distribution, suggesting the influence of higher plant input is limited to the outermost part of the sample.

Detected aliphatic hydrocarbons are mostly more abundant than in the procedural blank (< 3.4 pg / g sample) in all slices (Fig. 3.4a). However, their amount is close to the blank level for some compounds, indicating that the amount of hydrocarbons contained in this Archean rock is low. Although *n*-C_{11}, *n*-C_{12}, and *n*-C_{13} are also abundant in all slices except for slice 4, these compounds are also present in the procedural blank at similar abundances. Therefore, these *n*-alkanes are deemed

to be experimental contamination, and they were excluded from further analysis. *n*-Alkanes < *n*-C_9 were not recovered by the extraction procedure.

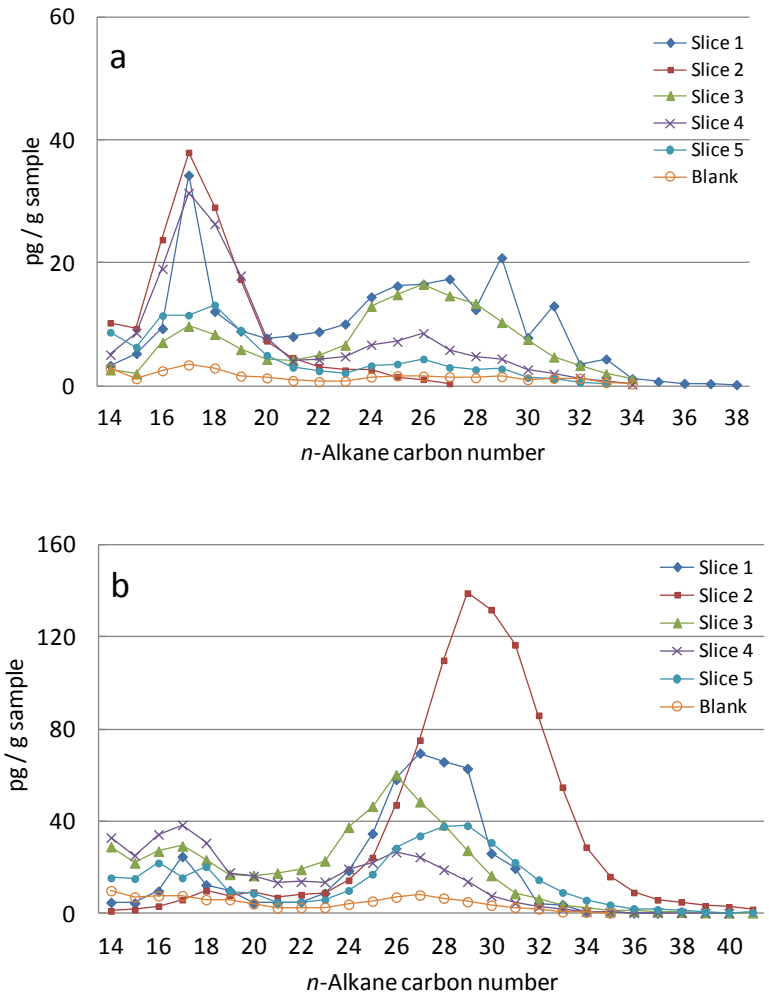

Figure 3.4. Amount and distribution of *n*-alkanes from Ext. I (a) and Ext. II (b) of the five slices and the procedural blank.

Monomethylalkanes (MMAs) were detected in the molecular weight range from C_{16} to C_{20} (Fig. 3.5). All possible isomers were identified, but their amounts were small (< 4 pg / g sample). The procedural blank does not contain any MMAs. One distinctive feature of the MMAs is that 7- and 6-methylheptadecane (7- and 6-MHeD) are the dominant MMAs in slice 1, these being more than 4 times more abundant than the other MMAs (Figs 3.5 and 3.6a), in contrast to the other slices which do not have such a high relative abundance of these isomers. In addition, *n*-C_{17} is also a distinctively large hydrocarbon in slice 1 (Figs 3.4a and 3.5), indicating the presence of cyanobacteria in slice 1 at some time.

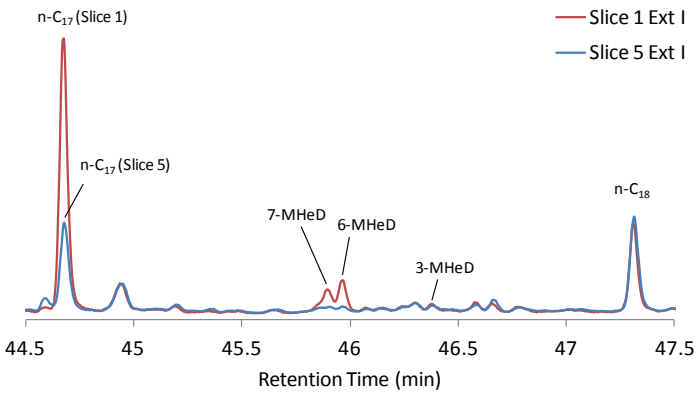

Figure 3.5. Partial m/z 57 mass chromatogram of C_{17} and C_{18} *n*-alkanes and the methylheptadecanes (MHeD) in slice 1 (red) and 5 (blue) in Ext. I.

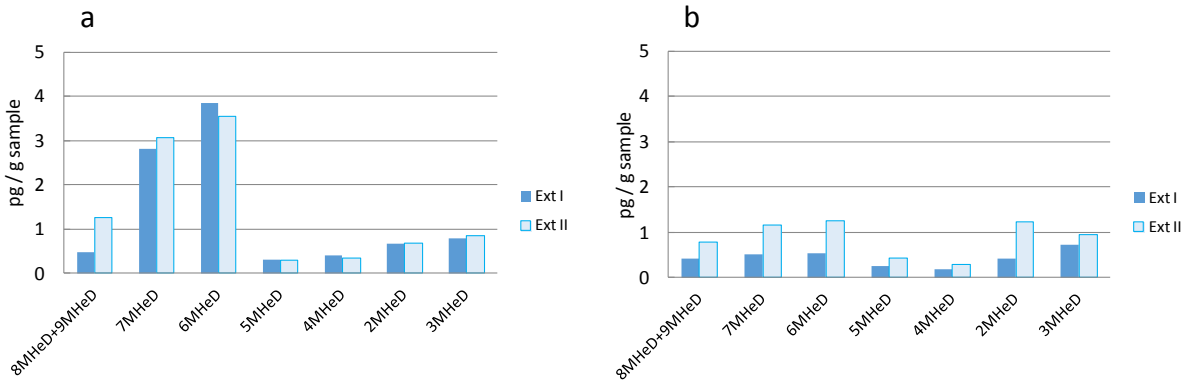

Figure 3.6. Histograms of methylheptadecane abundances in slice 1 (a) and 5 (b) for Ext. I (blue) and Ext. II (pale blue).

The selective production of *n*-C_{17} and 7-MHeD in extant cyanobacteria has been frequently reported (Schirmer et al., 2010; Coates et al., 2014). Deeper slices do not have the same anomalous abundances of *n*-C_{17} and 7-MHeD (Figs 3.5 and 3.6b). Therefore, evidence for the presence of cyanobacteria is limited to the surface of the rock. It is unlikely that these molecular fossils are of Archean origin, because their distribution is limited to the rock surface. These hydrocarbons might be the result of hydrocarbon migration, but more likely they represent the remains of an endolithic cyanobacterial colony that grew on the outside portion of the rock sample in outcrop (see also Chapter 6).

Alkylcyclohexanes (ACHs) and methylalkylcyclcohexanes (MACHs) ranging from C_{15} to C_{20} are also present in Ext. I of all slices (< 2 pg / g sample) (data now shown). The procedural blank does not contain any ACHs and MACHs. The amounts of ACHs and MACHs were generally proportional to those of *n*-alkanes with a similar molecular weight, indicating a common origin, but a high abundance of C_{17} ACHs and MACHs was not observed, unlike C_{17} *n*-alkane.

3.4.1.2. Aromatic hydrocarbons

The Ext. I fraction of all the slices only contained small amounts of naphthalene, phenanthrene, fluoranthene and pyrene (< 10 pg / g sample). The procedural blank only contains trace amounts of naphthalene and phenanthrene (1 pg / g sample). Alkylated aromatic hydrocarbons were not detected in any of the slices.

3.4.1.3. Biomarkers

The only detected biomarkers in the rock slices were regular isoprenoids, ranging from C_{13} to C_{20} (0.4-11 pg / g sample). C_{19} Pristane (Pr) and C_{20} Phytane (Ph) are more abundant than the other isoprenoids (Fig. 3.7a), and there is no clear trend between the slices. This may be because the amount of isoprenoids is too small to be interpreted quantitatively. The amount of *i*-C_{13} to *i*-C_{15} in the slices is comparable to the blank level, so it is likely that at least a part of what was analysed is not indigenous. The primary source of Pr and Ph is phytol, which is the side chain of chlorophyll a in cyanobacteria and green-plants, and bacteriochlorophyll a and b in purple sulphur bacteria (Brooks et al., 1969; Powell and McKirdy, 1973). In most slices, Pr/Ph = 0.8-1.3 (Table 3.1), suggesting an anoxic to suboxic depositional environment (Didyk et al., 1978).

No more specific biomarkers such as hopanes and steranes were detected in any of the slices or in the procedural blank. This contrasts with the distinctive *n*-C_{17} and 7- and 6-MHeD peaks in slice 1, which indicate the presence of cyanobacteria, and with the OEP derived from a higher plant input. However, considering that the detected amounts of *n*-alkanes are less than 20 pg / g sample on average, and because hopanes or steranes are normally 10 to 10,000 times less abundant than *n*-alkanes in rocks and oils (Brocks et al., 2003a; Waldbauer et al., 2009), hopanes or steranes are likely

to be much less abundant and in the range of 2 pg / g to 2 fg / g sample. Thus, it is likely that these biomarkers were below the detection limit of the instrument used. In addition, it is also likely the thermal maturity of the rock led to any pre-existing free biomarkers being thermally cracked and decomposed during burial and prehnite-pumpellyite facies metamorphism.

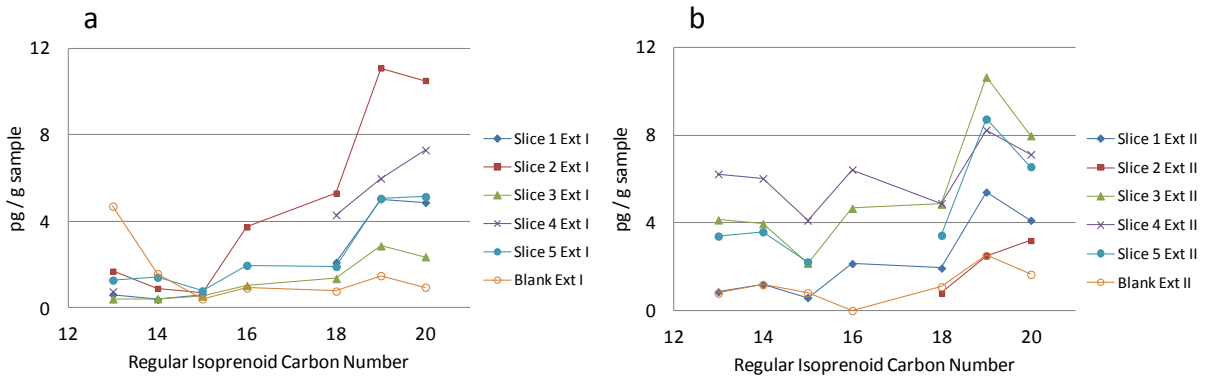

Figure 3.7. Amount and distribution of C_{13} to C_{20} regular isoprenoids from Ext. I (a) and Ext. II (b) of the five slices and the procedural blank. C_{19} = Pristane; C_{20} = Phytane.

Table 3.1. Alkanes and isoprenoid ratios of Ext. I and Ext. II aliphatic hydrocarbons.

Ext. I	Slice 1	Slice 2	Slice 3	Slice 4	Slice 5
Pr / Ph	1.03	1.06	1.21	0.82	0.98
Pr / *n*-C_{17}	0.15	0.29	0.30	0.19	0.44
Ph / *n*-C_{18}	0.40	0.36	0.28	0.28	0.39

Ext. II	Slice 1	Slice 2	Slice 3	Slice 4	Slice 5
Pr / Ph	1.31	0.78	1.34	1.16	1.33
Pr / *n*-C_{17}	0.22	0.41	0.17	0.16	0.56
Ph / *n*-C_{18}	0.33	0.32	0.13	0.17	0.32

3.4.2. The second solvent extraction (Ext. II)

3.4.2.1. Aliphatic hydrocarbons

The weight of each slice is 10-15% of its original weight after HCl treatment, due to the fact that the rock is predominantly composed of carbonate minerals. The distributions of *n*-alkanes from Ext. II are generally similar to those from Ext. I from *n*-C_{14} to *n*-C_{21} except slice 2 (Fig. 3.4b). However, all the

rock slices have large amounts of *n*-alkanes from C_{21} to C_{35}, with a smooth distribution maximising between *n*-C_{26} and *n*-C_{29} (26-139 pg / g sample) in significantly higher abundance than the blank (< 8 pg / g sample). These *n*-alkanes appeared after HCl treatment, so they were probably trapped within the carbonate minerals (Holman et al., 2012). Therefore, these *n*-alkanes in slices 2 to 5 are interpreted to be indigenous, and their origins are likely to be common, considering their preservational environment, although the maxima of their distributions do not always match (Fig. 3.4b). Slice 1 Ext. II contains an OEP between *n*-C_{26} and *n*-C_{34} as for Ext. I, and also a large amount of *n*-alkanes between C_{21} and C_{35}. This is consistent with slice 1 Ext. II being a mixture of non-indigenous hydrocarbons including higher plant input from outside the sample, and indigenous hydrocarbons from within the rock matrix that were released by the carbonate removal.

In contrast, an *n*-alkane maximum at *n*-C_{17}, high abundance of 7- and 6-MHeD in slice 1, and an EOP between *n*-C_{15} and *n*-C_{19} in slice 5, are common characteristics of both Ext. I and II (Figs 3.4b and 3.6). The abundance of *n*-C_{17} in slice 1 in Ext. II is higher than *n*-C_{16} and *n*-C_{18}, but is less distinctive than in Ext. II. *n*-C_{17} in slice 2 to 4 Ext. II is only slightly more abundant than *n*-C_{16} and *n*-C_{18}, and *n*-C_{17} is less abundant than in slice 1. This suggests that the influence of endolithic cyanobacteria is mainly limited to pores within the rock fabric. In contrast, the *n*-alkanes from C_{15} to C_{19} in slice 5 are probably indigenous, and the EOP between *n*-C_{15} and *n*-C_{19} reflects an original composition of organic matter at the time of deposition. The presence of ACHs, MACHs and MMAs in Ext. II extends to C_{34}, and this is consistent with the occurrence of high abundances of *n*-alkanes > *n*-C_{21} (data not shown). The ACH, MACH and MMA amounts are proportional to *n*-alkanes with a similar molecular weight, and are of low abundance (< 4 pg / g sample), similar to the amounts in Ext. I.

3.4.2.2. Aromatic hydrocarbons

Unlike Ext. I, Ext. II contains a variety of aromatic hydrocarbons, including naphthalene, phenanthrene, biphenyl, fluorene, and their alkylated compounds. The distribution of naphthalene and alkylated naphthalenes is shown in Fig. 3.8. Other aromatic hydrocarbons have a similar trend (Fig. 3.9).

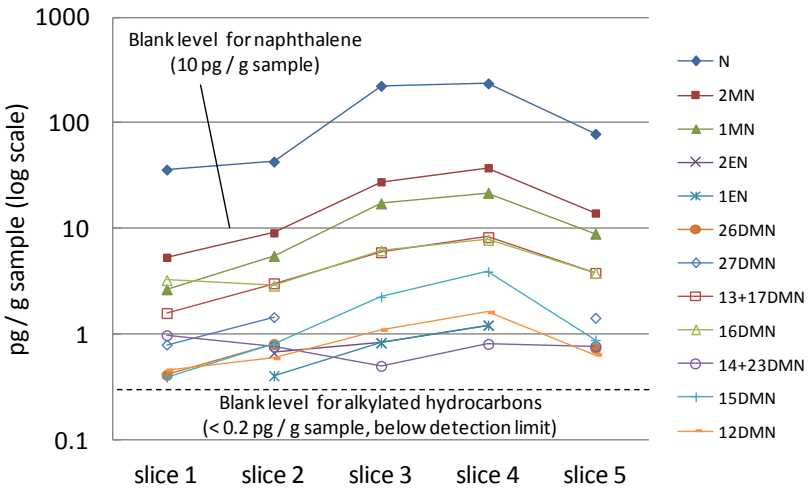

Figure 3.8. Amount and distribution of naphthalene and alkylated naphthalenes from Ext. II for the five slices. N = Naphthalene; MN = Methylnaphthalene; EN = Ethylnaphthalene; DMN = Dimethylnaphthalene.

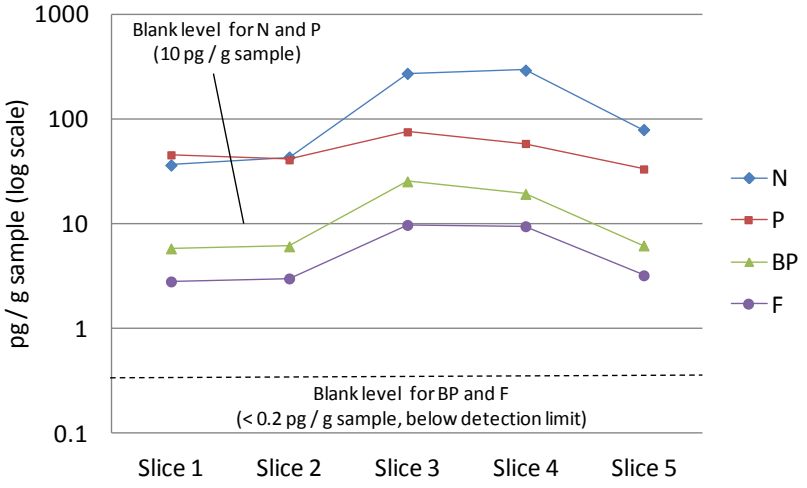

Figure 3.9. Amount and distribution of aromatic hydrocarbons from Ext. II for the five slices. N = Naphthalene; P = phenanthrene; BP = biphenyl; F = fluorene.

Alkylated hydrocarbons are always less abundant than their parent hydrocarbons. The important common feature among all slices is that these hydrocarbons could only be released by HCl treatment. Therefore, aromatic hydrocarbons are considered to have been trapped and preserved among the carbonate minerals, indicating that they are likely to be indigenous compounds of Archean origin. There are no known younger petroleum source rocks overlying the Fortescue Group in the study area. Most of the aromatic hydrocarbons have maxima between slices 3 and 4, rather than in the middle of the sample (slice 5), and thus have a rather heterogeneous distribution through

the rock. The rock sample was composed of many centimetre scale coniform stromatolites, which may have contributed to an abundance peak somewhere other than in the middle of the rock.

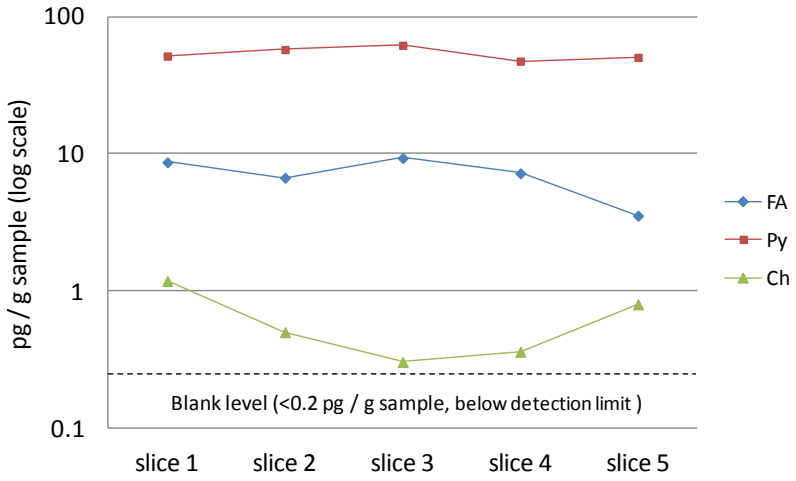

Figure 3.10. Amount and distribution of polycyclic aromatic hydrocarbons from Ext. II for the five slices. FA = fluoranthene; Py = pyrene; Ch = chrysene.

Several high molecular weight polycyclic aromatic hydrocarbons (PAHs) with four or more rings are present in all the slices, including fluoranthene, pyrene, and chrysene (Fig. 3.10). In slices 1 and 2, pyrene is more abundant than naphthalene, and is the most abundant aromatic hydrocarbon. No alkylated PAHs were detected except for 1-, 2- and 4-methylpyrenes. The distribution of PAHs is relatively homogenous throughout the rock, unlike other aromatic compounds. This may indicate a different origin for these PAHs.

Various aromatic hydrocarbon parameters that are useful for assessing the thermal maturity of a rock (e.g. Radke et al., 1982; Nabbefeld et al., 2010) were calculated for each slice (Table 3.2). Most of the calculated aromatic parameters indicate a very high thermal maturity for the rock. The methylphenanthrene index 1 (MPI-1) is less than 0.1 for all slices, and thus gives a calculated vitrinite reflectance equivalent (R_c) of 2.2-2.3% (-0.60 x MPI-1 + 2.30, Radke and Welte, 1983), assuming that this Phanerozoic calibration can be applied to the Archean (Dick et al., 2013). R_c increases with the maturity of a rock, and R_c>2.0 generally indicates the dry-gas zone (Peters et al., 2005). The methylnaphthalene ratio (MNR), the dimethylnaphthalene ratio 1 (DNR-1), the trimethylnaphthalene ratio 2 (TNR-2), the methylphenanthrene distribution fraction (MPDF) and the methylphenanthrene

ratio (MPR) have similar values to those from the Mesoproterozoic Velkerri Member in the McArthur Basin in Australia (McManus 1), that was reported as highly thermally mature and corresponding to the peak to late oil generation window (George and Ahmed, 2002). MNR, DNR-1, TNR-2, MPDF, and MPR are positively correlated with thermal maturity, due to a thermodynamic equilibrium towards particular structural isomers. The values of aromatic parameters are generally homogenous throughout the rock slices (Table 3.2). Therefore, even though the distribution of aromatic hydrocarbons is heterogeneous, their thermal history appears to be the same.

These aromatic hydrocarbon data are partially in agreement and partially not in agreement with a previous drill core study targeting the same region (Roy 1, Tum 1 and Rae 1 in Table 3.2) (Brocks et al., 2003a). In the previous study, several rocks from the Fortescue Group and from the Hamersley Group were investigated. Roy 1 and Tum 1 were from the Fortescue Group, and Rae 1 was from the Hamersley Group (Fig. 3.1). The thermal maturity of Roy 1 was estimated to be the early to late stage of oil generation based on MPDF and MPI-1 (R_c = 0.8, Radke and Welte, 1983) (Table 3.2). Tum 1 was considered to have a thermal maturity as high as the wet-gas zone, based on the phenanthrene to methylphenanthrene ratio (P / Σ MP), MPDF, MPR and MPI-1 (R_c = 2.0 %, Radke and Welte, 1983) (Table 3.2).

Although the rock in this study is also from the Fortescue Group, the observed distribution of aromatic hydrocarbons is different to the previous study. The ratios of parent aromatic hydrocarbons to alkylated hydrocarbons in this study are much higher (1.4-8.0; N / ΣMN, P / ΣMP, BP / ΣMBP, and F / ΣMF in table 3.2) compared to those in Roy 1 and Tum 1. Highly thermally mature rocks generally tend to have high aromatic to alkylated hydrocarbon ratios, because of the lower stability of alkylated hydrocarbons (Matthias et al., 1982; Price, 1993). P / Σ MP in Tum 1 had a relatively high value (1.5), but all other ratios were low (<< 1). These ratios indicated a low maturity of the examined rocks, but this was not thoroughly discussed in the previous study (Brocks et al., 2003a).

The other aromatic parameters such as MNR, DNR-1, TNR-2, MPDF and MPR previously reported for the Fortescue Group are generally similar to this study, except for DNR-1 and TNR-2 in Tum 1, which

are extremely high compared to this study and also compared to the work by George and Ahmed (2002). This might reflect the composition of the original organic matter in Tum 1. The Tum 1 MPI-1 suggested a high thermal maturity of the rocks (R_c = 2.0), but it is still lower than in this study.

Rae 1 from the Hamersley Group was more similar to the rock in this study than Roy 1 and Tum 1. Rae 1 was estimated to be very thermally mature and in the dry-gas zone in the previous study (Brocks et al., 2003a). The ratio of parent hydrocarbons to alkylated hydrocarbons was more than 1, and even larger than in this study. The DNR-1 and TNR-2 indicated a high thermal maturity, although the MPDF and the MPR indicated lower thermal maturities (Table 3.2). This may be caused by the reversals of thermal maturity parameters at high temperature (Dick et al., 2013). The MPI-1 of Rae 1 was similar to this study, corresponding to an R_c of ~2.3 (Radke and Welte, 1983).

Although the rock in this study is from the Fortescue Group, its thermal history seems to be closer to the previously analysed rock from the Hamersley Group. In contrast, both Roy 1 and Tum 1 from the Fortescue Group appear to have a lower thermal maturity. Tum1 comes from the Z1 metamorphism area of the Pilbara region (Smith et al., 1982), corresponding to prehnite-pumpellyite facies. Roy 1 and the rock in this study come from the Z2 metamorphism area (prehnite-pumpellyite-epidote facies), and Rae 1 comes from the Z3 area (prehnite-pumpellyite-epidote-actinolite facies). Therefore, the order of the thermal maturity (Rae 1 > this study > Roy 1 / Tum 1) is generally consistent with the geographical metamorphic gradient (White et al., 2014). The difference in thermal maturity between the rock in this study and Roy 1, both of which come from the same metamorphism area, may be due to local variations in thermal history between the localities. The difference in thermal maturity between Roy 1 and Tum 1 is more problematic. In the previous study (Brocks et al., 2003a), Tum 1 was estimated to be more thermally mature than Roy 1, which is not consistent with the geographic metamorphic gradient outlined above. This may suggest that the aromatic hydrocarbons in Tum 1 or in Roy 1 are at least partially contaminants, as was postulated by Brocks (2011).

Table 3.2. Ratios including thermal maturity parameters of Ext. II aromatic hydrocarbons. Roy 1 is from the Roy Hill Member, Jeerinah Formation, Fortescue Group. Tum 1 is from the Tumbiana Formation, Fortescue Group in Western Australia. Rae 1 is from the Mt McRae shale, Hamersley Group in Western Australia. McManus 1 is from the Mesoproterozoic Velkerri Member in the McArthur Basin in Australia.

	Slice 1	Slice 2	Slice 3	Slice 4	Slice 5	Roy 1[a]	Tum 1[a]	Rae 1[a]	McManus1[b]
N / Σ MN	4.5	2.9	2.6	3.6	3.4	0.03	0.15	3.5	-
P / Σ MP	7.4	6.0	8.0	3.4	7.4	0.36	1.5	11	-
BP / Σ MBP	2.4	2.2	1.6	1.4	1.8	0.35	0.15	6.4	-
F / Σ MF	1.6	1.9	1.5	1.9	1.9	0.24	0.41	5.3	-
MNR	2.0	1.6	1.8	1.8	2.1	-	-	-	2.2
DNR-1	4.9	5.5	7.1	6.3	7.2	5.8	12.6	3.5	8
TNR-2	0.46	0.38	0.82	0.79	0.77	0.76	1.7	0.58	1
MPI	0.08	0.11	0.09	0.20	0.06	0.71	0.46	0.06	1.6
R_c	2.25	2.24	2.25	2.18	2.26	0.83	2.02	2.26	1.34
MPDF	0.59	0.63	0.69	0.68	0.58	0.44	0.61	0.44	0.67
MPR	2.1	1.2	2.3	2.9	1.2	0.87	1.9	1.1	2.9

[a]Brocks et al. (2003a); [b]George and Ahmed (2002), the highest value is shown. Σ MN = 2-MN + 1-MN; Σ MP = 3-MP + 2-MP + 9-MP + 1-MP; Σ MBP = 2-MBP + 3-MBP + 4-MBP; Σ MF = 2-MF + 3-MF + 1-MF + 4-MF; MNR = 2-MN / 1-MN; DNR-1 = (2,6-DMN + 2,7-DMN) / 1,5-DMN; TNR-2 = (2,3,6-TMN + 1,3,7-TMN) / (1,4,6-TMN + 1,3,5-TMN + 1,3,6-TMN); MPI-1 = 1.5 x (3-MP + 2-MP) / (P + 9-MP + 1-MP); R_c = 0.60 x MPI-1 + 2.30; MPDF = (3-MP + 2-MP) / Σ MP; MPR = 2-MP / 1-MP. MN = methylnaphthalene; MP = methylphenanthrene; MBP = methylbiphenyl; MF = methylfluorene; TMN = trimethylnaphthalene, for other abbreviations see Figs 3.8 and 3.9.

3.4.2.3. Biomarkers

No source-specific biomarkers such as hopanes or steranes were detected in any of the Ext. II fractions from the rock slices, as was also observed for Ext. I. This would be expected, given the observations of the high thermal maturity of the rock. If any biomarkers were originally present, they seem to have decomposed under the high temperature conditions over geological time. Regular isoprenoids were detected in the Ext. II fractions from all the rock slices. These have a similar distribution to those in Ext. I (Fig. 3.7b). Regular isoprenoids from C_{13} to C_{16} in Ext. II are slightly more

abundant than in Ext. I. They do not have any particular trend between the rocks slices. Pr/Ph ratios for Ext. II are similar to those of Ext. I, but with slightly higher values (Table 3.1).

3.5. Discussion

3.5.1. Outer slice 1 aliphatic hydrocarbon distribution

The distribution of *n*-alkanes throughout the rock suggests several inputs of organic matter, or the mixing of these inputs and the original indigenous hydrocarbons. The OEP in the outer-most layer indicates the recent input of higher plant-derived organic matter (Fig. 3.4), which may be related to roots of plants, pollens, aerosols of vehicle fuels, or to the incorporation of debris from surrounding biomass. The large relative abundances of *n*-C_{17} and 7- and 6-MHeD in the outer slice also suggest the presence of cyanobacteria (see also Chapter 6). The lack of these hydrocarbons in deeper layers suggests the penetration of cyanobacterial biomass was limited to the rock surface, although a trace amount of *n*-C_{17} could possibly have migrated into the deeper part of the rock (slices 2-4) through pores in the rock fabric, as suggested by a slight higher abundance of *n*-C_{17} than those of *n*-C_{16} and *n*-C_{18} (Fig. 3.4a). A common endolithic cyanobacterium is the unicellular *Chroococcidiopsis,* which typically occurs along with several other genera such as *Gloeocapsa* and *Acaryochloris* (Friedmann, 1982; Büdel et al., 2004; de los Ríos et al., 2007). Although there is no direct evidence for the production of mid-chain branched MMAs by these cyanobacterial species, the biosynthesis of mid-chain branched MMAs seems to be ubiquitous within the cyanobacterial clade (Coates et al., 2014), and so it is possible that the observed MMAs and *n*-C_{17} are the remains of recent or living endolithic cyanobacterial activity.

One inconsistency between the MMA distribution in the outer-most layer and modern cyanobacterial MMA synthesis is that 6-MHeD is not a major product, although some cyanobacteria are known to produce it (Coates et al., 2014). However, in this study, 6-MHeD has a higher abundance than 7-MHeD. A possible explanation for the discrepancy is that the MMAs undergo a change in their relative abundance, due to differences in their thermal stability, during which it is possible that biologically-derived 7-MHeD undergoes kinetically-controlled isomerisation to produce

6-MHeD, and perhaps other MHeD isomers. Other possibilities are that the cyanobacteria that inhabited this rock surface produced MMAs with a different relative abundance to that known from laboratory-cultured cyanobacteria, or that there are unknown extant cyanobacteria living today in the Pilbara which predominantly produce 6-MHeD. It is possible that these hydrocarbons are derived from living cyanobacteria. However, no functionalised lipid compounds were detected from the outer-most layer of the rock. Considering the depositional history of the Fortescue Group, the first appearance of the investigated rock to the surface would have been during the Cenozoic or later (M. Van Kranendonk, personal communication), thus putting a maximum age constraint on endolithic cyanobacteria inhabiting this rock surface.

3.5.2. Other aliphatic hydrocarbon distributions

A large amount of high molecular weight *n*-alkanes > *n*-C_{21} appeared in all slices after the HCl treatment (Fig. 3.4b). These *n*-alkanes could be the diagenetic products of more complex biomolecules produced by thermal cracking during deep burial and heating. There are no theoretical constraints to limit the cracking products of diagenesis within the molecular weight range of *n*-C_{21} to C_{35}. Low molecular weight *n*-alkanes might have been selectively removed by weathering through pore spaces in the rock fabric because of their small size, or may have undergone biodegradation preferentially affecting low molecular weight hydrocarbons (Wenger et al., 2002). The slight EOP between *n*-C_{15} and *n*-C_{19} in slice 5 might reflect such events in the past. An alternative explanation is that the high molecular weight *n*-alkanes > *n*-C_{21} are not diagenetic products, but instead are the direct remains of host organisms. One such candidate group of organisms is sulphate-reducing bacteria, some of which are known to produce long chain *n*-alkanes ranging from *n*-C_{25} to C_{35} (Ladygina et al., 2006; Melendez et al., 2013). The high molecular weight *n*-alkanes > *n*-C_{21} were only present after the HCl treatment, suggesting they may have an Archean origin. However, *n*-alkanes are very common hydrocarbons and cannot be used to identify a specific bacterial clade.

3.5.3. Aromatic hydrocarbon distribution and thermal maturity

The relative abundance of aromatic hydrocarbons in Ext. II is in sharp contrast with the scarcity of aromatic hydrocarbons in Ext. I (Figs 3.8-3.10). Aromatic hydrocarbons might have been removed

from the more open and less protected pore space by weathering over geological time. The amount of naphthalene and phenanthrene in the Ext. I slices was quite small (mostly < 20 pg /g sample), and no alkylated hydrocarbons could be detected. In contrast, the aromatic hydrocarbons in Ext. II seem to have been protected within the carbonate minerals and thus survived weathering. It has been proven that the acid treatment of rock samples effectively releases indigenous hydrocarbons without significantly altering the original composition of preserved hydrocarbons (Sherman et al., 2007). Although the samples were heated at 70 °C, this is much lower than the temperatures the samples would have experienced during burial (see below).

A high thermal maturity of the investigated rock is suggested by aromatic parameters such as MNR, DNR-1, TNR-2, MPI-1, MPDF and MPR. The ratios of parent aromatic hydrocarbons to alkylated hydrocarbons also suggest a high maturity. The suggested maturity is generally higher than the previously studied Fortescue Group rocks and is close to that of Hamersley Group rocks (see Brocks et al., 2003a). The high thermal maturity is consistent with the lack of any polycyclic biomarkers such as hopanes and steranes, because these compounds thermally crack at high temperatures (van Graas, 1990; George et al., 2008), or are below detection limit even if they are present. The high thermal maturity of the rock, as deduced by the hydrocarbon distribution, is corroborated by the metamorphic grade of prehnite-pumpellyite facies (175-280 °C) of the Fortescue Group in this part of the Pilbara (Smith et al., 1982). A more concerted regional survey of rocks of this age is necessary to establish if any zones of lower thermal maturity have survived. There may also be lithological variations, such as degree of cementation, which may help to preserve hydrocarbons in rocks of this age.

Although no specific biomarkers were found, and the discovered aromatic hydrocarbons are too common or ubiquitous to pinpoint any one taxonomic group, the aromatic hydrocarbons preserved in this sample could be still useful for investigating Archean ecosystems. There have been only a few papers reporting the presence of high molecular weight PAHs in Archean rocks (Brocks et al., 2003b; Marshall et al., 2007; Holman et al., 2014). Although they are supposedly biogenic, there is no

consensus in regards to their origin. The formation of PAHs is a temperature-dependent process, and thus they were probably produced by post-depositional diagenesis (Williford et al., 2011). Hydrothermal activity is known to be one mechanism to form PAHs (Kawka and Simoneit, 1990; Simoneit and Fetzer, 1996), and the interaction of organic matter with hydrothermal fluids might have produced PAHs in Archean rocks. The distribution of most of the aromatic hydrocarbons is heterogeneous, whereas high molecular weight PAHs have a homogeneous distribution, consistent with the post-depositional diagenetic production of these PAHs.

There is a possibility that meteoric water circulation through the rock may have caused the recrystallisation of carbonate minerals and removed the aromatic HCs in the carbonate minerals in the outer slices (Figs. 3.8 and 3.9) (supergene; Alpers and Brimhall, 1988). However, the homogeneous distribution of high molecular weight PAHs is inconsistent with the supergene model (Fig. 3.10). These PAHs, possibly produced by hydrothermal activity during burial and before uplift to the Earth's surface, should also be subject to the same weathering process, and thus, have a similar spatial distribution to other aromatic HCs. Therefore, the influence of weathering on the heterogeneous distribution of aromatic HCs in Ext. II is considered to not be significant.

The relative scarcity of aliphatic hydrocarbons and the richness of aromatic hydrocarbons in Archean rocks has previously been reported (Brocks et al., 2003b; French et al., 2013). Type III kerogen in post-Silurian sediments is typically aromatic (Tissot et al., 1974). Although Precambrian organic matter was predominantly microbially derived, it might have had a similar composition to Phanerozoic organic matter such as dinosporin, which is composed of condensed and aromatic recalcitrant macromolecules used in resting cyst walls of dinoflagellates (Brocks et al., 2003b). Indeed, cell wall materials of some Neoproterozoic acritarchs were shown to have a similar polyaromatic composition (Arouri et al., 2000), which might also represent the composition of Archean microorganisms investigated in this study.

3.6. Conclusions

The composition and origin of organic matter preserved in an Archean rock were investigated. Aliphatic hydrocarbons in the freely extractable fraction (Ext. I) likely originated from several different inputs of organic matter after deposition, and do not seem to be syngenetic. The lack of most aromatic hydrocarbons in Ext. I is attributed to be the result of severe weathering since uplift and exposure of the outcrop during the Cenozoic. The presence of living or recent endolithic cyanobacteria on the rock surface is suggested by an *n*-alkane maximum at *n*-C_{17} and the 7- and 6-MHeD abundance in the outer slice. Aliphatic hydrocarbons in the fraction released after acid removal of the carbonate minerals (Ext. II) have a smooth distribution of high molecular weight *n*-alkanes, suggesting a high thermal maturity of the rock. A variety of aromatic hydrocarbons were only found in Ext. II, indicating their presence is due to the protection from weathering of the carbonate minerals, and suggesting their indigeneity. Various aromatic parameters such as the methylphenanthrene index, alkylnaphthalene ratios, and the dominance of parent PAH over alkylated equivalents suggest a high thermal maturity of the rock, consistent with prehnite-pumpellyite facies metamorphism.

The results of this study show a different preservation history of aliphatic hydrocarbons and aromatic hydrocarbons within the same rock. Aliphatic hydrocarbons seem to be a mixture of indigenous compounds and later contamination, although it is possible that any indigenous hydrocarbons might have been completely removed by weathering, as was the case for most of the original aromatic hydrocarbons. However, some aromatic hydrocarbons are preserved inside the carbonate minerals, and these could reflect the original composition of Archean organic matter. These results suggest future investigations of this unit should take similar and additional steps to prevent contamination of analyses, especially removal of the outer-most layer.

3.7. Acknowledgements

We thank the Geological Survey of Western Australia (GSWA) for logistical field support and scientific assistance, particularly from Kath Grey and Arthur Hickman. Y.H. was supported by a Macquarie

University Research Excellence Scholarship. D.T.F. was supported by an Australian Government Postgraduate Award. M.R.W. acknowledges the Australian Research Council for a Discovery Grant and a Professorial Fellowship. S.C.G. acknowledges the Australian Research Council for a Discovery Grant. All authors acknowledge support from the Australian Centre for Astrobiology. We thank the three journal reviewers for their helpful comments that improved the earlier draft of this paper.

3.8. References

Alpers, C.N. and Brimhall, G.H. (1988) Middle Miocene climatic change in the Atacama Desert, northern Chile: Evidence from supergene mineralization at La Escondida. Geological Society of America Bulletin 100, 1640-1656.

Anbar, A.D., Duan, Y., Lyons, T.W., Arnold, G.L., Kendall, B., Creaser, R.A., Kaufman, A.J., Gordon, G.W., Scott, C., Garvin, J. and Buick, R. (2007) A whiff of oxygen before the Great Oxidation Event? Science 317, 1903-1906.

Arndt, N.T., Nelson, D.R., Compston, W., Trendall, A.F. and Thorne, A.M. (1991) The age of the Fortescue Group, Hamersley Basin, Western Australia, from ion microprobe zircon U-Pb results. Australian Journal of Earth Sciences 38, 261-281.

Arouri, K.R., Greenwood, P.F. and Walter, M.R. (2000) Biological affinities of Neoproterozoic acritarchs from Australia: microscopic and chemical characterisation. Organic Geochemistry 31, 75-89.

Awramik, S.M. and Buchheim, H.P. (2009) A giant, Late Archean lake system: The Meentheena Member (Tumbiana Formation; Fortescue Group), Western Australia. Precambrian Research 174, 215-240.

Bekker, A., Holland, H.D., Wang, P.L., Rumble, D., Stein, H.J., Hannah, J.L., Coetzee, L.L. and Beukes, N.J. (2004) Dating the rise of atmospheric oxygen. Nature 427, 117-120.

Brocks, J.J. (2001) Molecular Fossils in Archean Rocks. Ph.D. dissertation, University of Sydney.

Brocks, J.J. (2011) Millimeter-scale concentration gradients of hydrocarbons in Archean shales: Live-oil escape or fingerprint of contamination? Geochimica Et Cosmochimica Acta 75, 3196-3213.

Brocks, J.J., Buick, R., Logan, G.A. and Summons, R.E. (2003a) Composition and syngeneity of molecular fossils from the 2.78 to 2.45 billion-year-old Mount Bruce Supergroup, Pilbara Craton, Western Australia. Geochimica Et Cosmochimica Acta 67, 4289-4319.

Brocks, J.J., Logan, G.A., Buick, R. and Summons, R.E. (1999) Archean molecular fossils and the early rise of eukaryotes. Science 285, 1033-1036.

Brocks, J.J., Love, G.D., Snape, C.E., Logan, G.A., Summons, R.E. and Buick, R. (2003b) Release of bound aromatic hydrocarbons from late Archean and Mesoproterozoic kerogens via hydropyrolysis. Geochimica Et Cosmochimica Acta 67, 1521-1530.

Brocks, J.J., Love, G.D., Summons, R.E., Knoll, A.H., Logan, G.A. and Bowden, S.A. (2005) Biomarker evidence for green and purple sulphur bacteria in a stratified Palaeoproterozoic sea. Nature 437, 866-870.

Brocks, J.J. and Summons, R.E. (2003) 8.03 - Sedimentary Hydrocarbons, Biomarkers for Early Life, in: Editors-in-Chief: Heinrich, D.H., Karl, K.T. (Eds.), Treatise on Geochemistry. Pergamon, Oxford, pp. 63-115.

Brooks, J.D., Gould, K. and Smith, J.W. (1969) Isoprenoid Hydrocarbons in Coal and Petroleum. Nature 222, 257-259.

Büdel, B., Weber, B., Kuhl, M., Pfanz, H., Sultemeyer, D. and Wessels, D. (2004) Reshaping of sandstone surfaces by cryptoendolithic cyanobacteria: bioalkalization causes chemical weathering in arid landscapes. Geobiology 2, 261-268.

Buick, R., Thornett, J.R., McNaughton, N.J., Smith, J.B., Barley, M.E. and Savage, M. (1995) Record of emergent continental crust 3.5 billion years ago in the Pilbara craton of Australia. Nature 375, 574-577.

Coates, R., Podell, S., Korobeynikov, A., Lapidus, A., Pevzner, P., Sherman, D., Allen, E., Gerwick, L. and Gerwick, W. (2014) Characterization of cyanobacterial hydrocarbon composition and distribution of biosynthetic pathways. PloS one 9, e85140.

Coffey, J.M. (2011) A paleoenvironmental study of the 2.7 Ga Tumbiana Formation, Fortescue Basin, Western Australia. Ph.D. dissertation, University of New South Wales, Sydney.

Coffey, J.M., Flannery, D.T., Walter, M.R. and George, S.C. (2013) Sedimentology, stratigraphy and geochemistry of a stromatolite biofacies in the 2.72Ga Tumbiana Formation, Fortescue Group, Western Australia. Precambrian Research 236, 282-296.

de los Ríos, A., Grube, M., Sancho, L. and Ascaso, C. (2007) Ultrastructural and genetic characteristics of endolithic cyanobacterial biofilms colonizing Antarctic granite rocks. FEMS microbiology ecology 59, 386-395.

Dick, J.M., Evans, K.A., Holman, A.I., Jaraula, C.M.B. and Grice, K. (2013) Estimation and application of the thermodynamic properties of aqueous phenanthrene and isomers of methylphenanthrene at high temperature. Geochimica Et Cosmochimica Acta 122, 247-266.

Didyk, B.M., Simoneit, B.R.T., Brassell, S.C. and Eglinton, G. (1978) Organic geochemical indicators of palaeoenvironmental conditions of sedimentation. Nature 272, 216-222.

Dutkiewicz, A., Volk, H., George, S., Ridley, J. and Buick, R. (2006) Biomarkers from Huronian oil-bearing fluid inclusions: An uncontaminated record of life before the Great Oxidation Event. Geology 34, 437-440.

Eglinton, G. and Hamilton, R.J. (1967) Leaf Epicuticular Waxes. Science 156, 1322-1335.

Eglinton, G., Scott, P.M., Belsky, T., Burlingame, A.L. and Calvin, M. (1964) Hydrocarbons of Biological Origin from a One-Billion-Year-Old Sediment. Science 145, 263-264.

Eigenbrode, J.L., Freeman, K.H. and Summons, R.E. (2008) Methylhopane biomarker hydrocarbons in Hamersley Province sediments provide evidence for Neoarchean aerobiosis. Earth and Planetary Science Letters 273, 323-331.

Flannery, E.N. and George, S.C. (2014) Assessing the syngeneity and indigeneity of hydrocarbons in the ~1.4 Ga Velkerri Formation, McArthur Basin, using slice experiments. Organic Geochemistry, submitted.

French, K.L., Hallman, C., Hope, J.M., Buick, R., Brocks, J.J. and Summons, R.E. (2013) Archean hydrocarbon biomarkers: Archean or not?, Goldschmidt 2013 Conference Abstract.

Friedmann, E. (1982) Endolithic microorganisms in the antarctic cold desert. Science 215, 1045-1053.

George, S. and Ahmed, M. (2002) Use of aromatic compound distributions to evaluate organic maturity of the Proterozoic middle Velkerri Formation, McArthur Basin, Australia. The Sedimentary Basins of Western Australia III: Proceedings of the West Australasian Basins Symposium (WABS) III.

George, S.C., Volk, H., Dutkiewicz, A., Ridley, J. and Buick, R. (2008) Preservation of hydrocarbons and biomarkers in oil trapped inside fluid inclusions for > 2 billion years. Geochimica Et Cosmochimica Acta 72, 844-870.

Grice, K. and Eiserbeck, C. (2014) 12.3 - The Analysis and Application of Biomarkers, in: Holland, H.D., Turekian, K.K. (Eds.), Treatise on Geochemistry (Second Edition). Elsevier, Oxford, pp. 47-78.

Holland, H.D. (2002) Volcanic gases, black smokers, and the great oxidation event. Geochimica Et Cosmochimica Acta 66, 3811-3826.

Holman, A.I., Grice, K., Jaraula, C.M.B. and Schimmelmann, A. (2014) Bitumen II from the Paleoproterozoic Here's Your Chance Pb/Zn/Ag deposit: Implications for the analysis of depositional environment and thermal maturity of hydrothermally-altered sediments. Geochimica Et Cosmochimica Acta 139, 98-109.

Holman, A.I., Grice, K., Jaraula, C.M.B., Schimmelmann, A. and Brocks, J.J. (2012) Efficiency of extraction of polycyclic aromatic hydrocarbons from the Paleoproterozoic Here's Your Chance Pb/Zn/Ag ore deposit and implications for a study of Bitumen II. Organic Geochemistry 52, 81-87.

Jackson, M.J., Powell, T.G., Summons, R.E. and Sweet, I.P. (1986) Hydrocarbon shows and petroleum source rocks in sediments as old as 1.7 x 10^9 years. Nature 322, 727-729.

Kawka, O.E. and Simoneit, B.R.T. (1990) Polycyclic aromatic hydrocarbons in hydrothermal petroleums from the Guaymas Basin spreading center. Applied Geochemistry 5, 17-27.

Ladygina, N., Dedyukhina, E. and Vainshtein, M. (2006) A review on microbial synthesis of hydrocarbons. Process Biochemistry 41, 1001-1014.

Lipple, S.L. (1975) Definitions of new and revised stratigraphic units of the eastern Pilbara region. Annual Report - Western Australia, Geological Survey 1974, 58-63.

Lyons, T., Reinhard, C. and Planavsky, N. (2014) The rise of oxygen in Earth's early ocean and atmosphere. Nature 506, 307-315.

Marshall, C.P., Love, G.D., Snape, C.E., Hill, A.C., Allwood, A.C., Walter, M.R., Van Kranendonk, M.J., Bowden, S.A., Sylva, S.P. and Summons, R.E. (2007) Structural characterization of kerogen in 3.4 Ga Archaean cherts from the Pilbara Craton, Western Australia. Precambrian Research 155, 1-23.

Matthias, R., Dietrich, H.W. and Helmut, W. (1982) Geochemical study on a well in the Western Canada Basin: relation of the aromatic distribution pattern to maturity of organic matter. Geochimica Et Cosmochimica Acta 46, 1-10.

Melendez, I., Grice, K., Trinajstic, K., Ladjavardi, M., Greenwood, P. and Thompson, K. (2013) Biomarkers reveal the role of photic zone euxinia in exceptional fossil preservation: An organic geochemical perspective. Geology 41, 123-126.

Nabbefeld, B., Grice, K., Schimmelmann, A., Summons, R.E., Troitzsch, U. and Twitchett, R.J. (2010) A comparison of thermal maturity parameters between freely extracted hydrocarbons (Bitumen I) and a second extract (Bitumen II) from within the kerogen matrix of Permian and Triassic sedimentary rocks. Organic Geochemistry 41, 78-87.

Ourisson, G., Rohmer, M. and Poralla, K. (1987) Prokaryotic Hopanoids and other Polyterpenoid Sterol Surrogates. Annual Review of Microbiology 41, 301-333

Peters, K.E., Walters, C.C. and Moldowan, J.M. (2005) The biomarker guide: Biomarkers and isotopes in petroleum exploration and Earth history. Cambridge University Press Volume 2.

Planavsky, N.J., Asael, D., Hofmann, A., Reinhard, C.T., Lalonde, S.V., Knudsen, A., Wang, X., Ossa, F.O., Pecoits, E., Smith, A.J.B., Beukes, N.J., Bekker, A., Johnson, T.M., Konhauser, K.O., Lyons, T.W. and Rouxel, O.J. (2014) Evidence for oxygenic photosynthesis half a billion years before the Great Oxidation Event. Nature Geoscience 7, 283-286.

Powell, T.G. and McKirdy, D.M. (1973) Relationship between Ratio of Pristane to Phytane, Crude Oil Composition and Geological Environment in Australia. Nature Physical Science 243, 37-39.

Price, L.C. (1993) Thermal stability of hydrocarbons in nature: Limits, evidence, characteristics, and possible controls. Geochimica Et Cosmochimica Acta 57, 3261-3280.

Radke, M. and Welte, D. (1983) The Methylphenanthrene index (MPI). A Maturity parameter based on aromatic hydrocarbons, in: Bjorøy, M., Albrecht, C., Cornford, C. (Eds.), Advances in Organic Geochemistry. John Wiley & Sons, New York, pp. 504-512.

Radke, M., Willsch, H., Leythaeuser, D. and Teichmüller, M. (1982) Aromatic components of coal: relation of distribution pattern to rank. Geochimica Et Cosmochimica Acta 46, 1831-1848.

Rashby, S.E., Sessions, A.L., Summons, R.E. and Newman, D.K. (2007) Biosynthesis of 2-methylbacteriohopanepolyols by an anoxygenic phototroph. Proceedings of the National Academy of Sciences of the United States of America 104, 15099-15104.

Rasmussen, B., Fletcher, I.R., Brocks, J.J. and Kilburn, M.R. (2008) Reassessing the first appearance of eukaryotes and cyanobacteria. Nature 455, 1101-1104.

Sakurai, R., Ito, M., Ueno, Y., Kitajima, K. and Maruyama, S. (2005) Facies architecture and sequence-stratigraphic features of the Tumbiana Formation in the Pilbara Craton, northwestern Australia; implications for depositional environments of oxygenic stromatolites during the late Archean. Precambrian Research 138, 255-273.

Schirmer, A., Rude, M.A., Li, X., Popova, E. and Del Cardayre, S.B. (2010) Microbial biosynthesis of alkanes. Science 329, 559-562.

Sherman, L.S., Waldbauer, J.R. and Summons, R.E. (2007) Improved methods for isolating and validating indigenous biomarkers in Precambrian rocks. Organic Geochemistry 38, 1987-2000.

Simoneit, B. and Fetzer, J. (1996) High molecular weight polycyclic aromatic hydrocarbons in hydrothermal petroleums from the Gulf of California and Northeast Pacific Ocean. Organic Geochemistry 24, 1065-1077.

Smith, R.E., Perdrix, J.L. and Parks, T.C. (1982) Burial Metamorphism in the Hamersley Basin, Western Australia. Journal of Petrology 23, 75-102.

Summons, R.E., Bradley, A.S., Jahnke, L.L. and Waldbauer, J.R. (2006) Steroids, triterpenoids and molecular oxygen. Philosophical Transactions of the Royal Society B: Biological Sciences 361, 951-968.

Summons, R.E., Jahnke, L.L., Hope, J.M. and Logan, G.A. (1999) 2-Methylhopanoids as biomarkers for cyanobacterial oxygenic photosynthesis. Nature 400, 554-557.

Summons, R.E., Powell, T.G. and Boreham, C.J. (1988) Petroleum geology and geochemistry of the Middle Proterozoic McArthur Basin, Northern Australia: III. Composition of extractable hydrocarbons. Geochimica Et Cosmochimica Acta 52, 1747-1763.

Thorne, A.M. and Trendall, A.F. (2001) Geology of the Fortescue Group, Pilbara Craton, Western Australia. Bulletin - Geological Survey of Western Australia, 249.

Tissot, B., Durand, B., Espitalie, J. and Combaz, A. (1974) Influence of nature and diagenesis of organic matter in formation of petroleum. AAPG Bulletin 58, 499-506.

van Graas, G.W. (1990) Biomarker maturity parameters for high maturities: Calibration of the working range up to the oil/condensate threshold. Organic Geochemistry 16, 1025-1032.

Volk, H., George, S.C., Dutkiewicz, A. and Ridley, J. (2005) Characterisation of fluid inclusion oil in a Mid-Proterozoic sandstone and dolerite (Roper Superbasin, Australia). Chemical Geology 223, 109-135.

Waldbauer, J.R., Sherman, L.S., Sumner, D.Y. and Summons, R.E. (2009) Late Archean molecular fossils from the Transvaal Supergroup record the antiquity of microbial diversity and aerobiosis. Precambrian Research 169, 28-47.

Walter, M. (1983) Archean stromatolites: Evidence of the Earth's earliest benthos, in: Schopf, J. (Ed.), Earth's Earliest Biosphere: It's Origin and Evolution. Princeton University Press, Princeton, pp. 187-213.

Welander, P.V., Coleman, M.L., Sessions, A.L., Summons, R.E. and Newman, D.K. (2010) Identification of a methylase required for 2-methylhopanoid production and implications for the interpretation of sedimentary hopanes. Proceedings of the National Academy of Sciences 107, 8537-8542.

Wenger, L.M., Davis, C.L. and Isaksen, G.H. (2002) Multiple controls on petroleum biodegradation and impact on oil quality. SPE Reservoir Evaluation & Engineering 5, 375-383.

White, A.J.R., Smith, R.E., Nadoll, P. and Legras, M. (2014) Regional-scale Metasomatism in the Fortescue Group Volcanics, Hamersley Basin, Western Australia: Implications for Hydrothermal Ore Systems. Journal of Petrology 55, 977-1009.

Williford, K.H., Grice, K., Logan, G.A., Chen, J. and Huston, D. (2011) The molecular and isotopic effects of hydrothermal alteration of organic matter in the Paleoproterozoic McArthur River Pb/Zn/Ag ore deposit. Earth and Planetary Science Letters 301, 382-392.

Chapter 4.

Significance of hydrocarbon biomarkers discovered in an Archean stromatolite at 2.7 Ga from the Fortescue Group, Pilbara Craton, Western Australia

Y. Hoshino [1,2], D. T. Flannery [2,3], M. R. Walter [2,3], S. C. George [1,2]

[1] *Department of Earth and Planetary Sciences, Macquarie University, Sydney, Australia*

[2] *Australian Centre for Astrobiology, University of New South Wales, Australia*

[3] *School of Biotechnology and Biomolecular Sciences, University of New South Wales, Australia*

Statement of authors' contribution

This Chapter is to be submitted soon to *Geochimica et Cosmochimica Acta*. This paper has been formatted to conform to the font and referencing style adopted in this thesis. Figures and tables included within the text are prefixed with the chapter number.

I am the primary author (95% of the effort). I collected the sample with the help of David Flannery (University of New South Wales, Australia). I examined the sample, including sample cutting, grinding, and solvent extractions. I performed gas chromatography-mass spectroscopy. I processed and interpreted all the data derived from the measurements. I processed and designed the structure of the paper. All co-authors carefully reviewed and provided feedback and valuable refinements on the final version of the manuscript, and approved it for submission. Neither this manuscript nor one with similar content under our authorship has been published or is being considered for publication elsewhere, except as described above.

Abstract

2α-Methylhopanes, steranes and mid-chain branched monomethylalkanes, indicative of cyanobacteria and atmospheric oxygen, have been found coexisting in an Archean stromatolite outcrop. The sample was collected from the Fortescue Group, the Pilbara region, Western Australia. Experimental contamination was reduced to picogram levels and the detected biomarker abundance is above the blank level, but it is still quantitatively low (only a few pg / g sample). The distribution of the biomarkers reveals that the detected hydrocarbons have two different origins: (1) recent cyanobacterial input in the outer-most layer of the rock; and (2) the remains of ancient, possibly Archean, cyanobacterial and eukaryotic input preserved deep inside the rock. The recent cyanobacterial biomarkers are limited to pore spaces near the rock's surfaces, whereas the ancient cyanobacterial and eukaryotic biomarkers primarily exist within the carbonate minerals, and have a higher abundance towards the inside of the rock, indicating that they have been isolated from the outside environment and are better preserved in the innermost part of the rock. The syngeneity and indigeneity of the discovered biomarkers and their implications are discussed.

4.1. Introduction

The Fortescue Group is one of only two areas in the world which contains low-metamorphosed and relatively pristine Archean crust (Smith et al., 1982). The abundance of outcropping stromatolites and the possibility of preserved hydrocarbons (HCs) in such very old rocks have attracted significant attention for the study of Neoarchean ecosystems. The increase of atmospheric oxygen after the Archean during the Great Oxidation Event (GOE) at 2.45-2.32 Ga drastically changed the environment of the early Earth and eventually the evolutionary direction of early life (Holland, 2006; Sessions et al., 2009; Rezende, 2013). Some oxygen could have been produced abiogenically through atmospheric photochemical reactions via hydrogen peroxide intermediates, but this process could only lead to quite low concentrations, up to 1.5×10^{-5} of the present atmospheric level (Haqq-Misra et al., 2011). Thus, it is generally considered that the vast majority of oxygen at the GOE was introduced by the oxygenic photosynthesis invented by cyanobacteria (Kopp et al., 2005; Kirschvink and Kopp, 2008).

However, there is uncertainty about the timing of the emergence of oxygenic photosynthesis. Recent lines of evidence such as geochemical analyses of redox-sensitive elements suggest the presence of atmospheric oxygen, and therefore by deduction, cyanobacteria before the GOE (Anbar et al., 2007; Kump and Barley, 2007; Gaillard et al., 2011; Crowe et al., 2013; Lyons et al., 2014; Planavsky et al., 2014). One difficulty in assessing the presence of cyanobacteria in the Archean is that there are no unambiguous physical fossils. Although there have been numerous studies of cyanobacterial-like microfossils and Archean stromatolites in pre-GOE rocks, the validity of these interpretations is highly controversial (Brasier et al., 2006; Schopf, 2006; Bosak et al., 2013).

Biomarkers, preserved HCs within sedimentary rocks sometimes linked to specific groups of species or taxa, have the potential to help assess the presence of cyanobacteria in geological records, and thus constrain the uncertainty surrounding the precise timing of cyanobacterial evolution (Eglinton et al., 1964; Briggs and Summons, 2014). There are several possible cyanobacterial biomarkers: 2α-methylhopanes and mid-chain branched monomethylalkanes (MMAs). 2α-Methylhopanes were once

thought to be exclusive biomarkers for cyanobacteria (Brocks et al., 1999; Summons et al., 1999), but it has been shown that several other bacteria such as proteobacteria and acidobacteria can produce 2α-methylhopanoids, the precursor molecule of the biomarker (Rashby et al., 2007; Welander et al., 2010). It is also clear that not all cyanobacteria (only 19 % of all sequenced cyanobacterial genera) possess the gene *hpn P* which encodes the enzyme responsible for methylating hopanoids at the C-2 position (Welander et al., 2010; Ricci et al., 2013). Thus, 2α-methylhopanes are not a common product from cyanobacteria, nor are they derived exclusively from the cyanobacterial clade, and so they cannot be used as sole evidence for cyanobacteria. However, with accompanying other evidence, they might be used to constrain the specific hopanoid-producing cyanobacterial clade.

Mid-chain branched MMAs are characteristic constituents of cyanobacterial lipids (Shiea et al., 1990; Shiea et al., 1991; Thiel et al., 1999; Schirmer et al., 2010; Coates et al., 2014). Whereas geological production of mid-chain branched MMAs is possible, no mechanism is known to selectively produce them. Therefore, a selective abundance of mid-chain branched MMAs may be used as cyanobacterial biomarkers. They occur in about two thirds of the cyanobacterial species examined, and cyanobacteria are the only microorganisms known to produce mid-chain branched MMAs (Shiea et al., 1990). In pure-cultured cyanobacteria, the biosynthesis of mid-chain branched MMAs are mainly limited to 7- and 8-methylheptadecanes, but some cyanobacteria produce other isomers / homologues in the C_{16}-C_{21} range, with one report suggesting up to C_{28} (Paoletti et al., 1976), depending on the species and the culture conditions (Shiea et al., 1990; Coates et al., 2014).

There are many examples of ancient mid-chain branched MMAs from the Precambrian era (Summons et al., 1988; Brocks et al., 2003b). However, these samples generally contain all possible isomers in approximately equal proportions, unlike the heterogeneous distribution of mid-chain branched MMAs of cyanobacterial origin in the Phanerozoic, where MMA distributions are broadly dominated by the 2- and 3-methyl homologues (e.g. Summons, 1987). Some Precambrian examples show specific MMA isomer distributions such as the dominance of 5- to 10-MMAs at longer carbon numbers (C_{22}-C_{25}) from the Neoproterozoic oils in Oman (Klomp, 1986) and from the Neoproterozoic

(Vendian) oils of the Siberian platform (Fowler and Douglas, 1987), but they do not match any known MMA productions of cyanobacterial origin. There is one example of a high relative abundance of 7- and 8-MMAs in a fluid inclusion oil of possible cyanobacterial origin from Jurassic reservoirs in Australia (the Nancar oil family) (George et al., 2002).

Steranes can also be indirect indicators of the presence of cyanobacteria, because sterols, the precursor biomolecules of steranes, require molecular oxygen to be synthesised, and the oxygen is considered to be produced by cyanobacteria (Summons et al., 2006). In addition, alkylated sterols today are exclusively produced by eukaryotes, with only a few exceptions in bacteria that have no side-chain alkylation (Pearson et al., 2003; Desmond and Gribaldo, 2009). Thus, the presence of steranes in Archean rocks would mean the evolution of eukaryotes before the GOE. Currently, there have been no convincing reports of eukaryotic fossils in the Archean era. The oldest eukaryotic body fossils date back to 1.9 Ga (*Grypania*) (Knoll et al., 2006).

Despite its huge potential, biomarker analyses are frequently subject to trace contamination problems. The biomarker evidence of cyanobacteria in the Archean has been questioned by demonstrating that in some cases these biomarkers are contaminants (Rasmussen et al., 2008). The consensus for the oldest certainly authentic biomarkers is from the McArthur Basin and McArthur Group sediments at only 1.4-1.6 Ga (Summons et al., 1988; Brocks et al., 2005), although recent fluid inclusion evidence for hopane and sterane biomarkers in rocks aged 2.1 and 2.4 Ga arguably pushes the date considerably further back (Dutkiewicz et al., 2007; George et al., 2008).

Two types of contamination are serious problems for biomarker analyses: contamination during experiments, and HC migration after the initial deposition of the sediments. In this study, the contamination level during the experiments was kept very low (~pg / g sample), enabling trace amounts of indigenous organic molecules to be unambiguously detected. Later HC migration was monitored by measuring concentration gradients by slicing the rock sample and analysing HCs in each slice separately from the outside towards the inside (Brocks, 2001; Sherman et al., 2007). The

contamination from the outside environment would be expected to have the maximum concentration at the surface, and then it would decline towards the inside. In contrast, any indigenous organic compounds would have the higher abundance in the deeper part of the samples, where they would have been more protected from weathering and alteration, and would decrease towards the outside.

Distributions of biomarkers were further analysed by two different extraction procedures. The first extraction was performed immediately after crushing a rock, where HCs mainly in pore spaces and fissures in the rock fabric are expected to be extracted. In contrast, the second extraction was carried out after carbonate mineral removal by hydrochloric acid treatment of the rock sample, where HCs are expected to come from within the carbonate minerals, and would have been less susceptible to HC migration from the outside environment and weathering. In this study, a slice experiment reveals a variety of possibly indigenous organic compounds including biomarkers for cyanobacteria and eukaryotes in an Archean stromatolite, and also records the variation of the biomarker distributions throughout the rock.

4.2. Geological setting

The sample was collected from the Tumbiana Formation in the Fortescue Group, Pilbara region, Western Australia. The area has been well studied and described in detail (e.g. Thorne and Trendall, 2001). The Fortescue Group, a volcano-sedimentary succession, is the basal member of the Mount Bruce Supergroup (Arndt et al., 1991; Barley et al., 1997), and overlies granite-greenstone basement rocks of the Pilbara Craton (the Pilbara Supergroup) (Fig. 4.1). The Fortescue Group was deposited between 2775 and 2630 Ma during a period of rifting and extensive volcanism (Thorne & Trendall, 2001).

The Tumbiana Formation is a thin unit of mainly carbonate rocks, and generally conformably overlies the Kylena Formation and underlies the Maddina Formation, both of which mainly comprise basalt lava flows. The Tumbiana Formation is divided into the lower Mingah Member, consisting primarily

of sandstones and subaerial lava flows with minor stromatolitic carbonate rocks, and the overlying Meentheena Member, consisting of abundant stromatolitic limestones and recessive shales (Lipple, 1975; Coffey et al., 2013). The depositional age of the Tumbiana Formation is provided by detrital zircon recovered from tuffaceous sandstones (2715 ± 6 Ma, Arndt et al., 1991; 2719 ± 6 Ma, Nelson, 2001; 2721 ± 4 Ma, Blake et al., 2004).

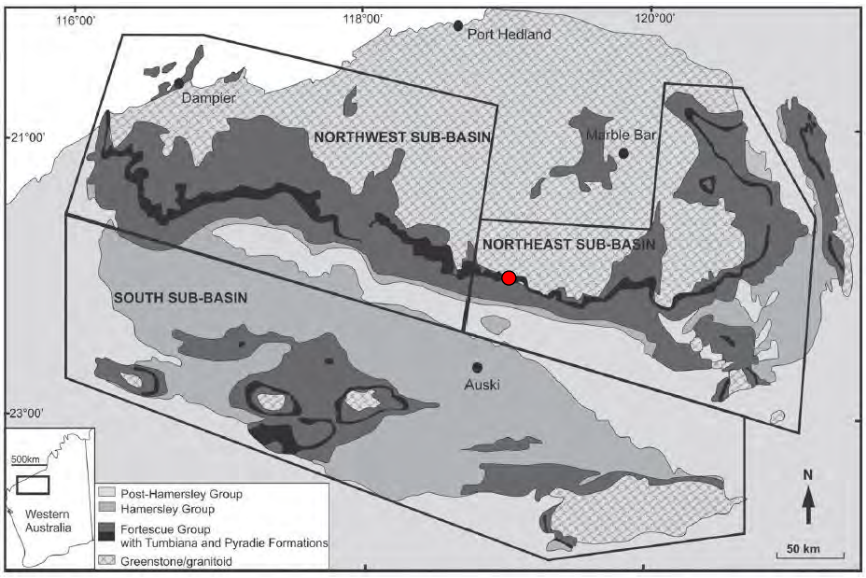

Figure 4.1. Location map showing the Fortescue Group and the Tumbiana Formation in the Pilbara Craton in Western Australia. The red dot shows the sampling location. Modified after Throne and Trendall, 2001.

The depositional setting of the Tumbiana Formation is either a shallow marine environment (e.g. Thorne and Trendall, 2001; Sakurai et al., 2005), or a lacustrine environment (e.g. Walter, 1983; Awramik and Buchheim, 2009; Coffey et al., 2013). A recent study to resolve this issue concluded that a lacustrine paleoenvironment was most likely (Coffey et al., 2013). The Tumbiana Formation experienced prehnite-pumpellyite facies metamorphism (175-280 °C) in the northeast (this study) and northwest sub-basins, and actinolite facies metamorphism (300-350 °C) in the southern sub-basin (Fig. 4.1). These temperatures are quite low compared to many other Archaean terrains (Smith et al., 1982).

The investigated locality, “Martin’s Hill”, is one of the outcrops in the hills around Redmont Railway Camp. It is very close to the site known as “Knossos” which hosts numerous domical stromatolites (Walter, 1983; Coffey et al., 2011). At “Martin’s Hill”, conically laminated columnar stromatolites (*Conophyton*) are observed (Fig. 4.2). *Conophyton* is well known for its possible association with cyanobacteria, and the sample examined in this study appear to be one of the oldest examples of *Conophyton* (Flannery, 2013). A basaltic lava flow from the nearby overlying Maddina Formation was sampled for use as a procedural blank.

Figure 4.2. Field photograph of the investigated locality “Martin’s Hill”, showing the conical stromatolite from the Meentheena Member that was sampled. The height of the chisel is about 20 cm.

4.3. Experimental procedure

4.3.1. Solvents and glassware

Dichloromethane (DCM) (Macron, H485-10) and methanol (MeOH) (Honeywell Burdick & Jackson, GC230-4) (9:1 v/v) were used to extract HCs from the sample. All solvents were checked for purity by gas chromatography-mass spectroscopy (GC-MS) as described below. All glassware was combusted in an oven at 400 °C for 3 hours before use.

4.3.2. Sample preparation

The rock sample was sliced using a diamond blade (Diatrenn, D0) from the outside towards the inside, producing approximately 1 cm thick slices. Each slice was then cut into approximately 1 cm^3 pieces. About 100 g of rock pieces was used for the analysis of each slice. The procedural blank was processed first. Between each slice experiment all equipment was washed with filtered water, MeOH and DCM and checked for purity by GC-MS. Fine particles on sample surfaces were removed by ultrasonication in filtered water for 10 min. Organic contamination on surfaces was removed by ultrasonication in a mixture of DCM and MeOH (9:1, v/v) for two cycles of 10 min., with a new solvent mixture each time. The last solvent mixture was analysed by GC-MS for purity and surface checking. If the cleaning was insufficient, additional ultrasonication was performed.

The rock was then ground to < 200 mesh grain size in a tungsten carbide ring-mill. The mill was cleaned between samples. Fine particles in the mill were removed by manual scrubbing by a metal brush and water washing. The mill was then repeatedly rinsed with a solvent mixture of the same composition as described above. If the cleaning was insufficient, additional rinsing of the ring-mill was performed.

4.3.3. First solvent extraction (Ext. I)

Extraction of HCs from the rock powder was carried out by ultrasonication with 200 mL of the solvent mixture described above for two cycles of 10 min. Between the sonications, the solution was stirred using a glass rod and left to stand still for a few minutes. The solvent was collected in a round-bottom flask. The powder was further sonicated with a fresh 100 mL aliquot of DCM for 10 min to retrieve organic residues, particularly aliphatic HCs, in the mixed slurry of powder and solvent. The second solvent was added to the first solvent. An instrument such as an Accelerated Solvent Extractor was not used because of the possibility of contamination.

The obtained solution volume was reduced by rotary evaporation to 30-40 mL. The solution was then centrifuged for 3 min at 2,000 rpm to remove suspended rock particles. The volume was then further

reduced by rotary evaporation to approximately 5 mL. If the amount of suspended solids was low, the centrifuge step was omitted and the solvent was directly reduced to approximately 5 mL. Even after the centrifuge step, there were still some very fine rock particles suspended in the solvent. These were removed by filtering the solvent/sample mixture through silica gel (silica gel 60, 0.063-0.200 mm, Merck), which was activated at 120 °C for > 4 hours before use. Column fractionation of the extractable organic matter (EOM) was not performed because the yield was very small (< 100 ng / g sample), because the interference between aliphatic and aromatic HCs was not serious, and also to prevent the loss of HCs.

The EOM was spiked with three compounds as internal standards by adding 1 mL of a DCM solution containing about 50 ng of each: anthracene-d_{10} (98 atom %D, Isotec), p-terphenyl-d_{14} (98 atom %D, Isotec), and tetraeicosane-d_{50} (98 atom %D, Isotec). The volume of solvent containing the EOM was further reduced on a hot plate at 40 °C under a gentle nitrogen flow, until approximately 50 µL remained.

4.3.4. Second solvent extraction (Ext. II)

After the first solvent extraction, the residual rock powder was treated with hydrochloric acid (HCl; 36%, RCI Labscan) to remove the carbonate minerals. 100-150 mL of HCl solution was added to the powder (~100 g) on a hot plate at 70 °C until effervescence stopped. The resultant solution was washed with 500 mL of filtered water six times. The surplus acid-water mixture was discarded and the remaining powder slurry was air dried. Extraction of the decarbonated rock powder was performed as described above for the first extraction. Acid treatment was found to release a large amount of elemental sulphur, which can damage GC-MS instruments and interfere with HC identification and quantification. Thus, elemental sulphur was removed by treatment of the EOM with activated copper. 5 g of copper particles (metal turnings, TG, Chem-Supply) were first treated with 36% HCl to remove CuO surficial layers and any remaining CuS residues from the previous experiment, and then washed with MeOH twice and DCM twice. The activated copper was added to the EOM and stirred for a minute. This simple procedure was enough to remove most sulphur so that

reflux of the solution was not performed. Then, the copper particles were removed. The resultant EOM was spiked with standards and prepared for GC-MS using the same procedure as for the first extraction.

4.3.5. Third solvent extraction (Ext. III)

The powder residue was further treated with hydrofluoric acid (HF) (40%, Merck) to remove silicate minerals. Only 4 g of powder was used because of the danger caused by the reaction of a large amount of sample with HF. 20 mL of HF solution was added to the powder on a hot plate at 70 °C and then left on the plate for 3-4 hours. This procedure was repeated three times to make sure the reaction completed. The resultant solution was washed with filtered water. The surplus water was discarded and the remaining solution was dried in the air. Then, the extraction was performed by the same procedure as the second extraction.

4.3.6. Gas Chromatography-Mass Spectroscopy (GC-MS)

GC-MS analysis was carried out on an Agilent GC (6890N) coupled to an Agilent Mass Selective Detector (5975B). 1 µL of the EOM solution was injected into a Programmable Temperature Vaporization (PTV) inlet operating in splitless mode with a J&W DB5MS capillary column (length 60 m, inner diameter 0.25 mm, film thickness 0.25 um). The PTV inlet was ramped from 35 °C (3 min. isothermal) to 310 °C (0.5 min. isothermal) at a rate of 700 °C / min. Helium was used as the carrier gas (1.5 mL / min., constant flow), and the temperature of the GC oven was ramped from 30 °C (2 min. isothermal) to 310 °C (30 min. isothermal) at a rate of 4 °C / min. The MS data were acquired in single ion monitoring (SIM) mode. HC identification was based on comparisons of relative GC retention times and mass spectra with those previously reported. Semi-quantitative analyses were performed using the tetraeicosane-d_{50} internal standard, not taking into account any response factor. The other two standards were used to check sensitivity and repeatability of the measurement, but were not used for the quantification.

4.3.7. Further biomarker analysis

Detected biomarkers such as hopanes and steranes were present in quite low amounts and it was not possible to quantify them, except for a few compounds. Therefore, selected samples and blanks were further analysed by a Thermo Trace Ultra GC interfaced with a high resolution Thermo DFS GC-MS system. Column separation was carried out on a J&W DB5MS capillary column (length 60 m, inner diameter 0.25 mm, film thickness 0.25 um). Helium was used as the carrier gas (1.5 mL / min., constant flow). 1 µL of the EOM solution was injected into a split/splitless inlet operating at 260 °C in splitless mode. The MS was tuned to 1,000 resolution (electron energy 70eV; source temperature 280 °C). The oven was ramped from 40 °C (2 min. isothermal) to 200 °C at a rate of 4 °C / min., then to 310 °C (30 min. isothermal) at a rate of 2 °C / min. The MS data were acquired in SIM mode. Observed biomarkers were further analysed by metastable reaction monitoring (MRM), but their abundance was too low to allow detection. Thus, the identification of biomarkers was performed using their retention time and mass spectral behaviour in comparison with the NSO-1 reference oil (Weiss et al., 2000). Semi-quantitative analyses were performed using the *p*-terphenyl-d_{14} internal standard, not taking into account any response factor.

4.3.8. Derivatisation experiment

The sample rock surface was analysed for functionalised HCs to investigate the presence of recent inputs from extant organisms. The EOM after Ext. I and II was dried to remove methanol from the samples. Two drops of bis-trimethylsilyltrifluoroacetamide (BSTFA) solution (Grace & Co., Maryland) was added to the EOM, which was then heated at 60 °C for 30 min to derivatise the EOM. DCM was added to the resultant solution to make up approximately 50 µL, and then analysed by the GC-MS with the procedure as mentioned above. A pure BSTFA solution was analysed as a blank by the GC-MS before any derivatisation experiment.

4.4. Results

4.4.1. Hopanes and steranes

Various hopane and sterane isomers are present in all four slices in both Ext. I and II, although their abundance is low (0.1-3 pg / g sample, Figs 4.3 and 4.4). Methylhopanes were only observed in Slice 4 Ext. II, (roughly 0.02 pg / g sample; Fig. 4.3b), which is close to the detection limit of the DFS GC-MS system. No hopanes or steranes were detected in Ext. III, perhaps due to the small amount of treated sample. No hopanes and steranes were detected in the procedural blank (Figs 4.3 and 4.4).

The abundance of the biomarkers in Ext. I is the highest in slice 1, and is low in the inner slices with the lowest value in slice 2 (Fig. 4.5). In contrast, the abundance of the biomarkers in Ext. II is the highest in slice 4, and is low in the outer slices with the lowest value in slice 2 (Fig. 4.5). Also, the concentration of the biomarkers decreases in slice 1 from Ext. I to Ext. II, but increases in the inner slices, particularly in slice 4 from Ext. I to Ext. II (Fig. 4.6). These observations indicate that there are two different origins of hopanes and steranes in this rock sample; (1) pore spaces in the rock limited to near the rock's surface, and (2) within the carbonate minerals in the inner part of the rock.

The biomarkers in the pore spaces in the rock could be extracted without HCl treatment. Their limited distribution mainly near the rock's surface indicates that they are a recent input from the surrounding environment since uplift and exposure to the Earth's surface during the Cenozoic (M. Krarendonk, personal communication). In contrast, the biomarkers in the inner slices are mainly confined within the carbonate minerals, and are interpreted to have been isolated from the outside environment and to be less affected by late migration (Sherman et al., 2007). The increase of the biomarker concentrations towards the inside of the rock suggests a lesser effect of weathering towards the inside.

(a)

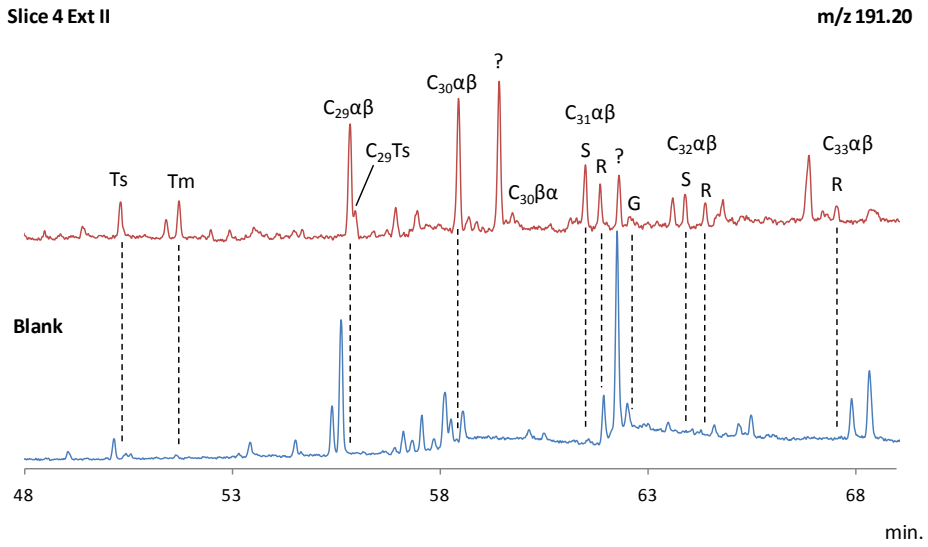

(b)

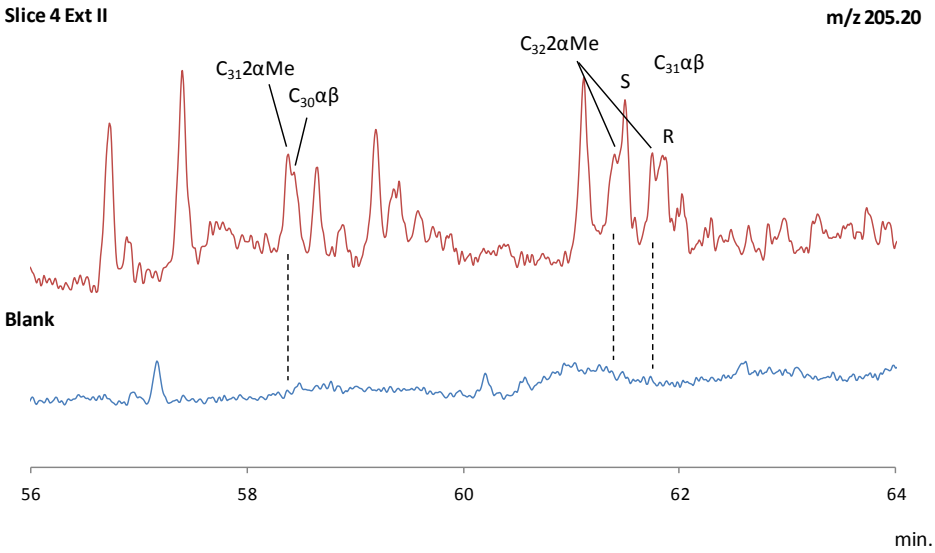

Figure 4.3. Partial mass chromatograms of hopanes and methylhopanes in slice 4 Ext. II, compared to the procedural blank. (a) Hopanes (m/z 191.20), and (b) methylhopanes (m/z 205.20). Compound abbreviations are defined in Table A4.1.

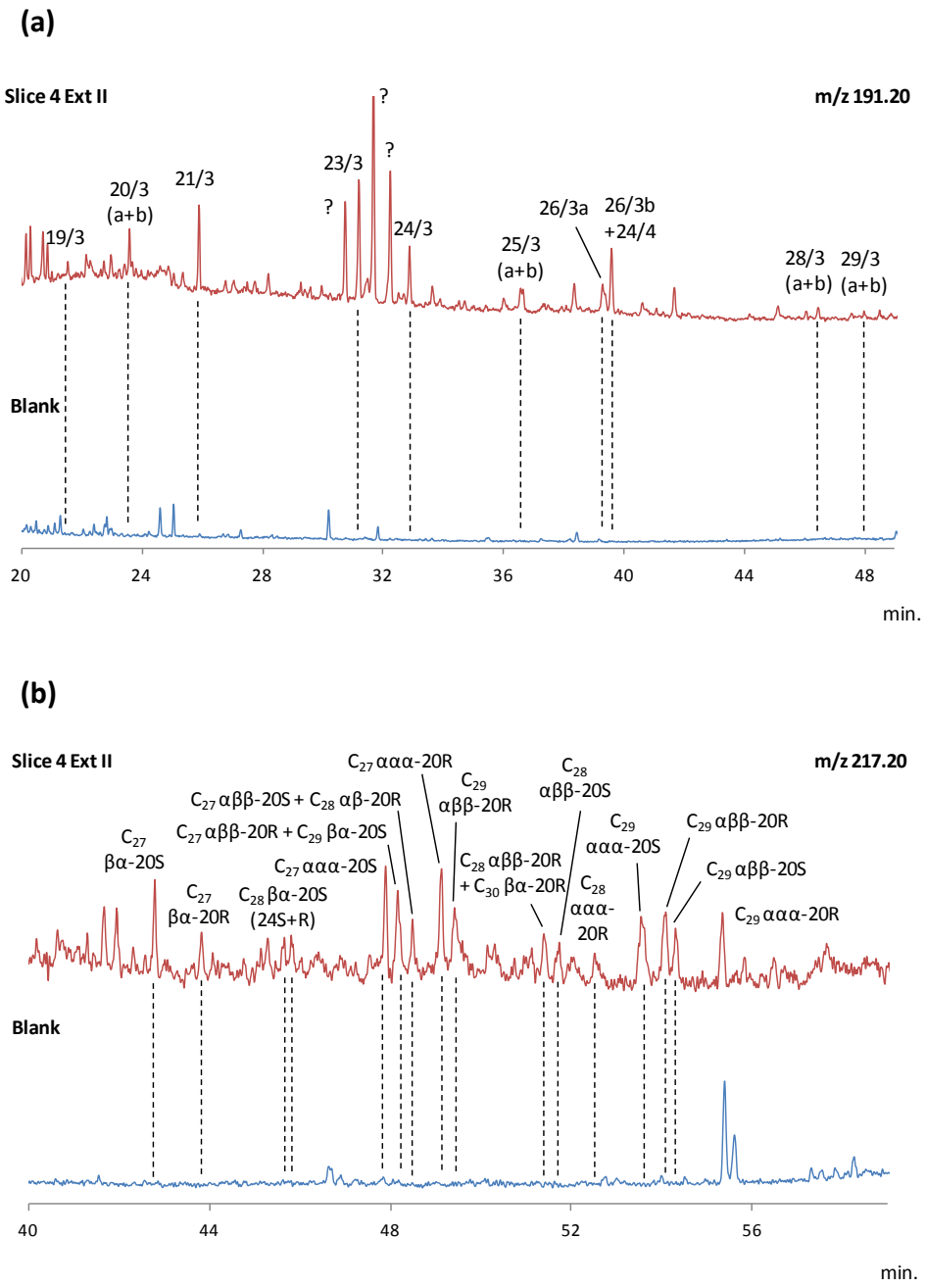

Figure 4.4. Partial mass chromatogram of tricyclic terpanes and steranes in slice 4 Ext. II, compared to the procedural blank. (a) Tricyclic terpanes (m/z 191.20) and (b) steranes (m/z 217.20). Compound abbreviations are defined in Table A4.1.

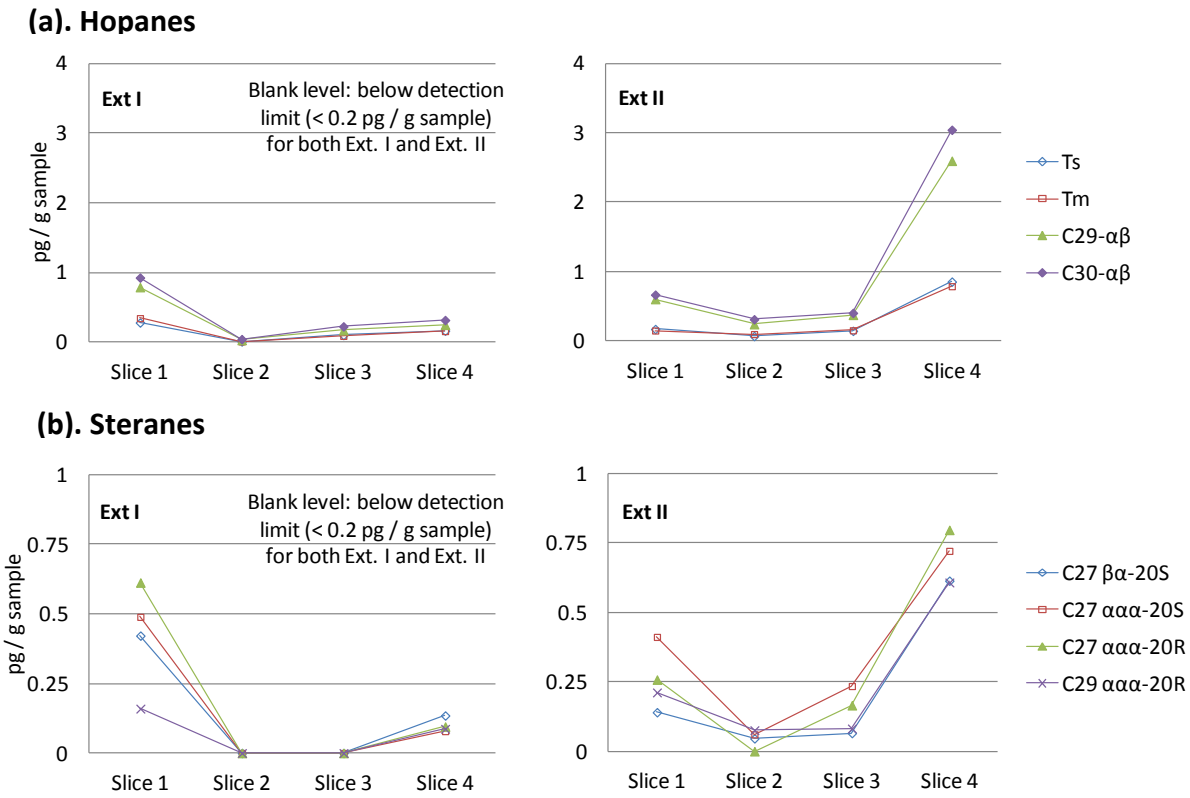

Figure 4.5. Amount and distribution of selected hopanes and steranes. (a) Hopanes in Ext. I and Ext. II, (b) steranes in Ext. I and Ext. II. Compound abbreviations are defined in Table A4.1.

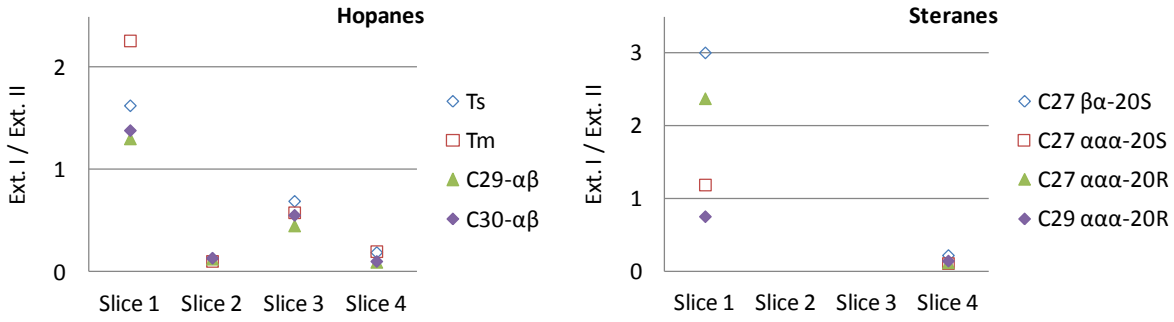

Figure 4.6. Ratios of abundance of biomarkers in Ext. I to that in Ext. II, for hopanes and steranes. Value > 1 means biomarkers are more abundant in Ext. I than in Ext. II. Value < 1 means they are more abundant in Ext. II than in Ext. I. Compound abbreviations are defined in Table A4.1.

4.4.2. Hopane and sterane thermal maturity parameters

Thermal maturity parameters based on the detected hopanes and steranes generally indicate a high thermal maturity of the rock, but there is a difference of the values between the outer slices (slices 1-2) and the inner slices (slices 3-4) (Table 4.1).

Table 4.1. Source and thermal maturity parameters of hopanes and steranes.

	Hopanes & Tricyclic terpanes							
	Ext I				**Ext II**			
	Slice 1	Slice 2	Slice 3	Slice 4	Slice 1	Slice 2	Slice 3	Slice 4
Ts / (Ts + Tm)	0.45	0.48	0.53	0.51	0.53	0.42	0.49	0.52
C_{27} / C_{29}	0.79	0.65	1.12	1.29	0.54	0.70	0.80	0.63
C_{29} / C_{30}	0.85	0.72	0.76	0.79	0.91	0.78	0.93	0.85
C_{31} / C_{30}	0.81	0.81	0.50	0.68	0.68	0.82	1.02	0.72
C_{29}Ts / (C_{29}Ts + C_{29})	0.22	0.11	0.12	0.15	0.17	0.21	0.14	0.19
C_{31}S / (S + R)	0.54	0.68	0.53	0.55	0.64	0.61	0.59	0.64
C_{32}S / (S + R)	0.63	0.63	-	0.48	0.47	0.67	0.58	0.60
Tricyclics / 17α-hopanes	0.75	1.07	2.44	2.18	0.72	1.62	1.27	0.73
(23/3) / C_{30}	0.86	0.85	1.34	1.43	0.76	1.61	1.69	0.76
(24/3) / C_{30}	0.48	0.47	0.66	-	0.37	0.53	0.59	0.44

	Steranes							
	Ext I				**Ext II**			
	Slice 1	Slice 2	Slice 3	Slice 4	Slice 1	Slice 2	Slice 3	Slice 4
C_{27}S / (S + R)	0.44	-	-	0.45	0.61	-	0.59	0.48
C_{29}S / (S + R)	-	-	-	0.33	0.15	-	0.43	0.60
C_{29}ββ / (αα + ββ)	-	-	-	0.39	0.46	-	0.53	0.43
C_{29} / C_{27} ααα**R**	0.26	-	-	0.92	0.82	-	0.49	0.76

Hopane biomarker ratios: **C_{27} / C_{29}** = (Ts + Tm) / C_{29}αβ; **C_{29} / C_{30}** = C_{29}αβ / C_{30}αβ; **C_{31} / C_{30}** = (C_{31}αβ-22S + C_{31}αβ-22R) / C_{30}αβ; **C_{29}Ts / (C_{29}Ts + C_{29})** = C_{29}Ts / (C_{29}Ts + C_{29}αβ); **C_{31}S / (S + R)** = C_{31}αβ-22S / (C_{31}αβ-22S + C_{31}αβ-22R); **C_{32}S / (S + R)** = C_{32}αβ-22S / (C_{32}αβ-22S + C_{32}αβ-22R); **Tricyclics / 17α-hopanes** = (19/3 + 20/3a + 20/3b + 21/3 + 23/3 + 24/3 + 25/3a + 25/3b + 26 / 3a + 26/3b + 28/3a + 28/3b) / (C_{29}αβ + C_{30}αβ + C_{31}αβ-22S + C_{31}αβ-22R + C_{32}αβ-22S + C_{32}αβ-22R + C_{33}αβ-22S + C_{33}αβ-22R + C_{34}αβ-22S + C_{35}αβ-22R + C_{35}αβ-22S + C_{35}αβ-22R). **Sterane** biomarker ratios: **C_{27}S / (S + R)** = C_{27}ααα-20S / (C_{27}ααα-20S + C_{27}ααα-20R); **C_{29}S / (S + R)** = C_{29}ααα-20S / (C_{29}ααα-20S + C_{29}ααα-20R); **C_{29}ββ / (αα + ββ)** = (C_{29}αββ-20S + C_{29}αββ-20R) / (C_{29}αββ-20S + C_{29}αββ-20R + C_{29}ααα-20S + C_{29}ααα-20R); **C_{29} / C_{27}αααR** = C_{29}ααα-20R / C_{27}ααα-20R. See Appendix 1 for compound abbreviations.

Although the variation is clear in Ext. I such as C_{27}/C_{29}, C_{31}/C_{30}, and $C_{29}Ts/(C_{29}Ts+C_{29})$, it becomes less distinctive in Ext. II. This may reflect the two different origins of the hopanes and steranes as suggested by their spatial distribution (Fig. 4.5). Within Ext. II, there are still some variations such as C_{31}/C_{30}, C_{32} S/(S+R) and C_{29}S/(S+R). Not many parameters can be calculated due to the low abundance of hopanes and steranes. For example, only very low concentrations of moretanes ($\beta\alpha$ hopanes) could be reliably detected, which is likely to reflect the high thermal maturity of the rock.

Application of hopane and sterane parameters for estimating a thermal maturity of rocks is generally limited up to the top of the oil generation window, as most of the ratios reach equilibrium values, and it is problematic to apply them to overmature bitumens (van Graas, 1990). Similar fluctuations in Archean rocks have been reported previously (Brocks et al., 2003a). Thus, the variations may have been caused by the over-maturity of the rock. The hopane and sterane thermal maturity parameters for slice 4 are mostly consistent with the prehnite-pumpellyite facies metamorphism (175–280 °C) that the rock experienced. However, thermal maturity parameters for slice 1 are also suggestive of a similar high maturity as for the inner slices. The reason is uncertain, but may relate to an external highly thermally mature anthropogenic input.

4.4.3. Tri- and tetracyclic terpanes

Tri- and tetracyclic terpanes were detected in all four slices, with a similar abundance and spatial distribution among the slices as for the hopanes and steranes (Fig. 4.4, and Fig. S4.1). No tri- and tetracyclic terpanes were detected in the procedural blank (Fig. 4.4). As for the hopanes and steranes, tri- and tetracyclic terpanes are most abundant in slice 1 in Ext. I, but their concentration decreases in Ext. II (Figs S4.1 and S4.2). In contrast, tri- and tetracyclic terpanes become more abundant in the inner slices in Ext. II, with the highest value in slice 4. Therefore, it is likely that there are two different origins of the tri- and tetracyclic terpanes, and that they share the same two origins as for the hopanes and steranes. One is a more recent input from the outside environment, and the other is a more ancient input, possibly indigenous Archean organic matter which has been preserved over geological time.

A high abundance of tri- and tetracyclic terpanes relative to hopanes and steranes suggests a high thermal maturity beyond the peak-oil window throughout the rock (Table 4.1) (George et al., 2008). There is a variation of tri- and tetracyclic terpane parameters among the slices. The values gradually increase from the outside towards the inside the rock, except for slice 4 Ext. II (Table 4.1). This means that the relative amount of tri- and tetracyclic terpanes increases compared to hopanes and steranes. The variation may be explained by the influence of weathering and preservational environment of the rock. It has been suggested that tri- and tetracyclic terpanes are more mobile than pentacyclic terpanes (hopanes and steranes), and pentacyclic terpanes have more affinity to the rock matrix (Zhusheng et al., 1988; Kruge et al., 1990). Therefore, tri- and tetracyclic terpanes are thought to be more subject to weathering, which may have led to the decrease of the tri- and tetracyclic terpane parameters in the outer slices. The low values of the parameters in slice Ext. II is due to the particular high abundance of hopanes and steranes in slice 4 Ext. II.

4.4.4. Mid-chain branched monomethylalkanes (MMAs) and C_{17} n-alkane (n-C_{17})

4.4.4.1. Slice 1 (outer-most layer)

Extremely high abundances of 7- and 6-MMA in the range from methylheptadecane (MHeD, C_{18}) to methyleicosane (MED, C_{21}) were observed in slice 1 in all extractions (I-III), always accompanying a large relative abundance of *n*-C_{17} (Fig. 4.7). 7-MMA coelutes with 8-MMA and 9-MMA, so were quantified together, but the retention time of the peak and the mass spectrum indicate that 7-MMA is dominant. The relative abundance of 8- and 9-MMA to 7-MMA in the combined peak is estimated to be about 15 % at most. Other MMAs are much less abundant than 7- and 6-MMAs. The dominance of 7- and 6-MMA in slice 1 decreases from MHeD to MED (Fig. 4.8). High abundances of *n*-C_{17} and mid-chain branched MMAs, especially 7-MHeD, are typical characteristics of some cyanobacteria (Schirmer et al., 2010; Coates et al., 2014).

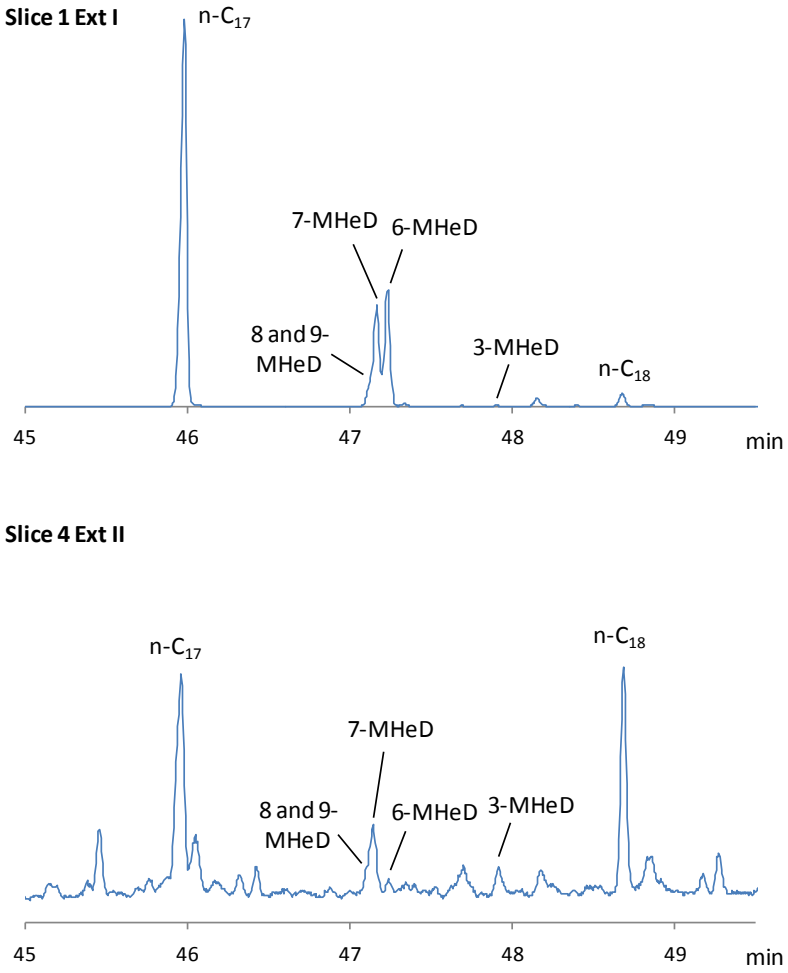

Figure 4.7. Partial m/z 57 mass chromatograms of methylheptadecanes (MHeDs) in (a) Slice 1 Ext. I and in (b) Slice 4 Ext. II.

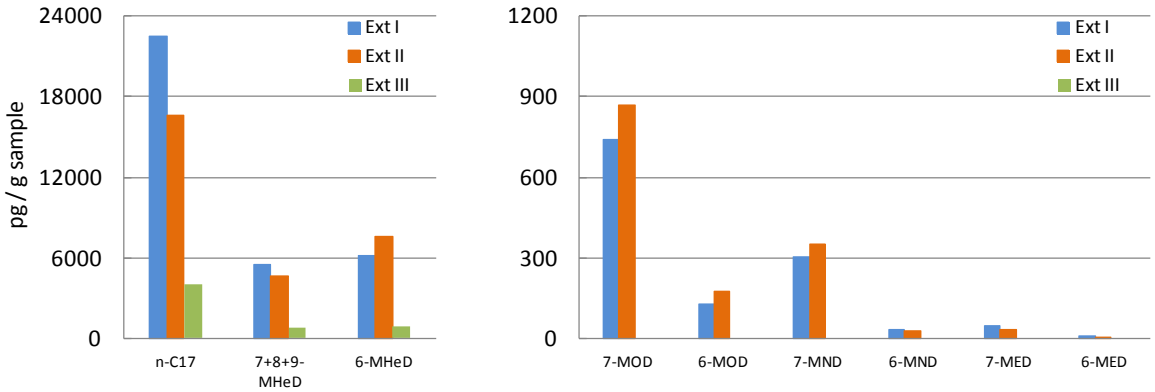

Figure 4.8. Amount of *n*-C_{17}, and 7- and 6-MMA in slice 1 Ext. I (blue), Ext. II (orange) and Ext. III (green). **MHeD** = methylheptadecane (C_{18}); **MOD** = methyloctadecane (C_{19}); **MND** = methylnonadecane (C_{20}); **MED** = methyleicosane (C_{21}).

The extremely high relative abundance of both 7- and 6-MMA is limited only to slice 1. Thus, the 7- and 6-MMAs in slice 1 are interpreted as a recent cyanobacterial input. These MMAs dominantly occur within 1 cm from the rock surface, indicating that the cyanobacteria are an endolithic species. A similar distribution of these compounds and the presence of endolithic cyanobacteria has recently been reported (Hoshino et al., 2014) (see also Chapters 3 and 6). The abundance of these MMAs and *n*-C_{17} decreases slightly from Ext. I to Ext. II, and drastically from Ext. II to Ext. III (Fig. 4.8), indicating that the presence of 7- and 6-MMA in slice 1 is mainly in the pore space of the rock fabric (Ext. I) and within the carbonate minerals (Ext. II), but not within the silicate minerals (Ext. III). This may suggest that cyanobacterial inhabitation penetrates into the carbonate minerals but not into the silicate minerals.

There is a possibility of extant cyanobacteria being the direct producer of these MMAs. In that case, functionalised organic compounds directly produced by their metabolisms are expected to be detected because they are not thermally altered yet. The presence of functionalised organic compounds in slice 1 was tested by derivatisation of the sample solutions after the third extraction (Ext. III). Only several fatty acids (<C_{20}) were detected, but their abundance was below the blank level (<1 ng). Therefore, the high abundance of *n*-C_{17} and 7- and 6-MHeD are probably not a direct input of modern living cyanobacteria.

4.4.4.2. Slices 2–4 (Inner layers)

7-MHeD is the most abundant compound of the detected isomers in the inner slices, even though the extremely high abundance of *n*-C_{17} and the 7- and 6-MMAs seen in slice 1 is not present (Fig. 4.7). The retention time of the peak and the mass spectrum indicate that 7-MHeD is dominant over 8- and 9-MHeD in slices 2–4, as well as in slice 1. The abundance of 7-MHeD in Ext. I constantly decreases towards the inside, but it is broadly the same in Ext. II, with slightly higher abundances in slice 3 and 4 than in slice 2 (Fig. 4.9). The abundance of 6-MHeD also decreases towards the inside. The abundance of 7-MMA in Ext. I is lower than that in Ext. II in slice 4, and in this slice 7-MMA is of no

greater abundance than the other isomers. Thus, the 7-MHeD in Ext. I appears to be a remnant of the 7-MHeD in slice 1. In contrast, the 7-MHeD in Ext. II seems to have a different origin that is more similar to that of the hopanes and steranes. The huge amount of 7-MHeD on the rock surface slightly permeates into a deeper part of the rock, as suggested in Ext. I. However, 7-MHeD in slices 2–4 is considered to be mainly confined within the carbonate minerals, and are possibly the remains of ancient cyanobacterial inhabitation within the stromatolites.

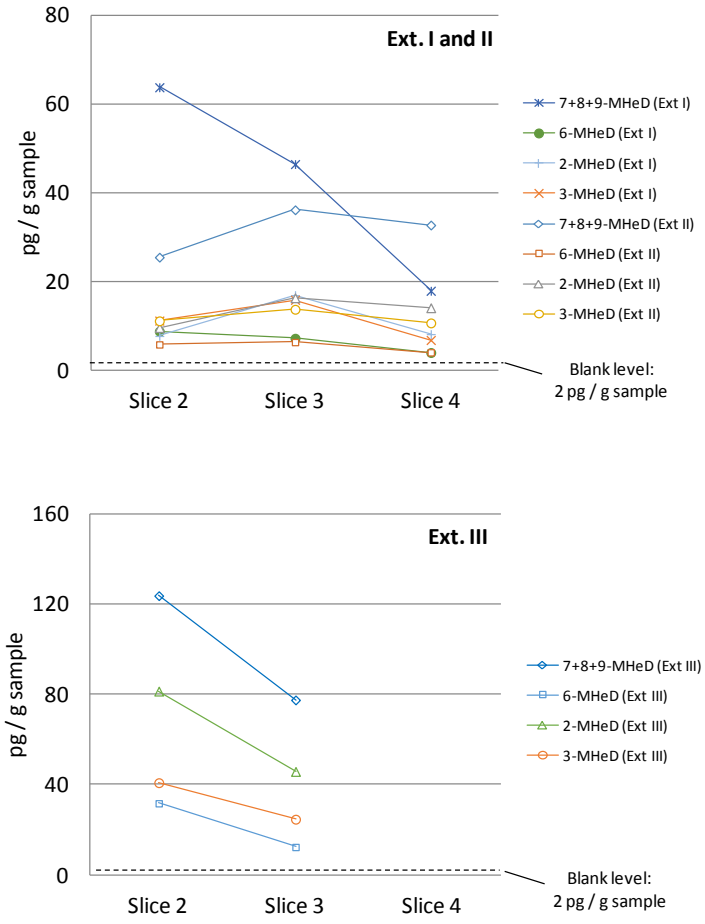

Figure 4.9. Abundance of selected $C_{17\text{-}20}$ mid-chain branched MMAs in Ext. I, II and III.

The compositional difference in MHeD isomers between slice 1 and slices 2–4 may indicate two different types of cyanobacteria (Fig. 4.10). MHeDs in slice 1 Ext. I have a high abundance of 7- and 6-MHeDs, whereas those in slices 2–4 Ext. II have a high abundance of only 7-MHeD. Another possibility is that biologically-derived 7-MHeD partly isomerises by rearrangement reactions to other MHeD isomers over geological time (Hoshino et al., 2014) (see also Chapter 6). The disappearance of

n-C_{17} may have been caused by long-term mild biodegradation, possibly induced by weathering at outcrop. A selective decrease of *n*-alkanes compared to MMAs has been reported by the comparison of modern and Holocene cyanobacterial mats (Kenig et al., 1995), and preferential biodegradation of *n*-alkanes is well known (Wenger et al., 2002).

The MHeD distribution between slices in Ext. III is different from that in Ext. I and II, but the isomer composition is similar to that of Ext. II (Figs 4.9 and 4.10). 7-MHeD in slices 2 and 3 of Ext. III has a higher abundance than for other MHeDs, as is also the case for Ext. II, but to a lesser degree. 2-MHeD is relatively abundant compared to the other isomers. The entire abundance of MHeDs decreases from slice 2 to slice 3, and slice 4 does not contain any MHeDs. Slice 4 Ext. III only contains a trace amount of $<C_{19}$ *n*-alkanes and does not contain any other aliphatic HCs nor any aromatic HCs. There is a possibility of experimental failure, but the extraction experiment was performed twice independently, and there was no difference between the two results. The decline of MHeD concentration towards the inside of the rock in Ext. III might suggest a sight influence of recent cyanobacterial input in slice 1 as well. The relative high abundance of 2-MHeD could be due to a different source compared to the MMAs in Ext. I and II, or to a difference in the preservation environment within the carbonate minerals compared to within the silicate minerals, that might have caused a different isomerisation pattern from a shared original composition. Currently, it is not clear that Ext. III properly preserve the original composition of organic matter at the time of deposition, because of the large differences of HC distribution between each slice. HCs in Ext. III were retrieved from small amounts of sample (4 g), so there were also more uncertainties in quantification.

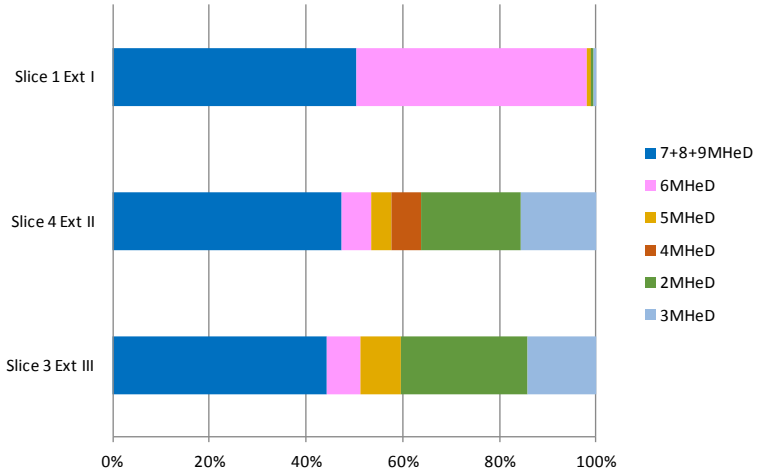

Figure 4.10. Abundance of MHeD isomers in a different part of the rock.

4.4.5. Other biomarkers

Regular isoprenoids in the range C_{13} to C_{20} were detected in all the slices in all three extractions except for slice 4 Ext. III (Fig. S4.3). They were also detected in the procedural blank, but with a much lower abundance (<4.7 pg / g sample in Ext. I, <2.5 pg / g sample in Ext. II, not detected in Ext. III). There is heterogeneity in the pristane/phytane (Pr/Ph) ratio between slice 1 and slices 2–4 for Ext. 1 and Ext. II (Fig. 4.11), indicating different origins of Pr and Ph in slice 1 and slices 2–4. In contrast, Pr/Ph in Ext. III is almost constant through slices 1–3 (slice 4 does not contain Pr nor Ph). Thus, Pr and Ph in the silicate minerals may not have been affected by recent input from the outside environment and weathering. However, the abundance of both Pr and Ph generally decreases towards the inside for all three extract fractions (Fig. S4.3). Thus, even if the isoprenoids in slices 2–4 have a different origin from those in slice 1, it is not clear that they are certainly indigenous HCs. Other isoprenoids (C_{13}-C_{18}) do not have any particular trends (Fig. S4.3).

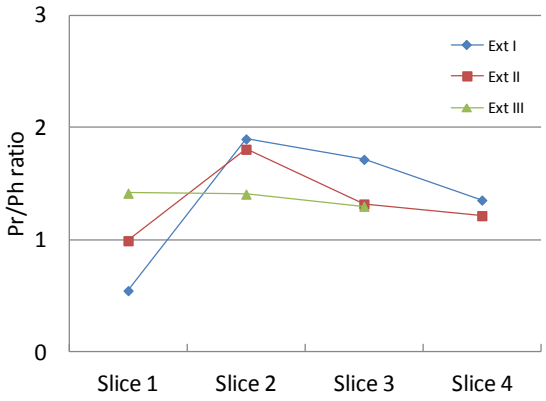

Figure 4.11. Pristane/phytane (Pr/Ph) ratio in slices 1 – 4 in Ext. I, II and III.

4.4.6. Other aliphatic HCs

4.4.6.1. n-Alkanes (slice 1)

The concentration of detected *n*-alkanes is mostly at least 10 times higher than the procedural blank, indicating these *n*-alkanes are indigenous (Fig. 4.12). Slice 1 has a very high abundance of the C_{17} *n*-alkane as already discussed, more than 30 times higher than *n*-C_{16} and *n*-C_{18} in Ext. I and Ext. II, but only 13 times higher than *n*-C_{16} and *n*-C_{18} in Ext. III. Slice 1 also has an odd-over-even carbon preference (OEP) between *n*-C_{28} and *n*-C_{35} (Table 4.2), indicating recent higher plant input (Eglinton and Hamilton, 1967). The OEP $((C_{29}+ 6C_{31} + C_{33}) / (4C_{30} + 4C_{32}))$ is very clear in Ext. I (1.90) and II (1.85), whereas it is reduced in Ext. III (1.10), suggesting that the influence of the higher plant input reaches within the carbonate minerals of slice 1, but not within the silicate minerals, as already shown for the MMAs. The procedural blank does not have an OEP. Another characteristic of the *n*-alkane distribution in slice 1 is that there are large amounts of high molecular weight *n*-alkanes (>C_{21}), and the *n*-alkane distribution shifts towards longer chain lengths from Ext. I to Ext. III. The *n*-alkanes in Ext. II may be a mixture of the recent input in Ext. I and the ancient *n*-alkanes in Ext. III.

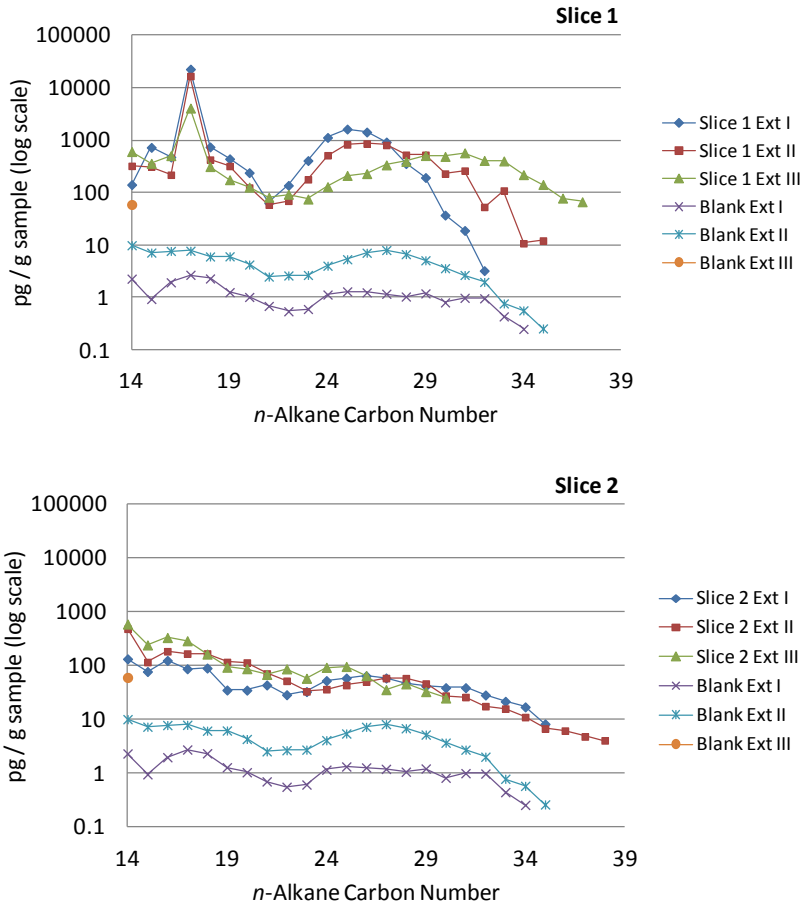

Figure 4.12. Amount and distribution of *n*-alkanes in slice 1 and slice 2 for Ext. I, II and III, compared to that in the procedural blank. Note that a log abundance scale is used in order to visualise all the data.

4.4.6.2. n-Alkanes (slices 2–4)

The high relative abundance of *n*-C_{17} and the OEP between *n*-C_{28} and *n*-C_{35} that are seen in slice 1 are absent in slices 2–4 (Fig. 4.12 and Fig. S4.4). Only slice 3 has a large amount of *n*-alkanes > C_{21}, and thus appears somewhat similar to slice 1 in Ext. I and Ext. II (Fig. 4.12). The origin of the relatively high abundance of >C_{21} *n*-alkanes in slice 3 is not clear, but it is not likely that they are indigenous HCs because this distribution is not seen in Ext. III. Thus, they are considered to be experimental contamination. The abundance of < C_{21} *n*-alkanes in slices 2-4 is generally similar to slice 1 and there is no particular difference between Ext. I, II and III, except for slice 4 Ext. III which only contains a trace amount of *n*-alkanes as already discussed in Section 4.4.4.2. (Fig. S4.4). The abundance of the low molecular weight *n*-alkanes is well above the blank level, and these *n*-alkanes are considered to

be indigenous. The tendency of a high abundance of lower molecular weight *n*-alkanes is consistent with a high thermal maturity of the rock sample.

4.4.6.3. Alkylcyclohexanes and methylalkylcyclohexanes

Alkylcyclohexanes (ACHs) were detected in all the slices in Ext. I and II, and were not detected in the procedural blank. The distribution of ACHs is different from that of the *n*-alkanes. Slices 1 and 2 Ext. I have a strong ACH OEP between C_{13} and C_{23} (Fig. 4.13). Slice 1 Ext. II also has the same distribution pattern, but with a lower abundance, and the ACH OEP is absent in slice 2 Ext. II (Fig. 4.13). Slices 3 and 4 do not have an ACH OEP trend in either Ext. I or Ext. II. Thus, this characteristic distribution of ACHs is likely to be a recent input from the outside environment, which is most marked in slice 1. The origin of the $< C_{23}$ ACHs is different from that of the *n*-alkanes as they have a different distribution pattern. On the other hand, most ACHs in slice 3 and 4 are likely to be indigenous HCs, as they do not have any carbon number preference and are absent from the blank. ACHs in slices 1 and 3 in both Ext. I and II have maxima around C_{28} (Fig. 4.13). This corresponds to the large amount of $>C_{21}$ *n*-alkanes in slices 1 and 3, and the ACHs in this molecular weight range probably share the same non-indigenous origin as the $>C_{21}$ *n*-alkanes.

Methylalkylcyclohexanes (MACHs) were detected in some slices and extraction experiments. In contrast with the ACHs, MACHs do not have any OEP, and their abundance is low (data not shown). This could mean that either MACHs have a different origin from the ACHs, or that the apparent discrepancy between the ACHs and the MACHs is within experimental error.

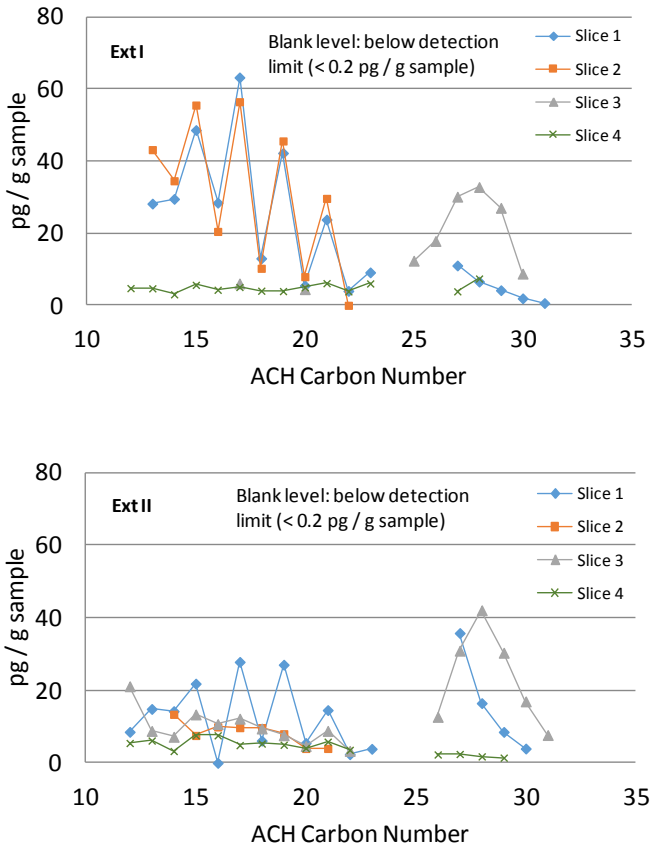

Figure 4.13. Amount and isomeric distribution of ACHs in slices 1–4 for Ext. I and Ext. II.

4.4.7. Aromatic HCs

The distribution of the aromatic HCs in the four slices and three extractions is more complicated than that of the aliphatic HCs, and also varies with the type of aromatic HC. The detected aromatic HCs include naphthalene (N), alkylated naphthalenes, phenanthrene (P), alkylated phenanthrenes, biphenyl, alkylated biphenyls, fluorene, alkylated fluorenes, dibenzothiophene, alkylated dibenzothiophenes, and polycyclic aromatic HCs (PAHs) with four rings (pyrene and chrysene). Procedural blank only contained small amounts of N and P (10 pg / g sample of N and P in both Ext. I and II, and 210 pg / g sample of N in Ext. III), and no alkylated aromatic HCs were detected. The abundance of aromatic HCs is generally in the order of Ext. III > Ext. II > Ext. I in slices 2–4 (Fig. 4.14). Only slice 1 has a higher abundance of aromatic HCs in Ext. I than in Ext. II (Fig. 4.14). This is interpreted to be due to a recent input into slice 1, as is the case for hopanes and steranes. Slice 4 Ext. III does not contain any aromatic HCs, as is also seen for the aliphatic HCs.

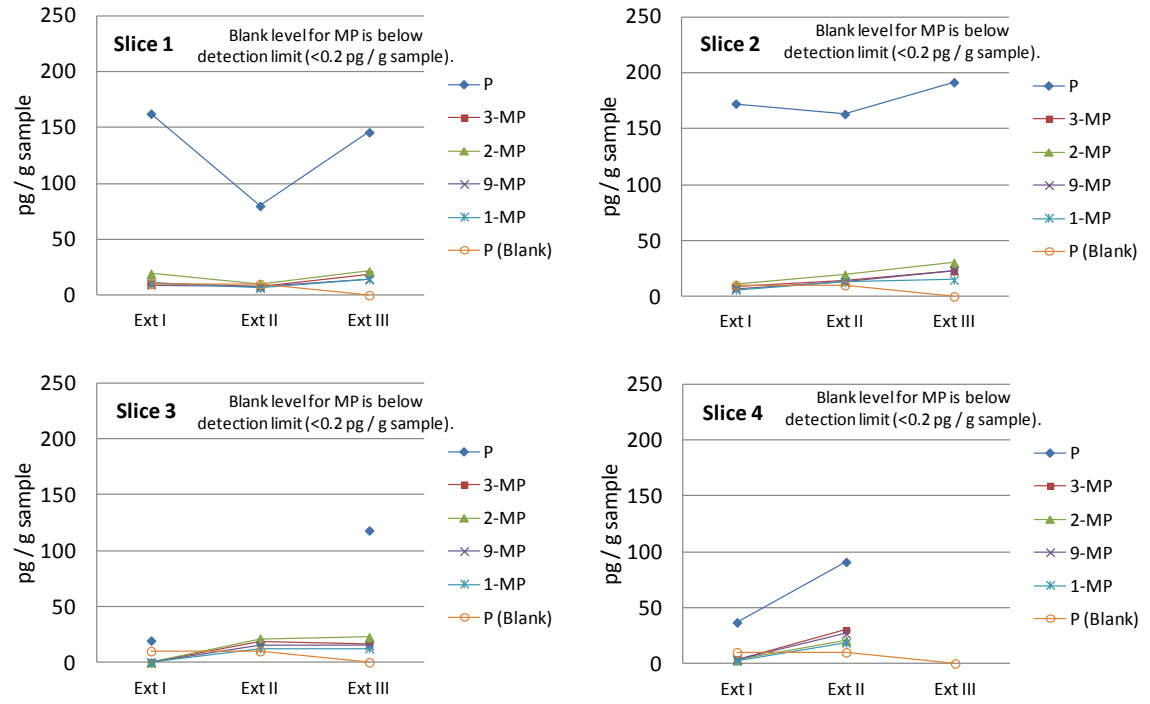

Figure 4.14. Comparison of amount and distribution of phenanthrene and alkylated phenanthrenes among Ext. I, Ext. II, and Ext. III for the four slice experiments. **P** = phenanthrene; **MP** = methylphenanthrene.

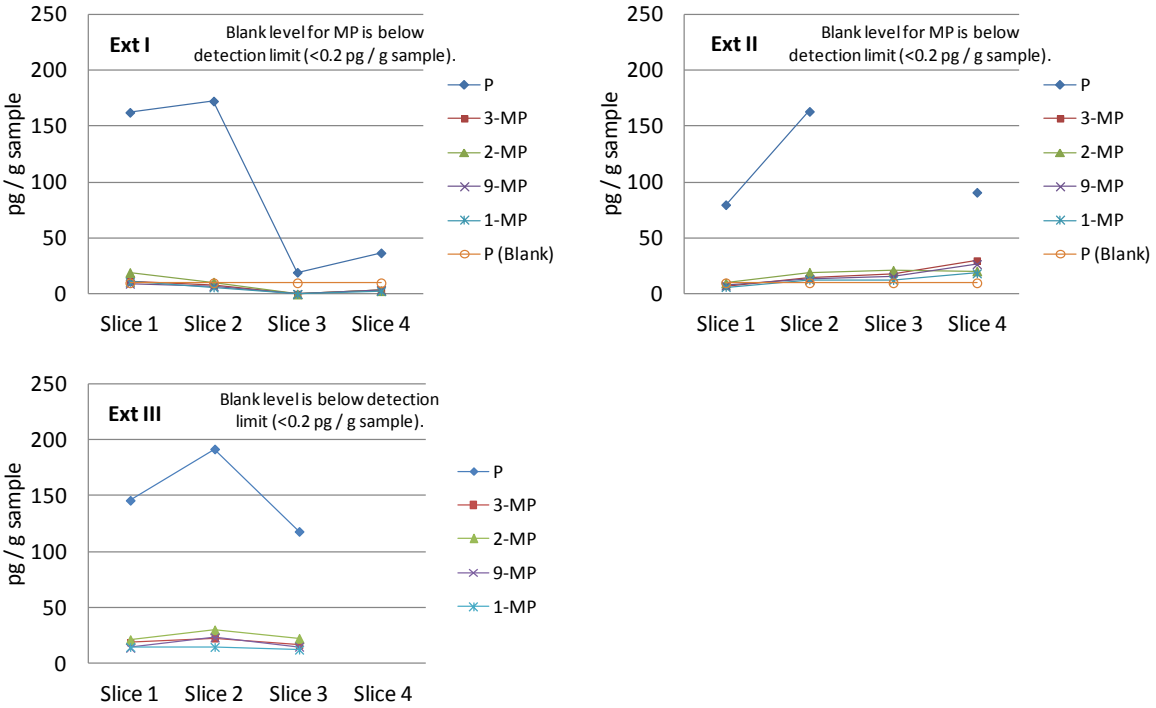

Figure 4.15. Comparison of amount and distribution of phenanthrene and alkylated phenanthrenes in the four slices for the three extraction experiments.

The abundance of aromatic HCs in Ext. I is generally in the order of slice 1 > slice 2 > slice 3 ~ slice 4 (Fig. 4.15). This distribution is considered to be the influence of a recent input from outside the sample as is the case for 7-MHeD. In contrast, the abundance of aromatic HCs in Ext. II is generally in the order slice 1 < slice 2 < slice 3 < slice 4 (Fig. 4.15), which is a similar trend to the hopanes and steranes, and 7-MHeD (see Sections 4.4.1 and 4.4.4.2). In Ext. III, there are not huge differences between the slices (Fig. 4.15). Thus, most of the aromatic HCs in Ext. II and III seem to be indigenous compounds preserved within the carbonate minerals and the silicate minerals. The exceptions are naphthalene, alkylated naphthalenes, phenanthrene, and biphenyl in slice 2 Ext. II and III (Fig. 4.15 and Fig. S4.5). These compounds have a higher abundance in slice 2 than in slice 3 and 4, and this might reflect a local heterogeneity of thermal alteration, or a more complicated preservation history of HCs than interpreted in this study.

4.4.8. Aromatic maturity parameters

Various aromatic HC parameters that are useful for assessing the thermal maturity of a rock (e.g. Radke et al., 1982) were calculated for each slice (Table 4.2). Unlike the heterogeneous distribution of amounts of aromatic HCs through the entire rock, aromatic maturity parameters are generally homogenous, and are interpreted as indicating a high thermal maturity of the rock. The methylphenanthrene index 1 (MPI-1) gives a calculated vitrinite reflectance equivalent (R_c) of ~2.2 throughout the rock (based on Radke and Welte, 1983). The methylnaphthalene ratio (MNR), dimethylnaphthalene ratio 1 (DNR-1), trimethylnaphthalene ratio 2 (TNR-2), methylphenanthrene distribution fraction (MPDF), methylphenanthrene ratio (MPR) and dimethyldibenzothiophene ratio (DMDR) have mostly similar values to those from the basal half of McManus-1 in the Mesoproterozoic Velkerri Member in the McArthur Basin in Australia (George and Ahmed, 2002). Based on multiple parameters, the McManus-1 sequence was estimated to be highly thermally mature, corresponding to the late oil generation window.

There are two clear differences between the three extraction experiments. DNR-1 and TNR-2 in Ext. II are apparently different from Ext. I and III in all the slices (Table 4.2). DNR-1 in Ext. II indicates a higher thermal maturity than in Ext. I and III, whereas TNR-2 in Ext. II suggests a lower thermal maturity, and thus are not consistent with each other. These values may reflect the different preservation history of three different environments in the rock (pore space, within the carbonate minerals and within the silicate minerals).

Table 4.2. Ratios and thermal maturity parameters of aliphatic and aromatic HCs for the four slices and the three extraction experiments.

	Ext I				
	Slice 1	Slice 2	Slice 3	Slice 4	Blank
OEP	1.9	1.02	0.96	-	1
MNR	2.03	2.46	2.33	1.76	-
DNR-1	4.72	3.46	-	3.39	-
TNR-2	0.90	1.05	-	-	-
MPI	0.18	0.11	-	0.17	-
MPDF	0.60	0.59	-	0.52	-
MPR	1.79	1.78	-	1.16	-
DMDR	1.05	-	-	0.88	-
	Ext II				
	Slice 1	Slice 2	Slice 3	Slice 4	Blank
OEP	1.85	1.12	0.99	1.07	0.95
MNR	2.17	2.16	2.47	2.26	-
DNR-1	6.55	12.38	8.56	8.27	-
TNR-2	3.38	0.43	0.64	0.62	-
MPI	0.20	0.20	-	-	-
MPDF	0.55	0.57	0.59	0.53	-
MPR	1.57	1.54	1.70	1.11	-
DMDR	1.06	0.87	0.35	0.67	-
	Ext III				
	Slice 1	Slice 2	Slice 3	Slice 4	Blank
OEP	1.1	-	0.87	-	-
MNR	2.23	1.81	1.88	-	-
DNR-1	4.80	2.36	5.66	-	-
TNR-2	0.92	0.81	0.89	-	-
MPI	0.25	0.25	0.30	-	-
MPDF	0.58	0.58	0.59	-	-
MPR	1.46	2.04	1.81	-	-
DMDR	-	-	0.79	-	-

OEP = odd-over-even carbon number preference: (n-C_{29}+ 6 n-C_{31} + n-C_{33})/(4 n-C_{30} + 4 n-C_{32}); **MNR** = 2-MN/1-MN; **DNR-1** = (2,6-DMN + 2,7-DMN)/1,5-DMN; **TNR-**2 = (2,3,6-TMN + 1,3,7-TMN)/(1,4,6-TMN + 1,3,5-TMN + 1,3,6-TMN); **MPI-1** = 1.5 x (3-MP + 2-MP)/(P + 9-MP + 1-MP); **MPDF** = (3-MP + 2-MP)/(3-MP + 2-MP + 9-MP + 1-MP); **MPR** = (2-MP / 1-MP); **DMDR** = 4,6-DMDBT / (3,6-DMDBT + 2,6-DMDBT); **MN** = methylnaphthalene; **DMN** = dimethylnaphthalene; **TMN** = trimethylnaphthalene; **MP** = methylphenanthrene; **DMDBT** = dimethyldibenzothiophene.

4.5. Discussion

4.5.1. Reliability of HC data

Experimental contamination levels have been reduced to picogram levels in this study, and most detected HCs in the inner slices in all three extraction experiments are considered to be indigenous, including biomarkers such as hopanes, steranes and tri- and tetracyclic terpanes. The procedural blank does not contain these biomarkers, except for Pr and Ph, or they are at least below detection limit (<0.2 pg / g sample) (Fig. 4.5 and Fig. S4.1). Hopanes and steranes in some previous Archean drill cores, which were collected by a conventional drilling method, are now considered to be contamination during drilling and storage (French et al., 2013). However, as the investigated rock in this study is an outcrop sample, common contamination sources for drill core samples, such as drilling mud or lubricating oil, are not applicable to this study (see Section 4.5.2 for more details). Instead, the rock was covered with aluminium foil and sealed in a plastic pail in the field. These materials could be a contamination source, and part of the HCs detected on the rock surface may come from them. However, the clear distinction of HC composition between the outer and the inner slices suggest that the influence of the field contamination is limited to the rock surface. Lubricant water, the saw blade and the ring-mill can be contamination sources during rock handling, but the procedural blank data clearly indicate that these contamination sources do not contain any biomarkers, except for Pr and Ph, and their contribution is at most 10 pg.

Recently, airborne HC contamination inside laboratories, including hopanes and steranes was reported (Illing et al., 2014). Multiple contamination sources are expected, and the contamination particularly accumulates in fume cupboards. The rock in this study may have been exposed to the same contamination sources. However, the airborne HC contamination is not considered to have been a serious matter in this study. Although all slices and the procedural blank were examined in a laboratory with similar equipment to the one described by Illing et al. (2014), there is a clear distinction in the HC composition and abundance between the investigated stromatolite rock and the

procedural blank. Each slice also has a completely different composition. This is unlikely if the detected HCs share common origins in the laboratory. Therefore, the biomarkers detected in this study are not likely to be due to any experimental contamination.

4.5.2. Relative merits of drill core and outcrop samples for analysis of Archean biomarkers

A recent study of drill cores collected by ultraclean sampling from the Pilbara region did not find any biomarkers in 2.6–3.5 Ga rocks, and the authenticity of Archean biomarkers discovered in the past drill core projects is strongly questioned (French et al., *in prep*) (see also Chapter 5). Drill cores are commonly considered to be less susceptible to contamination than outcrop rocks, although there is substantial evidence in earlier studies on non-ultraclean drill core that the detected biomarkers are mainly contamination (Rasmussen et al., 2008; Brocks, 2011). Drilling fluid contaminants, core storage and sawing of cores have all been implicated in providing extraneous biomarkers that have contaminated Archean drill cores (Brocks, 2011; French et al., 2013). In addition, the amount of material collected from drill cores is very limited. The core needs to be sliced into outside and inside parts at least (preferably more slices as described in this chapter), so as to distinguish contamination from drilling and storage, so the amount of each slice is very small, typically 20-50 g. Thus, it is commonly difficult to obtain sufficient material to test the presence of biomarkers in cored Archean rocks.

The surface of the rock analysed in this study was found to be heavily influenced by recent HC input. However, it was also proven that the inside of the rock has a completely different HC distribution, and especially HCs preserved within the carbonate minerals are interpreted as likely indigenous. Therefore, outcrop samples still have the possibility of holding an intact record of ancient organisms that inhabited Earth. Advantages of analysing outcrop samples are that they are visible in geological context, it is easy to obtain a large amount of material, and it is possible to examine the spatial distribution of HCs. Even after slicing the rock, each slice weighed at least 100 g in this study. However, the amount of detected biomarkers in the deepest part of rock is still <3 pg /g for hopanes and <1 pg / g for steranes, which is almost below the detection limit of the GC-MS.

It is also possible that the investigated stromatolite (*Conophyton*) has a different preservation environment from the shale drill core samples (French et al., 2013), and may have higher abundance of biomarkers. The development of *Conophyton* is suggested to have a specific link to the phototrophic movement of cyanobacteria (Walter et al., 1976; Allwood et al., 2006), and therefore it might contain a large amount of cyanobacterial biomarkers. So far, all the cyanobacterial biomarker evidence in the Archean has come from shale drill core samples (Brocks et al., 1999; Brocks et al., 2003a; Eigenbrode et al., 2008; Waldbauer et al., 2009), and these are now called into question (Rasmussen et al., 2008; Brocks, 2011; French et al., 2013). Further study of Archean stromatolite outcrops may provide new information about the Archean ecosystem.

4.5.3. HC distribution on the rock surface

The influence of the recent HC input onto the rock surface can be seen by the heterogeneous distribution of aliphatic HCs such as *n*-alkanes, MMAs, ACHs, regular isoprenoids, hopanes, steranes, and aromatic HCs between the outer slices (slice 1) and the inner slices (slices 2-4). However, the origins of HCs on the rock surface are not necessarily shared. Hopanes, steranes and some aromatic HCs in slice 1 could have the same origin as they similarly suggest a high thermal maturity (Table 4.1 and 4.2), and share the same spatial distribution in Ext. I and II (Figs 4.5 and 4.14). The distribution of 7-MHeD and *n*-C_{17} on the rock surface clearly indicates the presence of endolithic cyanobacteria in the past or at present (Hoshino et al., 2014) (see also Chapter 6). However, no functionalised organic compounds were detected by the derivatisation experiment on the extract solution. Thus, their inhabitation is considered to not be modern, but at some point since the Cenozoic. The cyanobacterial input did not experience high temperature alteration, so the origin of the hopanes and steranes is probably different from the endolithic cyanobacteria. The OEP in the high molecular weight *n*-alkane distribution suggests an input of higher plant material. The irregular OEP in the low molecular weight ACH distribution implies another source of HCs. The origin of the detected organic matter on the rock surface may be associated with roots of plants, pollens, aerosols of vehicle fuels,

aluminium foil and plastic pails used for rock storage, or the incorporation of debris from surrounding biomass (e.g. Schauer et al., 1999).

4.5.4. Constraints on the endolithic cyanobacteria

The composition of MMAs may be used to identify more specific types of cyanobacteria. The cyanobacteria on the rock surface have predominantly produced 7- and 6-MMAs (MHeD, MOD, MND and MED), whereas 2-, 3-, 4- and 5-MMAs were not major products (Fig. 4.7). The ability to synthesise mid-chain branched MMAs is considered to be universal within the cyanobacterial clade (Shiea et al., 1990; Coates et al., 2014). The main product is mostly 7-MHeD, but the detailed compositions of MMA isomers synthesised by each cyanobacterial species are diverse. Some cyanobacteria are known to produce MHeD, MOD and MND, such as have been found in this study (Fig. 4.8) (Coates et al., 2014). The discovered cyanobacterial biomarkers in slice 1 may suggest the presence of one or a mixture of such particular types of cyanobacteria on the surface of stromatolitic carbonate rocks in the Pilbara region (see Chapter 6 for more details). However, there is a possibility that the original composition of MMA isomers from an endolithic cyanobacterium may have been altered through weathering or diagenetic rearrangement over geological time. Thus, the original composition could have been different, and different cyanobacteria may be responsible for the observed MMA composition on the rock surface.

4.5.5. HC distribution in the inner parts of the sample

Hopanes, steranes and 7-MHeD in the inner slices are interpreted to be ancient indigenous HCs within the rock, possibly of Archean era. A low amount of 2α-methylhopanes was also detected in the deepest part of the rock (slice 4). The source of these biomarkers inside the rock are likely to be common for all biomarker classes detected, although their distribution is not exactly the same across the inner slices and extraction experiments. All the polycyclic terpane biomarkers (hopanes, steranes, and tri- and tetracyclic terpanes) detected in the inner slices have a higher abundance within the carbonate minerals (Ext. II) than in the pore space outside the minerals (Ext. I) (Fig. 4.5). Furthermore, the biomarkers in Ext. II increase in abundance towards the inside of the rock (Fig. 4.5), indicating

that the deeper part of the rock protected the biomarkers better from weathering or alteration. This sort of concentration profile is typical of indigenous biomarkers (Sherman et al., 2007; Brocks, 2011), and cannot be due to a recent input from outside the rock.

The indigenous MHeDs inside the rock are slightly influenced by the extremely abundant MHeDs on the rock surface, which appears to penetrate into the deeper parts of the rock. Although the abundance of 7-MHeD in slice 2 and 3 is higher in Ext. I than in Ext. II, the 7-MHeD abundance in Ext. I decreases towards the inside of the rock, and becomes lower than that in Ext. II in slice 4 (Fig. 4.9). In addition, the abundance of 7-MHeD in Ext. II is constantly higher than the other MHeD isomers throughout the inner slices. Thus, the 7-MHeD in Ext. II appears to have been isolated from the outside environment within the carbonate minerals, and is a signature of possible Archean cyanobacterial input. Hopanes, steranes and MHeDs all reside within the carbonate minerals and have a similar spatial distribution, so probably have a common origin. The abundance of MHeDs in Ext. III is higher in the outer parts of the rock, and it is not possible to conclude that there are indigenous (Fig. 4.9). However, based on the possible shared origin of some aliphatic and aromatic HCs in Ext. III with those in Ext. II, Ext. III may also contain some indigenous MHeDs.

Based on traditional biomarker geochemistry interpretation (Peters et al., 2005), the combination of mid-chain branched MMAs and 2α-methylhopanes indicates the presence of cyanobacteria, although 2α-methylhopanes cannot be used alone as evidence for cynaobacteria any more (Rashby et al., 2007; Welander et al., 2010; Ricci et al., 2013). It is possible to constrain to some extent particular cyanobacterial species responsible for the production of these biomarkers. Some studies indicate the diversification of multicellularity occurred at the time of the GOE (e.g. Schirrmeister et al., 2013). Their work implies that cyanobacterial morphologies were much simpler and mostly unicellular before the GOE. A recent phylogenetic analysis proved that many unicellular cyanobacteria possess the biosynthetic pathway of mid-chain branched MMA, and one of the most ancient types of unicellular cyanobacterium, *G. violaceus*, is also found to possess the MMA production pathway

(Coates et al., 2014). *G. violaceus* also has the gene *hpn P* which encodes the enzyme responsible for methylating hopanoids at the C-2 position (Talbot et al., 2008; Welander et al., 2010). The observed biomarkers (7-MHeD and 2α-methylhopanes) are consistent with the presence of such an ancient unicellular species. The suggestion of cyanobacteria in the Archean is consistent with recent several new lines of evidence provided by some redox-sensitive metal element analyses, which also indicate the presence of atmospheric oxygen before the GOE (e.g. Planavsky et al., 2014).

4.5.6. Interpretation of the biomarkers at "Martin's Hill"

Although there is a possibility of HC migration after the initial deposition in the Fortescue Group, the Pilbara region, it is not likely for the biomarkers in this study. Four other stromatolite rocks, and two Maddina Formation basalt rocks from different localities have also been examined, including the "Knossos" locality (see Chapter 7). None of these rocks contain any biomarkers, and their HC compositions are also different from each other. In particular, the "Knossos" locality is very close, within a few kilometres, to the "Martin's Hill" locality (this study). If a HC migration had occurred in this area, both localities should have experienced the same migration event. These data are indicative that a pervasive HC migration event has not occurred in the Pilbara region.

Hopanes, 2α-methylhopanes and steranes have previously been discovered in an Archean rock from the same locality at "Martin's Hill" (Coffey, 2011). The abundance of the biomarkers in the previous study has a similar trend to this study, with the outside surface having a higher abundance than in the second outer-most layer, and the abundance gradually increasing towards the inside layer. The rock samples were collected from the same locality as this study, but the sampling point was slightly different, and they were examined by a different person independently at a different time. Thus, the biomarkers discovered twice at "Martin's Hill" are not likely to be mere experimental contamination. The most likely possibility is that this locality is one of only a few places in which indigenous HCs were luckily preserved. Further comprehensive study of "Martin's Hill" is required to corroborate and test these two studies. In addition, further exploration of other localities in the Pilbara region is essential to test how unusual the situation at "Martin's Hill" is (see Chapter 7 for more details).

4.5.7. Implication of steranes at 2.7 Ga

Generally, the presence of steranes is interpreted to indicate the presence of eukaryotes, and atmospheric oxygen because the biosynthesis of sterols requires molecular oxygen (Summons et al., 2006). The current consensus for the emergence of atmospheric oxygen is at the GOE around 2.4 Ga, so the steranes at 2.7 Ga requires the reassessment of the evolutionary history of cyanobacteria and oxygenic photosynthesis. The search for anoxic sterol synthesis pathways is underway by some researchers, but currently there is no clear evidence of its existence (Summons et al., 2006). Therefore, the presence of steranes at 2.7 Ga implies the appearance of cyanobacteria earlier than 2.7 Ga.

However, there is a hypothesis that low amounts of oxygen produced by abiogenic processes before the invention of oxygenic photosynthesis were enough to develop some aerobic metabolisms (e.g. Brochier-Armanet et al., 2009). Also, the biosynthesis of sterols is proven possible by dissolved oxygen in the nanomolar range (Waldbauer et al., 2011). In this case, the synthesis of sterols in ancient eukaryotes might have already been possible, regardless of the presence of cyanobacteria and oxygenic photosynthesis. The divergence of the domain Bacteria from the eukaryotic and archaeal lineages is considered to have been much earlier than the advent of cyanobacteria. The fact that no extant archaea have sterols may indicate that sterols appeared after the divergence of the domain Archaea and the domain Eukaryotes, but the advent of sterols could have been before the emergence of cyanobacteria.

Steranes are not the only compounds that require oxygen for their biosynthesis. Recent studies have suggested that the biosynthesis of mid-chain branched MMAs in cyanobacteria also needs oxygen (Li et al., 2011; Li et al., 2012). Thus, the presence of mid-chain branched MMAs produced by cyanobacteria also implies the presence of oxygen. However, it is not clear that the MMA biosynthesis pathway appeared after oxygenic photosynthesis, or before it as might be the case for sterol biosynthesis. A physiological study of MMA production in cyanobacteria, the MMA counterpart

of the oxygen requirement test for sterol biosynthesis (Waldbauer et al., 2011), would be beneficial. Further, comprehensive genomic analysis for aerobic metabolism, including sterol and MMA biosynthesis will be required to decipher the history of oxygen on Earth, and the development of aerobic metabolisms in the early life.

4.6. Conclusions

Various hopanes, 2α-methylhopanes, steranes, and mid-chain branched MMAs were found in the internal parts of an Archean rock from the Pilbara region. The rock surface also has these biomarkers, but with a different distribution, which is considered to be a mixture of the input from endolithic organisms, and overprinting from the outside environment. The biomarkers are more abundantly preserved within the carbonate minerals, and to some extent within the silicate minerals as well, indicating that they are indigenous HCs of a probable Archean origin. The distribution of biomarkers on the rock surface has the opposite trend, and reside more in the pore spaces in the rock, which supports their recent origin from the outside. The distribution of some of the aliphatic and aromatic HCs is not the same as that of these biomarkers, implying a complex thermal alteration and preservational history over geological time. 2α-Methylhopanes and mid-chain branched MMAs suggest the presence of cyanobacteria, and steranes suggest the presence of eukaryotes in the Archean. However, the evidence is still limited and further investigation is necessary to definitely conclude their presence in the Archean in terms of biomarker authenticity. The rock surface may also have harboured endolithic cyanobacteria since uplift of the Fortescue Group stromatolites during the Cenozoic, indicated by the presence of characteristic high abundances of 7-MHeD and 6-MHeD on the rock surface. Therefore, the investigated stromatolite rock is found to have both recent and ancient cyanobacterial sources.

4.7. Acknowledgements

We thank the Geological Survey of Western Australia for logistical field support and scientific assistance, particularly from Kath Grey and Arthur Hickman. Y.H. is supported by a Macquarie

University Research Excellence Scholarship. D.T.F. was supported by an Australian Government Postgraduate Award. M.R.W. acknowledges the Australian Research Council for a Discovery Grant and a Professional Fellowship. S.C.G. acknowledges the Australian Research Council for a Discovery Grant.

4.8. Appendix

Table A4.1. Compound abbreviations for hopanes, steranes, and tricyclic terpanes. Compound order follows the elution order in the chromatograms.

Abbreviation	Name
Ts	18α(H)-22,29,30-Trisnorneohopane
Tm	17α(H)-22,29,30-Trisnorhopane
C_{29} αβ	17α(H), 21β(H)-29-Norhopane
C_{29} Ts	18α(H)-30-Norneohopane
C_{30} αβ	17α(H), 21β(H)-Hopane
C_{30} βα	17β(H), 21α(H)-Hopane
C_{31} αβ-22S	17α(H), 21β(H)-Homohopane (22S)
C_{31} αβ-22R	17α(H), 21β(H)-Homohopane (22R)
G	Gammacerane
C_{32} αβ-22S	17α(H), 21β(H)-Bishomohopane (22S)
C_{32} αβ-22R	17α(H), 21β(H)-Bishomohopane (22R)
C_{33} αβ-22R	17α(H), 21β(H)-Trishomohopane (22R)
C_{31} 2α-Me	2α-methyl-17β(H), 21α(H)-Hopane
C_{32} 2α-Me 22S	2α-methyl-17α(H), 21β(H)-Homohopane (22S)
C_{32} 2α-Me 22R	2α-methyl-17α(H), 21β(H)-Homohopane (22R)
C_{27} βα-20S	13β(H), 17α(H)-diacholestane (20S)
C_{27} βα-20R	13β(H), 17α(H)-diacholestane (20R)
C_{28} βα-20S 24S	24-methyl-13β(H), 17α(H)-diacholestane (20S)(24S)
C_{28} βα-20S 24R	24-methyl-13β(H), 17α(H)-diacholestane (20S)(24R)
C_{27} ααα-20S	5α(H), 14α(H), 17α(H)-cholestane (20S)
C_{27} αββ-20R	5α(H), 14β(H), 17β(H)-cholestane (20R)
C_{29} βα-20S	24-ethyl-13β(H), 17α(H)-diacholestane (20S)
C_{27} αββ-20S	5α(H), 14β(H), 17β(H)-cholestane (20S)
C_{28} αβ-20R	24-methyl-13α(H), 17β(H)-diacholestane (20R)
C_{27} ααα-20R	5α(H), 14α(H), 17α(H)-cholestane (20R)
C_{29} βα-20R	24-ethyl-13β(H), 17α(H)-diacholestane (20R)
C_{28} αββ-20R	24-methyl-5α(H), 14β(H), 17β(H)-cholestane (20R)
C_{30} βα-20R	24-n-propyl-13β(H), 17α(H)-diacholestane (20R)
C_{28} αββ-20S	24-methyl-5α(H), 14β(H), 17β(H)-cholestane (20S)
C_{28} ααα-20R	24-methyl-5α(H), 14α(H), 17α(H)-cholestane (20R)
C_{29} ααα-20S	24-ethyl-5α(H), 14α(H), 17α(H)-cholestane (20S)
C_{29} αββ-20R	24-ethyl-5α(H), 14β(H), 17β(H)-cholestane (20R)
C_{29} αββ-20S	24-ethyl-5α(H), 14β(H), 17β(H)-cholestane (20S)
C_{29} ααα-20R	24-ethyl-5α(H), 14α(H), 17α(H)-cholestane (20R)
19/3	C_{19} 13β(H), 14α(H)-cheilanthane
20/3 a	C_{20} 13β(H), 14α(H)-cheilanthane
20/3 b	C_{20} 13β(H), 14α(H)-cheilanthane
21/3	C_{21} 13β(H), 14α(H)-cheilanthane
23/3	C_{23} 13β(H), 14α(H)-cheilanthane
24/3	C_{24} 13β(H), 14α(H)-cheilanthane
25/3 a	C_{25} 13β(H), 14α(H)-cheilanthane (22S)

25/3 b	C_{25} 13β(H), 14α(H)-cheilanthane (22R)
26/3 a	C_{26} 13β(H), 14α(H)-cheilanthane (22S)
26/3 b	C_{26} 13β(H), 14α(H)-cheilanthane (22R)
24/4	C_{24} 17α(H), 21β(H)-Secohopane
28/3 a	C_{28} 13β(H), 14α(H)-cheilanthane (22S)
28/3 b	C_{28} 13β(H), 14α(H)-cheilanthane (22R)
29/3 a	C_{29} 13β(H), 14α(H)-cheilanthane (22S)
29/3 b	C_{29} 13β(H), 14α(H)-cheilanthane (22R)

4.9. Supplementary Information

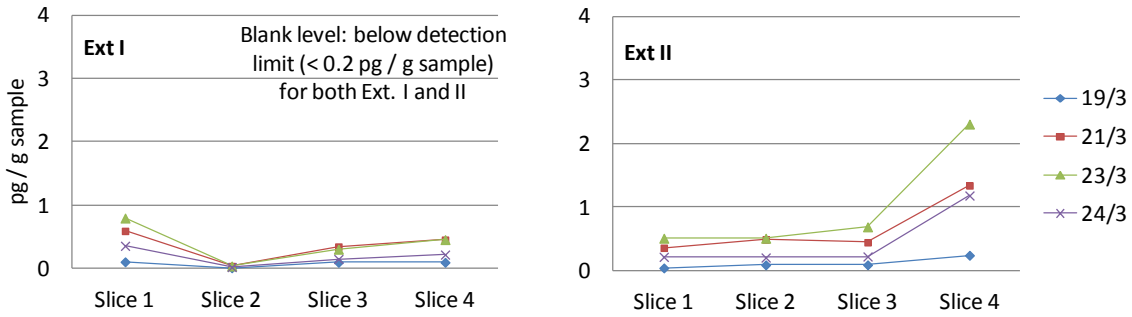

Figure S4.1. Amount and distribution of selected tricyclic terpanes in the four slices in (a) Ext. I, and (b) Ext. II.

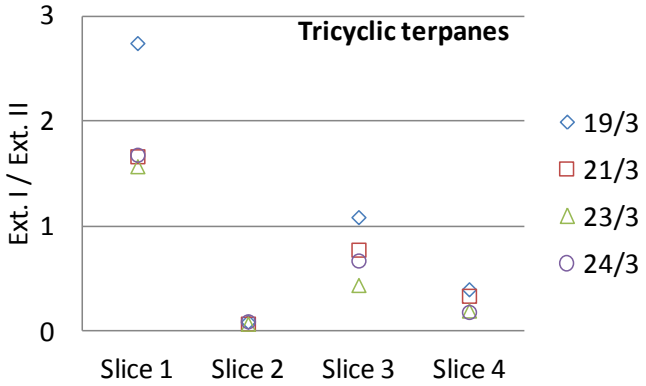

Figure S4.2. Ratios of abundance of selected tricyclic terpanes in Ext. I to that in Ext. II.

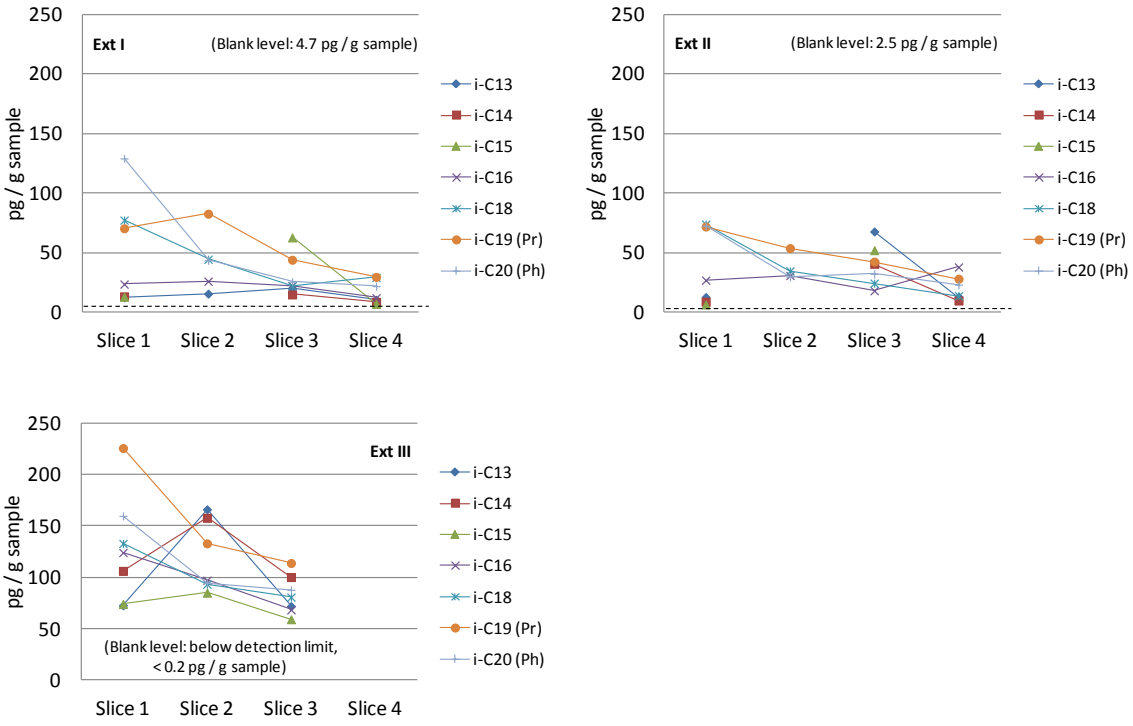

Figure S4.3. Amount and distribution of regular isoprenoids in the four slices in Ext. I, Ext. II, and Ext. III.

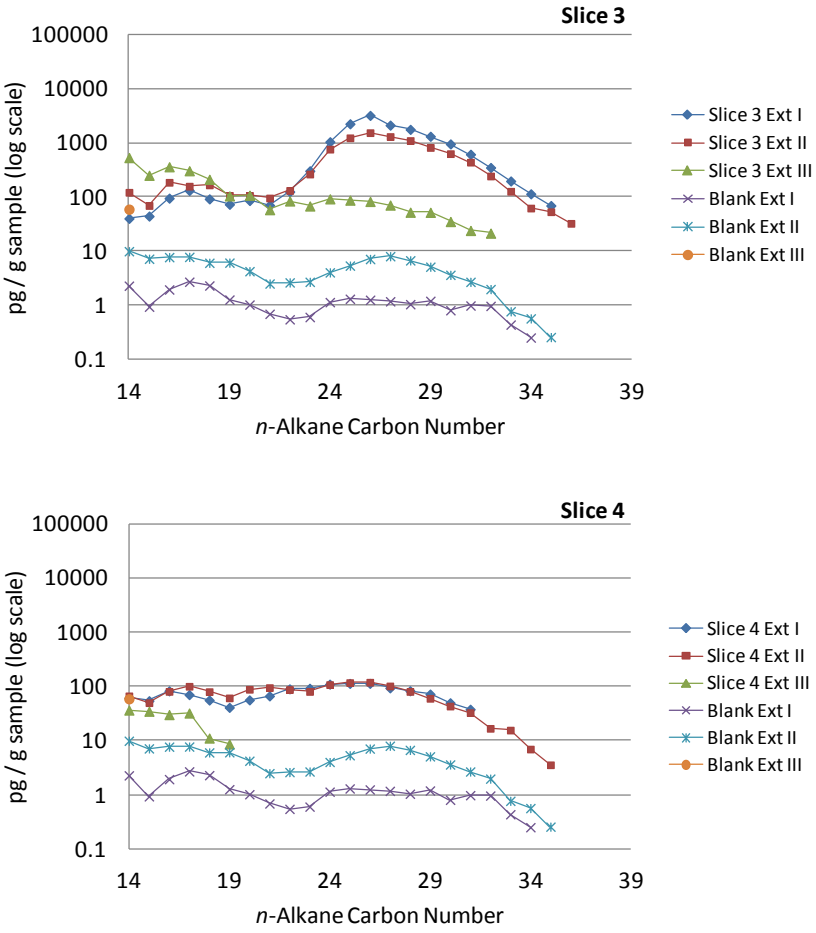

Figure S4.4. Amount and distribution of *n*-alkanes in the three extraction experiments for slice 3 and slice 4, and the amount of *n*-alkanes in the basalt blank. Note that a log abundance scale is used in order to visualise all the data.

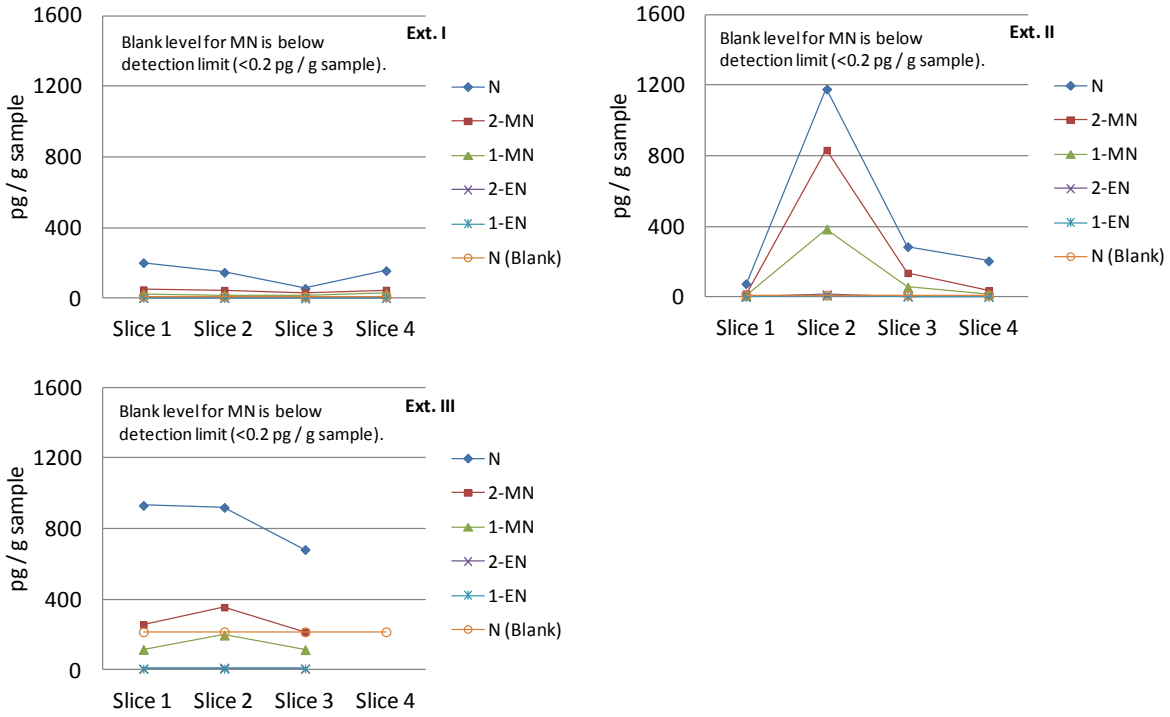

Figure S4.5. Amount and distribution of naphthalene and alkylated naphthalenes in the four slices in Ext. I, Ext. II, and Ext. III. **N** = naphthalene; **MN** = methylnaphthalene; **EN** = ethylnaphthalene.

4.10. References

Allwood, A., Walter, M., Kamber, B., Marshall, C. and Burch, I. (2006) Stromatolite reef from the Early Archaean era of Australia. Nature 441, 714-718.

Anbar, A.D., Duan, Y., Lyons, T.W., Arnold, G.L., Kendall, B., Creaser, R.A., Kaufman, A.J., Gordon, G.W., Scott, C., Garvin, J. and Buick, R. (2007) A whiff of oxygen before the Great Oxidation Event? Science 317, 1903-1906.

Arndt, N.T., Nelson, D.R., Compston, W., Trendall, A.F. and Thorne, A.M. (1991) The age of the Fortescue Group, Hamersley Basin, Western Australia, from ion microprobe zircon U-Pb results. Australian Journal of Earth Sciences 38, 261-281.

Awramik, S.M. and Buchheim, H.P. (2009) A giant, Late Archean lake system: The Meentheena Member (Tumbiana Formation; Fortescue Group), Western Australia. Precambrian Research 174, 215-240.

Barley, M.E., Pickard, A.L. and Sylvester, P.J. (1997) Emplacement of a large igneous province as a possible cause of banded iron formation 2.45 billion years ago. Nature 385, 55-58.

Blake, T.S., Buick, R., Brown, S.J.A. and Barley, M.E. (2004) Geochronology of a late Archaean flood basalt province in the Pilbara Craton, Australia; constraints on basin evolution, volcanic and sedimentary accumulation, and continental drift rates. Precambrian Research 133, 143-173.

Bosak, T., Knoll, A.H. and Petroff, A.P. (2013) The Meaning of Stromatolites. Annual Review of Earth and Planetary Sciences 41, 21-44.

Brasier, M., McLoughlin, N., Green, O. and Wacey, D. (2006) A fresh look at the fossil evidence for early Archaean cellular life. Philosophical Transactions of the Royal Society B: Biological Sciences 361, 887-902.

Briggs, D.E.G. and Summons, R.E. (2014) Ancient biomolecules: Their origins, fossilization, and role in revealing the history of life. BioEssays 36, 482-490.

Brochier-Armanet, C., Talla, E. and Gribaldo, S. (2009) The multiple evolutionary histories of dioxygen reductases: Implications for the origin and evolution of aerobic respiration. Molecular biology and evolution 26, 285-297.

Brocks, J.J. (2001) Molecular Fossils in Archean Rocks. Ph.D. dissertation, University of Sydney.

Brocks, J.J. (2011) Millimeter-scale concentration gradients of hydrocarbons in Archean shales: Live-oil escape or fingerprint of contamination? Geochimica Et Cosmochimica Acta 75, 3196-3213.

Brocks, J.J., Buick, R., Logan, G.A. and Summons, R.E. (2003a) Composition and syngeneity of molecular fossils from the 2.78 to 2.45 billion-year-old Mount Bruce Supergroup, Pilbara Craton, Western Australia. Geochimica Et Cosmochimica Acta 67, 4289-4319.

Brocks, J.J., Buick, R., Summons, R.E. and Logan, G.A. (2003b) A reconstruction of Archean biological diversity based on molecular fossils from the 2.78 to 2.45 billion-year-old Mount Bruce Supergroup, Hamersley Basin, Western Australia. Geochimica Et Cosmochimica Acta 67, 4321-4335.

Brocks, J.J., Logan, G.A., Buick, R. and Summons, R.E. (1999) Archean molecular fossils and the early rise of eukaryotes. Science 285, 1033-1036.

Brocks, J.J., Love, G.D., Summons, R.E., Knoll, A.H., Logan, G.A. and Bowden, S.A. (2005) Biomarker evidence for green and purple sulphur bacteria in a stratified Palaeoproterozoic sea. Nature 437, 866-870.

Coates, R., Podell, S., Korobeynikov, A., Lapidus, A., Pevzner, P., Sherman, D., Allen, E., Gerwick, L. and Gerwick, W. (2014) Characterization of cyanobacterial hydrocarbon composition and distribution of biosynthetic pathways. PloS one 9, e85140.

Coffey, J.M. (2011) A paleoenvironmental study of the 2.7 Ga Tumbiana Formation, Fortescue Basin, Western Australia. Ph.D. dissertation, University of New South Wales, Sydney.

Coffey, J.M., Flannery, D.T., Walter, M.R. and George, S.C. (2013) Sedimentology, stratigraphy and geochemistry of a stromatolite biofacies in the 2.72Ga Tumbiana Formation, Fortescue Group, Western Australia. Precambrian Research 236, 282-296.

Coffey, J.M., Walter, M.R., George, S.C. and Hill, A.C. (2011) Paleontology and field observations of the ~2720 Ma Tumbiana Formation in the Northwest Pilbara, Western Australia. Geological Survey of Western Australia, Record 2011/8., pp. 22.

Crowe, S., Døssing, L., Beukes, N., Bau, M., Kruger, S., Frei, R. and Canfield, D. (2013) Atmospheric oxygenation three billion years ago. Nature 501, 535-538.

Desmond, E. and Gribaldo, S. (2009) Phylogenomics of Sterol Synthesis: Insights into the Origin, Evolution, and Diversity of a Key Eukaryotic Feature. Genome Biology and Evolution 1, 364–381.

Dutkiewicz, A., George, S.C., Mossman, D., Ridley, J. and Volk, H. (2007) Oil and its biomarkers associated with the Palaeoproterozoic Oklo natural fission reactors, Gabon. Chemical Geology 244, 130-154.

Eglinton, G. and Hamilton, R.J. (1967) Leaf Epicuticular Waxes. Science 156, 1322-1335.

Eglinton, G., Scott, P.M., Belsky, T., Burlingame, A.L. and Calvin, M. (1964) Hydrocarbons of Biological Origin from a One-Billion-Year-Old Sediment. Science 145, 263-264.

Eigenbrode, J.L., Freeman, K.H. and Summons, R.E. (2008) Methylhopane biomarker hydrocarbons in Hamersley Province sediments provide evidence for Neoarchean aerobiosis. Earth and Planetary Science Letters 273, 323-331.

Flannery, D.T. (2013) Palaeobiology of the Neoarchean Fortescue Group, Pilbara Craton, Western Australia. Ph.D. dissertation, University of Sydney.

Fowler, M.G. and Douglas, A.G. (1987) Saturated hydrocarbon biomarkers in oils of Late Precambrian age from Eastern Siberia. Organic Geochemistry 11, 201-213.

French, K.L., Hallman, C., Hope, J.M., Buick, R., Brocks, J.J. and Summons, R.E. (2013) Archean hydrocarbon biomarkers: Archean or not?, Goldschmidt 2013 Conference Abstract.

French, K.L., Hallmann, C., Hope, J.M., Hoshino, Y., Peters, C., George, S.C., Buick, R., Brocks, J.J. and Summons, R.E. (*in prep*) Archean hydrocarbon biomarkers: Indigenous or not? Proceedings of National Academy of Science USA.

Gaillard, F., Scaillet, B. and Arndt, N. (2011) Atmospheric oxygenation caused by a change in volcanic degassing pressure. Nature 478, 229-232.

George, S. and Ahmed, M. (2002) Use of aromatic compound distributions to evaluate organic maturity of the Proterozoic middle Velkerri Formation, McArthur Basin, Australia. The Sedimentary Basins of Western Australia III: Proceedings of the West Australasian Basins Symposium (WABS) III.

George, S., Volk, H., Ruble, T. and Brincat, M. (2002) Evidence for a new oil family in the Nancar Trough area, Timor Sea. APPEA journal 42, 387-404.

George, S.C., Volk, H., Dutkiewicz, A., Ridley, J. and Buick, R. (2008) Preservation of hydrocarbons and biomarkers in oil trapped inside fluid inclusions for > 2 billion years. Geochimica Et Cosmochimica Acta 72, 844-870.

Haqq-Misra, J., Kasting, J. and Lee, S. (2011) Availability of O_2 and H_2O_2 on pre-photosynthetic Earth. Astrobiology 11, 293-302.

Holland, H.D. (2006) The oxygenation of the atmosphere and oceans. Philosophical Transactions of the Royal Society B: Biological Sciences 361, 903-915.

Hoshino, Y., Flannery, D., Walter, M. and George, S.C. (2014) Investigation of hydrocarbons preserved in a 2.7 Ga Archean rock from the Fortescue Group, Pilbara Craton, Western Australia. Geobiology submitted.

Illing, C.J., Hallmann, C., Miller, K.E., Summons, R.E. and Strauss, H. (2014) Airborne hydrocarbon contamination from laboratory atmospheres. Organic Geochemistry 76, 26-38.

Kenig, F., Damsté, J.S.S., Dalen, A.C.K.-v., Rijpstra, W.I.C., Huc, A.Y. and Leeuw, J.W.d. (1995) Occurrence and origin of mono-, di-, and trimethylalkanes in modern and Holocene cyanobacterial mats from Abu Dhabi, United Arab Emirates. Geochimica Et Cosmochimica Acta 59, 2999-3015.

Kirschvink, J.L. and Kopp, R.E. (2008) Palaeoproterozoic ice houses and the evolution of oxygen-mediating enzymes: the case for a late origin of photosystem II. Philosophical Transactions of the Royal Society B: Biological Sciences 363, 2755-2765.

Klomp, U.C. (1986) The chemical structure of a pronounced series of iso-alkanes in South Oman Crudes, in: Leythaeuser, D., Rullkcöte, J. (Eds.), Advances in Organic Geochemistry Part II. Pergamon Journals, Oxford, pp. 807-814.

Knoll, A.H., Javaux, E.J., Hewitt, D. and Cohen, P. (2006) Eukaryotic organisms in Proterozoic oceans. Philosophical Transactions of the Royal Society B: Biological Sciences 361, 1023-1038.

Kopp, R.E., Kirschvink, J.L., Hilburn, I.A. and Nash, C.Z. (2005) The Paleoproterozoic snowball Earth; a climate disaster triggered by the evolution of oxygenic photosynthesis. Proceedings of the National Academy of Sciences of the United States of America 102, 11131-11136.

Kruge, M.A., Hubert, J.F., Bensley, D.F., Crelling, J.C., Akes, R.J. and Meriney, P.E. (1990) Organic geochemistry of a lower jurassic synrift lacustrine sequence, Hartford Basin, Connecticut, U.S.A. Organic Geochemistry 16, 689-701.

Kump, L. and Barley, M. (2007) Increased subaerial volcanism and the rise of atmospheric oxygen 2.5 billion years ago. Nature 448, 1033-1036.

Li, N., Chang, W.-C., Warui, D., Booker, S., Krebs, C. and Bollinger, J. (2012) Evidence for only oxygenative cleavage of aldehydes to alk(a/e)nes and formate by cyanobacterial aldehyde decarbonylases. Biochemistry 51, 7908-7916.

Li, N., Nørgaard, H., Warui, D., Booker, S., Krebs, C. and Bollinger, J. (2011) Conversion of fatty aldehydes to alka(e)nes and formate by a cyanobacterial aldehyde decarbonylase: cryptic redox by an unusual dimetal oxygenase. Journal of the American Chemical Society 133, 6158-6161.

Lipple, S.L. (1975) Definitions of new and revised stratigraphic units of the eastern Pilbara region. Annual Report - Western Australia, Geological Survey 1974, 58-63.

Lyons, T., Reinhard, C. and Planavsky, N. (2014) The rise of oxygen in Earth's early ocean and atmosphere. Nature 506, 307-315.

Nelson, D.R. (2001) Compilation of geochronology data. 2000: Record 2001/2.

Paoletti, C., Pushparaj, B., Florenzano, G., Capella, P. and Lercker, G. (1976) Unsaponifiable matter of green and blue-green algal lipids as a factor of biochemical differentiation of their biomasses: I. Total unsaponifiable and hydrocarbon fraction. Lipids 11, 258-265.

Pearson, A., Budin, M. and Brocks, J.J. (2003) Phylogenetic and biochemical evidence for sterol synthesis in the bacterium Gemmata obscuriglobus. Proceedings of the National Academy of Sciences of the United States of America 100, 15352-15357.

Peters, K.E., Walters, C.C. and Moldowan, J.M. (2005) The biomarker guide: Biomarkers and isotopes in the environment and human history. Cambridge University Press Volume 1.

Planavsky, N.J., Asael, D., Hofmann, A., Reinhard, C.T., Lalonde, S.V., Knudsen, A., Wang, X., Ossa, F.O., Pecoits, E., Smith, A.J.B., Beukes, N.J., Bekker, A., Johnson, T.M., Konhauser, K.O., Lyons, T.W.

and Rouxel, O.J. (2014) Evidence for oxygenic photosynthesis half a billion years before the Great Oxidation Event. Nature Geoscience 7, 283-286.

Radke, M. and Welte, D. (1983) The Methylphenanthrene index (MPI). A Maturity parameter based on aromatic hydrocarbons, in: Bjorøy, M., Albrecht, C., Cornford, C. (Eds.), Advances in Organic Geochemistry. John Wiley & Sons, New York, pp. 504-512.

Radke, M., Willsch, H., Leythaeuser, D. and Teichmüller, M. (1982) Aromatic components of coal: relation of distribution pattern to rank. Geochimica Et Cosmochimica Acta 46, 1831-1848.

Rashby, S.E., Sessions, A.L., Summons, R.E. and Newman, D.K. (2007) Biosynthesis of 2-methylbacteriohopanepolyols by an anoxygenic phototroph. Proceedings of the National Academy of Sciences of the United States of America 104, 15099-15104.

Rasmussen, B., Fletcher, I.R., Brocks, J.J. and Kilburn, M.R. (2008) Reassessing the first appearance of eukaryotes and cyanobacteria. Nature 455, 1101-1104.

Rezende, E. (2013) Evolution. Better oxygen delivery. Science 340, 1293-1294.

Ricci, J., Coleman, M., Welander, P., Sessions, A., Summons, R., Spear, J. and Newman, D. (2013) Diverse capacity for 2-methylhopanoid production correlates with a specific ecological niche. The ISME journal 8, 675-684.

Sakurai, R., Ito, M., Ueno, Y., Kitajima, K. and Maruyama, S. (2005) Facies architecture and sequence-stratigraphic features of the Tumbiana Formation in the Pilbara Craton, northwestern Australia; implications for depositional environments of oxygenic stromatolites during the late Archean. Precambrian Research 138, 255-273.

Schauer, J.J., Kleeman, M.J., Cass, G.R. and Simoneit, B.R.T. (1999) Measurement of Emissions from Air Pollution Sources. 2. C_1 through C_{30} Organic Compounds from Medium Duty Diesel Trucks. Environmental Science & Technology 33, 1578-1587.

Schirmer, A., Rude, M.A., Li, X., Popova, E. and Del Cardayre, S.B. (2010) Microbial biosynthesis of alkanes. Science 329, 559-562.

Schirrmeister, B., de Vos, J., Antonelli, A. and Bagheri, H. (2013) Evolution of multicellularity coincided with increased diversification of cyanobacteria and the Great Oxidation Event. Proceedings of the National Academy of Sciences of the United States of America 110, 1791-1796.

Schopf, J.W. (2006) Fossil evidence of Archaean life. Philosophical Transactions of the Royal Society B: Biological Sciences 361, 869-885.

Sessions, A., Doughty, D., Welander, P., Summons, R. and Newman, D. (2009) The continuing puzzle of the great oxidation event. Current biology 19, R567-574.

Sherman, L.S., Waldbauer, J.R. and Summons, R.E. (2007) Improved methods for isolating and validating indigenous biomarkers in Precambrian rocks. Organic Geochemistry 38, 1987-2000.

Shiea, J., Brassel, S.C. and Ward, D.M. (1991) Comparative analysis of extractable lipids in hot spring microbial mats and their component photosynthetic bacteria. Organic Geochemistry 17, 309-319.

Shiea, J., Brassell, S.C. and Ward, D.M. (1990) Mid-chain branched mono- and dimethyl alkanes in hot spring cyanobacterial mats: A direct biogenic source for branched alkanes in ancient sediments? Organic Geochemistry 15, 223-231.

Smith, R.E., Perdrix, J.L. and Parks, T.C. (1982) Burial Metamorphism in the Hamersley Basin, Western Australia. Journal of Petrology 23, 75-102.

Summons, R.E. (1987) Branched alkanes from ancient and modern sediments: Isomer discrimination by GC/MS with multiple reaction monitoring. Organic Geochemistry 11, 281-289.

Summons, R.E., Bradley, A.S., Jahnke, L.L. and Waldbauer, J.R. (2006) Steroids, triterpenoids and molecular oxygen. Philosophical Transactions of the Royal Society B: Biological Sciences 361, 951-968.

Summons, R.E., Jahnke, L.L., Hope, J.M. and Logan, G.A. (1999) 2-Methylhopanoids as biomarkers for cyanobacterial oxygenic photosynthesis. Nature 400, 554-557.

Summons, R.E., Powell, T.G. and Boreham, C.J. (1988) Petroleum geology and geochemistry of the Middle Proterozoic McArthur Basin, Northern Australia: III. Composition of extractable hydrocarbons. Geochimica Et Cosmochimica Acta 52, 1747-1763.

Talbot, H.M., Summons, R.E., Jahnke, L.L., Cockell, C.S., Rohmer, M. and Farrimond, P. (2008) Cyanobacterial bacteriohopanepolyol signatures from cultures and natural environmental settings. Organic Geochemistry 39, 232-263.

Thiel, V., Jenisch, A., Wörheide, G., Löwenberg, A., Reitner, J. and Michaelis, W. (1999) Mid-chain branched alkanoic acids from "living fossil" demosponges: a link to ancient sedimentary lipids? Organic Geochemistry 30, 1-14.

Thorne, A.M. and Trendall, A.F. (2001) Geology of the Fortescue Group, Pilbara Craton, Western Australia. Bulletin - Geological Survey of Western Australia, 249.

van Graas, G.W. (1990) Biomarker maturity parameters for high maturities: Calibration of the working range up to the oil/condensate threshold. Organic Geochemistry 16, 1025-1032.

Waldbauer, J.R., Newman, D.K. and Summons, R.E. (2011) Microaerobic steroid biosynthesis and the molecular fossil record of Archean life. Proceedings of the National Academy of Sciences 108, 13409-13414.

Waldbauer, J.R., Sherman, L.S., Sumner, D.Y. and Summons, R.E. (2009) Late Archean molecular fossils from the Transvaal Supergroup record the antiquity of microbial diversity and aerobiosis. Precambrian Research 169, 28-47.

Walter, M. (1983) Archean stromatolites: Evidence of the Earth's earliest benthos, in: Schopf, J. (Ed.), Earth's Earliest Biosphere: It's Origin and Evolution. Princeton University Press, Princeton, pp. 187-213.

Walter, M.R., Bauld, J. and Brock, T.D. (1976) Microbiology and morphogenesis of columnar stromatolites (Conophyton, Vacerrila) from hot springs in Yellowstone National Park. Elsevier, New York.

Weiss, H.M., Wilhelms, A., Mills, N., Scotchmer, J., Hall, P.B., Lind, K. and Brekke, T. (2000) NIGOGA - The Norwegian Industry Guide to Organic Geochemical Analyses [online], http://www.npd.no/engelsk/nigoga/default.htm.

Welander, P.V., Coleman, M.L., Sessions, A.L., Summons, R.E. and Newman, D.K. (2010) Identification of a methylase required for 2-methylhopanoid production and implications for the interpretation of sedimentary hopanes. Proceedings of the National Academy of Sciences 107, 8537-8542.

Wenger, L.M., Davis, C.L. and Isaksen, G.H. (2002) Multiple controls on petroleum biodegradation and impact on oil quality. SPE Reservoir Evaluation & Engineering 5, 375-383.

Zhusheng, J., Philp, R.P. and Lewis, C.A. (1988) Fractionation of biological markers in crude oils during migration and the effects on correlation and maturation parameters. Organic Geochemistry 13, 561-571.

Chapter 5.

Indigeneity of hydrocarbons preserved in Archean drill cores from the Fortescue Group, Pilbara Craton, Western Australia

Y. Hoshino [1,2], C. Peters [1], S. C. George [1,2]

[1] *Department of Earth and Planetary Sciences, Macquarie University, Sydney, Australia*

[2] *Australian Centre for Astrobiology, University of New South Wales, Australia*

Statement of authors' contribution

This Chapter is a part of an article in review with *Proceedings of the National Academy of Sciences*, after modifications based on comments from reviewers were finalised on 6 Feb. 2015. The article combines four independently obtained sets of data from four different laboratories, including Macquarie University. Figures and tables included within the text are prefixed with the chapter number.

I am a co-author with 65 % contribution to this chapter, with another 30 % contribution made by Carl Peters (Macquarie University, Australia). The investigated samples were collected by Katherine French (Massachusetts Institute of Technology, the United States). Examination of the samples, including sample cutting, grinding, and solvent extraction was carried out by Yosuke Hoshino and Carl Peters. Gas chromatography-mass spectroscopy was performed by Yosuke Hoshino and Carl Peters, with help from Se Gong (The Commonwealth Scientific and Industrial Research Organisation, Australia), and Jochen Brocks (Australian National University, Australia). Processing and preliminary analysis of all the data derived from the measurements was performed by Yosuke Hoshino and Carl Peters. Detailed interpretation of the data was performed by Yosuke Hoshino. I processed and designed the structure of this chapter. Simon George (Macquarie University, Australia) organised the Macquarie University contribution to the collaboration, and carefully reviewed and provided feedback and valuable refinements on the final version of the manuscript (5% contribution).

Abstract

The composition of preserved hydrocarbons in three Archean drill cores was analysed, and the indigeneity of the detected hydrocarbons was investigated. The drill cores were collected according to an unprecedented ultraclean geochemical protocol. Not many aliphatic hydrocarbons were detected above the levels of experimental contamination, but $<C_{18}$ *n*-alkanes, monomethylalkanes and regular isoprenoids in some samples are above the contamination level. Diamondoids are always above the contamination level, and aromatic hydrocarbons are mainly above the contamination level. The distribution of diamondoids and aromatic hydrocarbons generally indicates a high thermal maturity for all three drill cores. Specific biomarkers such as hopanes and steranes were detected in some samples, but their abundance is comparable to the laboratory blank level, or was below the detection limit. The lack of these biomarkers is consistent with the high thermal maturity indicated by the diamondoids and aromatic hydrocarbons, and suggests that the previous evidence for biomarkers of cyanobacteria and eukaryotes in nearby commercially-drilled Archean cores needs to be reassessed.

5.1. Introduction

The rise of oxygen on Earth was of importance because it paved the way for the development of aerobiosis and complex multicellular organisms (Lyons et al., 2014). It is well accepted that the concentration of atmospheric oxygen arose by the Great Oxidation Event (GOE) around 2.4-2.3 Ga (e.g. Holland, 2002), and that this was associated with oxygenic photosynthesis invented by cyanobacteria (Kopp et al., 2005). However, it is not clear exactly when oxygenic photosynthesis emerged. Some biomarker analyses have indicated the presence of cyanobacteria and eukaryotes hundreds of millions of years preceding the GOE, by the presence of methylhopanes and steranes, diagnostic biomarkers for cyanobacteria and eukaryotes, at 2.7 Ga (Brocks et al., 1999; Brocks et al., 2003a; Eigenbrode et al., 2008; Waldbauer et al., 2011). However, the biomarker evidence has been contentious due to trace contamination problems (Rasmussen et al., 2008; Brocks, 2011). In contrast, other lines of independent geochemical evidence have suggested the presence of oxygen in the Archean (e.g. Anbar et al., 2007; Planavsky et al., 2014). Therefore, it is critical to assess the biomarker evidence for cyanobacteria and eukaryotes in the Archean so as to decisively constrain the timing of their emergence and to understand the evolutionary history of these organisms on Earth.

There are not many places on Earth in which Archean crust is preserved at a relatively low metamorphic grade. One such area is the Fortescue Group, Pilbara region, Western Australia (Smith et al., 1982). Biomarker evidence for oxygenic photosynthesis in the Archean has been reported by analysis of drill cores from the Fortescue Group (Brocks et al., 1999; Brocks et al., 2003a; Eigenbrode et al., 2008). However, conventional drilling is now regarded as inappropriate for providing rocks for trace biomarker analyses, because there are many anthropogenic contamination sources such as drilling fluids and sample storage bags (Sherman et al., 2007; Brocks, 2011; Schinteie and Brocks, 2014). Therefore, it is essential to test the validity of the previous biomarker analyses (Brocks et al., 1999; Brocks et al., 2003a; Eigenbrode et al., 2008) with newly collected drill cores obtained using a more reliable drilling method.

The new drill cores were collected according to an unprecedented organic geochemical protocol by the 2012 Agouron Institute Drilling Program (AIDP) (French et al., 2013). The study reported here is a part of multi-laboratory study. The drill cores were delivered to several different laboratories around the world, and were analysed separately to test the reproducibility of the results. The combined results are soon to be published (French et al., *in prep*). In this Chapter, the data obtained from the cores delivered to the Macquarie University organic geochemistry lab are presented and discussed in more detail.

The possibility of later hydrocarbon (HC) migration was monitored by measuring concentration gradients by slicing the rock samples from the outside towards the inside, and analysing HCs in each slice separately (Brocks, 2001; Sherman et al., 2007). Any contamination from the outside environment would be expected to have a maximum concentration at the surface, and then it would decline towards the inside. In contrast, any indigenous organic compounds would have the higher abundance in the deeper part of the samples, and would decrease in concentration towards the outside due to weathering processes.

5.2. Geological setting

Samples were collected from three drill cores (AIDP-1, 2, and 3) from the Pilbara region, Western Australia (Fig. 5.1). AIDP-1 is a drill core that intersected volcanic strata at the greenschist metamorphic grade (300-500 °C). This core was selected as a negative control due to its igneous origin and the high metamorphic grade that the strata experienced. AIDP-2 was recovered from the Ripon Hills region, which is thought to have experienced prehnite-pumpellyite metamorphism (175-280 °C) (Smith et al., 1982). AIDP-2 intersected the Hamersley Group Carawine Dolomite Formation and the Fortescue Group Jeerinah Formation (~2.65 Ga), and is an analogue of the previously drilled Archean core RHDH2A that was obtained with conventional drilling methods, which reportedly contained indigenous Archean biomarkers (Eigenbrode and Freeman, 2006; Eigenbrode et al., 2008). RHDH2A is spatially separated by only 2.5 km from AIDP-2. AIDP-3 intersects the Hamersley Group Wittenoom Dolomite Formation, Marra Mamba Iron Formation and the Fortescue Group Jeerinah

Formation which includes the Roy Hill shale member, and is a deep water age-equivalent of the Rippon Hills region. Six core samples were analysed; one from AIDP-1 and 3, respectively, and four from AIDP-2 (Table 5.1).

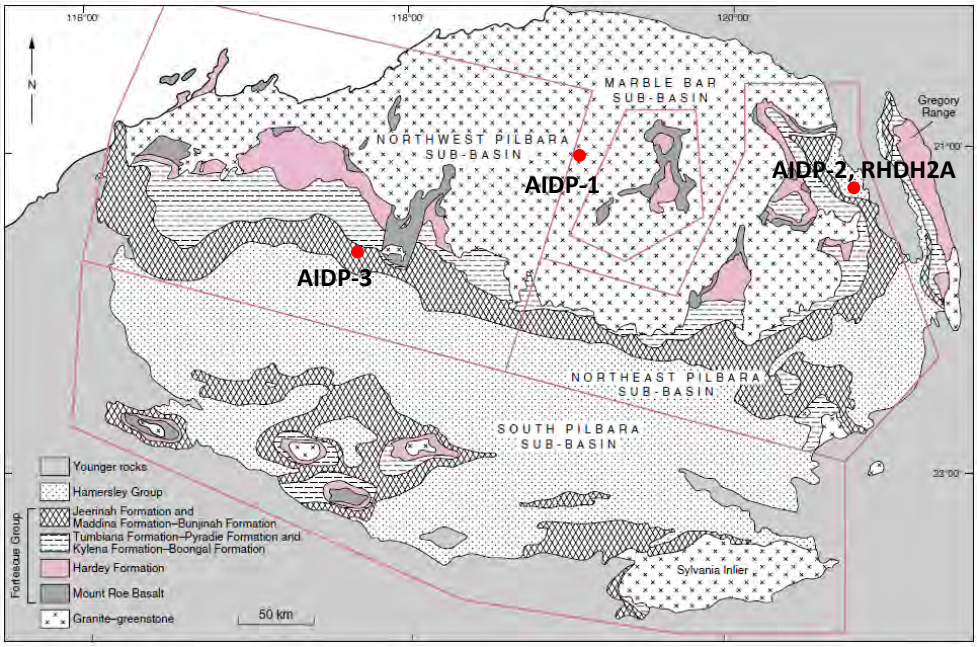

Figure 5.1. Geological map of the Fortescue Group (adapted from Thorne and Trendall, 2001) and the drilling locations of newly collected drill cores AIDP-1, 2 and 3, and the previously collected core RHDH2A.

Table 5.1. Sample list of analysed drill cores.

Label	Depth (m)	Borehole	Description
1	186	AIDP-1	dolerite
3	130.3	AIDP-3	black shale
2-1	146.2	AIDP-2	kerogen rich shale
2-2	197.2	AIDP-2	black shale
2-3	327.42	AIDP-2	black shale
2-4	291.28	AIDP-2	dark kerogenous shale

The Fortescue Group, a volcano-sedimentary succession, is the basal member of the Mount Bruce Supergroup (Arndt et al., 1991; Barley et al., 1997), and overlies granite-greenstone basement rocks of the Pilbara Craton (the Pilbara Supergroup) (Fig. 5.1). The Fortescue Group was deposited between 2775 and 2630 Ma during a period of rifting and extensive volcanism (Thorne and Trendall, 2001). The depositional setting of the Fortescue Group is either a shallow marine environment (e.g.

Thorne and Trendall, 2001; Sakurai et al., 2005), or a lacustrine environment (e.g. Walter, 1983; Awramik and Buchheim, 2009; Coffey et al., 2013). The Jeerinah Formation in the Fortescue Group is mostly composed of argillite with minor sandstone, dolomite, chert and volcanic rocks (Thorne and Trendall, 2001). The age of the Jeerinah Formation is constrained by the 2717 Ma date of the underlying Maddina Formation (Kojan and Hickman, 1998), and by the 2629±5 Ma, 2684±6 Ma and 2690±16 Ma dates obtained from upper units of the Jeerinah Formation (Arndt et al., 1991; Nelson et al., 1999; Trendall et al., 2004). A basaltic lava flow from a Fortescue Group Maddina Formation outcrop was tested as a procedural blank.

5.3. Experimental procedure

5.3.1. Drill core sampling

Three drill cores were recovered in June-July 2012. Only water (i.e. no drilling additives) was used as the drilling fluid, but biphenyl-d_{10} was intentionally added to the drilling fluid to check the influence of drilling fluids on the HC analysis. In addition, *n*-octacosane (C_{28})-d_{60} was added to the drilling equipment. Within minutes of recovery, portions of the core selected as biomarker targets were rinsed with Milli-Q Type-1 ultrapure water in the core tray before being placed into organic-clean Teflon bags containing several millilitres of ultrapure water to prevent the core material from drying out. After purging with high purity Ar, the bags were sealed and samples were frozen at -20 °C in the dark. Each individual participating laboratory sliced their half cores into interior and exterior pieces before powdering and solvent extraction, in order to allow the identification of surficial hydrocarbon enrichments.

5.3.2. Solvents and glassware

Dichloromethane (DCM) (Macron, H485-10) and methanol (MeOH) (Honeywell Burdick & Jackson, GC230-4) (9:1 v/v) were used to extract HCs from the sample. All solvents were checked for purity by gas chromatography-mass spectroscopy (GC-MS) as described below. All glassware was combusted in an oven at 400 °C for 3 hours before use.

5.3.3. Sample preparation

The rock samples were sliced using a diamond blade (BUEHLER, BUE11-4267) into exterior (Ext.) and interior (Int.) portions. The slice pattern was based on the work by Sherman et al. (2007). The thickness of Ext. was typically 1-2 mm. Both Ext. and Int. were further cut into approximately 1 cm^3 pieces. The weight of Ext. was 30-130 g, and that of Int. was 20-120 g, but typically less than 60 g for both Ext. and Int. The procedural blank was analysed first. The blank was combusted at 400°C for 3+ hours before cutting to eliminate possible hydrocarbon contamination. Between each slice experiment, all equipment, including the saw blade and the ring-mill, was washed with filtered water, MeOH and DCM and checked for purity by GC-MS.

Fine particles on sample surfaces were removed by ultrasonication in filtered water for 10 min. Organic contamination on surfaces was removed by ultrasonication in a mixture of DCM and MeOH (9:1, v/v) for two cycles of 10 min, with a new solvent mixture each time. The last solvent mixture was analysed by GC-MS for purity and surface checking. If the cleaning was not sufficient, additional ultrasonication was performed.

The rock was then ground to < 200 mesh grain size in a ring-mill. The mill was cleaned between samples. Fine particles in the mill were removed by water washing and scrubbing by a metal brush. The mill was then repeatedly rinsed with a solvent mixture of the same composition as described above. If the cleaning was insufficient, additional rinsing of the ring-mill was performed.

5.3.4. Solvent extraction

Extraction of HCs from the rock powder was carried out by ultrasonication with 200 ml of the solvent mixture described above for two cycles of 10 min. Between the sonications, the solution was stirred using a glass rod and left to stand still for a few minutes. The solvent was collected in a round-bottom flask. The powder was further sonicated with a fresh 100 ml aliquot of DCM for 10 min to retrieve organic residues, particularly aliphatic HCs, in the mixed slurry of powder and solvent. The second

solvent was added to the first solvent. An instrument such as an Accelerated Solvent Extractor was not used because of the possibility of trace inter-sample contamination.

The obtained solution volume was reduced by rotary evaporation to 30-40 ml. The solution was then centrifuged for 3 min at 2,000 rpm to remove suspended rock particles. The volume was then further reduced by rotary evaporation to approximately 5 ml. If the amount of suspended solids was low, the centrifuge step was omitted and the solvent was directly reduced to approximately 5 ml. Even after the centrifuge step, there were always some very fine rock particles suspended in the solvent. These were removed by filtering the solvent/sample mixture through silica gel (silica gel 60, 0.063-0.200 mm, Merck), which was activated at 120 °C for > 4 hours before use. Column fractionation of the extractable organic matter (EOM) was not performed (1) because the yield was very small (< 100 ng / g sample), (2) because the interference between aliphatic and aromatic HCs was not serious, and (3) also so as to prevent the loss of HCs.

The EOM was spiked with three compounds as internal standards by adding 1 ml of a DCM solution containing about 50 ng of each: anthracene-d_{10} (98 atom %D, Isotec), *p*-terphenyl-d_{14} (98 atom %D, Isotec), and tetraeicosane-d_{50} (98 atom %D, Isotec). The volume of solvent containing the EOM was further reduced on a hot plate at 40 °C under a gentle nitrogen flow, until approximately 50 µl remained.

5.3.5. Gas Chromatography-Mass Spectroscopy (GC-MS)

GC-MS analysis was carried out on an Agilent GC (6890N) coupled to an Agilent Mass Selective Detector (5975B). 1 µL of the EOM solution was injected into a Programmable Temperature Vaporization (PTV) inlet operating in splitless mode with a J&W DB5MS column (length 60 m, inner diameter 0.25 mm, film thickness 0.25 um). The inlet was ramped from 35 °C (3 min. isothermal) to 310 °C (0.5 min. isothermal) at a rate of 700 °C / min. Helium was used as the carrier gas (1.5 ml / min.), and the temperature of the GC oven was ramped from 30 °C (2 min. isothermal) to 310 °C (30 min. isothermal) at a rate of 4 °C / min. The MS data were acquired in single ion monitoring mode.

Hydrocarbon identification was based on comparisons of relative GC retention times and mass spectra with those previously reported. Semi-quantitative analyses were performed using the tetraeicosane-d_{50} internal standard, not taking into account any response factors. The other two standards were used to check sensitivity and repeatability of the measurement, but were not used for the quantification.

5.3.6. Biomarker analyses

Detected biomarkers such as hopanes and steranes by the Agilent GC-MS were present in very low amounts, so it was not possible to quantify them as they were mostly below the level of detection. Therefore, selected samples and blanks were further analysed by either a Thermo Trace Ultra GC interfaced with a high resolution Thermo DFS GC-MS system, or a GC-linked Micromass Autospec Premier. Samples 1 and 3 were run by the former, but the DFS system then had a technical problem, and caused a long holdup, so samples 2-1, 2-2, 2-3, and 2-4 were run by the latter instrument. Semi-quantitative analyses were performed using the *p*-terphenyl-d_{14} internal standard, not taking into account any response factors. The procedural blank was measured by both instruments. The data obtained by the DFS were integrated into the main set of data that were acquired by the Autospec, by comparing the peak areas of the internal standard in the procedural blanks obtained by the DFS and the Autospec.

In the DFS measurements, GC separation was carried out on a J&W DB5MS capillary column (length 60 m, inner diameter 0.25 mm, film thickness 0.25 um). Helium was used as the carrier gas (1.5 ml / min). 1 µL of the EOM solution was injected into an inlet operating at 260 °C in splitless mode. The MS was tuned to 1,000 resolution (electron energy 70eV; source temperature 280 °C). The oven was ramped from 40 °C (2 min isothermal) to 200 °C at a rate of 4 °C / min, then to 310 °C (30 min isothermal) at a rate of 2 °C / min. The MS data were acquired in SIM mode.

The Autospec measurements were carried out on a Micromass AutoSpec Premier GC-MS equipped with an Agilent 6890 GC and a J&W DB5MS capillary column (length 60 m, inner diameter 0.25 mm,

film thickness 0.25 µm). Helium was the carrier gas (1.5 ml / min). 1 µL of the EOM solution was injected into a PTV injector in splitless mode. The injector was ramped from 60 °C (2 min, isothermal) to 300 °C. The MS source was operated at 260 °C in EI-mode at 70 eV ionization energy, and with an acceleration voltage of 8000 V. The GC oven was ramped from 60 °C (4 min, isothermal) to 315 °C (32.3 min isothermal) at a rate of 4 °C / min. The MS data were acquired in SIM mode.

5.4. Results

5.4.1. Aliphatic HCs

5.4.1.1. n-Alkanes

n-Alkanes were detected in all six samples (0.01-3.66 ng / g sample; Fig. 5.2). Samples 1, 3, 2-1 and 2-3 have a higher abundance of $<C_{18}$ *n*-alkanes than the procedural blank, although the abundance of these in samples 1 and 2-1 is almost comparable to the blank. Sample 1 has a higher abundance of $>C_{19}$ *n*-alkanes than the other samples in both the Int. and Ext. fractions, but the abundance is close to the blank level, and their distribution pattern is similar to that of the blank. Thus these high molecular weight *n*-alkanes in sample 1 seem to be experimental contamination. Samples 2-2 and 2-4 have a lower abundance of all *n*-alkanes than the blank, and no certainly indigenous *n*-alkanes were detected. Even though sample 1 has $<C_{18}$ *n*-alkanes above the blank level, it is a dolerite, and was collected as a negative control. The sample contained several quartz veins, and the detected *n*-alkanes may have migrated through the veins. No intentionally added deuterated compounds (*n*-C_{28}-d_{60} and biphenyl-d_{10}) were observed in the Int. or Ext. fractions of any samples, suggesting no contamination from drilling equipment or fluids.

A characteristic of the $<C_{18}$ *n*-alkane distribution of samples 3, 2-1 and 2-3 is the elevated abundance of *n*-C_{16}, *n*-C_{17} and *n*-C_{18} compared to other *n*-alkanes, and an even-over-odd preference of C_{16} and C_{18} over C_{17} (Fig. 5.3). The $<C_{18}$ *n*-alkane distribution pattern of sample 1 Int. is slightly similar to the samples 3, 2-1 and 2-3, but there is no clear even-over-odd preference pattern in either the Int. or the Ext. fractions. The $<C_{18}$ *n*-alkane distribution pattern of samples 2-2 and 2-4, and the procedural

blank does not have this even-over-odd preference, and supports the implication that the origin of *n*-alkanes in samples 2-2 and 2-4 are different from that in the other samples.

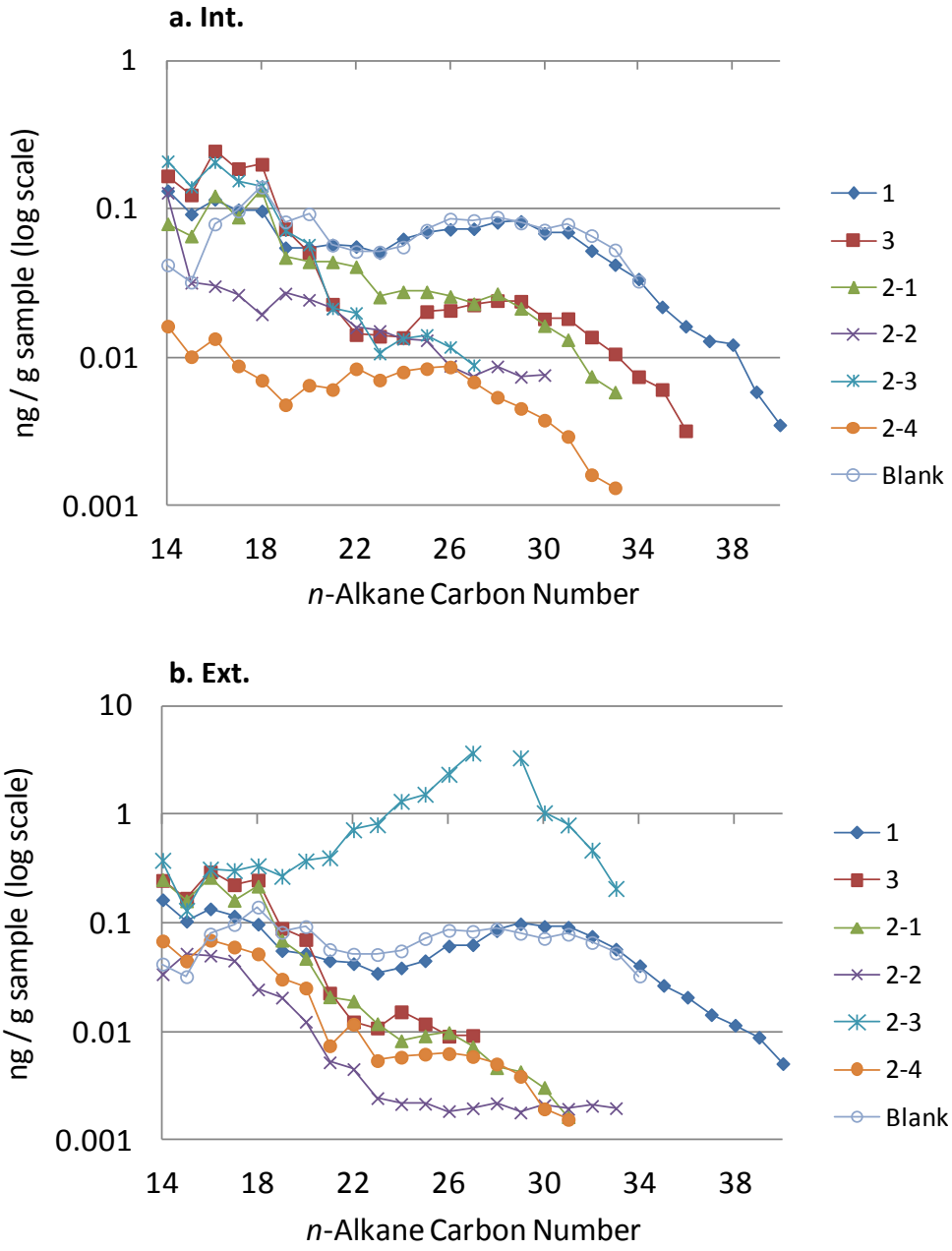

Figure 5.2. Total *n*-alkane distributions in the Int. (a) and the Ext. (b) fractions of all samples and the blank.

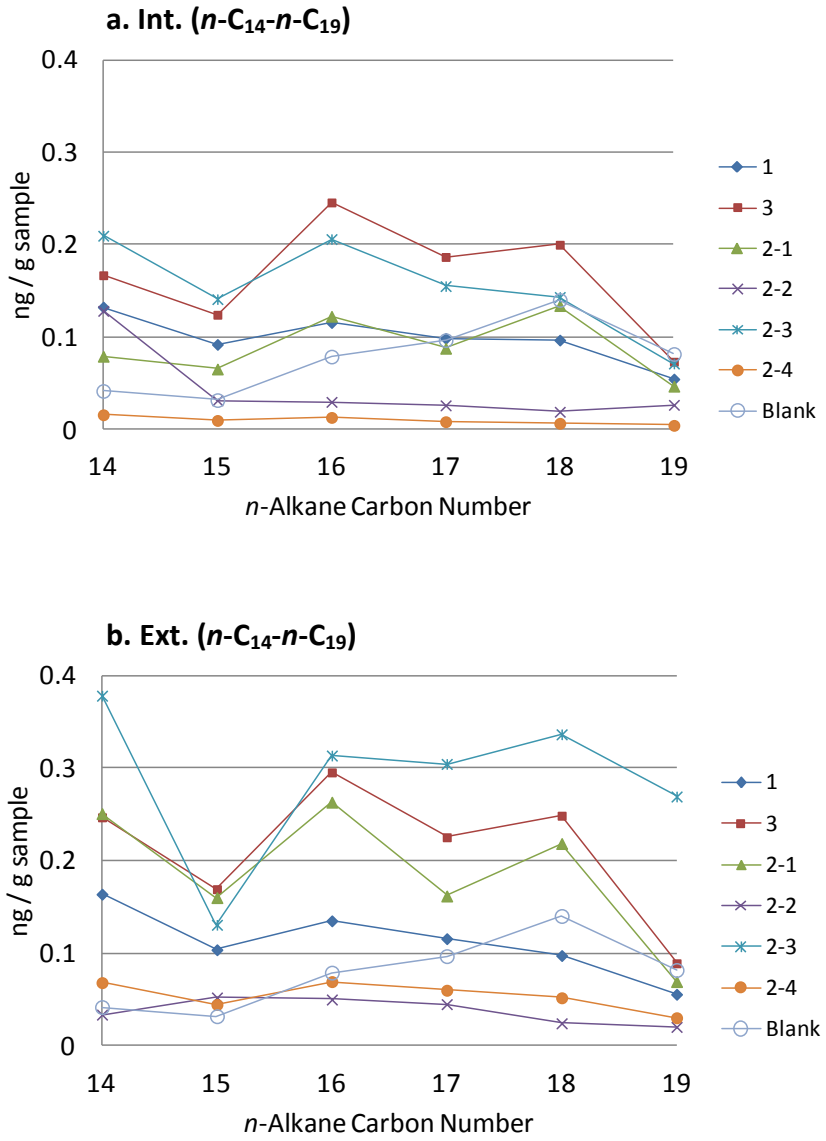

Figure 5.3. Possibly indigenous $C_{14\text{-}19}$ *n*-alkane distributions in the Int. (a) and the Ext. (b) fractions of all samples and the blank.

For the four samples which may contain indigenous *n*-alkanes (1, 3, 2-1 and 2-3), samples 1 and 3 have an abundance of $<C_{18}$ *n*-alkanes in Int. as high as in Ext. (Figs 5.3a and 5.3b), and have a similar distribution pattern between Int. and Ext. However, the $<C_{18}$ *n*-alkane abundance of samples 2-1 and 2-3 in Int. is lower than in Ext. (by about a half), and the distribution pattern of $<C_{18}$ *n*-alkanes are also different between Int. and Ext. The abundance of $C_{14\text{-}16}$ *n*-alkanes in sample 2-3 is almost the same in both Int. and Ext. fractions, but the amount of *n*-alkanes then monotonously increases in sample 2-3 Ext from *n*-C_{19} to *n*-C_{27} (Fig. 5.3b). As these high molecular weight *n*-alkanes were

interpreted as experimental contamination, the C_{17} and C_{18} *n*-alkanes in sample 2-3 are considered to be the mixture of indigenous *n*-alkanes and experimental contamination, and the C_{14-16} *n*-alkanes in sample 2-3 are probably all indigenous. The $<C_{18}$ *n*-alkanes in sample 2-3 Int. may also be indigenous as the distribution pattern of $<C_{18}$ *n*-alkanes in samples 1, 3 and 2-3 Int. are similar and more abundant than in the procedural blank (Fig. 5.3a). In contrast, the distribution pattern of the $<C_{18}$ *n*-alkanes in the Int. and Ext. fractions of sample 2-1 is similar, and the difference in the abundance of *n*-alkanes between the Int. and Ext. fractions may reflect the spatial concentration gradient of *n*-alkanes in the sample. Therefore, although the $<C_{18}$ *n*-alkane abundance in sample 2-1 is close to that of the procedural blank, the distribution pattern is similar to that of samples 1, 3 and 2-3, and thus the *n*-alkanes in sample 2-1 may also be indigenous. Samples 2-2 and 2-4 have a higher abundance of $<C_{18}$ *n*-alkanes in the Ext. fraction than in the Int. fraction, but these are of lower abundance than in the procedural blank. Thus, it cannot be concluded that any of the *n*-alkanes in samples 2-2 and 2-4 are indigenous.

5.4.1.2. Monomethylalkanes (MMAs)

MMAs were detected in five of the six samples (0.01-0.05 ng / g sample), from C_{16} methylpentadecanes to C_{19} methyloctadecanes. Figure 5.4 gives the example of the C_{18} methylheptadecanes, which have similar distributions to the C_{16}, C_{17}, and C_{19} isomers, the exception being in sample 2-3, where MMAs were masked by other small unknown compounds and could not be reliably identified. The abundance of MMAs in samples 1, 3 and 2-1 is higher than that of the blank, and is generally proportional to that of *n*-alkanes with the same carbon number in the three samples, indicating a likely common origin of MMAs and *n*-alkanes. In contrast, the abundance of MMAs in sample 2-2 and 2-4 is comparable to or lower than that of the procedural blank, except for 2- and 3-MMAs in sample 2-2 Ext. fraction, which coincides with the low abundance of *n*-alkanes in samples 2-2 and 2-4. In samples 1, 3 and 2-1, the combined abundance of the 7-, 8- and 9-methylheptadecanes (MHeDs) is higher than that of the 2- and 3-MHeDs, but it was not possible to quantify each of the 7-, 8- and 9-MHeDs separately, as these isomers typically coelute (Summons,

1987). Therefore, no clear dominance of a specific MMA was observed in any sample. In samples 1 and 3, the abundance of MMAs in the Int. fraction relative to the Ext. fraction is the same. However, in sample 2-1, the Ext. fraction has a higher abundance of MMAs than the Int. fraction, as is also the case for the *n*-alkanes.

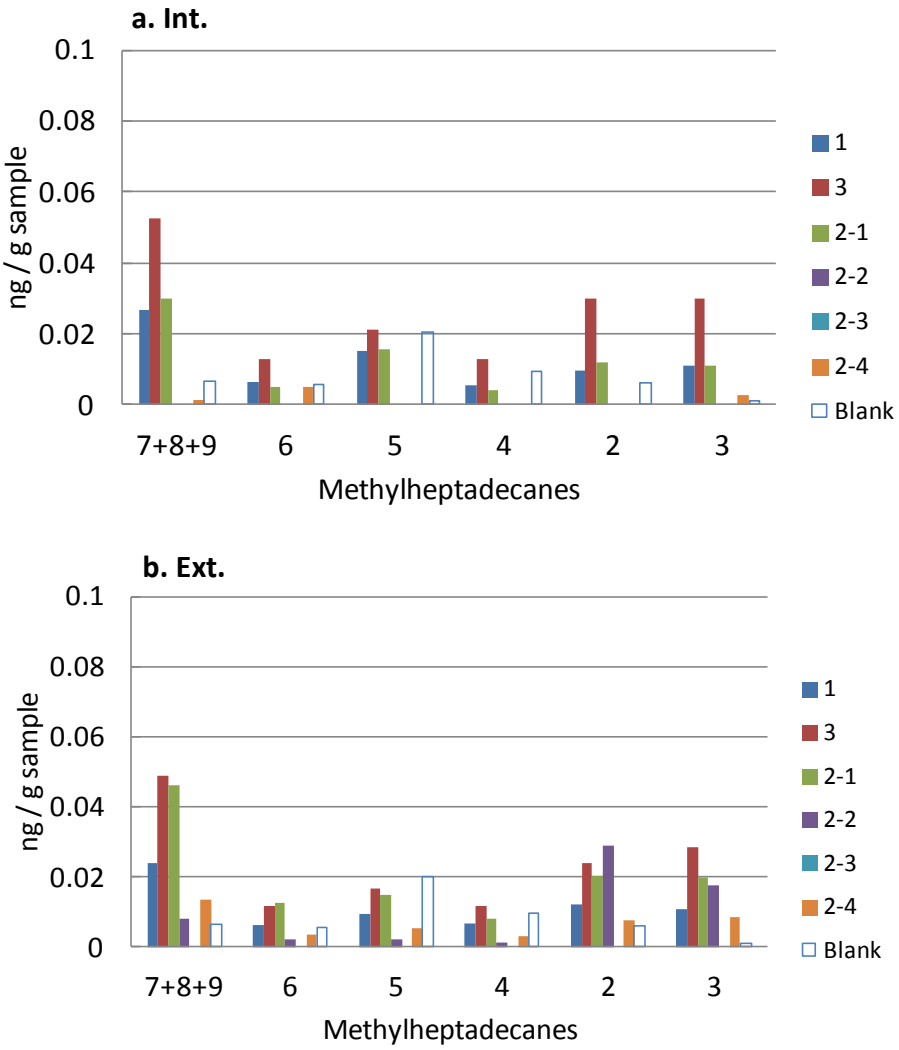

Figure 5.4. Methylheptadecane distributions in the Int. (a) and the Ext. (b) fractions of all samples and the blank.

5.4.1.3. Regular isoprenoids

Regular isoprenoids from *i*-C_{13} to *i*-C_{20} were detected in all samples for both Int. and Ext. fractions (0.01-0.12 ng / g sample; Fig. 5.5). Although the detected isoprenoids ranged from *i*-C_{13} to *i*-C_{20}, not all compounds were detected in each sample or fraction. The abundance of isoprenoids in samples 2-2 and 2-4 is generally comparable to or lower than in the procedural blank, which is consistent with

the low amounts of *n*-alkanes and MMAs in these two samples, the exceptions being Pr and Ph in samples 2-2 and 2-4 Ext. fractions. The other four samples (1, 3, 2-1 and 2-3) generally have a higher abundance of *i*-C_{15} to *i*-C_{20} isoprenoids than for the blank. The abundance of isoprenoids in samples 1 and 3 is similar for the Int. and Ext. fractions. In samples 2-1 and 2-3, the abundance of isoprenoids in the Int. fraction is lower than in the Ext. fraction (by about a half), as was also the case for *n*-alkanes and MMAs. The distribution pattern for the Int. and Ext. fractions of sample 2-3 is also different, as for the *n*-alkanes. Therefore, the regular isoprenoids in sample 2-3 Ext. may be contaminants.

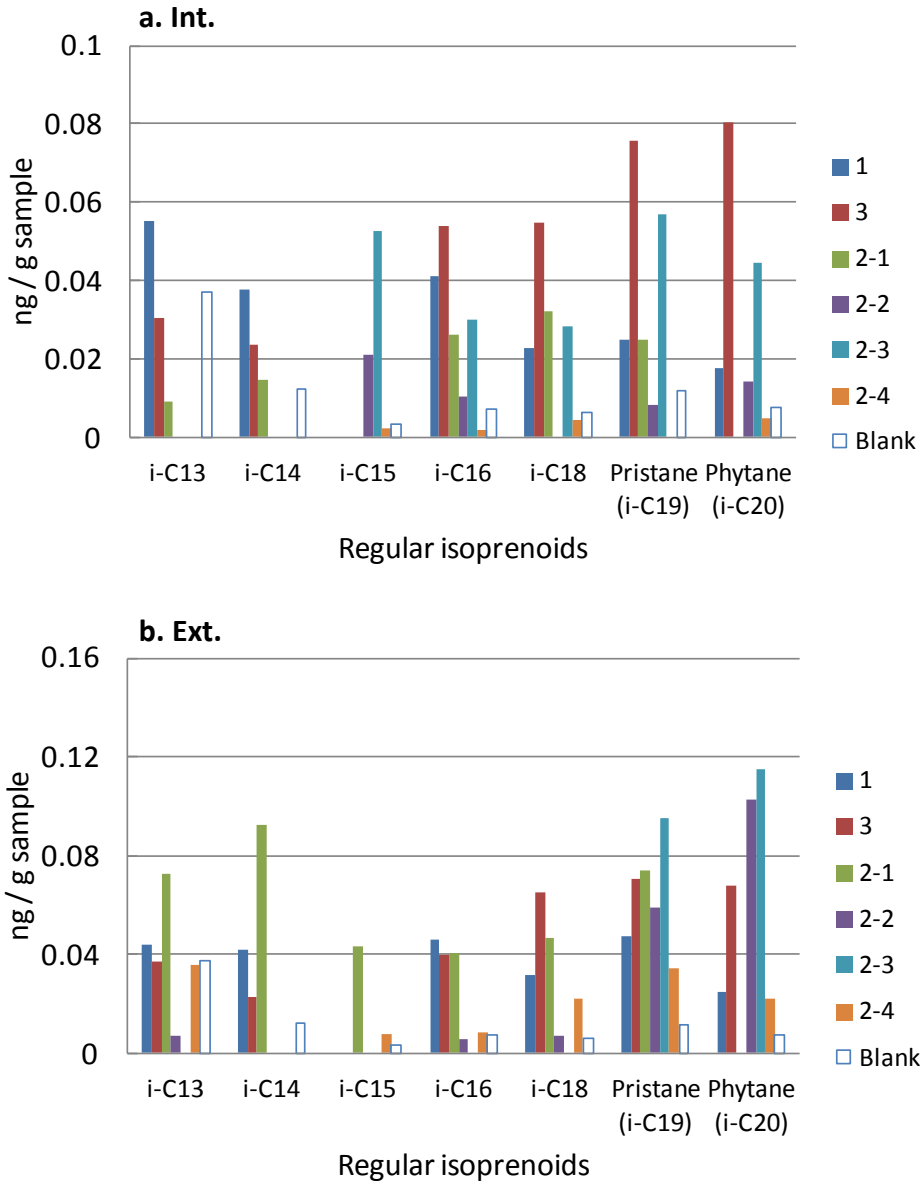

Figure 5.5. Regular isoprenoid distributions in the Int. (a) and the Ext. (b) fractions of all samples and the blank.

The pristane/phytane (Pr/Ph), Pr/*n*-C_{17}, and Ph/*n*-C_{18} ratios vary among the samples (Table 5.2). Pr and Ph cannot be quantified in samples 2-1 and 2-4 Int. due to coelution with an unknown compound. The Pr/Ph ratios of sample 1 are relatively high, and are the highest for the Int. fraction (1.9). In contrast, Pr/Ph of sample 3 is low (<1.1), which may indicate two different origins of regular isoprenoids for samples 1 and 3. The Pr/Ph ratio of sample 2-4 Ext. (1.5) is very close to the blank (1.6), which suggests that the isoprenoids in sample 2-4 are contamination, as has already been suggested by the low abundance of *n*-alkanes and MMAs comparable to the blank level. The Pr/Ph ratios of sample 2-3 have different values between the Int. and Ext. fractions, with values in Ext. closer to that of the blanks, which supports the influence of contamination in sample 2-3 Ext. The Pr/Ph ratios of sample 2-2, 2-3 Int. fraction and 3 are relatively low (0.6-1.1), whereas those of sample 1, 2-3 Ext. fraction, 2-4 Ext. fraction and the blank are high (1.3-1.9).

Table 5.2. Pr/Ph, Pr/*n*-C_{17} and Ph/*n*-C_{18} values (Pr = Pristane; Ph = Phytane).

		1	3	2-1	2-2	2-3	2-4	Blank
Pr/Ph	Int.	1.4	0.94	-	0.57	0.83	-	1.6
	Ext.	1.9	1.05	-	0.57	1.28	1.53	-
Pr/*n*-C_{17}	Int.	0.25	0.40	0.28	0.30	0.37	-	0.12
	Ext.	0.41	0.31	0.46	1.3	0.31	0.57	-
Ph/*n*-C_{18}	Int.	0.18	0.40	-	0.73	0.31	0.69	0.05
	Ext.	0.25	0.27	-	4.2	0.34	0.43	-

The Pr/*n*-C_{17} and Ph/*n*-C_{18} ratios have varying characteristics among the samples. All Int. and Ext. fractions have a higher value for these two ratios than the procedural blank (Table 5.2). This is caused by the low abundance of Pr and Ph in the blank relative to that in the drill core samples, even though the abundance of *n*-alkanes in the blank is comparable to that of the drill core samples. This may suggest that the experimental contamination in the procedural blank derived from highly thermally mature organic matter, as Pr and Ph are thermally less stable than *n*-alkanes, or contamination originated from anthropogenic organic matter without isoprenoids, as Pr and Ph are commonly derived from chlorophyll or bacteriochlorophyll (Brooks et al., 1969; Powell and McKirdy, 1973). Only sample 2-2 Ext. has extremely high values of the Pr/*n*-C_{17} and Ph/*n*-C_{18}, which may

indicate a different input from the other samples/fractions. Alternatively, it is possible that the Pr and Ph measurements of sample 2-2 Ext. were inflated due to coelution with an unknown compound, as the abundance of *n*-C_{17} and *n*-C_{18} in sample 2-2 Ext. is not different from those of other samples/fractions. Also, sample 1 generally has lower values of these two ratios relative to the other samples, which may suggest a different input of organic matter compared to the other samples.

5.4.1.4. Diamondoids

Adamantane, diamantane and their alkylated compounds were detected in all the AIDP-2 samples (0.02-10 ng / g sample; Fig. 5.6), except for sample 2-3 Ext. Diamondoids were not detected in the AIDP-1 or AIDP-3 samples. The procedural blank does not contain any diamondoids, and all samples which contain diamondoids have a similar abundance and distribution pattern for both the Int. and Ext. fractions, so all detected diamondoids are considered to be indigenous.

The distribution of diamondoids among the samples is different from that of the other aliphatic HCs, *n*-alkanes, MMAs and regular isoprenoids (Fig. 5.6). Sample 2-4 has the lowest abundance of diamondoids, which is consistent with the low amounts of the other aliphatic HCs in this sample. However, sample 2-2 has a higher abundance of diamondoids than samples 2-1 and 2-3, which is the opposite pattern to that for the other aliphatic HCs. The presence of diamondoids only in the AIDP-2 samples, and a different abundance pattern among samples, indicates a different origin of diamondoids from the other aliphatic HCs.

The methyladamantane index (MAI) and methyldiamantane index (MDI) indicate a high thermal maturity for all the AIDP-2 samples (Table 5.3) (Chen et al., 1996). The calculated vitrinite reflectance (R_c) is >1.3 for MAI, and >1.4 for MDI.

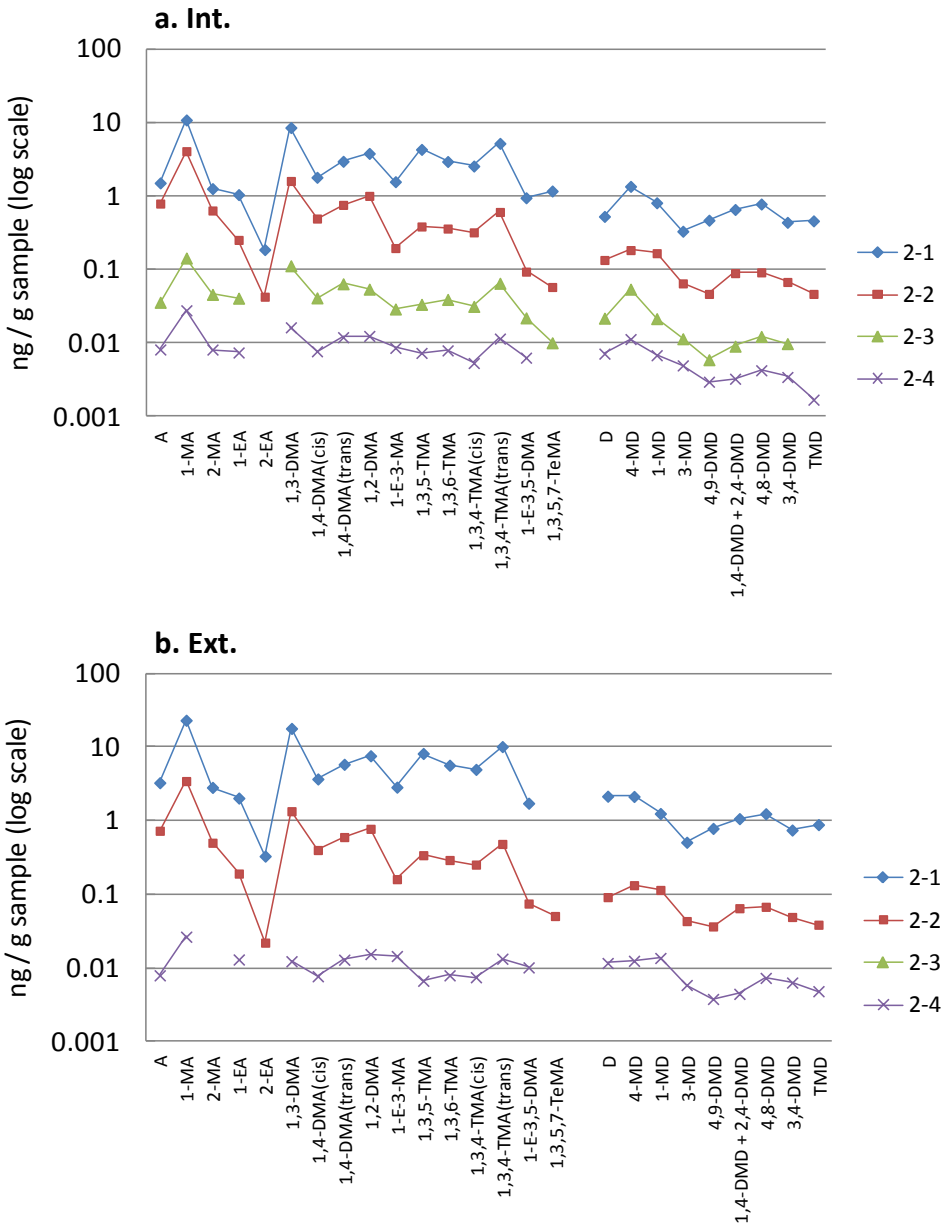

Figure 5.6. Diamondoid distributions in the Int. (a) and the Ext. (b) fractions of all samples and the blank. Adamantane series (left side); and diamantane series (right side). **A** = Adamantane; **MA** = Methyladamantane; **EA** = Ethyladamantane; **DMA** = Dimethyladamantane; **TMA** = Trimethyladamantane; **D** = Diamantane; **MD** = Methyldiamantane; **DMD** = Dimethyldiamantane; **TMD** = Trimethyldiamantane.

Table 5.3. Diamondoid thermal maturity parameters.

		2-1	2-2	2-3	2-4
MAI	Int.	0.90 (>1.9)	0.87 (1.6-1.9)	0.76 (1.3-1.6)	0.77 (1.3-1.6)
	Ext.	0.89 (1.6-1.9)	0.87 (1.6-1.9)	-	1.00 (>1.9)
MDI	Int.	0.54 (1.8)	0.44 (1.5)	0.62 (1.9)	0.49 (1.6)
	Ext.	0.55 (1.8)	0.46 (1.6)	-	0.39 (1.4)

MAI = Methyladamantane index; **MDI** = Methyldiamantane index. The values inside parentheses for MAI are the estimated range of the calculated vitrinite reflectance (R_c) (calculated from Radke and Welte, 1983). The values inside parentheses for MDI are the calculated vitrinite reflectance R_c (R_c = 2.4389 x MDI + 0.4364) (calculated from Zhang et al., 2005).

5.4.1.5. Polycyclic biomarkers

Trace amounts of hopanes (<2.1 pg / g sample; Fig. 5.7) and even lower amounts of steranes (<0.2 pg / g sample) were detected by DFS and Autospec GC-MS in all samples and fractions, but are in much lower amounts than for the other aliphatic and aromatic HCs (typically 0.01-10 ng / g sample). The procedural blank does not contain any steranes, but it does contain low levels of hopanes (Fig. 5.7). The abundance of hopanes is comparable to or lower than that of the procedural blank for both Int. and Ext. fractions in most samples. Only sample 1 Int. fraction has a slightly higher abundance of the biomarkers than the procedural blank. However, sample 1 Ext. fraction has a much lower abundance of the biomarkers. Also, the distribution of hopanes is completely different between the Int. and Ext. fractions for all samples. In addition, the crusher and the saw blade used in the study were tested for the purity every time between the cutting of each sample, and these occasionally contained comparable amounts of hopanes and steranes as were apparently detected in sample 1. Thus, the detected hopanes and steranes in the samples are considered to be experimental contamination for all samples, and the slightly higher abundance of the biomarkers in sample 1 Int. fraction is probably within experimental error. Therefore, no certainly indigenous hopanes and steranes were found in any drill core.

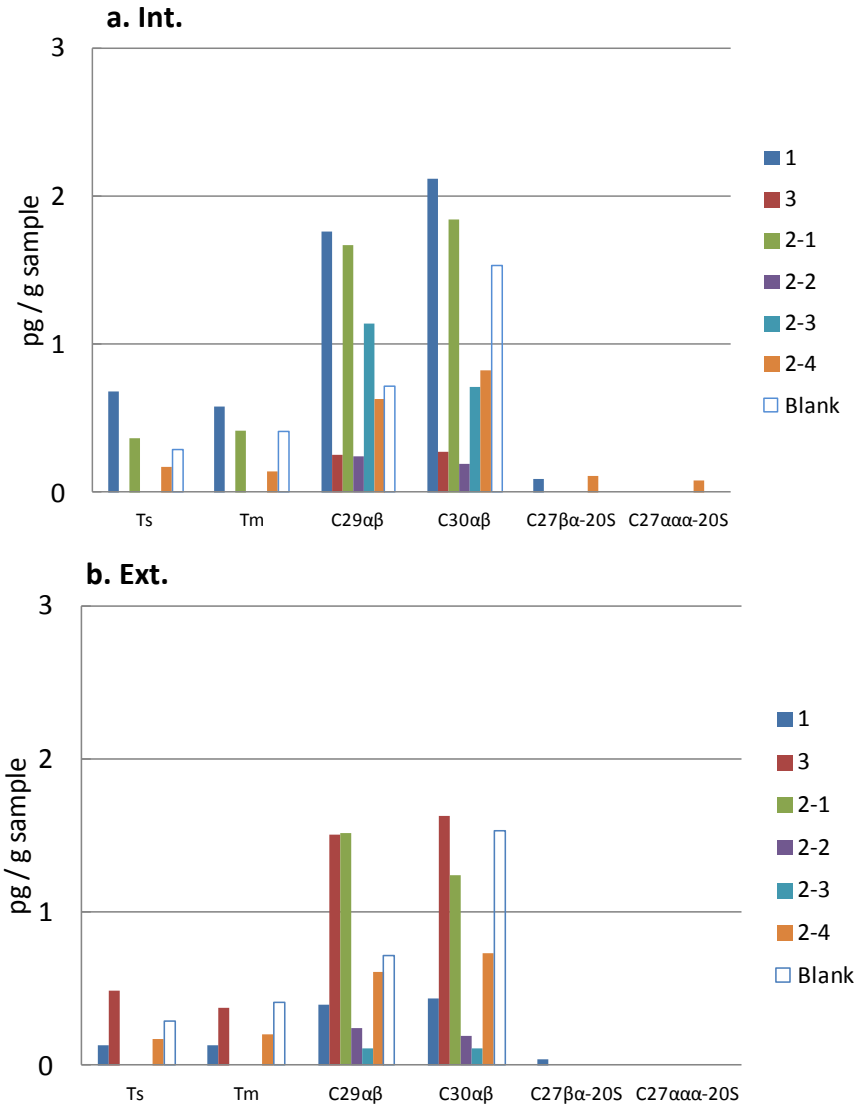

Figure 5.7. Selected hopane and sterane amounts in the Int. (a) and the Ext. (b) fractions of all samples and the blank. **Ts** = 18α(H)-22,29,30-Trisnorneohopane; **Tm** = 17α(H)-22,29,30-Trisnorhopane; **C_{29}αβ** = 17α(H), 21β(H)-29-Norhopane; **C_{30}αβ** = 17α(H), 21β(H)-Hopane; **C_{27}βα-20S** = 13β(H), 17α(H)-Diacholestane (20S); **C_{27}ααα-20S** = 5α(H), 14α(H), 17α(H)-Cholestane (20S).

5.4.1.6. Summary of aliphatic HCs

The <C_{18} *n*-alkanes in samples 1, 3, 2-1 and 2-3 appear to be indigenous, whereas any >C_{19} *n*-alkanes are probably contamination. These four samples have an elevated abundance of *n*-$C_{16\text{-}18}$ with an even-over-odd preference. The abundance of MMAs is generally proportional to that of the *n*-alkanes, indicating a common origin of MMAs with the *n*-alkanes. The regular isoprenoids from *i*-$C_{15\text{-}}$

$_{20}$ also appear to be indigenous in samples 1, 3, 2-1 and 2-3. Sample 1 (AIDP-1) has a relatively high Pr/Ph ratio, and a relatively low Pr/*n*-C_{17} and Ph/*n*-C_{18} values, and suggests a different origin of aliphatic HCs from the other samples (AIDP-2 and 3). Sample 2-3 Ext. may be a mixture of indigenous HCs and experimental contamination. Sample 2-1 has a lower abundance of aliphatic HCs in the Int. fraction than the Ext. fraction, but they are probably both indigenous. Diamondoids were only detected in the AIDP-2 samples, and are considered to be indigenous. The origin of the diamondoids may be different from the other aliphatic HCs for all the AIDP-2 samples. A high thermal maturity is suggested for all AIDP-2 samples based on the diamondoid distribution. The amount of aliphatic HCs in samples 2-2 and 2-4 are below the procedural blank level, except for the diamondoids. Although trace amount of hopanes and steranes were detected in some samples, but they are probably all experimental contamination.

5.4.2. Aromatic HCs

Various aromatic HCs were detected in all samples and fractions including naphthalene (N), phenanthrene (P), biphenyl (BP), fluorene (F), and their alkylated HCs (0.01-394 ng / g sample; Figs 5.8 and 5.9), with the exception of sample 2-3 Ext. fraction which only contains naphthalene. Polycyclic aromatic hydrocarbons (PAHs) with four rings (fluoranthene, pyrene and chrysene) were also detected (0.01-0.34 ng / g sample; Fig. 5.10). The procedural blank contains some parent aromatic HCs, and no alkylated HCs, except for some alkylated naphthalenes (0.03-0.33 ng / g sample; Figs 5.8 and 5.9). There is generally no difference in the abundance of aromatic HCs for the Int. and Ext. fractions, except for sample 2-1, in which aromatic HCs are more abundant in the Ext. (x2) fractions than in the Int. fraction (Fig. 5.9). However, the relative distribution pattern is the same between the Int. and Ext. fractions, as is also the case for aliphatic HCs in sample 2-1. Thus, the aromatic HCs in sample 2-1 are interpreted as being probably indigenous. In addition, sample 2-1 contains the largest amount of parent aromatic HCs (up to 158ng / g sample in the Int. fraction, and 394 ng / g sample in the Ext. fraction) compared to the other samples (up to 29.6 ng / g sample).

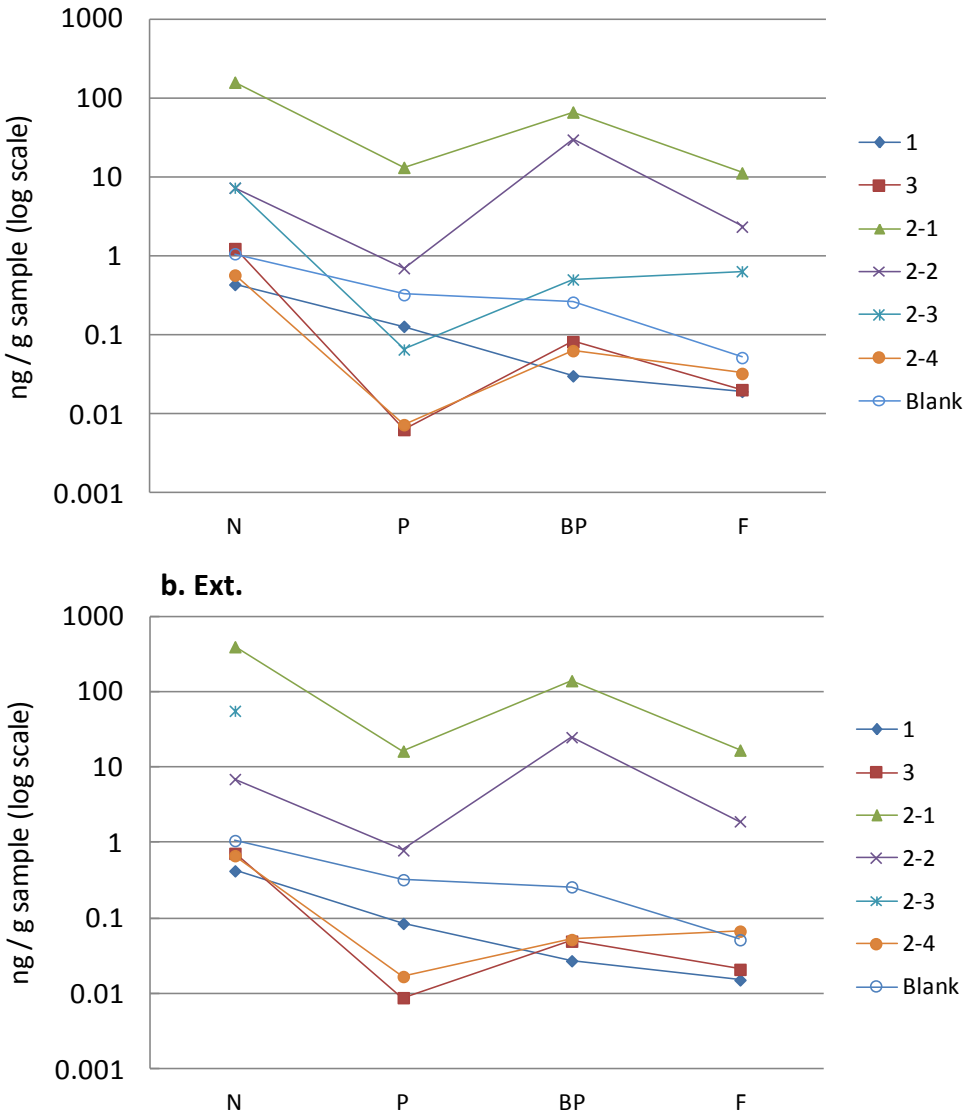

Figure 5.8. Abundance of parent aromatic compounds in the Int. (a) and the Ext. (b) fractions of all samples and the blank. **N** = Naphthalene; **P** = Phenanthrene; **BP** = Biphenyl; **F** = Fluorene.

The abundance of four parent aromatic HCs (N, P, BP and F) in the Int. and Ext. fractions of samples 2-1, 2-2 and 2-3 (all AIDP-2 samples) is higher than that of the procedural blank (Fig. 5.8). In contrast, samples 1 and 3 have a lower abundance of N, P, BP and F than the blank, unlike the higher abundance of some aliphatic HCs than the blank in these samples. Sample 2-4 has a lower abundance of N, P, BP and F than the blank, which coincides with the low abundance of aliphatic HCs in sample 2-4. Sample 1 has a distribution pattern similar to the blank (N > P > BP > F). In contrast, the other five samples have a different pattern, where P is the least abundant compound. N is the most abundant HC in all samples, except for sample 2-2 in which BP is the most abundant. The parent

aromatic HCs in samples 2-1 and 2-2 are particularly abundant compared to the alkylated aromatic HCs (see the N/Σ MN, P/Σ MP, BP/Σ MBP, and F/Σ MF ratios in Table 5.4).

The abundance of alkylated naphthalenes in samples 2-1, 2-2 and 2-3 is generally higher than that of the procedural blank (Fig. 5.9). As no other alkylated aromatic HCs were detected in the procedural blank, the alkylated phenanthrenes, biphenyls and fluorenes may be indigenous in all the samples, including in samples 1, 3, and 2-4 in which the abundance of N, P, BP and F is lower than the procedural blank. Sample 2-1 contains the most aromatic HCs of the sample set. The Int. fraction of sample 2-3 is richer in alkylnaphthalenes than sample 2-1 (Fig. 5.9c), but no similar trend is seen for the other aromatic HCs, and the abundance of aromatic HCs is generally in the order: 2-1 > 2-2 > 2-3. The abundance of alkylated aromatic HCs in samples 1, 3 and 2-4 is low compared to that of samples 2-1, 2-2 and 2-3 (Fig. 5.9). No methylphenanthrenes were detected in fraction 2-4 Ext. and sample 3 (both Int. and Ext. fractions), and no aromatic HCs were detected in sample 2-3 Ext. fraction, except for naphthalene.

Three aromatic hydrocarbon thermal maturity parameters were calculated for all samples: the methylphenanthrene index 1 (MPI-1), the methylphenanthrene distribution fraction (MPDF), and methylnaphthalene ratio (MNR) (Table 5.4). These thermal maturity parameters generally suggest a high thermal maturity for all samples. Samples 2-1 and 2-2 in particular have a very high thermal maturity based on MPI-1 (R_c >2.2) (calculated from Radke and Welte, 1983; Table 5.4).

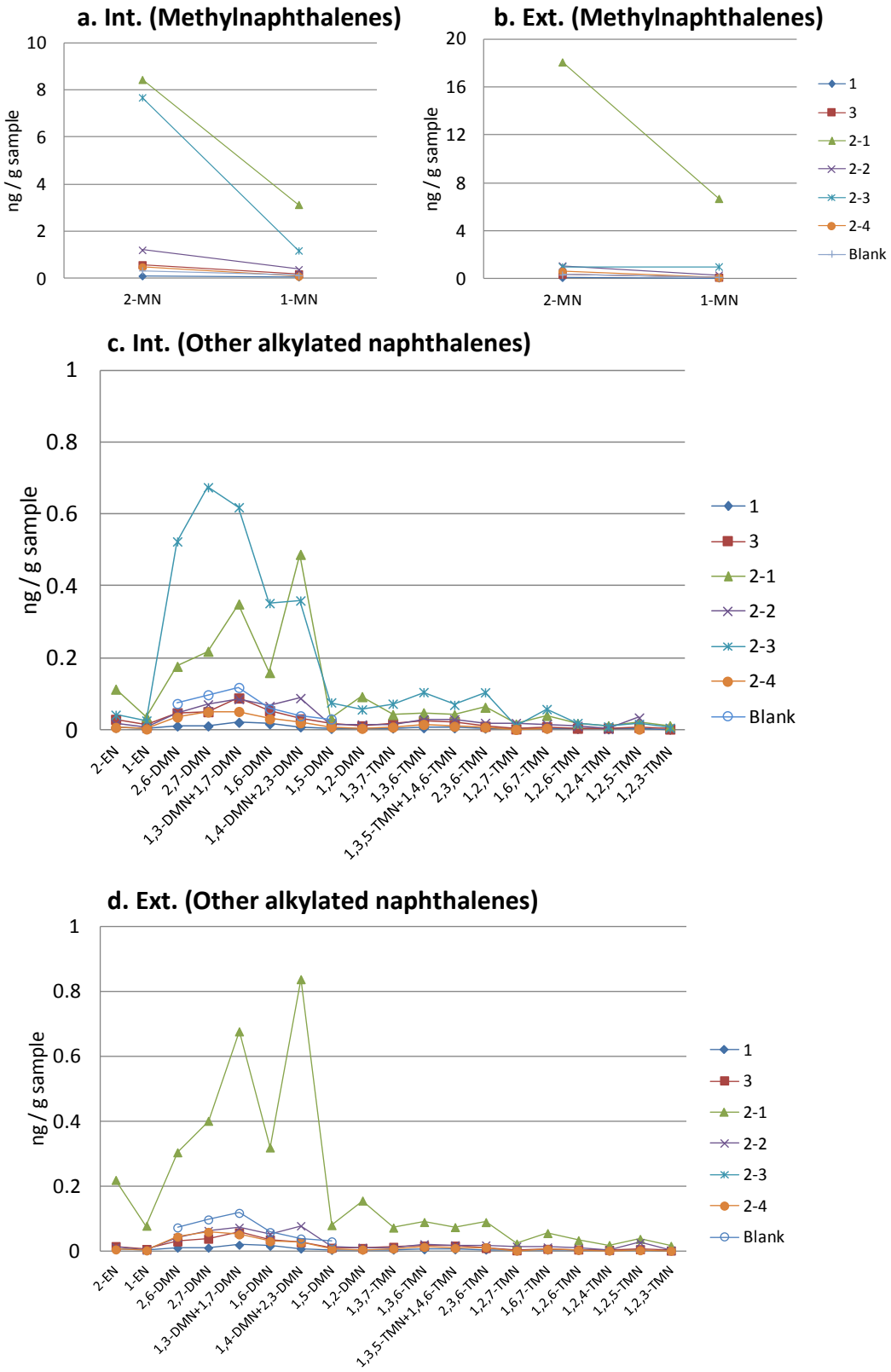

Figure 5.9. Methylnaphthalenes in the Int. (a) and the Ext. (b) fractions, and other alkylated naphthalenes in the Int. (c) and the Ext. (d) fractions of all samples and the blank. **MN** = Methylnaphthalene; **EN** = Ethylnaphthalene; **DMN** = Dimethylnaphthalene; **TMN** = Trimethylnaphthalene.

Table 5.4. Aromatic thermal maturity parameters.

		1	3	2-1	2-2	2-3	2-4	Blank	McManus 1
MPI-1	Ext.	0.25	-	0.02	0.08	-	-	-	-
	Int.	0.26	-	0.02	0.09	0.28	0.68	-	1.6
R_c	Ext.	2.2	-	2.3	2.3	-	-	-	-
	Int.	2.1	-	2.3	2.3	2.2	1.9	-	1.34
MPDF	Ext.	0.60	-	0.55	0.61	-	-	-	-
	Int.	0.59	-	0.55	0.61	0.6	0.63	-	0.67
F/P	Ext.	0.18	2.4	1.03	2.4	-	4.0	-	-
	Int.	0.15	3.2	0.85	3.3	9.8	4.5	-	-
P/Σ MP	Ext.	2.3	-	28.4	8.0	-	-	-	-
	Int.	2.1	-	29.6	6.9	1.9	0.72	-	-
MPR	Ext.	1.9	-	1.40	1.8	-	-	-	
	Int.	1.9	-	1.44	1.6	1.4	1.8	-	2.9
N/Σ MN	Ext.	3.0	1.5	15.9	5.0	-	0.98	-	-
	Int.	2.8	1.6	13.7	4.6	0.82	1.02	2.3	-
MNR	Ext.	2.0	3.1	2.70	3.4	-	7.2	-	
	Int.	1.8	3.1	2.70	3.2	6.5	6.0	2.6	2.2
DNR-1	Ext.	6.3	6.7	8.9	8.2	-	15.3	-	-
	Int.	6.3	5.9	12.9	8.4	15.8	11.1	5.7	8.0
TNR-2	Ext.	0.84	0.66	0.99	0.71	-	0.88	-	
	Int.	0.85	0.55	1.18	0.54	1.02	0.58	-	1.00
BP/Σ MBP	Ext.	0.82	1.47	21.9	13.0	-	1.40	-	-
	Int.	0.90	1.9	19.8	12.0	1.5	1.27	-	-
F/Σ MF	Ext.	1.33	1.5	8.5	5.8	-	1.41	-	-
	Int.	1.29	1.15	8.5	6.8	2.1	1.43	-	-

MPI-1 = methylphenanthrene index 1, = 1.5 x (3-MP + 2-MP) / (P + 9-MP + 1-MP) ; $\boldsymbol{R_c}$ = Calculated vitrinite reflectance from MPI-1, = -0.60 x MPI-1 + 2.30; **MPDF** = Methylphenanthrene distribution fraction = (3-MP + 2-MP) / Σ MP, ; **MPR** = Methylphenanthrene ratio, = 2-MP / 1-MPe; **MNR** = Methylnaphthalene ratio = 2-MN / 1-MN ; **DNR-1** = Dimethylnaphthalene ratio 1, = (2,6-DMN + 2,7-DMN) / 1,5-DMN; **TNR-2** = Trimethylnaphthalene ratio 2, = (2,3,6-TMN + 1,3,7-TMN) / (1,4,6-TMN + 1,3,5-TMN + 1,3,6-TMN). See Figure 5.7 and 5.8 for the abbreviations of N, P, BP, F, MN, MP, DMN, and TMN. McManus 1 is from the Mesoproterozoic Velkerri Member in the McArthur Basin in Australia (George and Ahmed, 2002).

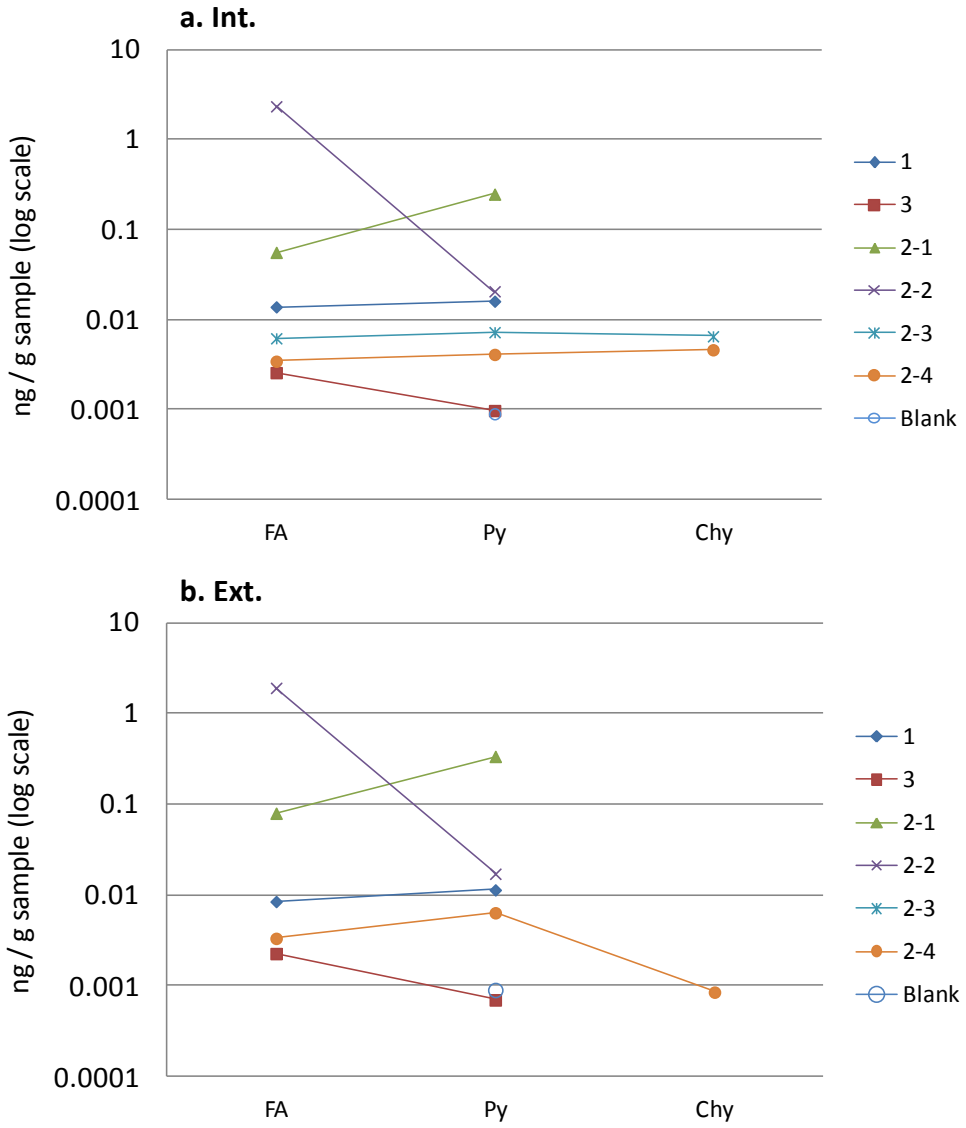

Figure 5.10. Abundance of high molecular weight PAHs in the Int. (a) and the Ext. (b) fractions of all samples and the blank. **FA** = Fluoranthene; **Py** = Pyrene; **Chy** = Chrysene.

Aromatic parameters from the Mesoproterozoic Velkerri Member in the McArthur Basin in Australia (McManus 1) that was reported as highly thermally mature, corresponding to the peak to late oil generation window (George and Ahmed, 2002), are shown in Table 5.4 for comparison. The DNR-1 is interpreted as indicating a high thermal maturity for the AIDP-2 samples, but not for the AIDP-1 and 3 samples. The DNR-1 values for the AIDP-2 samples are much higher than the blank, but those for the AIDP-1 and 3 samples are closer to the blank. The TNR-2 values vary depending on samples and the Int./Ext. fractions, and no particular trend was observed. Only the MPR generally shows a rather

low thermal maturity for all samples, and the reason for the difference for MPR compared to the other parameters is unclear.

The high molecular weight PAHs (fluoranthene, pyrene and chrysene), generally have a similar distribution pattern to other aromatic HCs (Fig. 5.10). The abundance of PAHs is almost the same for both the Int. and Ext. fractions. The procedural blank only contains a very small amount of pyrene (Fig. 5.10b). Chrysene was detected only in samples 2-3 and 2-4. Sample 2-1, 2-2 and 2-3 (all AIDP-2 samples) have a higher abundance of fluoranthene and pyrene than the procedural blank level and samples 3 and 2-4, as is the case for other aromatic HCs. However, sample 1 also has a higher abundance of fluoranthene and pyrene than the procedural blank and samples 3 and 2-4, which is unlike the case for the other aromatic HCs in which they are below the blank level in sample 1. This may indicate that the high molecular weight PAHs in sample 1 are indigenous, and their origin is different from other aromatic HCs.

5.4.2.1. Summary of aromatic HCs

The detected aromatic HCs in three of the AIDP-2 samples (2-1, 2-2 and 2-3) are interpreted to be indigenous. Although some alkylated aromatic HCs in the AIDP-1, 3 and 2-4 samples may also be indigenous, their abundance is always lower than that of the other three AIDP-2 samples. High molecular weight PAHs with four rings in sample 1 may also be indigenous. Most aromatic parameters suggest a high thermal maturity for all the samples, which is consistent with the high thermal maturity derived from the diamondoid distributions.

5.5. Discussion

5.5.1. Indigenous HC composition in the drill cores

The HC compositions of the three drill cores (AIDP-1, 2 and 3) are different from each other. AIDP-1 is a dolerite sample that was originally collected as a negative control, but this work shows that it contains some aliphatic HCs and various aromatic HCs. One possibility is that the HCs in AIDP-1 may have been introduced during the formation of quartz veins. Commonly occurred silicate and

carbonate veins in crustal rocks form via the "crack-seal" process (Ramsay, 1980). The cracking is the opening of a fluid-filled crack, and the sealing corresponds to the mineral precipitation. Organic matter can be deposited in the crack through fluid-rock interactions (Sracek and Zacharias, 2009).

AIDP-1 (sample 1) and 3 (sample 3) are richer in aliphatic HCs than aromatic HCs, but do not contain any diamondoids (Table 5.5). In contrast, the AIDP-2 core (samples 2-1 to 2-4) is richer in aromatic HCs than aliphatic HCs, and contains diamondoids (Table 5.5). Thus, the origin of the HCs in AIDP-2 is considered to be different from that in AIDP-1 and 3. The AIDP-1 and 3 cores have a similar aliphatic HC composition to each other compared to the AIDP-2 cores, but have different aliphatic parameters (Table 5.2) and aromatic parameters (Table 5.4), suggesting a different HC input history to each of these.

Table 5.5. Summary of possibly indigenous HCs in the AIDP cores. "Yes" means the detected HCs are interpreted to be indigenous. An empty space means absent or below the contamination level.

	AIDP-1	AIDP-3	AIDP-2			
	1	3	2-1	2-2	2-3	2-4
n-Alkanes	$<C_{18}$	$<C_{18}$	$<C_{18}$		$<C_{18}$	
MMAs	$C_{16\text{-}19}$	$C_{16\text{-}19}$	$C_{16\text{-}19}$		?	
Regular isoprenoids	*i*-$C_{15\text{-}20}$	*i*-$C_{15\text{-}20}$	*i*-$C_{15\text{-}20}$		*i*-$C_{15\text{-}20}$	
Diamondoids	Absent	Absent	Yes	Yes	Yes	Yes
Aromatic HCs	Partially yes	Partially yes	Yes	Yes	Yes	Partially yes

Table 5.6. Calculated peak temperatures for the AIDP-2 cores, and McManus 1 sample for a comparison (George and Ahmed, 2002). MaxT = (ln (R_c) + 1.78) / 0.0124 (Wang et al., 2005).

		MAI	MDI	MPI-1	MPI-1 (McManus 1)
Min.	R_c (%)	1.3	1.4	1.9	1.3
	MaxT (°C)	165	171	195	165
Max.	R_c (%)	1.9	1.9	2.3	-
	MaxT (°C)	195	195	211	-

The detected diamondoids and aromatic HCs in the AIDP-2 samples indicate a high thermal maturity of the AIDP-2 core (Tables 5.3 and 5.4). The calculated peak temperatures (MaxT) of the AIDP-2 samples range from 165-211 °C (R_c = 1.3-1.9) based on the calculated vitrinite reflectance (Wang et al., 2005) (Table 5.6), which is consistent with the prehnite-pumpellyite facies metamorphism (175-280 °C) that the Fortescue Group rocks are thought to have experienced (Smith et al., 1982). The parent/alkylated aromatic HC ratios (N/Σ MN, P/Σ MP, BP/Σ MBP, and F/Σ MF) are generally high (>1), and are also consistent with the suggested high thermal maturity (Table 5.4). The thermal maturity is higher than the most mature McManus I samples from the Mesoproterozoic Velkerri Member in the McArthur Basin in Australia (Tables 5.4 and 5.6), which was reported as highly thermally mature, corresponding to the peak to late oil generation window (George and Ahmed, 2002).

There is also a difference in the composition and the thermal history between the AIDP-2 samples. Samples 2-1 and 2-2 have a high abundance of parent aromatic HCs (Fig. 5.8), and therefore have a higher value of the parent/alkylated HC ratio compared to samples 2-3 and 2-4 (Table 5.4), suggesting a higher thermal maturity of sample 2-1 and 2-2 than sample 2-3 and 2-4. The R_c calculated from MPI-1 also indicates a higher thermal maturity of samples 2-1 and 2-2 than samples 2-3 and 2-4 (Table 5.4). Similarly, the diamondoids are much more abundant in samples 2-1 and 2-2 than samples 2-3 and 2-4 (Fig. 5.6), and the MAI and MDI of samples 2-1 and 2-2 are slightly higher on average than those of samples 2-3 and 2-4 (Table 5.3). Samples 2-1 and 2-2 come from the Carawine Dolomite in the Hamersley Formation, whereas samples 2-3 and 2-4 come from the Jeerinah Formation in the Fortescue Group. The difference in thermal maturity may reflect a different preservational history for these two groups of samples.

The even-over-odd preference of *n*-C_{16} and *n*-C_{18} over *n*-C_{17} in samples 1, 3, 2-1 and 2-3 is a clear characteristic of some samples (Fig. 5.3), and may indicate a certain biological input, but a specific origin is not clear. Most samples have no particular trend of MMA distribution, but only sample 2-2 Ext. fraction has a higher abundance of 2- and 3-MHeD than other isomers (Fig. 5.4b), which may indicate a bacterial input as 2- and 3-MHeD are common lipid membrane components of bacteria

(Fulco, 1983), and are found in some Precambrian rocks (Summons, 1987). However, considering its limited distribution in the Ext. fraction in only one sample, this bacterial input is not apparently indigenous organic matter. The lack of any preferential dominance of a specific MMA may be a result of thermal cracking induced by the suggested high thermal maturity. This is consistent with the lack of indigenous *n*-alkanes, except for only a small amount of $<C_{18}$ low molecular weight *n*-alkanes in some samples (Fig. 5.2). The Pr/Ph ratios are equal to or less than 1 for the AIDP-2 and 3 samples, except for samples 2-3 and 2-4 Ext. fractions (Table 5.2), which may indicate an anoxic to suboxic depositional environment for the AIDP-2 and 3 samples (Didyk et al., 1978).

5.5.2. Reliability of previous Archean HC data

Although various aliphatic and aromatic HCs were detected in all the drill cores, only a limited number of compounds have been proven to be indigenous. In this study, contamination level was reduced to pg levels, but the abundance of many of the detected HCs including hopanes and steranes is comparable to that of the procedural blank, and thus it cannot be concluded that they are indigenous. The lack of the complex multi-ring hopanes and steranes is consistent with the level of metamorphism that the samples are known to have experienced.

The results in this study are in sharp contrast to the previously analysed drill core RHDH2A, which reportedly contains hopanes and steranes (Eigenbrode and Freeman, 2006; Eigenbrode et al., 2008). The detected aliphatic and aromatic HCs in the RHDH2A core were enriched in the Ext. fractions, suggesting later migration or contamination during handling (Brocks, 2011). In contrast, the abundance of HCs in the samples analysed in this study is broadly comparable for the Int. and Ext. fractions, and does not show any apparent contamination. In addition, high molecular weight *n*-alkanes (C_{19+}) were typically abundant in previously analysed Archean drill cores (Brocks et al., 1999; Brocks et al., 2003a; Brocks et al., 2003b), whereas these *n*-alkanes were only detected below the procedural blank level in this study. In contrast, the abundance of aromatic HCs and diamondoids in this study is generally the same as previous studies (Brocks et al., 2003a; Brocks et al., 2003c). These compounds indicate a similar high thermal maturity of the drill cores both in this study and the

previous studies. Therefore, the aromatic HCs and diamondoids found in the previous studies may be indigenous compounds.

5.6. Conclusions

Newly collected Archean drill cores AIDP-1, 2 and 3 were analysed to establish whether they contain indigenous HCs. Many of the detected HCs were considered to be experimental contamination, but some aliphatic and aromatic HCs were interpreted to be indigenous, including *n*-alkanes, MMAs, regular isoprenoids, diamondoids, and aromatic HCs with two to four rings. Hopanes and steranes were not detected above the experimental contamination level. There is mostly no appreciable difference in the HC abundance between the exterior and the interior of the samples, indicating that the drilling procedure was sufficiently clean. In contrast, the previously studied RHDH2A cores showed a heterogeneous distribution of HCs enriched in the sample surfaces, suggesting contamination during drilling and/or storage.

The HC composition is different between the three AIDP cores. The AIDP-1 and 3 cores are generally richer in aliphatic HCs than aromatic HCs, whereas the AIDP-2 core samples are richer in aromatic HCs than aliphatic HCs. The HC composition of AIDP-1 and 3 cores is also different from each other according to several aliphatic and aromatic parameters. These differences may reflect a different depositional setting, different host organism ecosystem, and/or different preservational environment. Indeed, although the dolerite sample (AIDP-1) was collected as a negative control, it is revealed to contain some aliphatic and aromatic HCs, and these may reside in the observed veins. These HCs may have migrated during vein formation by fluid-rock interaction after the initial rock formation. A high thermal maturity of AIDP-2 cores around the late oil generation window or beyond is indicated based on the diamondoid and aromatic HC thermal maturity parameters, which is consistent with the prehnite-pumpellyite facies metamorphism that the Fortescue Group experienced.

5.7. Acknowledgements

The AIDP drilling project is supported by the Agouron Institute. Y.H. and C.P. are supported by Macquarie University Research Excellence Scholarships. S.C.G. acknowledges the Australian Research Council for a Discovery Grant. We thank Gordon Love, Roger Summons, Roger Buick, Jochen Brocks, Christian Hallmann, Kate French, for constructive discussions about interpretation of the hydrocarbon distributions in the AIDP cores. We also thank the Commonwealth Scientific and Industrial Research Organisation and the Australian National University for some of the GC-MS analysis.

5.8. References

Anbar, A.D., Duan, Y., Lyons, T.W., Arnold, G.L., Kendall, B., Creaser, R.A., Kaufman, A.J., Gordon, G.W., Scott, C., Garvin, J. and Buick, R. (2007) A whiff of oxygen before the Great Oxidation Event? Science 317, 1903-1906.

Arndt, N.T., Nelson, D.R., Compston, W., Trendall, A.F. and Thorne, A.M. (1991) The age of the Fortescue Group, Hamersley Basin, Western Australia, from ion microprobe zircon U-Pb results. Australian Journal of Earth Sciences 38, 261-281.

Awramik, S.M. and Buchheim, H.P. (2009) A giant, Late Archean lake system: The Meentheena Member (Tumbiana Formation; Fortescue Group), Western Australia. Precambrian Research 174, 215-240.

Barley, M.E., Pickard, A.L. and Sylvester, P.J. (1997) Emplacement of a large igneous province as a possible cause of banded iron formation 2.45 billion years ago. Nature 385, 55-58.

Brocks, J.J. (2001) Molecular Fossils in Archean Rocks. Ph.D. dissertation, University of Sydney.

Brocks, J.J. (2011) Millimeter-scale concentration gradients of hydrocarbons in Archean shales: Live-oil escape or fingerprint of contamination? Geochimica Et Cosmochimica Acta 75, 3196-3213.

Brocks, J.J., Buick, R., Logan, G.A. and Summons, R.E. (2003a) Composition and syngeneity of molecular fossils from the 2.78 to 2.45 billion-year-old Mount Bruce Supergroup, Pilbara Craton, Western Australia. Geochimica Et Cosmochimica Acta 67, 4289-4319.

Brocks, J.J., Buick, R., Summons, R.E. and Logan, G.A. (2003b) A reconstruction of Archean biological diversity based on molecular fossils from the 2.78 to 2.45 billion-year-old Mount Bruce Supergroup, Hamersley Basin, Western Australia. Geochimica Et Cosmochimica Acta 67, 4321-4335.

Brocks, J.J., Logan, G.A., Buick, R. and Summons, R.E. (1999) Archean molecular fossils and the early rise of eukaryotes. Science 285, 1033-1036.

Brocks, J.J., Summons, R.E., Buick, R. and Logan, G.A. (2003c) Origin and significance of aromatic hydrocarbons in giant iron ore deposits of the late Archean Hamersley Basin, Western Australia. Organic Geochemistry 34, 1161-1175.

Brooks, J.D., Gould, K. and Smith, J.W. (1969) Isoprenoid Hydrocarbons in Coal and Petroleum. Nature 222, 257-259.

Chen, J., Fu, J., Sheng, G., Liu, D. and Zhang, J. (1996) Diamondoid hydrocarbon ratios: novel maturity indices for highly mature crude oils. Organic Geochemistry 25, 179-190.

Coffey, J.M., Flannery, D.T., Walter, M.R. and George, S.C. (2013) Sedimentology, stratigraphy and geochemistry of a stromatolite biofacies in the 2.72Ga Tumbiana Formation, Fortescue Group, Western Australia. Precambrian Research 236, 282-296.

Didyk, B.M., Simoneit, B.R.T., Brassell, S.C. and Eglinton, G. (1978) Organic geochemical indicators of palaeoenvironmental conditions of sedimentation. Nature 272, 216-222.

Eigenbrode, J.L. and Freeman, K.H. (2006) Late Archean rise of aerobic microbial ecosystems. Proceedings of the National Academy of Sciences 103, 15759-15764.

Eigenbrode, J.L., Freeman, K.H. and Summons, R.E. (2008) Methylhopane biomarker hydrocarbons in Hamersley Province sediments provide evidence for Neoarchean aerobiosis. Earth and Planetary Science Letters 273, 323-331.

French, K.L., Hallman, C., Hope, J.M., Buick, R., Brocks, J.J. and Summons, R.E. (2013) Archean hydrocarbon biomarkers: Archean or not?, Goldschmidt 2013 Conference Abstract.

French, K.L., Hallmann, C., Hope, J.M., Hoshino, Y., Peters, C., George, S.C., Buick, R., Brocks, J.J. and Summons, R.E. (*in prep*) Archean hydrocarbon biomarkers: Indigenous or not? Proceedings of National Academy of Science USA.

Fulco, A. (1983) Fatty acid metabolism in bacteria. Progress in Lipid Research 22, 133-160.

George, S. and Ahmed, M. (2002) Use of aromatic compound distributions to evaluate organic maturity of the Proterozoic middle Velkerri Formation, McArthur Basin, Australia. The Sedimentary Basins of Western Australia III: Proceedings of the West Australasian Basins Symposium (WABS) III.

Holland, H.D. (2002) Volcanic gases, black smokers, and the great oxidation event. Geochimica Et Cosmochimica Acta 66, 3811-3826.

Kojan, C.J. and Hickman, A.H. (1998) Late Archaean volcanism in the Kylena and Maddina Formations, Fortescue Group, west Pilbara. Western Australia Geological Survey, Annual Review 1997–98, 43-53.

Kopp, R.E., Kirschvink, J.L., Hilburn, I.A. and Nash, C.Z. (2005) The Paleoproterozoic snowball Earth; a climate disaster triggered by the evolution of oxygenic photosynthesis. Proceedings of the National Academy of Sciences of the United States of America 102, 11131-11136.

Lyons, T., Reinhard, C. and Planavsky, N. (2014) The rise of oxygen in Earth's early ocean and atmosphere. Nature 506, 307-315.

Nelson, D.R., Trendall, A.F. and Altermann, W. (1999) Chronological correlations between the Pilbara and Kaapvaal cratons. Precambrian Research 97, 165-189.

Planavsky, N.J., Asael, D., Hofmann, A., Reinhard, C.T., Lalonde, S.V., Knudsen, A., Wang, X., Ossa, F.O., Pecoits, E., Smith, A.J.B., Beukes, N.J., Bekker, A., Johnson, T.M., Konhauser, K.O., Lyons, T.W. and Rouxel, O.J. (2014) Evidence for oxygenic photosynthesis half a billion years before the Great Oxidation Event. Nature Geoscience 7, 283-286.

Powell, T.G. and McKirdy, D.M. (1973) Relationship between Ratio of Pristane to Phytane, Crude Oil Composition and Geological Environment in Australia. Nature Physical Science 243, 37-39.

Radke, M. and Welte, D. (1983) The Methylphenanthrene index (MPI). A Maturity parameter based on aromatic hydrocarbons, in: Bjorøy, M., Albrecht, C., Cornford, C. (Eds.), Advances in Organic Geochemistry. John Wiley & Sons, New York, pp. 504-512.

Ramsay, J.G. (1980) The crack-seal mechanism of rock deformation. Nature 284, 135-139.

Rasmussen, B., Fletcher, I.R., Brocks, J.J. and Kilburn, M.R. (2008) Reassessing the first appearance of eukaryotes and cyanobacteria. Nature 455, 1101-1104.

Sakurai, R., Ito, M., Ueno, Y., Kitajima, K. and Maruyama, S. (2005) Facies architecture and sequence-stratigraphic features of the Tumbiana Formation in the Pilbara Craton, northwestern Australia; implications for depositional environments of oxygenic stromatolites during the late Archean. Precambrian Research 138, 255-273.

Schinteie, R. and Brocks, J. (2014) Evidence for ancient halophiles? Testing biomarker syngeneity of evaporites from Neoproterozoic and Cambrian strata. Organic Geochemistry 72, 46-58.

Sherman, L.S., Waldbauer, J.R. and Summons, R.E. (2007) Improved methods for isolating and validating indigenous biomarkers in Precambrian rocks. Organic Geochemistry 38, 1987-2000.

Smith, R.E., Perdrix, J.L. and Parks, T.C. (1982) Burial Metamorphism in the Hamersley Basin, Western Australia. Journal of Petrology 23, 75-102.

Sracek, O. and Zacharias, J. (2009) Fluids in geological processes, in: Cilek, V., Smith, R.H. (Eds.), Earth system: history and natural variability. Eolss, pp. 439-457.

Summons, R.E. (1987) Branched alkanes from ancient and modern sediments: Isomer discrimination by GC/MS with multiple reaction monitoring. Organic Geochemistry 11, 281-289.

Thorne, A.M. and Trendall, A.F. (2001) Geology of the Fortescue Group, Pilbara Craton, Western Australia. Bulletin - Geological Survey of Western Australia, 249.

Trendall, A.F., Compston, W., Nelson, D.R., Laeter, J.R.D. and Bennett, V.C. (2004) SHRIMP zircon ages constraining the depositional chronology of the Hamersley Group, Western Australia*. Australian Journal of Earth Sciences 51, 621-644.

Waldbauer, J.R., Newman, D.K. and Summons, R.E. (2011) Microaerobic steroid biosynthesis and the molecular fossil record of Archean life. Proceedings of the National Academy of Sciences 108, 13409-13414.

Walter, M. (1983) Archean stromatolites: Evidence of the Earth's earliest benthos, in: Schopf, J. (Ed.), Earth's Earliest Biosphere: It's Origin and Evolution. Princeton University Press, Princeton, pp. 187-213.

Wang, W., Zhou, Z.-Y. and Yu, P. (2005) Relations Between Vitrinite Reflectance, Peek Temperature and its Neighboring Temperature Variation Rate: A Comparison of Methods. Chinese Journal of Geophysics 48, 1443-1453.

Zhang, S., Huang, H., Xiao, Z. and Liang, D. (2005) Geochemistry of Palaeozoic marine petroleum from the Tarim Basin, NW China. Part 2: Maturity assessment. Organic Geochemistry 36, 1215-1225.

Chapter 6.

Cyanobacterial inhabitation on Archean rock surfaces in the Pilbara Craton, Western Australia

Y. Hoshino [1,2], S. C. George [1,2]

[1] *Department of Earth and Planetary Sciences, Macquarie University, Sydney, Australia*

[2] *Australian Centre for Astrobiology, University of New South Wales, Australia*

Statement of authors' contribution

This Chapter is a provisionally accepted article in *Astrobiology*, with some minor revisions. This paper has been formatted to conform to the font and referencing style adopted in this thesis. Figures and tables included within the text are prefixed with the chapter number.

I am the primary author (95% of the effort). I collected the samples with the help of David Flannery (University of New South Wales, Australia). I examined the samples, including sample cutting, grinding, and solvent extraction. I performed gas chromatography-mass spectroscopy. I processed and interpreted all the data derived from the measurements. I processed and designed the structure of the paper. The co-author carefully reviewed and provided feedback and valuable refinements on the final version of the manuscript, and approved it for the submission (5%). Neither this manuscript nor one with similar content under our authorship has been published nor is being considered for publication elsewhere, except as described above.

Final publication is available from Mary Ann Liebert, Inc., publishers https://doi.org/10.1089/ast.2014.1275

Abstract

A high abundance of 7- and 6-monomethylalkanes as well as C_{17} *n*-alkane, indicative of cyanobacteria, has been discovered on the surfaces of Archean carbonate rocks of the Fortescue Group in the Pilbara region, Western Australia. The presence of cyanobacterial biomarkers is mostly limited to the surface layer (< 1 cm thickness) of the rocks, indicating that the cyanobacteria are an endolithic species. Biomarkers are found in bitumen I (solvent-extracted rock) and also in bitumen II (solvent-extracted decarbonated rock), and the abundance of biomarkers is generally the same between both bitumen fractions in the surface layer, indicating that the cyanobacteria penetrated into the carbonate minerals. A trace amount of the biomarkers also diffuses into a deeper part of the rocks, but this influence is only seen in bitumen I. This indicates that hydrocarbons move towards the inside of the rock through pores and fissures in the rock fabric. In contrast, hydrocarbons in bitumen II, which mainly come from within the carbonate minerals, are isolated from the hydrocarbon migration from the outside of the rock, and may be ancient indigenous organic matter. To the best of our knowledge, this is the first report of the past or modern inhabitation of cyanobacteria on Archean rocks in the Pilbara region, using hydrocarbon biomarker analyses. The finding proves that the combination of the slice experiments and the two consecutive solvent extractions performed in this study is an effective method to distinguish modern or recent input from indigenous hydrocarbons.

6.1. Introduction

Cyanobacteria are of importance in the study of the early evolution of life on Earth. They are considered to have biologically produced molecular oxygen for the first time on Earth by oxygenic photosynthesis, which drastically changed the evolutionary direction of life towards aerobiosis (Lyons et al., 2014). The presence of cyanobacteria in ancient times may be detected by biomarker analysis. Biomarkers are hydrocarbons preserved within sedimentary rocks, which may be the direct remains of host organisms, or may be diagenetic products of original organic matter after deposition (e.g. Brocks and Summons, 2003; Grice and Eiserbeck, 2014). Although the evidence for cyanobacteria in the Archean has been suggested by some cyanobacterial biomarkers in Archean rocks (Brocks et al., 1999; Waldbauer et al., 2009), the syngeneity and indigeneity of the detected biomarkers is now called into question (Rasmussen et al., 2008; Brocks, 2011; French et al., 2013). One concern is the later input of cyanobacterial biomarkers over geological time, or during sample handling.

Methods to distinguish indigenous hydrocarbons from later contamination include using various types of slice experiments (Sherman et al., 2007; Brocks, 2011). Recent contamination from the external environment is likely to have a maximum concentration at the surface of the rock in the outer slice, and is expected to decline in concentration towards the inner slices. In contrast, any indigenous organic compounds will be more protected from weathering and alteration processes deep inside the rock. The original concentration of indigenous organic compounds may be retained in the middle of the rock, and would likely reduce towards the outer slices due to partial or complete removal by weathering.

Endolithic species were first described in 1914 (algae; Diels, 1914). Since then, detected microorganisms that inhabit endolithic environments include heterotrophic bacteria, fungi, eukaryotic algae, cyanobacteria and fungal/cyanobacterial symbionts (lichens) (Sigler et al., 2003). Especially cyanobacteria and eukaryotic algae have been reported from almost all endolithic ecosystems (Sigler et al., 2003; de los Ríos et al., 2007). Endoliths are classified into three classes: (i) chasmoendoliths colonise fissures and cracks in the rock; (ii) cryptoendoliths live in structural cavities

within porous rocks; and (iii) euendoliths actively penetrate into the inside of rocks such as carbonates or phosphates (Golubic et al., 1981). Identification of endolithic microorganisms had long been based on their morphologies, but recent extensive developments in molecular biotechnology have enabled molecular biology approaches to the study of endolithic communities (de los Ríos et al., 2007). The habitats of endoliths include extremely arid areas such as the Dry Valleys in Antarctica (de la Torre et al., 2003; Hughes and Lawley, 2003; de los Ríos et al., 2007), and the Atacama desert in Chile (Wierzchos et al., 2006; Dong et al., 2007; Neilson et al., 2012; Patzelt et al., 2014). The endolithic communities are frequently dominated by photoautotrophs, such as green algae and/or cyanobacteria. Typical endolithic cyanobacteria resistant to a harsh environment are some filamentous cyanobaceria, and the unicellular, primitive cyanobacteria genus *Chroococcidiopsis* (Phoenix et al., 2006; Cockell et al., 2008; Patzelt et al., 2014). However, actively boring endolithic cyanobacteria are limited to filamentous species (Zhang and Pratt, 2008). Fossils of endolithic cyanobacteria may date back to the Precambrian era (Zhang and Golubic, 1987; Zhang and Pratt, 2008), although possible evidence for microbial boring itself further dates back to 3.4-3.5 Ga, based on observations of volcanic glass (Furnes et al., 2004; Banerjee et al., 2007; Furnes et al., 2007).

Carbonate rocks are the most common substrates for cyanobacteria to bore into (Cockell and Herrera, 2008), including limestone and dolostone (Campbell, 1983). Sandstone, halite crusts and gypsum have also been reported to harbour endolithic communities (Stivaletta et al., 2010). Although endolithic inhabitation of carbonate rocks is quite common, the mechanisms of carbonate dissolution are poorly understood (Garcia-Pichel, 2006). However, in any case, the dissolution process is not merely an auxiliary result of photosynthesis, but is an active behaviour for survival, with the expense of cellular energy.

The presence of cyanobacteria can be suggested by their characteristic lipid component, mid-chain branched monomethylkanes (MMAs) (Shiea et al., 1990; Schirmer et al., 2010). A culture study of cyanobacteria indicates that the production of mid-chain branched MMAs is considered as universal in the cyanobacterial clade, with exception of several cyanobacterial species which instead produce terminal alkenes (Coates et al., 2014). The major product is 7-methylheptadecane (MHeD), typically

along with a high abundance of the C_{17} *n*-alkane. There are some other organisms which produce 7-MHeD, but the biosynthetic pathways differ from that of cyanobacteria (Gries et al., 1994; Shirai et al., 1999; Qiu et al., 2012). The biosynthetic pathway of 7-MHeD in cyanobacteria seems to be unique to the cyanobacterial clade so far (Coates et al., 2014), and requires molecular oxygen (Li et al., 2011; Li et al., 2012). Previously, 2α-methylhopanes were thought to be exclusive biomarkers for cyanobacteria (Summons et al., 1999), but now it is revealed that many other bacteria have the biosynthetic ability to produce 2α-methylhopanes, and cyanobacteria are only a part of these bacteria (Welander et al., 2010; Ricci et al., 2013). Therefore, the presence of 2α-methylhopanes was not investigated in this study.

Here we report that cyanobacteria have recently thrived on the surfaces of Archean rocks, and have left their biomarkers on the rock surfaces. To quantify indigenous hydrocarbon signals of the Archean era, these recent biomarkers must be carefully discounted. The inhabitation of such endolithic cyanobacteria is limited to within 1 cm from the surfaces. Also, the space within the carbonate minerals was less affected by these inputs and may have preserved indigenous hydrocarbons.

6.2. Geological setting

The Fortescue Group, a volcano-sedimentary succession, is the basal member of the Mount Bruce Supergroup, and overlies Palaeoarchaean granite-greenstone basement rocks of the Pilbara Craton (Fig. 6.1) (Thorne and Trendall, 2001). The Fortescue Group was deposited between 2775 and 2630 Ma during one or more periods of rifting and extensive volcanism (Thorne & Trendall, 2001). The group is predominantly composed of subaerial tholeiitic flood basalts, with subordinate siliciclastic, volcaniclastic and carbonate units. The depositional setting of the Fortescue Group is either a shallow marine environment (e.g. Thorne and Trendall, 2001; Sakurai et al., 2005), or a lacustrine environment (e.g. Walter, 1983; Awramik and Buchheim, 2009; Coffey et al., 2013).

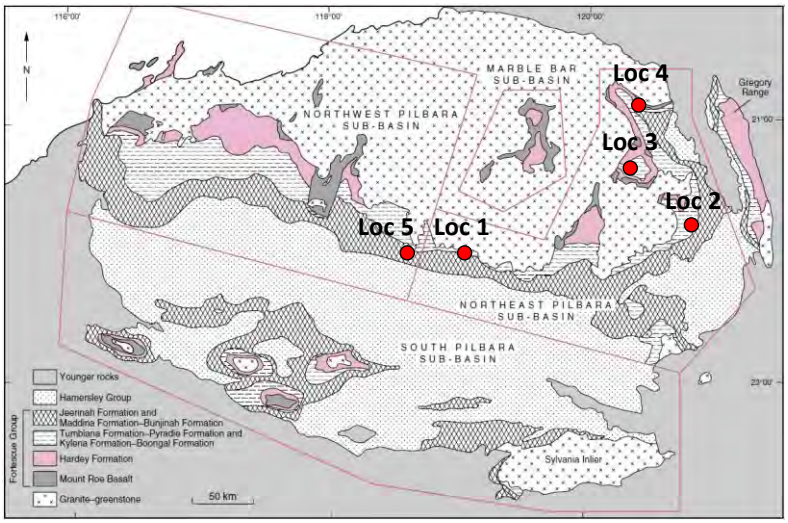

Figure 6.1. Geological map of the Fortescue Group (adapted from Thorne and Trendall, 2001) and the sampling locations of the stromatolite rocks (Locs 1-4) and a basaltic rock (Loc. 5). Locs 1, 3 and 4 are the Tumbiana Formation. Loc. 2 is the Kylena Formation, and Loc. 5 is the Maddina Formation.

The Fortescue Group is well known for broad morphologies of well preserved stromatolite fossils around 2.7-2.8 Ga that are among the oldest Precambrian stromatolites (Flannery and Walter, 2012). Stromatolites are microbially mediated finely laminated rock structures that are typically composed of carbonate minerals (e.g. $CaCO_3$). Modern major stromatolites include those at Shark Bay in Western Australia (Garby et al., 2013), and at the Highborne Cay in Bahamas (Baumgartner et al., 2009). Stromatolites are generally associated with cyanobacteria, because all modern stromatolites are produced by active involvement of cyanobacteria as well as many other microorganisms, including bacteria, archaea and eukaryotes (Allen et al., 2009; Garby et al., 2013; Edgcomb et al., 2014). By analogy, ancient stromatolites were likely produced by cyanobacteria (Walter, 1983). Further, conical stromatolites (*Conophyton*) found in the Fortescue Group have been associated with the presence of cyanobacteria because the phototaxis of cyanobacteria are thought to produce the conical shape (Flannery and Walter, 2012). Thus, the search for cyanobacterial biomarkers in the Fortescue Group stromatolite rocks has been a major topic for understanding the early evolution of life in the Archean.

The rock samples studied in this study were collected from the northeast sub-basin, where stromatolitic carbonate rocks are well preserved, including in three formations; the Tumbiana

Formation (Meentheena Member), the Kylena Formation (Mopoke Member), and the Maddina Formation (Table 6.1). The Tumbiana Formation was deposited between subaerial lava flows of the underlying Kylena and overlying Maddina formations. The Meentheena Member consists of dark, prominently outcropping, stromatolitic limestones and recessive mudstones (Lipple, 1975; Thorne and Hickman, 1998). The Kylena Formation is dominated by subaerial lava flows, with thin layers of carbonate, volcaniclastic and siliciclastic sedimentary rocks (Smithies, 1998). The Maddina Formation is predominantly a unit of subaerial lava flows, but contains stromatolitic carbonates as a minor component (Thorne and Trendall, 2001). Three samples were collected from carbonate units in the Tumbiana Formation, one from the Kylena Formation, and one from a basaltic lava flow from the Maddina Formation. The basalt sample was analysed for cyanobacterial biomarkers, and also as a procedural blank (the deepest part of the rock). One of three Tumbiana Formation samples (from Loc. 1) is shown in Fig. 6.2. The sample contains conically laminated columnar stromatolites.

Table 6.1. Sample list of analysed rocks.

Locality	Formation (Fm)	Lithology
Loc. 1	Tumbiana Fm	Carbonates
Loc. 2	Kylena Fm	Carbonates
Loc. 3	Tumbiana Fm	Carbonates
Loc. 4	Tumbiana Fm	Carbonates
Loc. 5	Maddina Fm	Basalt

6.3. Experimental procedure

6.3.1. Solvents and glassware

Dichloromethane (DCM) (Macron, H485-10) and methanol (MeOH) (Honeywell Burdick & Jackson, GC230-4) (9:1 v/v) were used to extract hydrocarbons from the samples. All solvents were checked for purity by gas chromatography-mass spectroscopy (GC-MS) as described below. All glassware was combusted in an oven at 400 °C for 3 hours before use.

Figure 6.2. Field photograph of one of the investigated localities (Loc. 1), showing the conical stromatolite from the Meentheena Member of the Tumbiana Formation that was sampled. The height of the chisel is about 20 cm.

6.3.2. Sample preparation

The rock samples were sliced using a diamond blade (Diatrenn, D0) from the outside towards the inside, producing approximately 1 cm thick slices. This study focuses on the rock surfaces, so not all slices were analysed. The Loc. 1 and 3 samples were analysed throughout the rocks (four slices for the Loc. 1 sample, and five slices for the Loc. 3 sample). The other two samples (Locs 2 and 4) were only analysed for slices 1 and 2. The Loc. 5 sample (basaltic rock) was analysed for slices 1 and 2, but slice 5 was also tested as a procedural blank. Each slice was then cut into approximately 1 cm^3 pieces. About 100 g of rock pieces were used for the analysis of each slice. The procedural blank was processed first. Between each slice experiment all equipment was washed with filtered water, MeOH and DCM and checked for purity by GC-MS. Fine particles on sample surfaces were removed by ultrasonication in filtered water for 10 min. Organic contamination on surfaces was removed by ultrasonication in a mixture of DCM and MeOH (9:1, v/v) for two cycles of 10 min., with a new solvent mixture each time. The last solvent mixture was analysed by GC-MS for purity and surface checking. If the cleaning was insufficient, additional ultrasonication was performed.

The rock was then ground to < 200 mesh grain size in a ring-mill. The mill was cleaned between samples. Fine particles in the mill were removed by manual scrubbing by a metal brush and water washing. The mill was then repeatedly rinsed with a solvent mixture of the same composition as described above. If the cleaning was insufficient, additional rinsing of the ring-mill was performed.

6.3.3. First solvent extraction (Ext. I)

Extraction of HCs from the rock powder was carried out by ultrasonication with 200 mL of the solvent mixture described above for two cycles of 10 min. Between the sonications, the solution was stirred using a glass rod and left to stand still for a few minutes. The solvent was collected in a round-bottom flask. The powder was further sonicated with a fresh 100 mL aliquot of DCM for 10 min to retrieve organic residues, particularly aliphatic HCs, in the mixed slurry of powder and solvent. The second solvent was added to the first solvent. An instrument such as an Accelerated Solvent Extractor was not used because of the possibility of contamination.

The obtained solution volume was reduced by rotary evaporation to 30-40 mL. The solution was then centrifuged for 3 min at 2,000 rpm to remove suspended rock particles. The volume was then further reduced by rotary evaporation to approximately 5 mL. If the amount of suspended solids was low, the centrifuge step was omitted and the solvent was directly reduced to approximately 5 mL. Even after the centrifuge step, there were still some very fine rock particles suspended in the solvent. These were removed by filtering the solvent/sample mixture through silica gel (silica gel 60, 0.063-0.200 mm, Merck), which was activated at 120 °C for > 4 hours before use. Column fractionation of the extractable organic matter (EOM) was not performed because the yield was very small (< 100 ng / g sample), because the interference between aliphatic and aromatic HCs was not serious, and also to prevent the loss of HCs.

The EOM was spiked with three compounds as internal standards by adding 1 mL of a DCM solution containing about 50 ng of each of: anthracene-d_{10} (98 atom %D, Isotec), p-terphenyl-d_{14} (98 atom %D, Isotec), and tetraeicosane-d_{50} (98 atom %D, Isotec). The volume of solvent containing the EOM was further reduced on a hot plate at 40 °C under a gentle nitrogen flow, until approximately 50 µL remained.

6.3.4. Second solvent extraction (Ext. II)

After the first solvent extraction, the residual rock powder was treated with hydrochloric acid (HCl; 36%, RCI Labscan) to remove the carbonate minerals. 100-150 mL of HCl solution was added to the powder (~100 g) on a hot plate at 70 °C until effervescence stopped. The resultant solution was washed with 500 mL of filtered water six times. The surplus acid-water mixture was discarded and the remaining powder slurry was air dried. Extraction of the decarbonated rock powder was performed as described above for the first extraction. Acid treatment was found to release a large amount of elemental sulphur, which can damage GC-MS instruments and interfere with HC identification and quantification. Thus, elemental sulphur was removed by treatment of the EOM with activated copper. 5 g of copper particles (metal turnings, TG, Chem-Supply) were first treated with 36% HCl to remove CuO surficial layers and any remaining CuS residues from the previous experiment, and then washed with MeOH twice and DCM twice. The activated copper was added to the EOM and stirred for a minute. This simple procedure was enough to remove most sulphur so that reflux of the solution was not performed. Then, the copper particles were removed. The resultant EOM was spiked with standards and prepared for GC-MS using the same procedure as for the first extraction.

6.3.5. Gas Chromatography-Mass Spectroscopy (GC-MS)

GC-MS analysis was carried out on an Agilent GC (6890N) coupled to an Agilent Mass Selective Detector (5975B). 1 µL of the EOM solution was injected into a Programmable Temperature Vaporization (PTV) inlet operating in splitless mode with a J&W DB5MS capillary column (length 60 m, inner diameter 0.25 mm, film thickness 0.25 um). The PTV inlet was ramped from 35 °C (3 min. isothermal) to 310 °C (0.5 min. isothermal) at a rate of 700 °C / min. Helium was used as the carrier gas (1.5 mL / min., constant flow), and the temperature of the GC oven was ramped from 30 °C (2 min. isothermal) to 310 °C (30 min. isothermal) at a rate of 4 °C / min. The MS data were acquired in single ion monitoring (SIM) mode. HC identification was based on comparisons of relative GC retention times and mass spectra with those previously reported. Semi-quantitative analyses were performed using the tetraeicosane-d_{50} internal standard, not taking into account any response factor.

The other two standards were used to check sensitivity and repeatability of the measurement, but were not used for the quantification.

6.3.6. Derivatisation experiment

The sample rock surface was analysed for functionalised HCs to investigate the presence of recent inputs from extant organisms. The EOM after Ext. I and II was dried to remove methanol from the samples. Two drops of bis-trimethylsilyltrifluoroacetamide (BSTFA) solution (Grace & Co., Maryland) was added to the EOM, which was then heated at 60 °C for 30 min to derivatise the EOM. DCM was added to the resultant solution to make up the volume to approximately 50 µL, and the solution was analysed by GC-MS using the procedure as described above.

6.4. Results

Each sample is examined in terms of its *n*-alkane and MMA distributions. The results for the Loc. 1 (carbonate rock) and 5 (basaltic rock) samples are shown as figures in the main text, and those of the other samples are shown in the supplementary information.

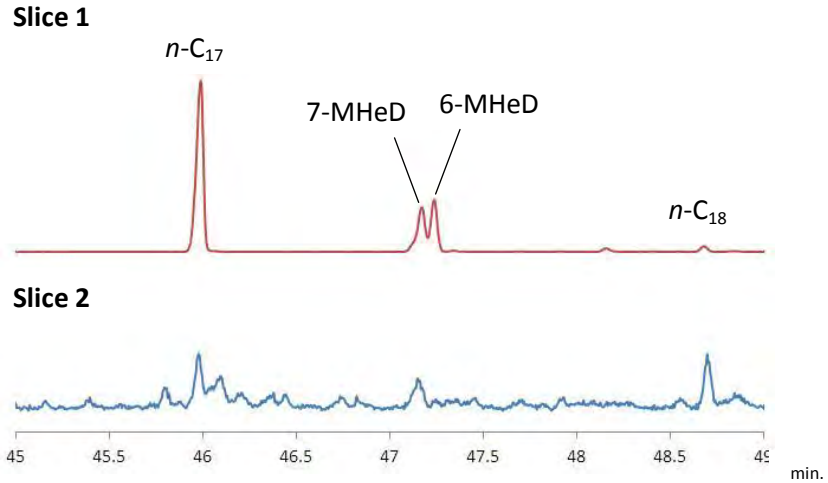

Figure 6.3. Partial mass chromatograms (m/z 57) of *n*-alkanes and MHeDs in slice 1 Ext. I, and slice 2 Ext. I of the Loc. 1 sample.

6.4.1. n-Alkanes

A higher abundance of *n*-C_{17} than other *n*-alkanes of similar molecular weight in the outer-most slice (Slice 1) was observed for all five samples (Figs 6.3, 6.4 and 6.5, and Figs S6.1, S6.2 and S6.3). The degree of the abundance of *n*-C_{17} varies among the samples. The procedural blank (slice 5 of the Loc. 5 sample) contains a series of *n*-alkanes from C_{14} to C_{35}, but their amount is very small (~1 pg / g sample) (Fig. 6.5). For the most part, all five samples contain much higher abundances of *n*-alkanes than the procedural blank. The Loc. 5 sample has a slightly higher abundance of *n*-C_{17} than other nearby *n*-alkanes as well (Fig. 6.5), but the difference is very small compared to the other four samples.

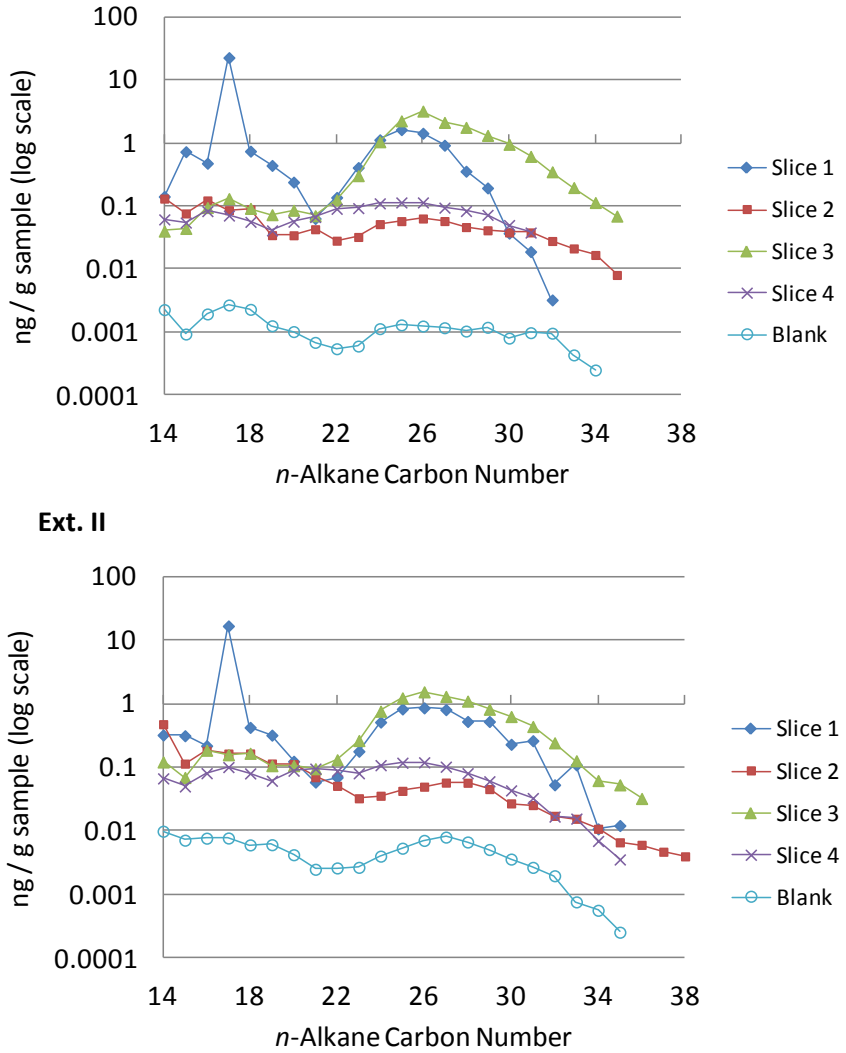

Figure 6.4. Amount and distribution of *n*-alkanes in all four slices of the Loc. 1 sample for Ext. I and II, and the procedural blank.

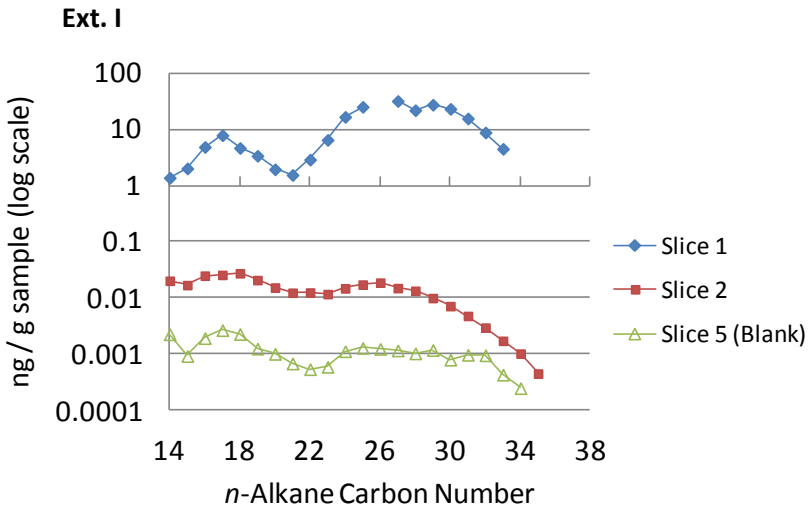

Figure 6.5. Amount and distribution of *n*-alkanes in slices 1, 2 and 5 of the Loc. 5 sample for Ext. I. Slice 5 of the Loc. 5 sample is used as the procedural blank in this study.

The high abundance of *n*-C_{17} in the Loc. 1 sample is limited to slice 1, so is within 1 cm of the rock surface (Figs 6.3 and 6.4). *n*-C_{17} is present in the inner slices, but its abundance is comparable to other <C_{21} *n*-alkanes. The Loc. 3 and 4 samples have a slightly higher abundance of *n*-C_{17} than other <C_{21} *n*-alkanes in slice 2, but the abundance in slice 2 is lower than that of slice 1 (Figs S6.2 and S6.3). The abundance of n-alkanes in the Loc. 5 sample (basaltic rock) is significantly different between slice 1 and slice 2 (Fig. 6.5). The *n*-alkane abundance in slice 1 of the Loc. 5 sample is higher than most stromatolite samples (Locs 1, 3 and 4), but that in slice 2 is much lower than those of any stromatolite samples (Locs 1-4). Also, the abundance of *n*-alkanes in slice 2 tends to be lower for higher molecular weight *n*-alkanes than lower molecular weight *n*-alkanes, compared to that of slice 1. Slice 5 of the Loc. 5 sample, which is the procedural blank, has an even lower abundance of *n*-alkanes than slice 2 (Fig. 6.5). This indicates a significant amount of hydrocarbon input onto the rock surface of the Loc. 5 sample from the surrounding environment, but the inner part of the rock stayed mostly intact from the contamination. However, a trace amount of hydrocarbons, especially low molecular weight compounds, appears to have reached a deeper part of the rock, which is consistent with the previous observation of higher mobility of lower molecular weight hydrocarbons through rocks (Brocks, 2011; Schinteie and Brocks, 2014).

In contrast, there is no particular difference in the relative abundance of *n*-C_{17} to other <C_{21} *n*-alkanes between Ext. I and II, for most stromatolite samples (Locs 1, 3 and 4) (Fig. 6.4, and Figs S6.2 and S6.3). The Loc. 5 sample is a basaltic rock, and does not contain carbonates, so the second solvent extraction experiment was not performed, except for slice 5 which was extracted for both Ext. I and II as a procedural blank (Fig. 6.4). The Loc. 2 sample is an exception, as slice 1 has a much higher abundance of *n*-alkanes in Ext. I than in Ext. II (Fig. S6.1). However, the relative abundance of *n*-C_{17} to other *n*-alkanes in slice 1 is lower in Ext. I than in Ext. II (Fig. S6.1). This may indicate an overprinting of another *n*-alkane input to the original distinctive *n*-C_{17} abundance, which has a larger influence on Ext. I than on Ext. II, whereas hydrocarbons in the carbonate minerals were more shielded from the outside environment.

The Loc. 1 and 3 samples were further analysed from the outside to the inside (Fig. 6.4 and Fig. S6.2). The inner slices of both the Loc. 1 and 3 samples never have a characteristic high abundance of *n*-C_{17}. Slices 2 and 4 of the Loc. 3 sample has a higher abundance of *n*-C_{17} relative to other *n*-alkanes, but the abundance is less distinctive. Both the Loc. 1 and 3 samples have an odd-over-even carbon preference (OEP) between *n*-C_{28} and *n*-C_{35} in slice 1, indicating a higher plant input (Eglinton and Hamilton, 1967). In contrast, the Loc. 2, 4 and 5 samples do not have an OEP in slice 1. The inner slices never have an OEP for any of the samples, so the influence of the higher plant input is limited to the rock surfaces, as is the case for *n*-C_{17}. The inner slices of the Loc. 3 sample have a large amount of >C_{21} *n*-alkanes only in Ext. II (Fig. S6.2), which may be ancient indigenous hydrocarbons preserved within the carbonate minerals.

6.4.1.1. Parameter calculation for n-C_{17} abundance

The relative abundance of *n*-C_{17} to the average of *n*-C_{16} and *n*-C_{18} was calculated (Table 6.2). The parameter is abbreviated as 17/(16+18) in this study, and is calculated as *n*-C_{17} / [(*n*-C_{16} + *n*-C_{18}) / 2]). The 17/(16+18) ratio reaches as high as 51.8 in slice 1 of the Loc. 1 sample. High values of 17/(16+18) are generally proportional to the overall amount of *n*-alkanes among the stromatolite samples (Locs 1-4). The Loc. 5 sample (basaltic) also has a >1 value for 17/(16+18), but the value is the lowest of the five samples. In contrast, slice 2 never has 17/(16+18) values as high as those in slice 1 for any of the

samples, and the limited influence of *n*-alkane input to slice 1 is confirmed. The inner slices generally have constant values of 17/(16+18) around 1 (0.7-1.4) for both the Loc. 1 and 3 samples for both Ext. I and II (Table 6.3), and *n*-C_{17} does not have any selective higher abundance compared to other *n*-alkanes.

Table 6.2. Relative abundance of *n*-C_{17} represented by the 17/(16+18) parameter for all five samples for Ext. I and II. The second extraction for slices 1 and 2 of the Loc. 5 sample was not performed. **17/(16+18)** = *n*-C_{17} / [(*n*-C_{16} + *n*-C_{18}) / 2].

	Slice 1		Slice 2	
	Ext. I	Ext. II	Ext. I	Ext. II
Loc. 1	37.0	51.8	0.81	0.95
Loc. 2	6.71	32.7	1.59	0.86
Loc. 3	3.20	2.23	1.44	0.92
Loc. 4	5.61	6.28	1.26	1.21
Loc. 5	1.65	-	0.98	-

Table 6.3. Variation of the 17/(16+18) parameter from the outside (Slice 1) towards the inside (Slices 4 or 5) of the Loc. 1, 3 and 5 samples for Ext. I and II. Extractions of slices 3 and 4 of the Loc. 5 sample were not performed.

Loc. 1	Slice 1	Slice 2	Slice 3	Slice 4
Ext. I	37.0	0.81	1.41	1.02
Ext. II	51.8	0.95	0.89	1.25

Loc. 3	Slice 1	Slice 2	Slice 3	Slice 4	Slice 5
Ext. I	3.20	1.44	1.26	1.38	0.93
Ext. II	2.23	0.92	1.03	1.21	0.73

Loc. 5	Slice 1	Slice 2	Slice 5
Ext. I	1.65	0.98	1.27

6.4.2. Monomethylalkanes (MMAs)

A high abundance of C_{18} 7- and 6-MHeDs was observed in slice 1 for all stromatolite samples (Locs 1-4) (Figs 6.3 and 6.6, and Figs S6.4, S6.5 and S6.6), but the basaltic sample (Loc. 5) does not have such a trend (Fig. 6.7).

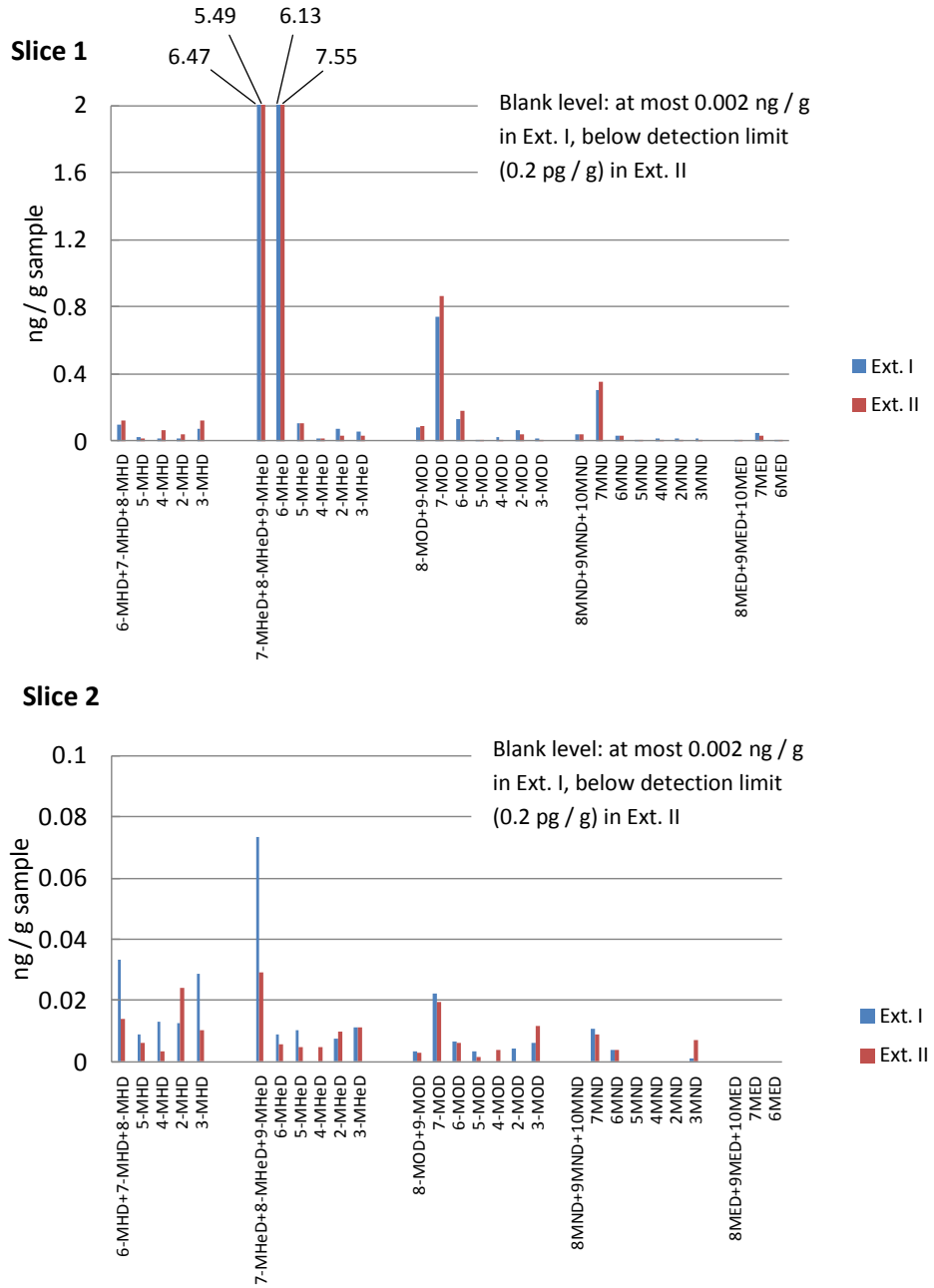

Figure 6.6. Histograms of MMA abundances in slices 1 and 2 of the Loc. 1 sample for Ext. I and II. **MHD** = methylhexadecane; **MHeD** = methylheptadecane; **MOD** = methyloctadecane, **MND** = methylnonadecane, **MED** = methyleicosane.

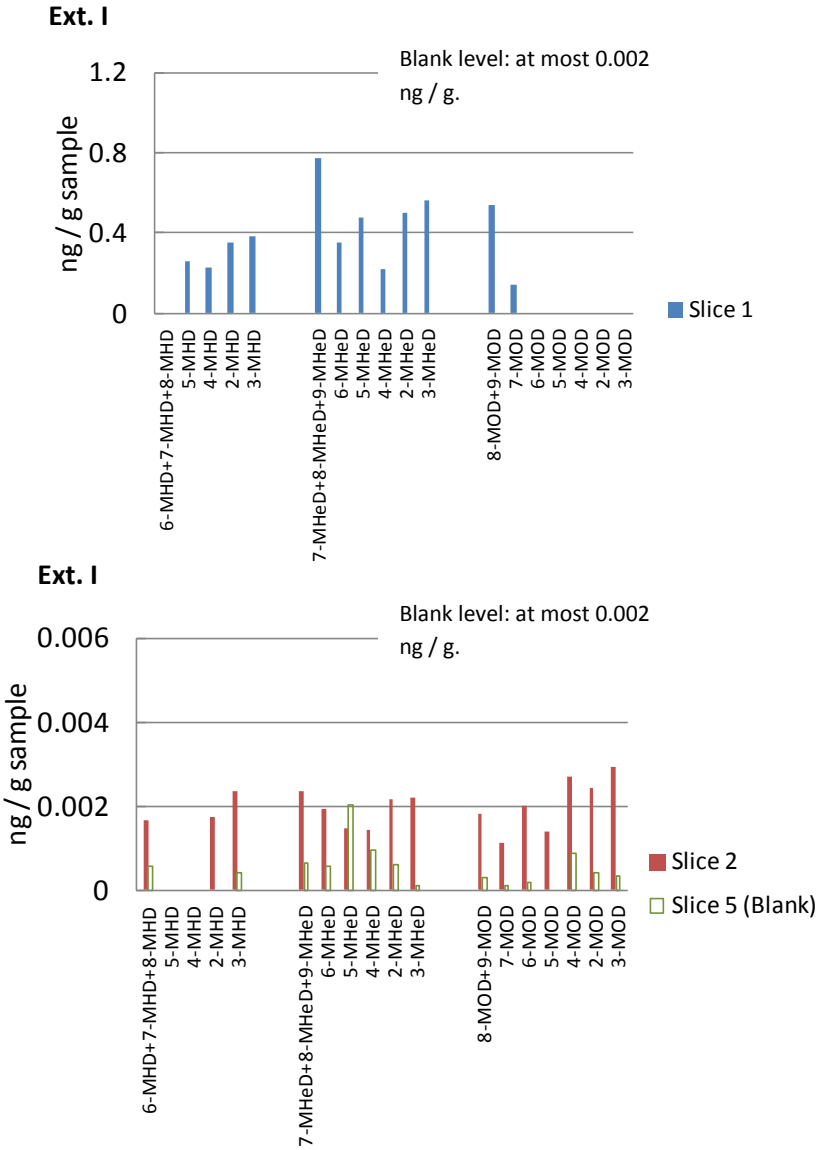

Figure 6.7. Histograms of MMA (MND, MHeD and MOD) abundances in slices 1, 2 and 5 of the Loc. 5 sample for Ext. I. Slice 5 of the Loc. 5 sample is used as the procedural blank in this study.

In the Loc. 1 and 5 samples, 8- and 9-MHeDs coelute with 7-MHeD, so these are all quantified together. However, the retention time of the peak and the mass spectrum indicate that 7-MHeD is dominant (Fig. 6.8). The relative abundance of 8- and 9-MHeD to 7-MHeD in the combined peak is estimated to be about 15 % at most. The high abundance of mid-chain isomers extends to C_{19} methyloctadecane (MOD), C_{20} methylnonadecane (MND) and C_{21} methyleicosane (MED) in the Loc. 1 sample (Fig. 6.6). 7- and 6-MMAs are more abundant than the other isomers for the $C_{18\text{-}21}$ MMA series (MHeD, MOD, MND and MED) in the Loc. 1 sample. In contrast, the C_{17} methylhexadecanes (MHDs) never have a high abundance of 7- or 6-MHD relative to other isomers. A similar distribution

pattern was observed for the other three stromatolite samples (Locs 2-4), and the high abundance of MMAs always starts from MHeD series for all samples (Figs S6.4, S6.5 and S6.6). Also, slice 1 Ext. II has a similar amount and distribution to Ext. I for three of the stromatolite samples (Locs 1, 3 and 4) (Fig. 6.6, and Figs S6.5 and S6.6), but not for the Loc. 2 sample (Fig. S6.4).

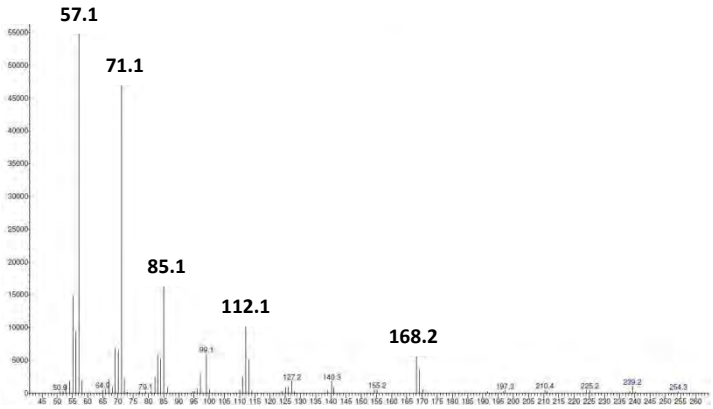

Figure 6.8. Mass spectrum of 7-MHeD in slice 1 Ext. I of the Loc. 1 sample. A prominent m/z 168.2 peak is a characteristic of 7-MHeD.

The different distribution of MMAs in the Loc. 2 sample may reflect the presence of more than one input sources. Slice 1 of the Loc. 2 sample has a significantly higher abundance of MMAs in Ext. I than in Ext. II (x 30; Fig. S6.4). Nevertheless, the relative abundance of 6- and 7-MMAs to other isomers is not distinctive in Ext. I. Furthermore, the abundance of 8- and 9-MMAs is comparable to or higher than that of 7- and 6-MMAs in Ext. I. In contrast, the high abundance of 6- and 7-MHeDs is apparent in Ext. II, although the overall amount of MMAs is very low compared to Ext. I. One interpretation of this observation is that the high abundance of 7- and 6-MHeDs is overprinted by another input of MMAs, which affects Ext. I more than Ext. II, as is already suggested by the *n*-alkane distribution of the Loc. 2 sample (Fig. S6.1).

The high abundance of 7- and 6-MMAs is mainly limited to the rock surface for all the stromatolite samples (Locs 1-4), as is the case for the *n*-alkanes (Figs 6.3 and 6.6, and Figs S6.4, S6.5 and S6.6). The relative abundance of 7- and 6-MMAs to other isomers in slice 2 is much lower than that in slice 1 in both Ext. I and II for all stromatolite samples. Also, the overall abundance of MMAs in slice 2 is much lower than that in slice 1 for all samples. However, a slight influence of MMAs on the rock surface

can be seen in slice 2. The abundance of 7-MHeD and 7-MOD in slice 2 of Loc. 1 sample is higher than the other isomers for both Ext. I and II (Fig. 6.6).

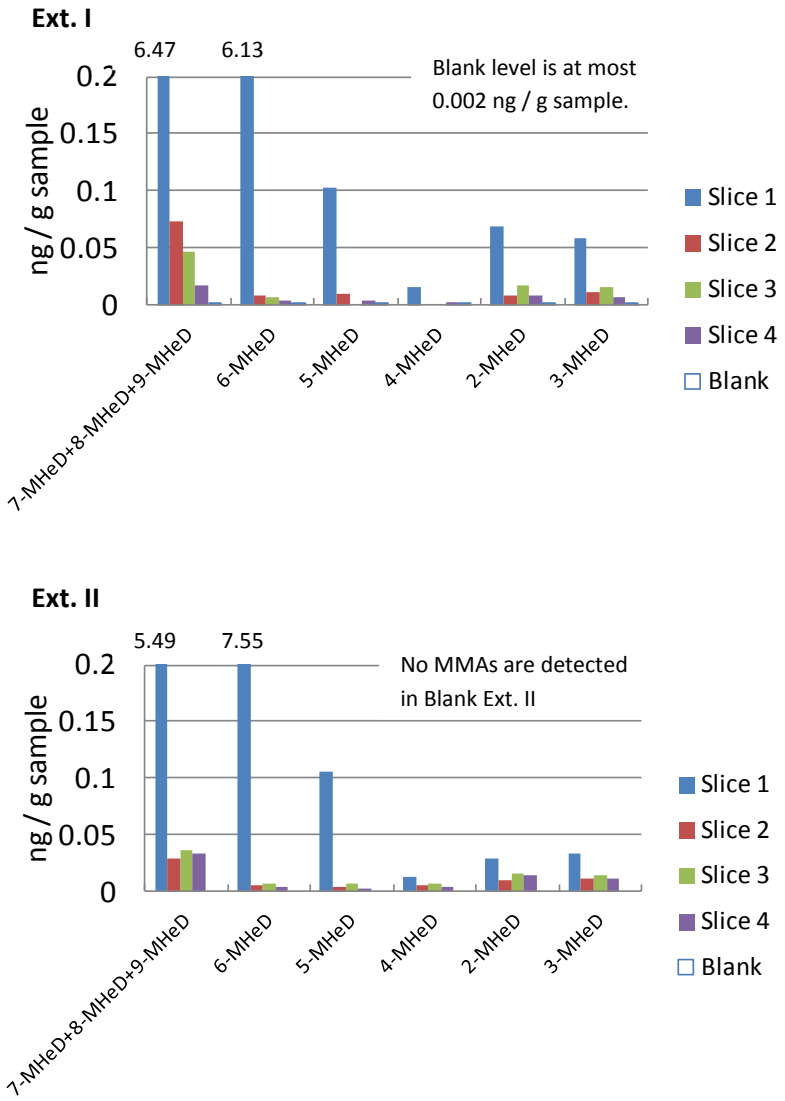

Figure 6.9. Histograms of MHeD abundances in all four slices of the Loc. 1 sample for Ext. I and II, and the procedural blank.

The influence of surficial MMAs can be further seen in the inner slices of the samples from Locs 1 and 3. The concentration of 7- and 6-MHeDs in the Loc. 1 sample slices continuously decreases towards the inside slice in Ext. I (Fig. 6.9), probably by the penetration of a small amount of MMAs towards the deeper part of the rock. In contrast, the abundance of 7- and 6-MHeDs in Ext. II is generally constant, and the influence of surficial MMAs is not observed. The concentration profile of MMAs in the Loc. 3 sample is more complicated (Fig. S6.5). The amount of detected MMAs is very small and

close to the blank level, so the experimental error may be larger than for the Loc. 1 sample. MHDs and MODs were not reliably identified in the Loc. 3 sample due to very small peaks. The high abundance of 7- and 6-MHeDs is seen in slices 1 and 2 in Ext. I, but only in slice 1 in Ext. II (Fig. S6.5). The amount of detected MHeDs is mostly higher in Ext. II than in Ext. I in the inner slices 3-5, but is lower or comparable in Ext. II than in Ext. I in slices 1 and 2. These observations suggest that the MMAs in Ext. II in the inner slices of both the Loc. 1 and 3 samples have a different origin from those in Ext. I, and are indigenous MMAs preserved within the carbonate minerals.

6.4.2.1. Parameter calculation for MMA abundance

The relative abundance of mid-chain branched MMAs was calculated as a relative ratio of the sum of 6-, 7-, 8- and 9-MMAs to the sum of 2-, 3-, 4- and 5-MMAs (Table 6.4). The parameter is abbreviated as the methylalkane parameter (MAP), and is defined for the first time in this study. There are three MAPs defined; MAP17 for the MHD series, MAP18 for the MHeD series, and MAP19 for the MOD series. Although 8- and 9-MMAs are not always abundant, they frequently coelute with 7-MMA and are difficult to separately quantify (for example in the Loc. 1 and 5 samples), so they are included in the sum of the 6- and 7-MMAs.

MAP17 is below 1 for both slices 1 and 2 in any sample for both Ext. I and II (Table 6.4), which means that the abundance of the combined 6-, 7-, 8- and 9-MHDs is lower than that of the combined 2-, 3-, 4- and 5-MHDs. The Loc. 5 sample does not contain MHDs, or MHDs are below the detection limit. In contrast, MAP18 is above 1 in slice 1 for all stromatolite samples for both Ext. I and II (Table 6.4), reflecting the dominance of 6- and 7-MHeDs, as already discussed. Only the basaltic sample (Loc. 5) has a MAP18 value lower than 1 in slice 1. The MAP18 for all the slice 2 samples is much lower than for slice 1 and becomes close to 1 for both Ext .I and II, expect for the Loc. 1 sample which still has a somewhat high value for Ext. I (2.8; Table 6.4). MAP19 is generally low (0.5-1.5) for both slices 1 and 2, and for both Ext. I and II, so a clear dominance of 6- and/or 7-MOD is not found for most samples (Locs 2-5) (Table 6.4), except for the Loc. 1 sample which has a distinctive high abundance of 7-MOD, and a high MAP19 value in slice 1. The MAP19 in slice 2 of the Loc. 1 sample is still high (Table 6.4).

The high values of both MAP18 and MAP19 for the Loc. 1 sample suggest an influence of mid-chain branched MHDs and MHeDs on the rock surface and into the deeper part of the rock.

Table 6.4. Methylalkane parameters (MAPs) for all five samples for Ext. I and II. The second extractions for slices 1 and 2 of Loc. 5 sample were not performed. **MAP17** = (6-MHD+7-MHD+8-MHD+9-MHD) / (2-MHD+3-MHD+4-MHD+5-MHD); **MAP18** = (6-MHeD+7-MHeD+8-MHeD+9-MHeD) / (2-MHeD+3-MHeD+4-MHeD+5-MHeD); and **MAP19** = (6-MOD+7-MOD+8-MOD+9-MOD) / (2-MOD+3-MOD+4-MOD+5-MOD).

		Slice 1		Slice 2	
	MAP	Ext. I	Ext. II	Ext. I	Ext. II
Loc. 1	*17*	0.72	0.50	0.52	0.31
	18	51	72	2.8	1.16
	19	8.5	17	2.2	1.7
Loc. 2	*17*	0.50	0.50	0.12	0.31
	18	1.5	4.5	0.68	0.84
	19	0.96	1.24	0.46	0.93
Loc. 3	*17*	0.23	0.25	-	-
	18	3.3	3.7	1.19	0.11
	19	0.70	0.52	-	-
Loc. 4	*17*	0.46	0.72	0.34	0.44
	18	2.1	2.3	1.23	1.39
	19	1.38	-	1.5	1.36
Loc. 5	*17*	-	-	0.40	-
	18	0.64	-	0.59	-
	19	-	-	0.52	-

Table 6.5. Variation of MAP18 for the Loc. 1, 3 and 5 samples for Ext. I and II, from the outside (Slice 1) towards the inside (Slices 4 or 5). Extractions for slices 3 and 4 of the Loc. 5 sample were not performed.

Loc. 1	Slice 1	Slice 2	Slice 3	Slice 4
Ext. I	51	2.5	1.6	0.98
Ext. II	72	1.03	0.97	1.15

Loc. 3	Slice 1	Slice 2	Slice 3	Slice 4	Slice 5
Ext. I	3.3	1.19	0.90	0.78	0.51
Ext. II	3.7	0.11	0.70	0.64	0.58

Loc. 5	Slice 1	Slice 2	Slice 5
Ext. I	0.64	0.59	0.33

The influence of surface MMAs on the inner slices is confirmed by the MAP18 values for the inner slices (Table 6.5). Because of the low abundance of MMAs in the inner slices, only the MAP18 was calculated. Samples 1 and 3 have the highest values of MAP18 in slice 1, and the values are lower in the inner slices (Table 6.5). The MAP18 values become lower from slice 1 towards the middle in Ext. I for both samples, whereas MAP18 values in Ext. II are generally constant throughout the inner slices, except for slice 2 of the Loc. 3 sample. This indicates that the influence of MMAs on rock surfaces is limited to Ext. I, and MMAs in Ext. II are generally free from later migration of hydrocarbons. The Loc. 5 basaltic sample does not have a high abundance of mid-chain branched MHeDs at all throughout the rock (Table 6.5), and the MAP18 is very low (0.3-0.6). The Loc. 3 sample reaches similar low MAP18 values in the inner slices in Ext. II (0.6-0.7; Table 6.5), and no sign of a high abundance of 6- or 7-MMA is seen (Fig. S6.5). In contrast, MAP18 values of the inner slices of the Loc. 1 sample in Ext. II are always around 1 (Table 6.5), and the abundance of 7-MHeDs is higher than that of the other isomers (Fig. 6.9). This may indicate a trace of indigenous cyanobacterial input preserved within the carbonate minerals throughout the inner part of the rock.

6.5. Discussion

6.5.1. Inhabitation of cyanobacteria on Archean rocks

The high values of both the 17/(16+18) and the MAP in slice 1 of the four stromatolitic carbonate rocks (Locs 1-4) clearly indicate the presence of cyanobacteria on the rock surfaces in the past or present. The limited distribution of a large amount of mid-chain branched MMAs to the rock surfaces suggests that the cyanobacteria are endolithic. In contrast, the low values of 17/(16+18) and MAP in slice 1 of the basalt sample (Loc. 5) make the presence of such cyanobacteria unlikely on the basaltic rock surface. The similar amount of MMAs in both Ext. I and II suggests that the endolithic cyanobacteria can get into the carbonate minerals, but mainly only within 1 cm of the rock surfaces (the thickness of slice 1). In contrast, the inner part of the rocks, particularly within the carbonate minerals, are isolated from the migration of hydrocarbons. The detected mid-chain branched MMAs

in the Loc. 1 sample may be indigenous MMAs of possibly Archean origin, and may suggest the presence of cyanobacteria in the Archean (see Chapter 4 for more evidence for cyanobacteria in the rock). In contrast, the source of MMAs in Locs 2-4 seems non-cyanobacterial, because it does not have a high abundance of 7-MHeD.

All four stromatolite rocks have a similar distribution of *n*-C_{17} and mid-chain branched MMAs. They were collected from four different localities, and from two different formations (the Tumbiana Formation and the Kylena Formation). Therefore, the presence of endolithic cyanobacteria on carbonate rocks is apparently common in the Pilbara region. The absence of endolithic cyanobacteria on the basaltic rock, at least in this study, suggests that the cyanobacterial inhabitation is selective and depends on the mineralogy of rocks.

Endolithic phototrophs typically reside a few millimetres beneath the surface, enough to protect them from exposure to extreme temperatures, ultraviolet light, and desiccation, yet allowing photosynthesis and N_2 fixation to occur (Stivaletta et al., 2010). This is consistent with the presence of cyanobacterial biomarkers within 1 cm of the rock surfaces.

MMAs are the direct products of cyanobacteria (Schirmer et al., 2010), and do not constrain the age of the actual input of these MMAs into the investigated rocks. The derivatisation experiments of the Loc. 1 and 3 slice 1 extractions do not show any functionalised organic compounds, or they are at least below the blank level. Therefore, the detected MMAs may be the remains of a past presence of cyanobacteria on the rock surfaces. The Fortescue Group stromatolites became exposed to the Earth's surface since uplift during the Cenozoic (M. Kranendonk, personal communication), so the inhabitation of endolithic cyanobacteria would have been at some point since that time. However, there is another possibility that any functionalised organic molecules could have been removed during the solvent washing performed to eliminate experimental contamination. Thus, the analysis of organic matter on rock surface needs to be carried out separately from the inner slices, without using pre-solvent washing, in future work designed to more extensively test for functionalised organic compounds.

The main products of MMA biosynthesis in cyanobacteria are *n*-C_{17} and 7-MHeD (Coates et al., 2014), and 6-MHeD is not usually a major product, which is different from the observations in this study, where 6-MHeD is also a major component along with 7-MHeD. In addition, 7-MOD, 7-MND and 7-MED were also observed in the Loc. 1 sample. The lack of these mid-chain branched MMAs in the other samples may suggest a different cyanobacterial species on those rock surfaces. Alternatively, this may be a matter of the amount of these MMAs, because the Loc. 1 sample has the largest amount of MMAs in this study, except for the overprinting of non-cyanobacterial input in the Loc. 2 sample. One possible explanation for the origin of MMAs other than 7-MHeD is a diagenetic rearrangement of 7-MHeD to 6-MHeD, and also to other MMA series (MOD, MND and MED). However, the complete lack of 7-MHD makes this possibility uncertain, because the production of 7-MHD is also expected on thermodynamic grounds. Alternatively, a specific cyanobacterial species, so far uncharcterised by anyone, may produce both 7- and 6-MHeDs as major products.

6.5.2. Identity of endolithic cyanobacteria

The endolithic cyanobacteria on carbonate rocks in the Pilbara region seem to penetrate into the carbonate minerals. Therefore, euendolithic cyanobacteria may be included in the endolithic community, thriving within carbonate mineral grains. Currently, euendolithic cyanobacteria discovered so far are filamentous from section III (Oscillatoriales) to IV (Nostocales), and V (Stigonematales) cyanobacteria (Garcia-Pichel, 2006), so the cyanobacteria in the Pilbara region found in this study may also include filamentous species. However, a literature survey suggests that there are no euendolithic cyanobacteria found in subaerial conditions, although there are many examples of euendolithic cyanobacteria in aquatic environments (both marine and freshwater) (Golubic et al., 1981; Garcia-Pichel, 2006; Cockell and Herrera, 2008; Cockell et al., 2009). Examples of endolithic cyanobacteria in subaerial conditions are limited to cryptoendoliths, chasmoendoliths, or hypoliths (microorganisms living underneath rocks). The possible explanations are: (1) there are undiscovered cyanobacterial species actively penetrating into carbonate minerals; or (2) cyanobacteria do not contribute to the boring itself, which may be carried out by other coexisting microorganisms such as endolithic lichens and algae.

Subaerial endolithic communities typically contain both filamentous and unicellular cyanobacteria, such as a unicellular genus *Chroococcidiopsis*, which is very common as a cryptoendolith and a chasmoendolith in arid environments (Bell, 1993; Gerrath et al., 2000). Most filamentous cyanobacteria and unicellular *Chroococcidiopsis* have the biosynthetic pathway to produce 7-MHeD (Coates et al., 2014), which is consistent with the high abundance of 7-MHeD in this study. In addition, *Chroococcus turgidus*, *Spirulina sp.*, *Calothrix sp.*, *Nostoc commune* and *Chlorogloea fritschii*, for example, are known to produce MHeD, MOD and MND, as have been found in this study, and *Fischerella sp.* produces 6-MHeD predominantly (Coates et al., 2014). Some of the cyanobacteria are known to grow in an extreme environment, for example *Chroococcus turgidus* in arid deserts (Potts and Friedmann, 1981), *Calothrix sp* on dolomite surfaces (Sigler et al., 2003) and *Nostoc commune* in an Antarctic stromatolitic community (Wynn-Williams et al., 1999). Thus, the endolithic cyanobacterial communities on the Fortescue Group carbonate rocks may be one or a mixture of these species. The lack of endolithic cyanobacteria on a basalt rock in the Pilbara region may further constrain the cyanobacterial species, but any comprehensive study about the mineral preference by particular cyanobacterial taxa has apparently not been carried out.

6.5.3. On the contamination problem for Archean biomarker research

Trace hydrocarbon contamination is a major obstacle to the study of Archean biomarkers. Previously reported Archean biomarkers (hopanes and steranes) are now called into question, as at least some of the detected biomarkers have been shown to be anthropogenic contamination, or due to later hydrocarbon migration (Rasmussen et al., 2008; Brocks, 2011; French et al., 2013).

The penetration of hydrocarbons towards the deeper part of a rock has been previously reported (Brocks, 2011; Schinteie and Brocks, 2014), and is consistent with the concentration gradient of the MMAs in this study. However, the ratio of migrating MMAs is very low compared to the amount of the MMAs on the rock surfaces, so the contamination from the surrounding environment is mostly limited to the rock surfaces, as recently suggested (Flannery and George, 2014). However, the influence of hydrocarbon migration from the outside is not negligible for an Archean biomarker study,

where only a very small amount of hydrocarbons is preserved in the rocks. Measurement of concentration gradients of hydrocarbons by slice experiment has been proven as effective to distinguish indigenous hydrocarbons from contamination (Hoshino et al., 2014; and Chapters 3-5). Furthermore, two extraction experiments, Ext. I and II, reveal that hydrocarbons in Ext. II are more protected from contamination from the outside than those in Ext. I.

6.6. Conclusions

Four stromatolitic carbonate rocks and one basaltic rock were investigated in terms of cyanobacterial inhabitation on their rock surfaces. All four carbonate rocks indicate the presence of cyanobacteria since the Cenozoic, but the basaltic rock does not have any sign of cyanobacteria. Therefore, the inhabitation of cyanobacteria may depend on the rock mineralogy. Also, based on the second solvent extraction experiments it is suggested that the endolithic cyanobacteria found in this study can penetrate into carbonate minerals. The influence of *n*-alkanes and monomethylalkanes is limited mainly to the rock surfaces, but a trace amount of monomethylalkanes is confirmed to migrate into deeper parts of the rocks, probably through pore spaces and fissures in the rock fabric. In contrast, the hydrocarbons within the carbonate minerals in the inner part of the rocks are generally isolated from such migration, and may preserve ancient indigenous hydrocarbons. It is demonstrated that the combination of slice experiment and two consecutive solvent extractions is an effective method to investigate ancient geological samples from the Precambrian era.

6.7. Acknowledgements

We thank the Geological Survey of Western Australia for logistical field support and scientific assistance. Y.H. is supported by a Macquarie University Research Excellence Scholarship. S.C.G. acknowledges the Australian Research Council for a Discovery Grant.

6.8. Supplementary information

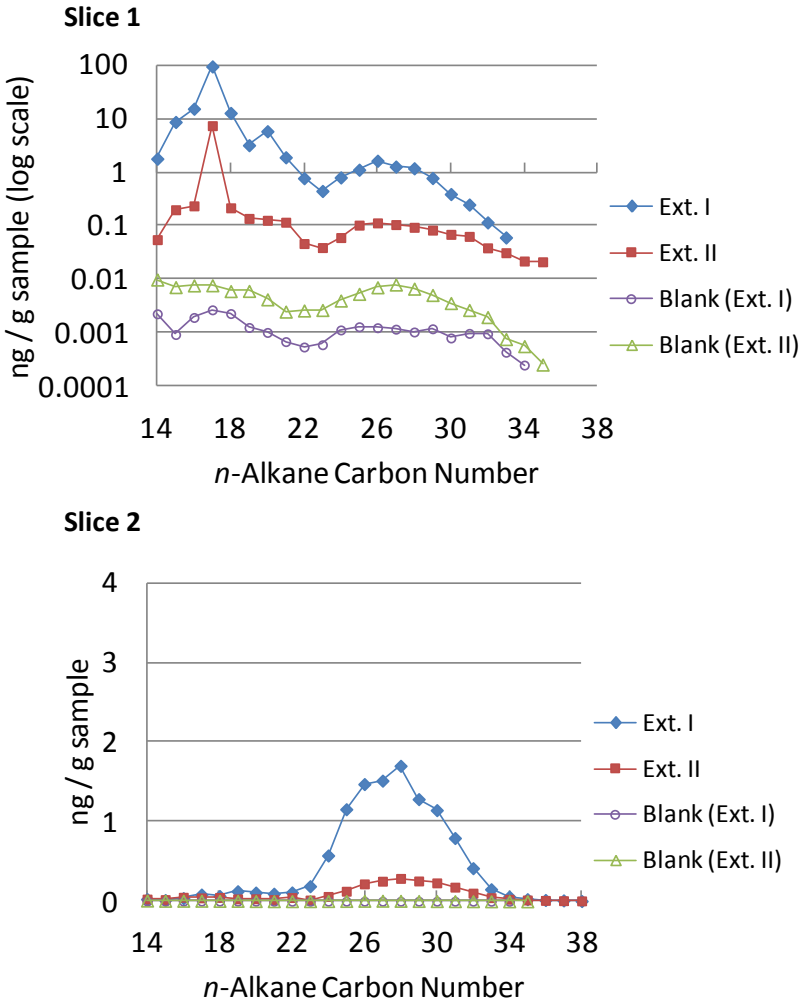

Figure S6.1. Amount and distribution of *n*-alkanes in slices 1 and 2 of the Loc. 2 sample, and the procedural blank for Ext. I and II.

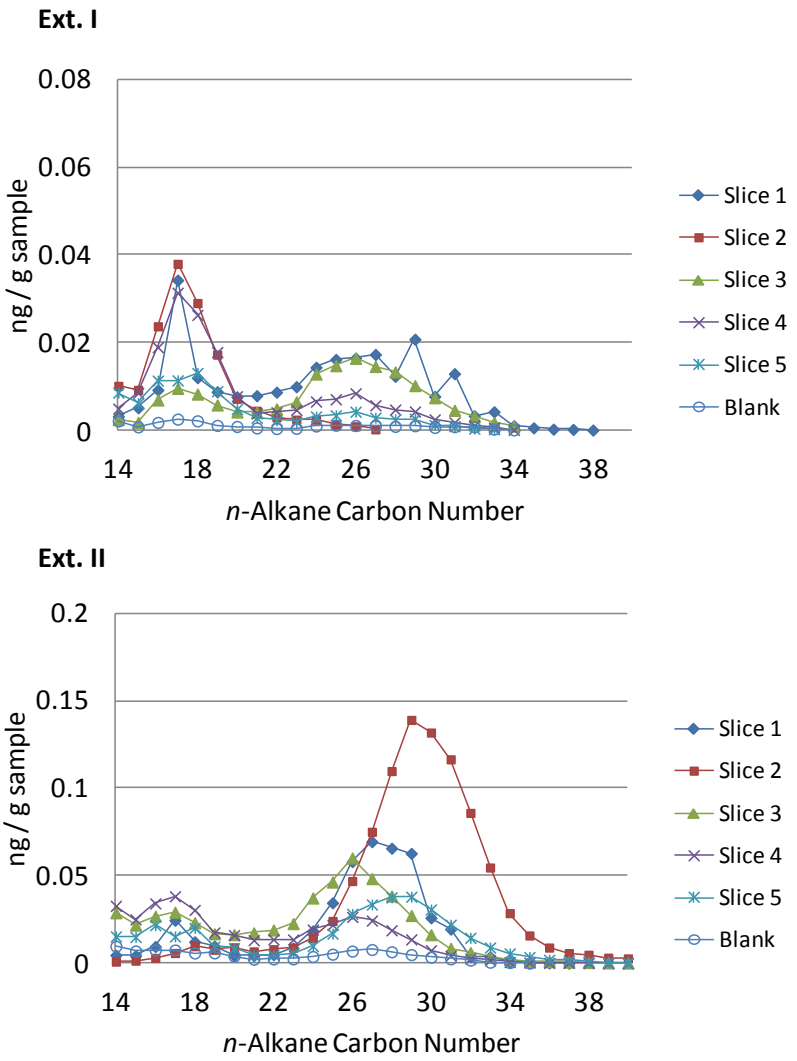

Figure S6.2. Amount and distribution of *n*-alkanes in all five slices of the Loc. 3 sample for Ext. I and II, and the procedural blank.

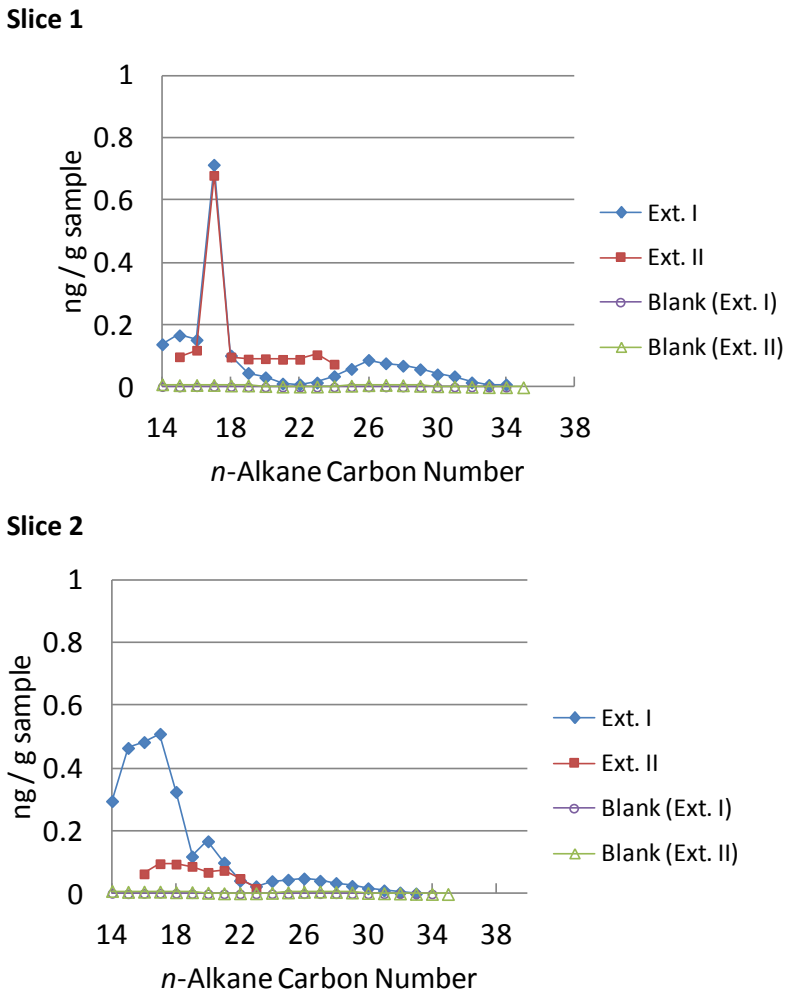

Figure S6.3. Amount and distribution of *n*-alkanes in slices 1 and 2 of the Loc. 4 sample, and the procedural blank for Ext. I and II.

Slice 1 Ext. I

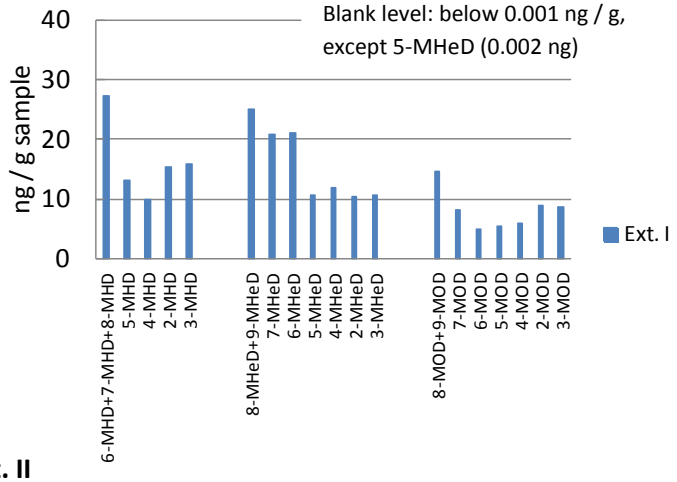

Slice 1 Ext. II

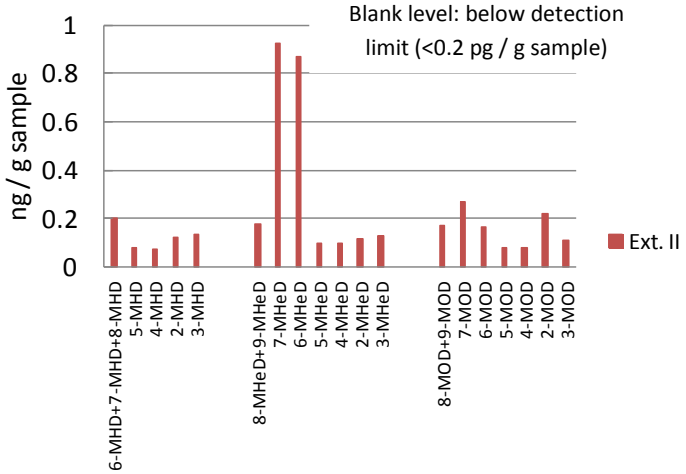

Slice 2

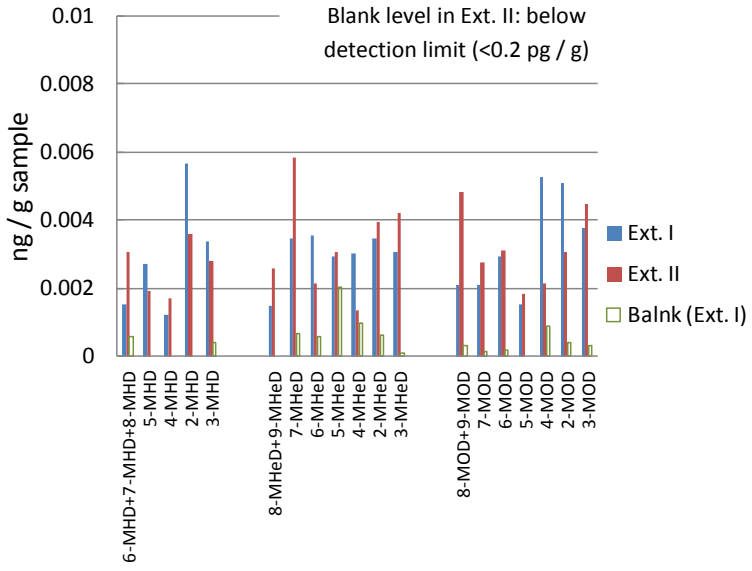

Figure S6.4. Histograms of MMA (MHD, MHeD and MOD) abundances in slices 1 and 2 of the Loc. 2 sample for Ext. I and II.

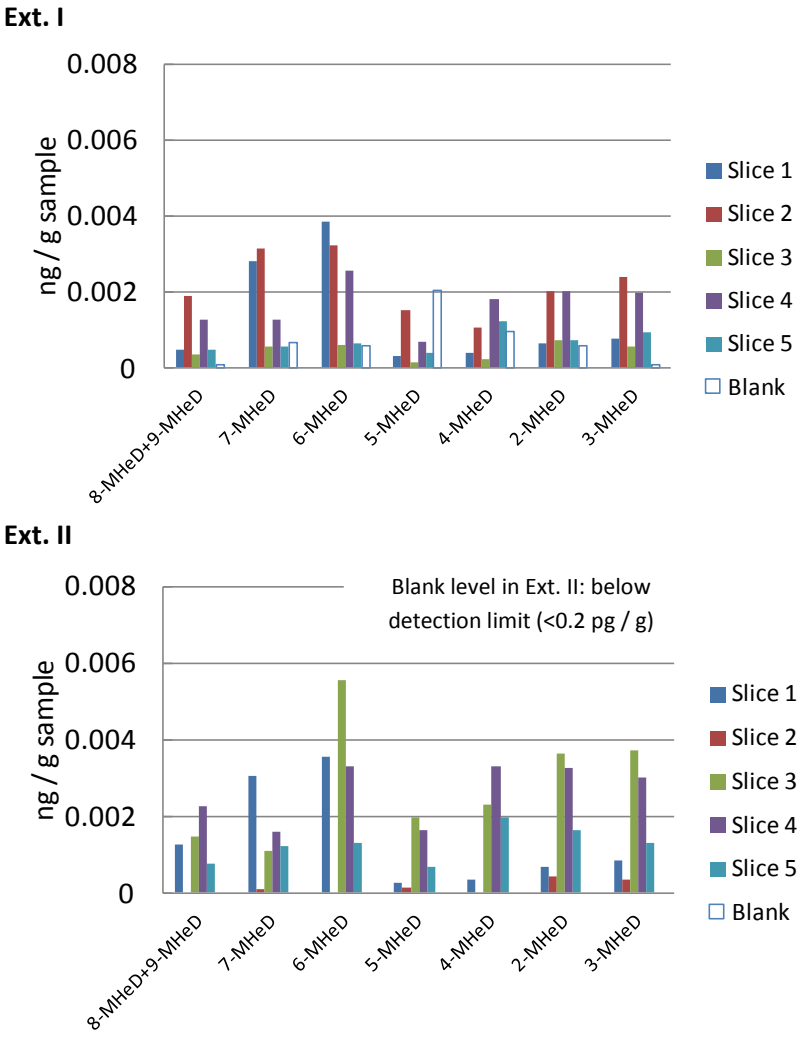

Figure S6.5. Histograms of MHeD abundances in all five slices of the Loc. 3 sample for Ext. I and II.

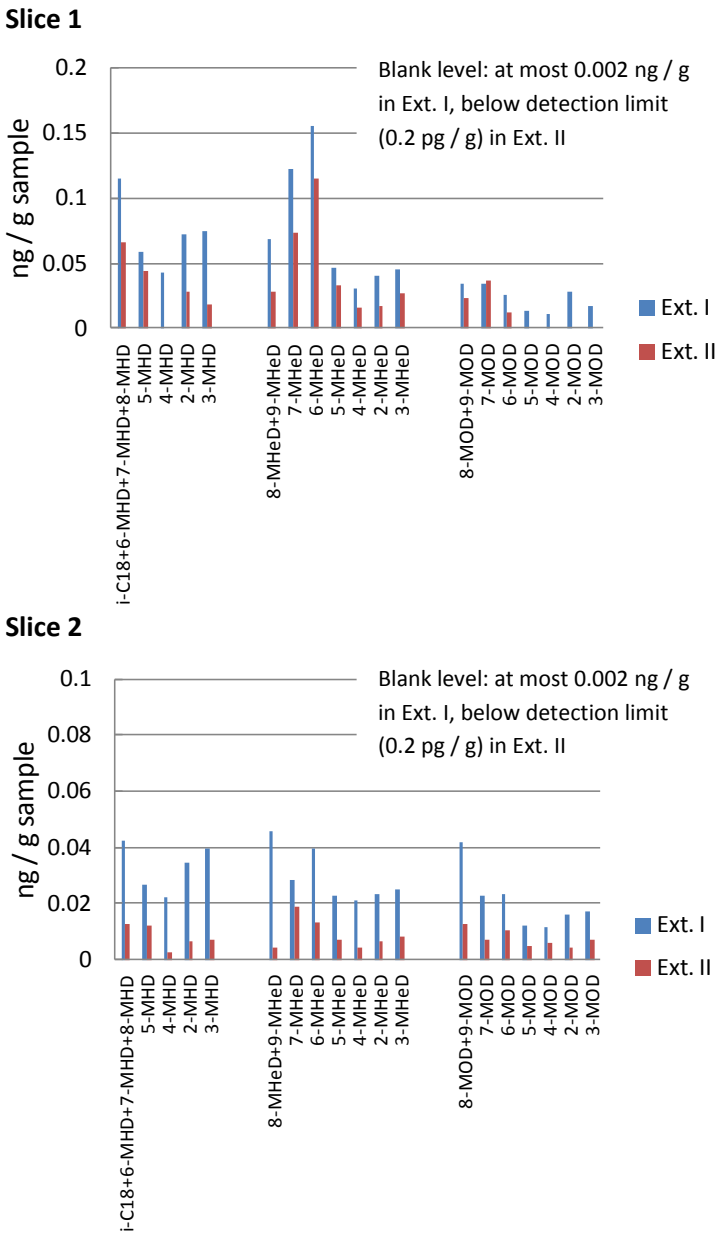

Figure S6.6. Histograms of MMA (MHD, MHeD and MOD) abundances in slices 1 and 2 of the Loc. 4 sample for Ext. I and II.

6.9. References

Allen, M.A., Goh, F., Burns, B.P. and Neilan, B.A. (2009) Bacterial, archaeal and eukaryotic diversity of smooth and pustular microbial mat communities in the hypersaline lagoon of Shark Bay. Geobiology 7, 82-96.

Awramik, S.M. and Buchheim, H.P. (2009) A giant, Late Archean lake system: The Meentheena Member (Tumbiana Formation; Fortescue Group), Western Australia. Precambrian Research 174, 215-240.

Banerjee, N.R., Simonetti, A., Furnes, H., Muehlenbachs, K., Staudigel, H., Heaman, L. and Van Kranendonk, M.J. (2007) Direct dating of Archean microbial ichnofossils. Geology 35, 487-490.

Baumgartner, L., Spear, J., Buckley, D., Pace, N., Reid, R., Dupraz, C. and Visscher, P. (2009) Microbial diversity in modern marine stromatolites, Highborne Cay, Bahamas. Environmental Microbiology 11, 2710-2719.

Bell, R.A. (1993) Cryptoendolithic algae of hot semiarid lands and deserts. Journal of Phycology 29, 133-139.

Brocks, J.J. (2011) Millimeter-scale concentration gradients of hydrocarbons in Archean shales: Live-oil escape or fingerprint of contamination? Geochimica Et Cosmochimica Acta 75, 3196-3213.

Brocks, J.J., Logan, G.A., Buick, R. and Summons, R.E. (1999) Archean molecular fossils and the early rise of eukaryotes. Science 285, 1033-1036.

Brocks, J.J. and Summons, R.E. (2003) 8.03 - Sedimentary Hydrocarbons, Biomarkers for Early Life, in: Editors-in-Chief: Heinrich, D.H., Karl, K.T. (Eds.), Treatise on Geochemistry. Pergamon, Oxford, pp. 63-115.

Campbell, S. (1983) The Modern Distribution and Geological History of Calcium Carbonate Boring Microorganisms, in: Westbroek, P., de Jong, E.W. (Eds.), Biomineralization and Biological Metal Accumulation. Springer Netherlands, pp. 99-104.

Coates, R., Podell, S., Korobeynikov, A., Lapidus, A., Pevzner, P., Sherman, D., Allen, E., Gerwick, L. and Gerwick, W. (2014) Characterization of cyanobacterial hydrocarbon composition and distribution of biosynthetic pathways. PloS one 9, e85140.

Cockell, C.S. and Herrera, A. (2008) Why are some microorganisms boring? Trends in Microbiology 16, 101-106.

Cockell, C.S., Kaltenegger, L. and Raven, J.A. (2009) Cryptic photosynthesis—extrasolar planetary oxygen without a surface biological signature. Astrobiology 9, 623-636.

Cockell, C.S., McKay, C.P., Warren-Rhodes, K. and Horneck, G. (2008) Ultraviolet radiation-induced limitation to epilithic microbial growth in arid deserts – Dosimetric experiments in the hyperarid core of the Atacama Desert. Journal of Photochemistry and Photobiology B: Biology 90, 79-87.

Coffey, J.M., Flannery, D.T., Walter, M.R. and George, S.C. (2013) Sedimentology, stratigraphy and geochemistry of a stromatolite biofacies in the 2.72Ga Tumbiana Formation, Fortescue Group, Western Australia. Precambrian Research 236, 282-296.

de la Torre, J.R., Goebel, B.M., Friedmann, E.I. and Pace, N.R. (2003) Microbial diversity of cryptoendolithic communities from the McMurdo Dry Valleys, Antarctica. Applied and environmental microbiology 69, 3858-3867.

de los Ríos, A., Grube, M., Sancho, L. and Ascaso, C. (2007) Ultrastructural and genetic characteristics of endolithic cyanobacterial biofilms colonizing Antarctic granite rocks. FEMS microbiology ecology 59, 386-395.

Diels, L. (1914) 64. L. Diels: Die Algen-Vegetation der Südtiroler Dolomitriffe. Berichte der Deutschen Botanischen Gesellschaft 32, 502-526.

Dong, H., Rech, J.A., Jiang, H., Sun, H. and Buck, B.J. (2007) Endolithic cyanobacteria in soil gypsum: Occurrences in Atacama (Chile), Mojave (United States), and Al-Jafr Basin (Jordan) Deserts. Journal of Geophysical Research: Biogeosciences 112, G02030.

Edgcomb, V.P., Bernhard, J.M., Summons, R.E., Orsi, W., Beaudoin, D. and Visscher, P.T. (2014) Active eukaryotes in microbialites from Highborne Cay, Bahamas, and Hamelin Pool (Shark Bay), Australia. ISME J 8, 418-429.

Eglinton, G. and Hamilton, R.J. (1967) Leaf Epicuticular Waxes. Science 156, 1322-1335.

Flannery, D.T. and Walter, M.R. (2012) Archean tufted microbial mats and the Great Oxidation Event: new insights into an ancient problem. Australian Journal of Earth Sciences 59, 1-11.

Flannery, E.N. and George, S.C. (2014) Assessing the syngeneity and indigeneity of hydrocarbons in the ~1.4 Ga Velkerri Formation, McArthur Basin, using slice experiments. Organic Geochemistry, submitted.

French, K.L., Hallman, C., Hope, J.M., Buick, R., Brocks, J.J. and Summons, R.E. (2013) Archean hydrocarbon biomarkers: Archean or not?, Goldschmidt 2013 Conference Abstract.

Furnes, H., Banerjee, N., Muehlenbachs, K., Staudigel, H. and De Wit, M. (2004) Early life recorded in Archean pillow lavas. Science 304, 578-581.

Furnes, H., Banerjee, N.R., Staudigel, H., Muehlenbachs, K., McLoughlin, N., de Wit, M. and Van Kranendonk, M. (2007) Comparing petrographic signatures of bioalteration in recent to Mesoarchean pillow lavas: Tracing subsurface life in oceanic igneous rocks. Precambrian Research 158, 156-176.

Garby, T.J., Walter, M.R., Larkum, A.W.D. and Neilan, B.A. (2013) Diversity of cyanobacterial biomarker genes from the stromatolites of Shark Bay, Western Australia. Environmental Microbiology 15, 1464-1475.

Garcia-Pichel, F. (2006) Plausible mechanisms for the boring on carbonates by microbial phototrophs. Sedimentary Geology 185, 205-213.

Gerrath, J.F., Gerrath, J.A., Matthes, U. and Larson, D.W. (2000) Endolithic algae and cyanobacteria from cliffs of the Niagara Escarpment, Ontario, Canada. Canadian Journal of Botany 78, 807-815.

Golubic, S., Friedmann, E.I. and Schneider, J. (1981) The lithobiontic ecological niche, with special reference to microorganisms. Journal of Sedimentary Research 51, 475-478.

Grice, K. and Eiserbeck, C. (2014) 12.3 - The Analysis and Application of Biomarkers, in: Holland, H.D., Turekian, K.K. (Eds.), Treatise on Geochemistry (Second Edition). Elsevier, Oxford, pp. 47-78.

Gries, R., Gries, G., Li, J., Maier, C., Lemmon, C. and Slessor, K. (1994) Sex pheromone components of the spring hemlock looper,Lambdina athasaria (Walker) (Lepidoptera: Geometridae). Journal of chemical ecology 20, 2501-2511.

Hoshino, Y., Flannery, D., Walter, M. and George, S.C. (2014) Investigation of hydrocarbons preserved in a 2.7 Ga Archean rock from the Fortescue Group, Pilbara Craton, Western Australia. Geobiology submitted.

Hughes, K. and Lawley, B. (2003) A novel Antarctic microbial endolithic community within gypsum crusts. Environmental Microbiology 5, 555-565.

Li, N., Chang, W.-C., Warui, D., Booker, S., Krebs, C. and Bollinger, J. (2012) Evidence for only oxygenative cleavage of aldehydes to alk(a/e)nes and formate by cyanobacterial aldehyde decarbonylases. Biochemistry 51, 7908-7916.

Li, N., Nørgaard, H., Warui, D., Booker, S., Krebs, C. and Bollinger, J. (2011) Conversion of fatty aldehydes to alka(e)nes and formate by a cyanobacterial aldehyde decarbonylase: cryptic redox by an unusual dimetal oxygenase. Journal of the American Chemical Society 133, 6158-6161.

Lyons, T., Reinhard, C. and Planavsky, N. (2014) The rise of oxygen in Earth's early ocean and atmosphere. Nature 506, 307-315.

Neilson, J., Quade, J., Ortiz, M., Nelson, W., Legatzki, A., Tian, F., LaComb, M., Betancourt, J., Wing, R., Soderlund, C. and Maier, R. (2012) Life at the hyperarid margin: novel bacterial diversity in arid soils of the Atacama Desert, Chile. Extremophiles : life under extreme conditions 16, 553-566.

Patzelt, D.J., Hodač, L., Friedl, T., Pietrasiak, N. and Johansen, J.R. (2014) Biodiversity of soil cyanobacteria in the hyper-arid Atacama Desert, Chile. Journal of Phycology 50, 698-710.

Phoenix, V.R., Bennett, P.C., Engel, A.S., Tyler, S.W. and Ferris, F.G. (2006) Chilean high-altitude hot-spring sinters: a model system for UV screening mechanisms by early Precambrian cyanobacteria. Geobiology 4, 15-28.

Potts, M. and Friedmann, E.I. (1981) Effects of water stress on cryptoendolithic cyanobacteria from hot desert rocks. Archives of microbiology 130, 267-271.

Qiu, Y., Tittiger, C., Wicker-Thomas, C., Goff, G.L., Young, S., Wajnberg, E., Fricaux, T., Taquet, N., Blomquist, G.J. and Feyereisen, R. (2012) An insect-specific P450 oxidative decarbonylase for cuticular hydrocarbon biosynthesis. Proceedings of the National Academy of Sciences 109, 14858-14863.

Rasmussen, B., Fletcher, I.R., Brocks, J.J. and Kilburn, M.R. (2008) Reassessing the first appearance of eukaryotes and cyanobacteria. Nature 455, 1101-1104.

Ricci, J., Coleman, M., Welander, P., Sessions, A., Summons, R., Spear, J. and Newman, D. (2013) Diverse capacity for 2-methylhopanoid production correlates with a specific ecological niche. The ISME journal 8, 675-684.

Sakurai, R., Ito, M., Ueno, Y., Kitajima, K. and Maruyama, S. (2005) Facies architecture and sequence-stratigraphic features of the Tumbiana Formation in the Pilbara Craton, northwestern Australia; implications for depositional environments of oxygenic stromatolites during the late Archean. Precambrian Research 138, 255-273.

Schinteie, R. and Brocks, J. (2014) Evidence for ancient halophiles? Testing biomarker syngeneity of evaporites from Neoproterozoic and Cambrian strata. Organic Geochemistry 72, 46-58.

Schirmer, A., Rude, M.A., Li, X., Popova, E. and Del Cardayre, S.B. (2010) Microbial biosynthesis of alkanes. Science 329, 559-562.

Sherman, L.S., Waldbauer, J.R. and Summons, R.E. (2007) Improved methods for isolating and validating indigenous biomarkers in Precambrian rocks. Organic Geochemistry 38, 1987-2000.

Shiea, J., Brassell, S.C. and Ward, D.M. (1990) Mid-chain branched mono- and dimethyl alkanes in hot spring cyanobacterial mats: A direct biogenic source for branched alkanes in ancient sediments? Organic Geochemistry 15, 223-231.

Shirai, Y., Seki, M. and Mori, K. (1999) Synthesis of All the Stereoisomers of 7 Methylheptadecane and 7, 11 Dimethylheptadecane, the Female Sex Pheromone Components of the Spring Hemlock Looper and the Pitch Pine Looper. European journal of organic chemistry 1999, 3139-3145.

Sigler, W., Bachofen, R. and Zeyer, J. (2003) Molecular characterization of endolithic cyanobacteria inhabiting exposed dolomite in central Switzerland. Environmental Microbiology 5, 618-627.

Smithies, R.H. (1998) Geology of the Mount Wohler 1:100 000 Sheet, Geological Survey of Western Australia. Explanatory Notes 1, 19.

Stivaletta, N., López-García, P., Boihem, L., Millie, D.F. and Barbieri, R. (2010) Biomarkers of Endolithic Communities within Gypsum Crusts (Southern Tunisia). Geomicrobiology Journal 27, 101-110.

Summons, R.E., Jahnke, L.L., Hope, J.M. and Logan, G.A. (1999) 2-Methylhopanoids as biomarkers for cyanobacterial oxygenic photosynthesis. Nature 400, 554-557.

Thorne, A.M. and Trendall, A.F. (2001) Geology of the Fortescue Group, Pilbara Craton, Western Australia. Bulletin - Geological Survey of Western Australia, 249.

Waldbauer, J.R., Sherman, L.S., Sumner, D.Y. and Summons, R.E. (2009) Late Archean molecular fossils from the Transvaal Supergroup record the antiquity of microbial diversity and aerobiosis. Precambrian Research 169, 28-47.

Walter, M. (1983) Archean stromatolites: Evidence of the Earth's earliest benthos, in: Schopf, J. (Ed.), Earth's Earliest Biosphere: It's Origin and Evolution. Princeton University Press, Princeton, pp. 187-213.

Welander, P.V., Coleman, M.L., Sessions, A.L., Summons, R.E. and Newman, D.K. (2010) Identification of a methylase required for 2-methylhopanoid production and implications for the interpretation of sedimentary hopanes. Proceedings of the National Academy of Sciences 107, 8537-8542.

Wierzchos, J., Ascaso, C. and McKay, C. (2006) Endolithic cyanobacteria in halite rocks from the hyperarid core of the Atacama Desert. Astrobiology 6, 415-422.

Wynn-Williams, D.D., Edwards, H.G.M. and Garcia-Pichel, F. (1999) Functional biomolecules of Antarctic stromatolitic and endolithic cyanobacterial communities. European Journal of Phycology 34, 381-391.

Zhang, X.-g. and Pratt, B.R. (2008) Microborings in Early Cambrian phosphatic and phosphatized fossils. Palaeogeography, Palaeoclimatology, Palaeoecology 267, 185-195.

Zhang, Y. and Golubic, S. (1987) Endolithic microfossils (cyanophyta) from early Proterozoic stromatolites, Hebei, China. Acta Micropaleontologica Sinica 4, 1-12.

Chapter 7.

Discussion and summary

7.1. Thermal maturity of the Fortescue Group rocks

The Fortescue Group rocks in the Pilbara region that were investigated in this study have organic geochemical attributes that generally indicate a high thermal maturity, beyond the late oil window. This is consistent with the prehnite-pumpellyite facies metamorphism (175-280 °C) that the Group is thought to have experienced, estimated by authigenic mineral growth in the Fortescue Group (Smith et al., 1982), although there are variations of metamorphic grade over the basin. A brief summary of the thermal maturity and hydrocarbon (HC) abundance data for Chapters 3-5 is shown in Table 7.1. Parts of samples that are overprinted by contamination or later hydrocarbon migration since their initial deposition are excluded from the data in Table 7.1 (the outer-most slices of outcrop samples in Chapters 3 and 4; and the Ext. fraction of sample 2-3 in Chapter 5).

The thermal maturity of the stromatolite outcrop rock in Chapter 3 (ST1) that is suggested by the aromatic HCs (R_c = 2.2-2.3) (Table 7.1, and Chapter 3, Table 3.2) is as high as the dry gas zone throughout the rock. ST1 contains few HCs in Ext. I, but Ext. II contains a variety of aliphatic and particularly aromatic HCs. The lack of HCs in Ext. I in ST1 is interpreted to be the result of severe weathering. In contrast, the HCs in Ext. II are considered to have been isolated from such weathering, and preserved over geological time. Another stromatolite outcrop sample that is documented in Chapter 4 (ST2) has a very similar high thermal maturity throughout the rock, (R_c = 2.1-2.2; Table 7.1; and Chapter 4, Table 4.2), although possibly slightly lower than ST1. ST2 is rich in aromatic HCs in both Ext. I and II, suggesting a lesser degree of weathering compared to ST1. Aromatic HCs are richer in Ext. II and III than in Ext. I, and are better preserved within the carbonate and silicate minerals (Chapter 4, Fig. 4.14).

Table 7.1. Maximum amounts of aliphatic and aromatic HCs, thermal maturity parameters, metamorphic grades, lithologies of the investigated rock samples in this study.

	Chapter 3	Chapter 4	Chapter 5					
	ST1[a]	ST2[b]	1	3	2-1	2-2	2-3[c]	2-4
Aliphatic HCs (ng / g)	0.14	0.58	0.16	0.3	0.26	0.13	0.21	0.07
Aromatic HCs (ng / g)	0.24	1.20	0.43	1.24	394	30	7.3	0.57
MPI-1	0.06-0.2	0.11-0.3	0.25-0.26	-	0.02	0.08-0.09	0.28	0.68
R_c	2.2-2.3	2.1-2.2	2.1-2.2	-	2.3	2.3	2.1	1.9
Metamorphic grade	Z2	Z2	Z1	Z2	Z2	Z2	Z2	Z2
Lithology	Carbonates	Carbonates	Dolerite	Shale	Shale	Shale	Shale	Shale
Formation	Tumbiana	Tumbiana	Coucal	Jeerinah	Carawine Dolomite	Carawine Dolomite	Jeerinah	Jeerinah

[a]Data from Ext. I and II of slices 2-5; [b]Data from Ext .I, II and III of slices 2-4; [c]Ext. Fraction excluded; **MPI-1** = methylphenanthrene index 1, = 1.5 x (3-MP + 2-MP) / (P + 9-MP + 1-MP); **P** = phenanthrene; **MP** = methylphenanthrene; $\boldsymbol{R_c}$ = calculated vitrinite reflectance from MPI-1, = -0.60 x MPI-1 + 2.30 (Radke and Welte, 1983); Z1 = the prehnite-pumpellyite facies, and Z2 = the prehnite-pumpellyite-epidote facies (Smith et al., 1982).

Three drill cores (AIDP-1, 2 and 3) recovered from the Pilbara region and described in Chapter 5 have heterogeneous thermal maturities. The AIDP-1 core (sample 1) is a dolerite of igneous origin, and was collected as a negative control. Nevertheless, sample 1 contains both aliphatic and aromatic HCs. These HCs may have been acquired through fluid-rock interactions during vein formation (Sracek and Zacharias, 2009), so are not indigenous. The age of the vein formation is not constrained. The AIDP-3 core (sample 3) is scarce in both aliphatic and aromatic HCs. It is difficult to constrain the thermal maturity of AIDP-3 sample, as it lacks the aromatic HCs required to calculate the MPI-1, the methylphenanthrene distribution fraction and the methylnaphthalene ratio data, which are all sensitive to thermal maturity and commonly used for maturity assessment (George and Ahmed, 2002). The AIDP-2 cores (samples 2-1 to 2-4) are rich in aromatic HCs, which is consistent with the two stromatolite outcrops (ST1 and 2) in Chapters 3 and 4. The AIDP-2 cores are rich in aromatic HCs

in Ext. I, unlike ST1, probably because of the protection of samples deep underground from weathering. The AIDP-2 cores have a high thermal maturity, varying from the late oil window (R_c~1.9) to the dry gas zone (R_c~2.3) (Table 7.1, and Chapter 5, Table 5.4), corresponding to two different depositional settings of the AIDP-2 core samples (Table 7.1). Two stromatolite samples (ST1 and 2) have intermediate thermal maturities between these two groups of drill core samples. ST1 is closer to samples 2-1 and 2-2, and ST2 is closer to samples 2-3 and 2-4 of AIDP-2.

7.2. Indigenous hydrocarbons in the Fortescue Group rocks, and the preservational potential of biomarkers

A variety of aliphatic and aromatic HCs were interpreted to be indigenous in the investigated Archean samples through Chapter 3-5, although the detected amount of HCs is very small. ST1 in Chapter 3 only contains a trace amount of aliphatic HCs (<0.04 ng / g sample) (Chapter 3, Fig. 3.4), and no aromatic HCs in Ext. I. But in Ext. II, it contains a higher abundance of >C_{21} *n*-alkanes (<0.14 ng / g sample) than in Ext. I (Table 7.1; and Chapter 3. Fig. 3.4), and various aromatic HCs such as naphthalene, phenanthrene, biphenyl, fluorene and their alkylated HCs (<0.24 ng / g sample) (Table 7.1; and Chapter 3, Fig. 3.8). These aliphatic and aromatic HCs in Ext. II are released by hydrochloric acid treatment, and are generally considered to be indigenous. The outer-most slice of ST1 has some characteristics of recent input such as higher plant material and lipid components of endolithic cyanobacteria, but the abundance of these HCs is not higher compared to the inner slices.

ST2 in Chapter 4 has a much higher abundance of aliphatic HCs (<22.5 ng / g sample) (Chapter 4, Fig. 4.12), and aromatic HCs (<1.2 ng / g sample) (Chapter 4, Fig. S4.5) in Ext. I, II and III, compared to ST1. As the outer-most slice of ST2 is overprinted by a recent input, the abundance of possible indigenous HCs in the inner slices is <0.6 ng / g sample for aliphatic HCs (Table 7.1; and Chapter 4, Fig. 4.12), and <1.2 ng / g sample for aromatic HCs (Table 7.1; and Chapter 4, Fig. S4.5). The large amount of >C_{21} *n*-alkanes in slice 3 (1.5-3.2 ng / g sample) (Chapter 4, Fig. S4.4) is also excluded from the calculation because these *n*-alkanes are probably experimental contamination.

The drill core samples in Chapter 5 have a comparable abundance of aliphatic HCs (<3.7 ng / g sample) (Chapter 5, Fig. 5.2) to ST2, and a significantly higher abundance of aromatic HCs (<390 ng / g sample) (Chapter 5. Fig. 5.7), although the abundance of aromatic HCs without sample 2-1 is much lower (<56 ng / g sample). Diamondoids are not included in this discussion because diamondoid analysis was performed only for the drill core samples, even though the abundance of diamondoids is higher than the other aliphatic HCs (<10 ng / g sample; Chapter 5, Fig. 5.5). Excluding the Ext. fraction of sample 2-3, which is probably contaminated as was suggested in Chapter 5, the abundance of possible indigenous HCs of drill core samples is <0.3 ng / g sample for aliphatic HCs (Table 7.1; and Chapter 5, Fig. 5.2), and <390 ng / g sample for sample 2-1, and <30 ng / g sample for the other drill core samples for aromatic HCs (Table 7.1; and Chapter 5, Fig. 5.8).

Although there is no major difference in the abundance of aliphatic HCs between each sample, ST2 in Chapter 4 has the highest abundance of aliphatic HCs compared to any other samples (Table 7.1). This may be associated with the fact that ST2 is the only sample that contains a trace amount of polycyclic biomarkers such as hopanes and steranes. The abundance of hopanes and steranes is 100-1000 times less abundant than the other aliphatic HCs (Chapter 4).

In contrast, aromatic HCs are rich in the drill core samples 2-1, 2-2 and 2-3 in Chapter 5 (7.3-394 ng / g sample, Table 7.1), which may be due to their preservational environment. Aromatic HCs in the two outcrop samples (Chapters 3 and 4) are scarce in Ext. I, and generally become more abundant in Ext. II and III, even though the abundance is still low compared to the drill core samples. This is interpreted to be due to severe weathering since uplift and exposure at the Earth's surface. In contrast, the drill core samples are considered to have been protected by weathering, and have still kept a high abundance of aromatic HCs. This suggests that aromatic HCs are more susceptible to weathering than aliphatic HCs. The solubility of aromatic hydrocarbons in water is much higher than that of aliphatic hydrocarbons (Polak and Lu, 1973), although the solubility gradually decreases with higher molecular weights (Bohon and Claussen, 1951). Thus, aromatic HCs may have been partially removed by the percolation of water (e.g. rain water). There is no difference in the abundance of

aliphatic HCs between the outcrop samples and drill core samples. In this sense, there may be no particular difference in the preservational potential of biomarkers such as hopanes and steranes between outcrops and drill cores, at least if biomarkers are strictly isolated and protected from weathering within minerals.

The thermal maturities of all the investigated samples are very high, between the late oil window and the dry-gas zone (Section 7.1), but the slight lower thermal maturity of ST2 in Chapter 4, and samples 2-3 and 2-4 in Chapter 5 (mostly MPI-1>0.1, and R_c<2.2), compared to ST1 in Chapter 3, and samples 2-1 and 2-2 in Chapter 5 (mostly MPI-1<0.1, and R_c>2.2), may have contributed to the better preservation of biomarkers in ST2. The lack of biomarkers in samples 2-3 and 2-4 may be associated with the content of clay minerals. Shales typically contain clays, which can catalyse the chemical breakdown of hydrocarbons (e.g. Johns, 1979; Wu et al., 2012). In contrast, carbonates may provide a more stable preservational environment.

7.2.1. Hydrocarbon compositions of other stromatolite samples

Four other stromatolite samples (ST3-6) and one basaltic rock (BS2) were analysed for biomarkers in this study (see Chapter 2, Table 2.2). Only the deepest part of the rocks was analysed to search for any indigenous biomarkers. ST3 and 4 have already been described in Chapter 6 (Locs 2 and 4). ST5 is a carbonate rock from the Tumbiana Formation (known as the "Knossos locality"), and ST6 is a chert from the Jeerinah Formation. BS2 is a basalt lava flow from the Maddina Formation, which is the same setting as another basaltic rock (BS1). The abundance of HCs in BS2 was comparable to BS1 (1-10 pg / g sample for both aliphatic and aromatic HCs), and the HCs in the deepest part of both BS1 and BS2 are considered to be experimental contamination.

No biomarkers were observed in samples ST3-6. ST3 and ST4 had a large amount of contamination during the experiment (~1 ng / g sample), and thus it is not clear that they contain any indigenous HCs. But in any case, biomarkers such hopanes and steranes were not detected, even in the contamination. The abundance of HCs in ST6 was also comparable to the blank level (<20 pg / g

sample). A trace amount of aliphatic HCs (<76 pg / g sample) and aromatic HCs (<143 pg / g sample) was detected in ST5 above the blank level (BS1 and BS2). The MPI-1 for ST5 is 0.34 (R_c = 2.1) (calculated from Radke and Welte, 1983), which is close to that for ST2. ST5 was collected from a nearby locality to ST2, and has a similar thermal maturity, but does not contain biomarkers. The abundance of HCs in ST5 is much lower than that of ST2. This is interpreted to be a result of weathering. Furthermore, the abundance of HCs has a major difference between Ext. I and Ext. II. The abundance of *n*-alkanes is 16 pg / g sample in Ext. I, and 76 pg / g sample (x 5) in Ext. II, and that of naphthalene is 18 pg / g sample in Ext. I, and 143 pg / g sample (x 8) in Ext. II. The HCs in Ext.II are interpreted to be indigenous, and the lower abundance of HCs in Ext. I may be due to weathering; aromatic HCs were probably removed more rapidly, as suggested in the above discussion. In other words, the difference in the abundance of HCs, especially that of aromatic HCs between Ext. I and II, may be an indicator for the degree of weathering. Thus ST5 is probably more influenced by weathering than ST1, and most of the HCs including biomarkers may have been already removed.

7.3. Inhabitation of endolithic cyanobacteria on the Fortescue Group rocks

The surface of four stromatolitic carbonate rocks (ST1-4) are inhabited by endolithic cyanobacteria, detected by the combination of high abundances of the C_{17} *n*-alkane and 7-monomethylalkanes (Chapter 6, Locs 1-4). The colonisation of cyanobacteria on carbonate rock surfaces seems to be widespread across the Pilbara region. In contrast, such a phenomenon was not observed on a basaltic rock (BS1) surface (Chapter 6, Loc. 5). Although there is a possibility that cyanobacterial biomarkers may be found in other basaltic rocks in the future, there may be a selectivity for cyanobacterial colonisation in association with the rock mineralogy and/or porosity. The slice experiments reveal that a trace amount of the C_{17} *n*-alkane and 7-monomethylalkanes may penetrate into the deeper part of the rocks through pore spaces, although the influence of these compounds is limited to Ext. I (Chapters 4 and 6). Therefore, the combination of the slice experiment and two consecutive solvent extractions is demonstrated to be an effective way to distinguish indigenous ancient HCs from contamination.

7.4. Towards a better understanding of the Archean biosphere

This study has suggested the possibility of the presence of cyanobacteria and eukaryotes in the Archean. More evidence will be needed to secure the presence of them before the Great Oxidation Event, and the methodology used in this study could be a standard for further searches for ancient biomarkers. The abundance of the biomarkers is very low in ancient rocks, so the analysis of HCs needs to be carried out with extreme care. The combination of the slice experiment and the two progressive solvent extractions has proven to be an effective method for such trace analyses. It has been clearly shown that the outer slices of the rocks are typically inhabited by modern cyanobacteria (Section 7.3), and influenced by recent inputs of organic matter such as higher plant material (Chapters 3 and 4). The influence of recent input is mainly limited to the rock surfaces, but a trace amount of HCs may migrate into the deeper part of the rock through pores (Chapters 4 and 6). Therefore, the distinction between the migrated HCs that can be extracted by the first extraction (Ext. I), and the HCs that can only be released by carbonate/silicate removal, and be extracted by the second extraction (Ext. II) is important.

The possibility of finding preserved ancient biomarkers seems to depend on (1) the mineralogy, (2) the degree of weathering, and (3) the thermal maturity of the host rock. Shale samples (AIDP-2 cores) may not be the perfect medium due to the catalytic breakdown of HCs by clay minerals (e.g. Johns, 1979; Wu et al., 2012), whereas carbonate minerals (stromatolite outcrop) are more inert, and may harbour HCs over geological time (Section 7.2). Weathering influences the preservation of aromatic HCs (Section 7.2), but it may not critically affect the preservation of aliphatic HCs. Nevertheless, severe weathering can eventually lower the total amount of HCs (ST5, Section 7.2.1). The sample which contains biomarkers (ST2) has indeed the highest abundance of aliphatic HCs (Section 7.1). The difference in the degree of weathering between ST2 and ST5 may have been caused by a local geographical condition. The suggested thermal maturity of the investigated rocks is generally consistent with the estimated metamorphic grade of the Fortescue Group. However, there are variations of thermal maturity between samples, and ST2 is estimated to be slightly less mature

than some other highly thermally mature rocks (e.g. ST1). The future search for biomarkers in the Fortescue Group should take these factors into account.

It is only one (ST2) out of six outcrop samples (ST1-6) that contain potential ancient biomarkers in this study. Drill core samples (AIDP-1 to AIDP-3) are considered to not contain any indigenous biomarkers. ST2 is thought to represent one of the lucky examples of a sample which still preserves ancient biomarkers constrained by the combination of the above three preservational conditions. It is clear from this study that the possibility of encountering ancient biomarkers in the Fortescue Group will be very rare, but at least we know one example, and there may be other such localities to be discovered.

Fluid inclusions (FIs) are another possibility that may preserve intact ancient biomarkers. The oldest biomarkers such as hopanes and steranes found in fluid inclusions push the boundary to samples deposited at 2.4 Ga, although the FIs were likely trapped a bit more recently than that (e.g. George et al., 2008). The FI record in Archean rocks goes even further back (Dutkiewicz et al., 1998), and these samples are an interesting target for further attempts at organic geochemical analyses of biomarkers trapped in FIs. Time-of-Flight Secondary Ion Mass Spectrometry is a recently developed technique that enables the analysis of a single inclusion without contaminating a sample (e.g. Toporski and Steele, 2004). In addition, hydropyrolysis was not performed in this study, but it may release a higher abundance of HCs including biomarkers from the kerogen preserved in a host rock, than by solvent extracting bitumen (e.g. Brocks et al., 2003). Thus, the rocks that do not contain any indigenous HCs might generate a certain amount of indigenous HCs, and perhaps biomarkers by hydropyrolysis. For future work, analysing more rocks, either outcrop or drill cores, as well as using these new techniques would be beneficial to shed more light on the Archean biosphere.

7.5. References

Bohon, R.L. and Claussen, W.F. (1951) The Solubility of Aromatic Hydrocarbons in Water1. Journal of the American Chemical Society 73, 1571-1578.

Brocks, J.J., Love, G.D., Snape, C.E., Logan, G.A., Summons, R.E. and Buick, R. (2003) Release of bound aromatic hydrocarbons from late Archean and Mesoproterozoic kerogens via hydropyrolysis. Geochimica Et Cosmochimica Acta 67, 1521-1530.

Dutkiewicz, A., Rasmussen, B. and Buick, R. (1998) Oil preserved in fluid inclusions in Archaean sandstones. Nature 395, 885-888.

George, S. and Ahmed, M. (2002) Use of aromatic compound distributions to evaluate organic maturity of the Proterozoic middle Velkerri Formation, McArthur Basin, Australia. The Sedimentary Basins of Western Australia III: Proceedings of the West Australasian Basins Symposium (WABS) III.

George, S.C., Volk, H., Dutkiewicz, A., Ridley, J. and Buick, R. (2008) Preservation of hydrocarbons and biomarkers in oil trapped inside fluid inclusions for > 2 billion years. Geochimica Et Cosmochimica Acta 72, 844-870.

Johns, W.D. (1979) Clay Mineral Catalysis and Petroleum Generation. Annual Review of Earth and Planetary Sciences 7, 183-198.

Polak, J. and Lu, B.C.Y. (1973) Mutual Solubilities of Hydrocarbons and Water at 0 and 25 °C. Canadian Journal of Chemistry 51, 4018-4023.

Radke, M. and Welte, D. (1983) The Methylphenanthrene index (MPI). A Maturity parameter based on aromatic hydrocarbons, in: Bjorøy, M., Albrecht, C., Cornford, C. (Eds.), Advances in Organic Geochemistry. John Wiley & Sons, New York, pp. 504-512.

Smith, R.E., Perdrix, J.L. and Parks, T.C. (1982) Burial Metamorphism in the Hamersley Basin, Western Australia. Journal of Petrology 23, 75-102.

Sracek, O. and Zacharias, J. (2009) Fluids in geological processes, in: Cilek, V., Smith, R.H. (Eds.), Earth system: history and natural variability. Eolss, pp. 439-457.

Toporski, J. and Steele, A. (2004) Characterization of purified biomarker compounds using time of flight-secondary ion mass spectrometry (ToF-SIMS). Organic Geochemistry 35, 793-811.

Wu, L.M., Zhou, C.H., Keeling, J., Tong, D.S. and Yu, W.H. (2012) Towards an understanding of the role of clay minerals in crude oil formation, migration and accumulation. Earth-Science Reviews 115, 373-386.

Appendix

Hydrocarbons preserved in a ~2.7 Ga outcrop sample from the Fortescue Group, Pilbara Craton, Western Australia

Y. Hoshino [1,2], D. T. Flannery [2,3], M. R. Walter [2,3], S. C. George [1,2]

[1] *Department of Earth and Planetary Sciences, Macquarie University, Sydney, Australia*

[2] *Australian Centre for Astrobiology, University of New South Wales, Australia*

[3] *School of Biotechnology and Biomolecular Sciences, University of New South Wales, Australia*

This appendix is the published article in *Geobiology* (see Chapter 3).

Y. Hoshino, D. T. Flannery, M. R. Walter, S. C. George, 2015. Hydrocarbons preserved in a ~2.7 Ga outcrop sample from the Fortescue Group, Pilbara Craton, Western Australia, *Geobiology* 13, 99-111.

Appendix of this thesis have been removed as they contain published material. Please refer to the following citation for details of the article contained in these pages.

Hoshino, Y., Flannery, D.T., Walter, M.R. and George, S.C. (2015), Hydrocarbons preserved in a ~2.7 Ga outcrop sample from the Fortescue Group, Pilbara Craton, Western Australia. *Geobiology*, 13(2), pp.99-111.

DOI: 10.1111/gbi.12117